SUSCEPTIBILITY OF BRIDGE STEEL AND CONCRETE COMPONENTS TO MICROBIOLOGICAL INFLUENCED CORROSION (MIC) AND MICROBIOLOGICAL INFLUENCED DETERIORATION (MID) IN FLORIDA

FINAL REPORT
Project BDV29-977-26
(800006816)

Submittd To:

FDOT Research Center
605 Suwannee Street
Tallahassee, FL 32399

Project Manager:
Matthew Duncan
Florida Department of Transportation, State Materials Office
5007 NE 39th Avenue
Gainesville, FL 32609

Submitted By:

Kingsley Lau
Florida International University
10555 W. Flagler Street
Miami, FL 33174

May 2019

Prepared by:

Samanbar Permeh
Mayrén Echeverría Boan
and Kingsley Lau

DISCLAIMER

This investigation was supported by the Florida Department of Transportation. The opinions, findings, and conclusions expressed here are those of the authors and not necessarily those of the Florida Department of Transportation or the U.S. Department of Transportation.

The assistance provided by Bin Li, Carla Reid, and other graduate research assistants as well as Dennis Baldi and others from FDOT State Materials Office during field testing is acknowledged and greatly appreciated.

Portions of the document were presented in conference proceedings, including:

1. S. Permeh, M.E. Echeverria, B. Tansel, K. Lau, and M. Duncan. “Exploration of the Influence of Microbe Availability on MIC of Steel Marine Fouling Environments.” NACE Corrosion/2019. Submitted
2. S. Permeh, M.E. Echeverria, B. Tansel, K. Lau, and M. Duncan. “Update on Mitigation of MIC of Steel In a Marine Environment with Coatings .” SSPC2019. Submitted.
3. S. Permeh*,* M.E. Boan*, B. Tansel, K. Lau, and M. Duncan. Poster. “Biofouling and MIC of Coated Steel in Marine Environments.” 19th International Congress on Marine Corrosion and Fouling. Melbourne, FL. June 24-29, 2018.
4. S. Permeh, B. Li, M. E. Boan, B. Tansel, A. Agarwal, K. Lau, M. Duncan. “Application of Coatings to Mitigate Degradation of Steel Subjected to Marine Fouling and MIC.” NACE Corrosion Risk Management Conference/ June 11-13, 2018. 13pp.
5. S. Permeh*, M, Echeverría*, B. Tansel, K. Lau, and M. Duncan. “Evaluation of Macrofouling Crevice Characteristics in MIC of Steel.” NACE Corrosion/2018. Paper No. 11529.
6. S. Permeh, C. Reid, M, Echeverría, B. Tansel, K. Lau, M. Duncan, and I. Lasa. “Microbiological Influenced Corrosion in Florida Marine Environment: A Case Study.” NACE Corrosion/2017. Paper No. 9536. 12pp.

APPROXIMATE CONVERSIONS TO SI UNITS

SYMBOL	WHEN YOU KNOW	MULTIPLY BY	TO FIND	SYMBOL
LENGTH				
in	inches	25.4	millimeters	Mm
mils	mils	25.4	micrometers	Mm
ft	feet	0.305	meters	M
yd	yards	0.914	meters	M
mi	miles	1.61	kilometers	km

SYMBOL	WHEN YOU KNOW	MULTIPLY BY	TO FIND	SYMBOL
AREA				
in^2	squareinches	645.2	square millimeters	mm^2
ft^2	squarefeet	0.093	square meters	m^2
yd^2	square yard	0.836	square meters	m^2
ac	acres	0.405	hectares	ha
mi^2	square miles	2.59	square kilometers	km^2

SYMBOL	WHEN YOU KNOW	MULTIPLY BY	TO FIND	SYMBOL
VOLUME				
fl oz	fluid ounces	29.57	milliliters	mL
gal	gallons	3.785	liters	L
ft^3	cubic feet	0.028	cubic meters	m^3
yd^3	cubic yards	0.765	cubic meters	m^3
NOTE: volumes greater than 1000 L shall be shown in m^3				

SYMBOL	WHEN YOU KNOW	MULTIPLY BY	TO FIND	SYMBOL
MASS				
oz	ounces	28.35	grams	g
lb	pounds	0.454	kilograms	kg
T	short tons (2000 lb)	0.907	megagrams (or "metric ton")	Mg (or "t")

SYMBOL	WHEN YOU KNOW	MULTIPLY BY	TO FIND	SYMBOL
TEMPERATURE (exact degrees)				
^{o}F	Fahrenheit	5 (F-32)/9 or (F-32)/1.8	Celsius	^{o}C
SYMBOL	**WHEN YOU KNOW**	**MULTIPLY BY**	**TO FIND**	**SYMBOL**
ILLUMINATION				
fc	foot-candles	10.76	lux	lx
fl	foot-Lamberts	3.426	candela/m^2	cd/m^2

SYMBOL	WHEN YOU KNOW	MULTIPLY BY	TO FIND	SYMBOL
FORCE and PRESSURE or STRESS				
lbf	poundforce	4.45	newtons	N
lbf/in^2	poundforce per square inch	6.89	kilopascals	kPa

APPROXIMATE CONVERSIONS TO US. CUSTOMARY UNITS

SYMBOL	WHEN YOU KNOW	MULTIPLY BY	TO FIND	SYMBOL
LENGTH				
mm	millimeters	0.039	inches	in
µm	micrometers	0.039	mils	mils
m	meters	3.28	feet	ft
m	meters	1.09	yards	yd
km	kilometers	0.621	miles	mi

SYMBOL	WHEN YOU KNOW	MULTIPLY BY	TO FIND	SYMBOL
AREA				
mm^2	square millimeters	0.0016	square inches	in^2
m^2	square meters	10.764	square feet	ft^2
m^2	square meters	1.195	square yards	yd^2
ha	hectares	2.47	acres	ac
km^2	square kilometers	0.386	square miles	mi^2

SYMBOL	WHEN YOU KNOW	MULTIPLY BY	TO FIND	SYMBOL
VOLUME				
mL	milliliters	0.034	fluid ounces	fl oz
L	liters	0.264	gallons	gal
m^3	cubic meters	35.314	cubic feet	ft^3
m^3	cubic meters	1.307	cubic yards	yd^3

SYMBOL	WHEN YOU KNOW	MULTIPLY BY	TO FIND	SYMBOL
MASS				
g	grams	0.035	ounces	oz
kg	kilograms	2.202	pounds	lb
Mg (or "t")	megagrams (or "metric ton")	1.103	short tons (2000 lb)	T

SYMBOL	WHEN YOU KNOW	MULTIPLY BY	TO FIND	SYMBOL
TEMPERATURE (exact degrees)				
^oC	Celsius	1.8C+32	Fahrenheit	^oF

SYMBOL	WHEN YOU KNOW	MULTIPLY BY	TO FIND	SYMBOL
ILLUMINATION				
lx	lux	0.0929	foot-candles	fc
cd/m^2	candela/m^2	0.2919	foot-Lamberts	fl

SYMBOL	WHEN YOU KNOW	MULTIPLY BY	TO FIND	SYMBOL
FORCE and PRESSURE or STRESS				
N	newtons	0.225	poundforce	lbf
kPa	kilopascals	0.145	poundforce per square inch	lbf/in^2

TECHNICAL REPORT DOCUMENTATION PAGE

1. Report No.	2. Government Accession No.	3. Recipient's Catalog No.
4. Title and Subtitle Susceptibility of Bridge Steel and Concrete Components to Microbiological Influenced Corrosion (MIC) and Microbiological Influenced Deterioration (MID) in Florida		5. Report Date February 2019 6. Performing Organization Code
7. Author(s) Samanbar Permeh, Mayrén Echeverría Boan, Berrin Tansel and Kingsley Lau		8. Performing Organization Report No.
9. Performing Organization Name and Address Florida International University 10555 W. Flagler St. Miami, FL 33174		10. Work Unit No. (TRAIS) 11. Contract or Grant No. BDV29-977-26
12. Sponsoring Agency Name and Address Florida Department of Transportation 605 Suwannee St. MS 30 Tallahassee, FL 32399		13. Type of Report and Period Covered: Draft Final Report March 16, 2016 - February 8, 2019 14. Sponsoring Agency Code
15. Supplementary Notes		

16. Abstract

Submerged steel piles had localized corrosion associated with microbiologically influenced corrosion (MIC). The site also had heavy marine growth. The effect of crevice environments created by the macrofoulers may support MIC. Also, concrete may be subject to deterioration by microbiologically influenced deterioration (MID). Field visits to Florida natural water sites and a review of the literature and databases indicated that there are locations in Florida that support MIC. Steel samples were installed at three sites (brackish and fresh waters). The presence of marine fouling was an important part of the corrosion system. Laboratory testing identified the effects of crevices and availability of bacteria and nutrients on MIC. The use of steel coatings and galvanic cathodic protection was assessed for mitigation of MIC in environments with marine fouling. The use of polyurea and a water-based copper-free antifouling coating was examined to identify mitigation. The anti-fouling coating showed less barnacle growth compared to polyurea and had generally lower surface populations of SRB, IRB, APB, and SFB. Complications in cathodic protection (CP) arise with the presence of MIC and marine fouling. Steel field specimens were coupled to a zinc anode at the test sites. Application of CP reduced the corrosion rate, but results indicated that there were portions of the steel array under marine fouling that did not receive sufficient cathodic polarization. In field testing of concrete immersed in the test sites, heavy marine fouling and bacteria developed on the specimen surface. No differentiation in bulk concrete characteristics relating to MID were identified. Application of a polyurea did not mitigate marine fouling or bacteria formation.

17. Key Word	18. Distribution Statement
Steel Bridge, Corrosion, Fouling, MIC, MID, Cathodic Protection, Coating, SRB	

19. Security Classif. (of this report)	20. Security Classif. (of this page)	21. No. of Pages	22. Price
unclassified	unclassified	279	

EXECUTIVE SUMMARY

Recent findings at a Florida bridge showed that submerged steel piles had severe localized corrosion cells and pits, up to 3" in diameter, that had penetrated through the steel thickness. Sampling and testing of water indicated strong presence of microbial growth that can be associated with microbiologically influenced corrosion (MIC). In particular, anaerobic sulfate-reducing bacteria (SRB), acid-producing bacteria (APB), and slime-producing bacteria (SPB) were recovered in cultures produced from the steel and water samples. In addition to the microorganisms that can cause corrosion, the affected site had heavy marine growth. It was thought that the effect of localized crevice environments created by the presence of the macrofoulers may support MIC. In addition to these field findings, concrete may be subject to significant deterioration due to microbiologically influenced deterioration (MID). The objective of the research was to identify if (1) if marine fouling can enhance proliferation of bacteria that can support MIC in Florida natural waters, (2) if macrofouling can affect the efficacy of cathodic protection to mitigate MIC, (3) if application of coatings can be used to mitigate marine fouling and bacteria settlement, and (4) if microbially influenced degradation of concrete can develop in natural waters. To address the research objectives, the following research questions were posed.

Field visits to five Florida natural water sites and a review of environmental databases were made to identify environmental conditions, water chemistry, microbial activity, and marine fouling. In light of the findings from the case study, review of the technical literature, and available environmental databases, there may be locations in Florida that meet environmental conditions and nutrients requirements for microorganism colonization and sustained activity. Steel samples were installed at three Florida sites that comprised estuarial, brackish, and fresh waters with environmental conditions that support MIC. All three test sites supported heavy marine growth, predominantly barnacles and marine flora. Microbiological analysis under the marine growth encrustations verified that bacteria associated with MIC had developed in the occluded spaces. Electrochemical testing and corrosion mass loss measurements of steel specimens submerged in the test river waters indicated highly aggressive corrosion conditions. The testing revealed significant localized corrosion that was associated with crevice conditions developed by marine fouling.

As field observations indicated that the presence of marine fouling was an important part of the corrosion system, laboratory testing was conducted to identify the effects of hard and porous crevice and availability of planktonic bacteria and nutrients to those crevices spaces on the development of MIC due to SRB. With pulse increments of SRB and nutrients, SRB activity can proliferate in supportive environments that include low oxygen levels. In lab tests, SRB activity could be maintained after an initial inoculation but was not differentiated by the level of initial nutrient concentrations. SRB activity was shown to be better supported under crevice environments. Laboratory specimens that developed corrosion in the SRB-inoculated solution exhibited potential ennoblement characteristics (due to cathodic depolarization by SRB),indicating that the corrosion can be accounted for reactions associated with MIC.

The use of steel coatings and galvanic cathodic protection was assessed for mitigation of MIC in environments with heavy marine fouling. The use of polyurea and a water-based copper-free antifouling coating was examined to identify their efficacy in mitigating degradation of submerged steel in natural waters susceptible to fouling and MIC. Field and lab assessments were conducted to identify bacteria proliferation, surface fouling, coating degradation, and steel substrate corrosion. The antifouling coating showed relatively better antifouling performance and less barnacle growth, compared to polyurea, and had generally lower surface populations of SRB, IRB, APB, and SFB over the time of exposure. The polyurea coating did not prevent marine growth regardless of its physical surface conditions, but larger barnacle basal plate sizes were observed for polyurea with higher roughness. Severe corrosion was observed for samples with heavy marine fouling, implicating the adverse effects of immersion and marine growth on coating durability. In lab tests, MIC due to SRB only occurred with the presence of coating defects. For the antifouling coating, it was posited that local concentration of the antifouling agents may be reduced near the steel defect interface.

Complications in cathodic protection of submerged steel arise with the presence of MIC and marine fouling. Steel field specimens were coupled to a zinc anode at the three river test sites where heavy marine fouling develops and where the environment supports MIC. Laboratory cathodic polarization tests were made for lab specimens with hard and porous crevice geometries. System potentials, ~-1,000 mV_{CSE}, developed with the coupling to a commercially available zinc anode. Current densities afforded to the steel array exceeded 30 mA/m^2. No major differentiation in current was observed between the presence of adhered mature barnacles and interlayered barnacle encrustation. Application of CP reduced the general apparent corrosion rate at the test sites, but results indicated that there were portions of the steel array that did not receive sufficient cathodic polarization. It was posited that the localized corrosion developed when marine fouling created local corrosion cells in unprotected regions. Lab testing indicated reduced CP current in occluded regions of specimens with crevices. In presence of SRB in crevices, irregular steel surface oxidation developed. The lab results indicated that in the presence of cathodic polarization, sulfate reduction reactions were still important.

In field testing of concrete immersed in the three river test sites, heavy marine fouling and bacteria developed on the specimen surface. Electrical measurements (bulk resistivity and EIS) showed electrical characteristics representative of the environmental exposure condition including salinity and moisture level. No differentiation in bulk concrete characteristics relating to MID was identified. Laboratory testing of concrete specimens in test solutions showed development of SRB activity, but the observed concrete deterioration (characterized by degradation of the cement paste) was associated with leaching of alkaline compounds from the concrete. Application of a polyurea coating did not mitigate marine fouling or bacteria formation.

TABLE OF CONTENTS

LIST OF FIGURES

LIST OF TABLES

LIST OF TABLES

1. INTRODUCTION

Recent findings at a Florida bridge (Figure 1.1) showed that submerged steel piles had severe corrosion. Localized corrosion cells/pits were of up to 3" in diameter and penetrated through the steel thickness (Figure 1.2). Sampling and testing of water associated with the anomalous corrosion observations indicated strong presence of microbial growth that can be associated with microbiologically influenced corrosion (MIC). ln particular, anaerobic sulfate reducing bacteria (SRB), acid producing bacteria (APB), and slime producing bacteria (SPB) were recovered in cultures produced from the steel and water samples. The water samples also showed high sulfate and chloride levels.

Figure 1.1. Picture of a Florida bridge over Matanzas River with Corrosion of Steel Piles.

In addition to the microorganisms that can cause corrosion, the affected site also had heavy marine growth (Figure 1.3). Although the role of the macrofoulers on the corrosion of the steel piles was not clear, the macrofoulers may have been associated with the corrosion development. It was thought that the effect of localized crevice environments created by the presence of the macrofoulers may support MIC.

In addition to these field findings, concrete may be subject to significant deterioration due to microbiologically influenced deterioration (MID). Concrete is usually immune to biological attack because of its high alkalinity, but over time, the pH of the alkaline concrete surface is gradually reduced by the carbonation and neutralization of hydrogen sulfide. Microbial colonization may then progress rapidly; further reducing the surface pH due to biogenic production of acids. Biogenic organic acids (acetic, lactic, butyric and the like) and carbon dioxide produced by microorganisms (bacteria and fungi) can be extremely damaging to concrete structures. Microorganisms can penetrate inside the concrete matrix even if there are no observable cracks in concrete.

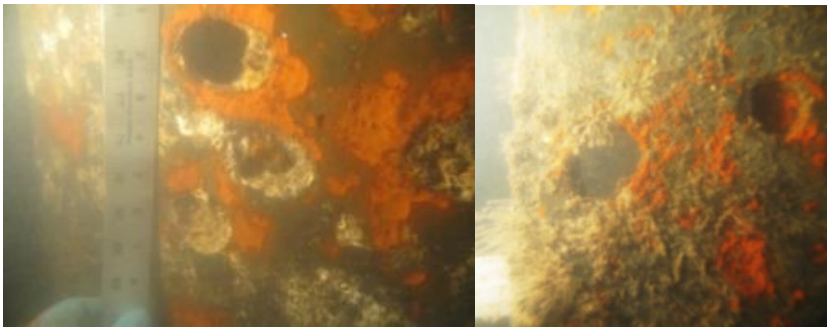

Figure 1.2. Picture of Corrosion Pits on Submerged Steel Piles.

Figure 1.3. Picture of Heavy Marine Biofouling.

MIC and MID has been identified in many environments associated with vital infrastructure including buried pipelines, marine structures, and waste water facilities. A vast array of various forms of microbial organisms has been reported to be associated with MIC and MID. As such, corrosion and degradation mechanisms can vary significantly depending on biological and chemical characteristics of microbial growth and activity, as well as the interaction with the environment for nutrient supply and sustainable growth. MIC and MID has not traditionally been a major durability concern for Florida coastal and inland bridges, but the recent findings compounded by greater service life performance expectations for transportation infrastructure has made determination of corrosion and material degradation susceptibility of embedded and immersed bridge components to degradation by microbial activity of vital interest.

The objective of the research was to identify if 1) marine fouling can enhance proliferation of bacteria that can support MIC in Florida natural waters, 2) if macrofouling can affect the efficacy of cathodic protection to mitigate MIC, 3) application of coatings can be used to mitigate marine fouling and bacteria settlement, and 4) if microbial influenced degradation of concrete can develop in natural waters.

To address the research objectives, the following research questions were posed:

1. Are there environments in Florida that are susceptible to MIC?
2. Can marine macrofouling create adverse crevice conditions that support MIC?
3. Can fouling crevice environments affect the proliferation of bacteria?

4. Can cathodic protection systems provide sufficient cathodic polarization to mitigate MIC in presence of marine foulers?
5. Can cathodic polarization affect bacteria growth and proliferation?
6. How do physical characteristics of marine foulers affect the efficacy of CP?
7. Can coatings be used to mitigate macrofouling and MIC?
8. Can proliferation of bacteria and settlement of bacteria cause concrete degradation.

Testing to address objective 1 included two major subsets of laboratory test setups and a set of field exposed steel coupons as shown in Figure 1.4. Laboratory experiments made under test setup A varied the availability of isolated sulfate reducing bacteria and nutrient levels. Experiments in test setup B followed a modified laboratory test setup and a single inoculation of isolated sulfate reducing bacteria was initially introduced and the level of biotic and electrochemical activity was continuously monitored. Field corrosion testing utilized freshly recovered steel coupons from test sites in natural waters in Florida to provide a control condition in real life natural conditions. Details of the test methodologies for each test setup is described in Chapters 4 and 5.

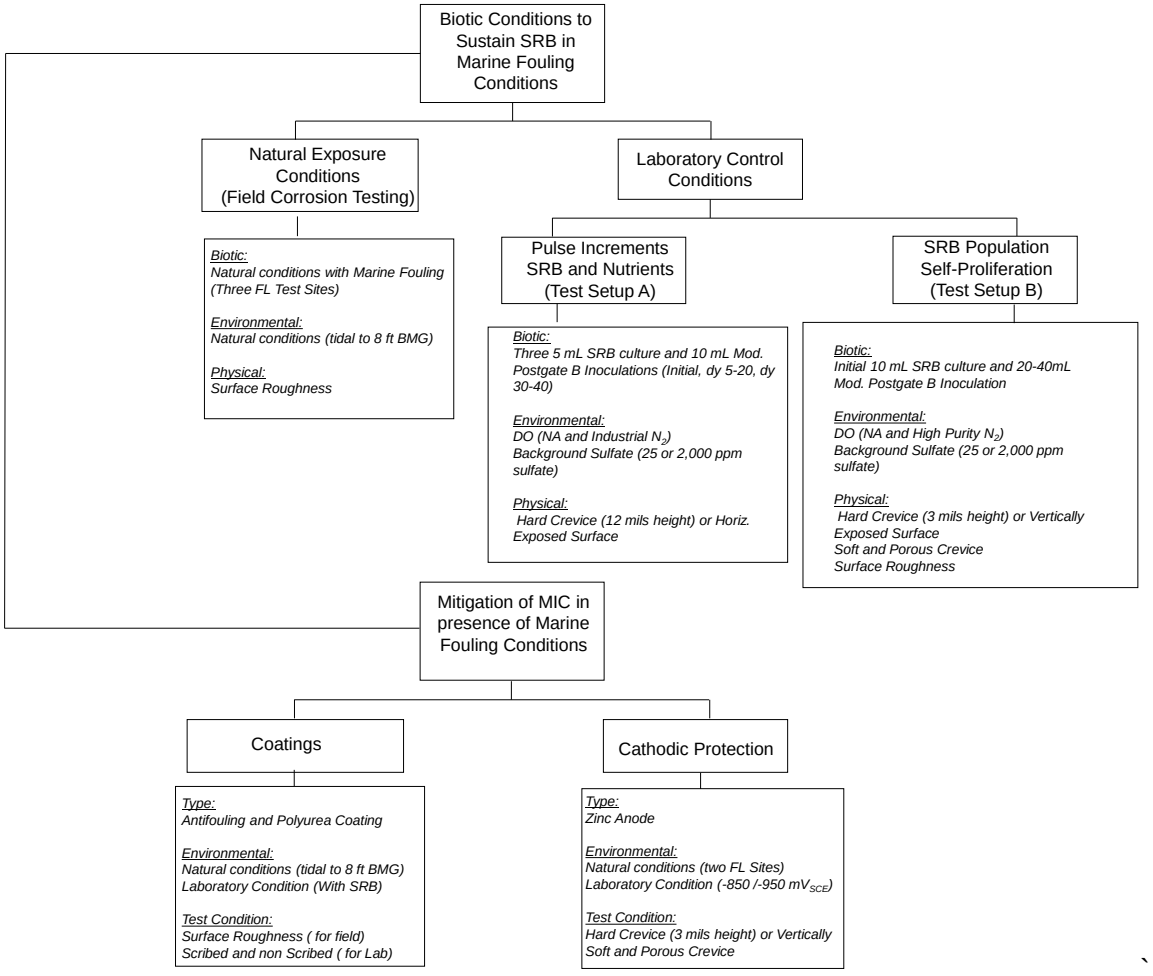

Figure 1.4. Test Approach.

Due to the large volume of work, the research is presented in the report as following:

1) Literature Review (Chapter 2)

2) Florida Natural Water Environments (Chapter 3)

The early case study identified by FDOT was reviewed to clarify chemical makeup and microbial composition. The information obtained from the test site as well as a review of the literature and available environmental databases was used to identify additional sites for sampling and inspection when possible.

3) Field Corrosion Testing- (Chapter 4)

Steel coupons were installed at three Florida water bodies (that could sustain microbiological activity associated with MIC as well as heavy marine fouling) at different water submergence level and periodically tested to identify microbial presence and corrosion activity. Steel Coupons were retrieved after longtime exposure and examined for fouling formation, microbial activity and corrosion development.

4) Laboratory Testing (Chapter 5)

Laboratory testing was conducted in simulated environments to identify pertinent parameters for sustained microbial and corrosion activity. The testing aimed to explore the role of micro-biotic conditions such as microbe availability, nutrient levels, and oxygen levels as well as physical environmental conditions (including steel surface conditions and development of fouling encrustations) that can regulate biotic conditions that may affect MIC.

5) Coatings to Mitigate Macro- and Micro-Fouling (Chapter 6)

Antifouling coating and a polyurea coating were used to evaluate its effectiveness of the two coating materials to mitigate degradation of steel in natural water environments that are susceptible to fouling and MIC. Field tests and laboratory examination were conducted to elucidate coating behavior pertaining to proliferation of bacteria, surface fouling, coating degradation, and steel substrate corrosion. Laboratory testing condition was applied for coated steel coupons in nutrient rich environment with presence of microbial inoculum.

6) Cathodic Protection to Mitigate MIC with Presence of Fouling (Chapter 7)

The effects of cathodic polarization on the development of corrosion on submerged steel samples subjected to marine fouling and MIC was investigated. Field testing incorporated steel plates submerged in two Florida natural water bodies that could sustain microbiological activity associated with MIC as well as heavy marine fouling. Other laboratory testing incorporated steel samples with fabricated crevices, placed in inoculated SRB media, subjected to potentiostatic or potentiodynamic polarizations.

7) Microbially Influenced Degradation of Concrete (Chapter 8)

Concrete cylinders were installed at three Florida water bodies (that could sustain microbiological activity associated with MIC as well as heavy marine fouling) at tidal water submergence level and tested to identify microbial presence and visual deterioration. Concrete cylinders were retrived after longtime exposure and examined for fouling formation, microbial activity. Laboratory testing was conducted in nutrient rich environment in presence of SRB. Laboratory and field tests were also conducted with concrete cylinders coated with polyurea to identify possible degradation mitigation.

2. LITERATURE REVIEW

2.1. Microbiologically Influenced Corrosion (MIC)

MIC is an important degradation mechanism for materials in a wide variety of industries. Considerable research has been conducted to understand the phenomenon of MIC. Even though much research has addressed the phenomenon for materials exposed in aqueous environments, the often narrow field of individual studies and the complexities involved with MIC presents difficulties to account for the wide variabilities in microbial biology as well as environmental, physical, and chemical factors (Borenstein, 1994; Mansfeld, 2007; Melchers, 2014). Furthermore, limited information has been readily disseminated in the literature on MIC of bridge infrastructure in marine environments. According to Lee *et al*. (1995) and Videla and Herrera (2009), microbial corrosion and degradation of marine steel infrastructures such as bridges, wharfs, platforms and pipeline systems due to the activity of microorganisms is responsible of 20% of corrosion costs (Lee *et al*., 1995). The main part of these costs are closely related to anaerobic corrosion by SRB (Videla and Herrera, 2009), where their activity often causes the formation of biofilms on iron and steel and tends to promote the formation of cavity on them.

Microorganisms associated with MIC are microscopic and submicroscopic and can include bacteria, microalgae and fungi. Some literature suggest that bacteria and fungi are of particular interest for MIC (Little and Lee, 2014), however, environmental parameters are important to sustain microbiological activities. The main types of bacteria traditionally studied in MIC have been SRB (anaerobic), sulfur/sulfide-oxidizing bacteria (SOB) (aerobic), iron/manganese–reducing bacteria (IRB) (aerobic) and bacteria secreting organic acids and slime (Beech *et al*., 2000).

Microorganisms in natural waters have the ability to adhere to most surfaces. There, they can reproduce, and many can produce exopolymers, also called extracellular polymeric substance (EPS) (Geesey *et al*., 1986). Some investigations have mentioned that a consortium of microorganisms is involved in the formation of biofilms and consequently different types of microorganisms can live together as a small unit (at least temporarily) (Kobrin, 1976; Linhardt, 2006; Geesey, 1993). The biofilm is constituted by immobilized cells (Dexter and La Fontaine, 1998) or EPS (Rajasekar and Ting, 2011) developed on the metal interface. EPS also mediate microorganism adhesion to surfaces allowing formation of a cohesive, three-dimensional polymer network that interconnects and transiently immobilizes biofilm cells. Under the biofilm, an occluded space may form where the chemical environment can differ from the bulk solution (Rajasekar and Ting, 2011).

Corrosion of steel can take place under the biofilm at the metal to solution interface (Melchers, 2014). The corrosion involves electrochemical processes where the microorganisms can influence the corrosion kinetics. In general, for MIC to occur, an energy source, a carbon source, an electron donator, an electron acceptor and water, are required (Melchers, 2014). The required energy and nutrients are found from the surrounding environment. At cathodic sites,

electrons are accepted from the anodic site (Rajasekar and Ting, 2011). More complicated steps involving charge transfer related to biotic reactions can also occur. For example, MIC due to SRB involves the reduction of inorganic sulfate ion in the presence of hydrogen or organic matter to produce hydrogen sulphide (Javaherdashti, 2008).

MIC does not necessarily occur in the presence of biofilm alone. The wide variety of microorganisms and their interaction with the environment and other organisms can create different electrochemical conditions that can accelerate corrosion and conversely, in some conditions, inhibit corrosion (Videla and Herrera, 2009). In addition, the chemical concentration at the metallic substrate can change significantly due to the extent of biofilm growth as the film can create diffusion conditions for oxygen and nutrients to the metallic surface (Javaherdashti, 2008). Once the biofilm is formed and developed, the outer cells start to consume the nutrients available to them more rapidly than the ones locates deeper within the biofilm. Consequently the activity and growth rate of the latter are reduced. Then, while the outer cells increase in number, the biofilm starts acting as a net, trapping more and more particles (organic and inorganic), thus increasing the biofilm thickness even further (Liu *et al.,* 2000). Factors such as pH, dissolved oxygen, etc. may be drastically different inside and outside the biofilm, thus causing changes in the electrochemistry of the biofilm-metal system. Differential chemistry and bioactivity can lead to a phenomenon known as potential ennoblement (documented for a range of metals and alloys at different salinities) that can result in an increase pitting susceptibility (Geesey, 1993, Dexter and La Fontaine, 1998; Dickinson, 1996; Videla, 1996). This would also coincide with possible changes in the cathodic reaction on the metal due to the microbial activity within the biofilm.

2.1.1. Corrosion Mechanisms Related to MIC in Aqueous Environments

Several damage mechanisms for MIC have been proposed in the literature. Mansfield (2007) pointed out that MIC leads to an increase in corrosion rates owing to the presence of bacteria that accelerate the rates of the anodic and/or cathodic corrosion reaction (Mansfield, 2007). Potekhina et al., 1999 suggested that there are two types of bacteria according to their capacity to induce or inhibit corrosion. The bacteria that causes corrosion are those which create an additional galvanic coupling between themselves and the metal. Under anaerobic conditions, the bacteria is the cathode and the metal is the anode and electrons will flow from metal to bacteria. Consequently, the open circuit potential of the metal increases and moves to more positive values as long as the bacteria are active. Hydrogen consuming bacteria like SRB, certain nitrate-reducing bacteria and phototrophic bacteria are some examples of corrosive bacteria.

SRB has been widely associated with MIC. It is known that SRB easily reduce inorganic sulfates into sulfides in the presence of hydrogen or organic matter and the process is facilitated on iron surface (Mansfeld, 2007), but there has been considerable controversy regarding the mechanism of anaerobic microbial corrosion. In 1934, Kuhr proposed the cathodic depolarization mechanism where it was posited that SRB removes atomic hydrogen from the iron surface (by the hydrogenase enzyme), providing cathodic reaction to accommodate accelerated corrosion of iron. However, the validity of this mechanism has been questioned as

corrosion has been observed on hydrogenase negative strain of SRB. Also, the reaction products (such as hydrogen sulfide and ferrous sulfide) also could act as depolarizing agents, which can account for high rate of corrosion. Costello (1974) also proposed that hydrogen sulfide, rather than the hydrogen ion, was the cathodic reactant. King and Miller (1971) indicated that the addition of chemically prepared ferrous sulfide to the system encourage depolarization. However, the cathodic reaction is considered to be either activation or concentration polarization controlled and hydrogenase may therefore have some role in removing molecular hydrogen and ensuring the supply of hydrogen sulfide for the cathodic reaction. Iverson (1981) suggested a more complex mechanism involving both sulfide and phosphide. Starkey (1986) suggested that several processes concerning the effect of ferrous sulfide, sulfur, ferrous hydrate, phosphide and other product are involved in anerobic corrosion. Other research supported the classical theory (Cord-Ruwisch ,1986; Pankhania et al.,1986; Hardy,1983).

Research by Herrera and Videla (2009) indicated that IRB can induce and enhance corrosion in the absence or presence of other bacteria. The common mechanism to promote corrosion is through reduction of Fe^{3+} corrosion products, which can subsequently exposes the metal surface to the corrosive medium. In addition, these bacteria are able to create anaerobic zones promoting SRB growth within biofilms where both bacteria are present (Herrera and Videla, 2009). Other authors that investigated steel corrosion influenced by anaerobic biofilm in natural sea water detected SRB and IRB bacteria in the anaerobic biofilm under the rust layer on carbon steel. SRB was located in the inner rust layer and IRB in middle and outer layers. Green rust was the main component in the inner rust layer, and both SRB and IRB contributed to the formation of green rust. The isolated SRB bacteria accelerated corrosion. However, the mixed anaerobic bacteria (SRB and IRB) was shown to have inhibited corrosion in part related to the formation of green rust under the biofilm (Duana et al., 2008).

Indeed, other studies have observed that large bacteria populations can inhibit corrosion of different metals and alloys in many corrosive environments (Mansfield, 2007). The other group of bacteria that inhibit corrosion both in aerobic (Pedersen and Hermansson, 1991) and anaerobic conditions (Jayaraman et al., 1997) removes oxygen, thus leading to a drop in the cathodic reaction and to a slowdown of metal dissolution. In this case, the protective bacteria act as an anode and the metal as a cathode. Videla and Herrera (2009) indicated that corrosion inhibition can occur at metal surfaces with biofilm, when the extracellular polymeric substances (EPS) of the biofilm impede the dissolution of Fe^{2+} corrosion products. Thus, the EPS behaves as a barrier between the metal and the environment (Videla and Herrera, 2009). The environmental characteristics of the metal/biofim/medium interface and its surroundings (pH, ionic composition, oxygen levels, EPS distribution) will control the chemical and physical nature of protective layers and may change microbial effects on the metal behavior from corrosive to protective (Herrera and Videla, 2009).

The microbial corrosion inhibition is not usually linked to a single mechanism or to a single species of microorganisms. They can induce corrosion inhibition in accordance with two general mechanisms or their combination: 1) neutralizing the action of corrosive substances present in the environment and 2) forming protective films or stabilizing pre-existing protective

films on a metal. However, authors have stressed that in some cases inhibitory action of bacteria can be reversed to a corrosive action in bacterial consortia located within biofilm thickness (Videla and Herrera, 2009)

2.1.2. Characteristics of Bacteria Related to MIC

The presence of microorganisms alone in a system does not necessarily indicate propensity for corrosion development. Some literature suggests that bacteria and fungi are of particular interest for MIC (Little, 2014). However, environmental parameters are important to sustain the microbiological activities. The type of bacteria can determine specific nutrient and environmental requirements.

There is a wide variability in microbiological organisms involved in MIC. The role of these microorganisms can vary significantly depending on environmental conditions that support their proliferation and therefore, degradation mechanisms can be complex. Also, the type of bacteria can determine specific nutrient and environmental requirements. In 1999, Gaylarde and Beech classified the types of organisms (related to corrosion failures of materials) into: sulfate-reducing bacteria (SRB), iron-oxidizing/reducing bacteria (IOB or IRB), manganese oxidizing bacteria, sulfur-oxidizing bacteria (SOB), and bacteria that secret organic acids and extracellular polymeric substances (EPS) or slime. In 2012, Rim-Rukeh reported that steel coupons corroded microbiologically at a rate of 0.79 mpy after 6920 hours of test periods. Total bacteria population varied from 10^5 CFU/mL to 10^6 CFU/mL in all water samples analyzed, indicating adequate bacterial population for microbiologically influence corrosion activity. It has been suggested that SRB level of 10^4 cell/cm^3 is a clear indication of possible corrosion problems, while a relative population of 10^6 cell/cm^3 of microorganisms indicate potential corrosion problems in an environment (Costello, 1969).

2.1.2.1. Sulfate-reducing Bacteria (SRB)

SRB are the organisms mostly identified with MIC (Hu, 2004; Little, 2009). SRB can exist in both marine and fresh water environments. A marine strain of SRB can gradually be converted to fresh water organism if the transition from salt water to a fresh water environment is not too abrupt (Donham, 1976). They are non-fermentative anaerobes that obtain their energy for growth from the oxidation of organic substances and using inorganic sulfur oxy-acids (sulfate) or nitrate as terminal electron acceptors, and reducing sulfate to sulfide/hydrogen sulfide (Feio *et al*., 2000). SRB include all unicellular bacteria that can reduce sulfate to sulfide. The sessile SRB are responsible for localized corrosion of mild steel in industrial and aquatic environments (Hu, 2004; Costerton and Boivin, 1991). Several corrosion mechanisms have been attributed to SRB, including cathodic depolarization by the enzyme dehydrogenase, anodic depolarization, release of exopolymers capable of binding metal ions, stress corrosion cracking, hydrogen induced cracking or blistering, and production of metal sulfides. Recent reviews suggest that SRB can influence a number of corrosion mechanisms simultaneously (Little, 2009).

SRB can grow in conditions within pH range from ~5.0 to 10.0 and temperature from 5°C to 50°C. The best temperature ranges from 25°C to 40°C (Javaherdashi, 1999). Also, they can tolerate pressure up to 500 atmospheres (Narayan, 2012). The corrosion process by SRB bacteria is characterized by the formation of black crusts and metal pitting (Donham, 1976). The general energy limitation for the growth of SRB bacteria is the carbon source, but in many systems with mixed population of organism, the carbon source is not restrictive, and the limitation is sulfate ions. The carbon source for SRB are always low molecular weight compound such as organic acids (lactate, pyruvate, formate), volatile acids (acetate), and alcohols (ethanol, propanol, methanol, and butanol) (Hao *et al.*, 1996). SRB needs a supply of sulfates for reduction to sulfides for their metabolism.

The counts obtained from water sampling are usually only an approximate indication of the actual bacterial population in the system (Donham, 1976). As SRB can be found in rich sulfate environment (Yuzwa, 1991), the sulfate concentration in a system has a direct influence on the growth and activity of SRB and the amount of sulfide produced (Sanders, 1988). It was found that the initiation of biocorrosion due to SRB only occurred in the presence of sulfate species. As such, the metabolic activity of SRB that causes accumulation of sulfide near metal surfaces can be evidence of potential SRB presence in the system(Little, 2009). Determination of total sulfide as H_2S, HS^-, S^{2-} , in water samples can be used to identify SRB activity (Melchers 2007). Also, Blackburn, 2004 pointed out that the presence of black color and odorous iron sulfide corrosion product (associated with orange bloom) can be a good indicator for MIC by SRB (Blackburn, 2004).

Fonseca *et al*., 1998 tested the corrosion of mild steel under different media both with and without sulfate ions. The corrosion current density showed an enhancement due to the SRB presence in the lactate/sulfate medium. On the other hand, Castaneda *et al*., (2008), characterized the electrochemical evolution of the interface formed in carbon steel samples exposed to artificial seawater with nutrients, in the presence and absence of mixed cultures that contained SRB. The anodic dissolution of carbon steel was the dominant process under the abiotic system over time, while the oxygen diffusion limited the corrosion process in the presence of SRB. Phosphorus-based corrosion products were detected in both systems; however, under SRB-biofilm presence the sulfides were also evident. Mohanty *et al.* (2000) also found that a high sulfate concentration in the medium could inhibit the sulfate reduction rate of SRB. SRB showed positive growth rate with the increase of biomass and N_2 concentration. In addition, the increase of sulfate and phosphate concentration decreased the bacterial growth.

The relationship between SRB and oxygen is complicated and will influence the corrosion process. The anaerobic bacteria may survive with temporarily exposure to oxygen and become active under anaerobic conditions. However, some genera can still grow at low dissolved oxygen concentrations (Hu, 2004; Hardy and Hamilton, 1981; Abdollahi et al., 1990). Although the oxygen content of seawater is in the range from 5 to 8 ppm, anaerobic microorganisms may survive in anaerobic micro-niches until conditions are suitable for their growth (Little, 2009). If the aerobic respiration rate within a biofilm is greater than the oxygen diffusion rate, the metal-biofilm interface can become anaerobic and provide a niche for sulfide

production by SRB (Hamilton, 1985). The critical biofilm thickness required to produce anaerobic conditions depends on availability of oxygen and the respiration rates of organisms in the biofilm. In 2002, Iversen noted that the critical DO concentration for sulfate reduction in wastewater plants was 0.1 to 1 mg/L. It was also mentioned that above a DO concentration of 1 m/L, sulfate reduction might be inhibited because of increase redox potential and inhibition of *Desulfovibrio*. Hamilton (2003), reported on anaerobic corrosion of carbon steel by SRB and concluded that oxygen was required for aggressive SRB-influenced corrosion. In corrosion of mild steel by SRB, oxygen is the ultimate electron acceptor through a series of coupled redox reactions. The interaction of SRB with corrosion process is represented in the following reactions (Borenstein,1994):

$4\ Fe \rightarrow 4\ Fe^{2+} + 8\ e^-$	(anodic reaction)	(2-1)
$8\ H^+ + 8\ e^- \rightarrow 8\ H$	(cathodic reaction)	(2-2)
$SO_4^{2-} + 8\ H \rightarrow S^{2-} + 4H_2O$	(cathodic depolarization by SRB)	(2-3)
$8\ H_2O \rightarrow 8\ OH^- + 8\ H^+$	(dissociation of water)	(2-4)
$2\ H^+ + S^{2-} \rightarrow H_2S$	(reversible reaction)	(2-5)
$Fe^{2+} + S^{2-} \rightarrow FeS$	(anode corrosion product)	(2-6)
$3\ Fe^{2+} + 6\ (OH)^- \rightarrow 3\ Fe(OH)_2$	(anode corrosion product)	(2-7)

2.1.2.2. Metal-reducing Bacteria (MRB)

As early as 1980, it was shown that corrosion reactions of metals can be affected by a variety of types of bacteria, such as *Pseudomonas* and *Shewanella,* which can carry out manganese and/or iron oxide reduction (Obuekwe *et al*., 1981; Myers and Nealson, 1988). While Mn (manganese) is soluble, all the various manganic (Mn^{2+}) oxidized forms are insoluble. Microbial deposits of manganese oxide on stainless steel samples exposed to freshwater have caused an increase in the corrosion potential (E_{corr}) and in the cathodic current density (Little, 2009; Dickinson, 1996).

Iron-reducing bacteria (IRB) are another group of microorganisms, which are of interest in MIC. This type of bacteria at near neutral pH, use insoluble ferric iron ion (Fe^{3+}) compounds as an energy source, reducing them into soluble ferrous ion (Fe^{2+}) compounds, exposing the metal beneath a ferric oxide protective layer to the corrosive environment (Javaherdashti, 2008). By dissolving the corrosion resistant oxide films or the protective films. In some cases the result is the formation of dense tubercles of filamentous iron oxides.

Some IRB species require ferric iron under anaerobic condition and some use nitrate for anaerobic respiration. Myers and Nealson, 1988 reported that IRB can use oxygen, Fe (III), Mn (IV), NO^{3-}, NO^{2-}, $S_2O_3^{2-}$, SO_3^{2-} and others. In a mixed population of microorganism in a biofilm, the redox potential start to decrease as oxygen is consumed so that reduction of nitrate, then manganic, ferric and sulfate ions can occur (Javaherdashti, 2016). IRB are capable of making the environment suitable for SRB growth. Authors have investigated steel corrosion influenced by anaerobic biofilm in natural seawater where SRB and IRB bacteria have been detected in the anaerobic biofilm under the rust layer on carbon steel. SRB was located in the inner rust layer

and IRB in middle and outer layer. Green rust has been the main component in the inner rust layer, and both SRB and IRB have affected the formation of green rust. The isolated SRB have accelerated corrosion and the mixed anaerobic bacteria (SRB and IRB) have inhibited corrosion. The main mechanism of corrosion inhibition is the biofilm-induced formation of green rust (Duan, 2008).

2.1.2.3. Slime-producing Bacteria (SPB)

Slime-producing microorganisms are also associated with localized attacks of steels (Hu, 2004). These organisms produce large quantities of extracellular polymeric substances (EPS) during their growth within biofilms and covered the steel surfaces. Most common SPB are including *Clostridium* spp*., Flavobacterium* spp*., Bacillus* spp*., Desulfovibrio* spp*., Desulfotomaculum* spp*.* and *Pseudomonas* spp*.* (Pope *et al*., 1984). The sticky polymers they produce referred to as "slime" affect the attachment of the cells to the surface and the permeation of substances through the deposit.

Microscopic amounts of EPS (10 ng/cm^2) can induce or provoke the initiation of microbial corrosion of stainless steels in natural seawater (Hu, 2004). The mechanisms of the EPS in the MIC of stainless steels are still not very clear.

2.1.2.4. Acid-producing Bacteria (APB)

These bacteria can produce large amounts of inorganic or organic acids as by- products during their metabolism, leading to serious corrosion damages. Heterotrophic organic acid produced is referred to as acid producing bacteria (APB). These bacteria have shown to cause the corrosion of carbon steel in some cases (Hu, 2004; Soracco et al., 1988; Little et al. 1988), also the corrosion of cathodically protected stainless steel was reported with certain acetic-producing bacteria. The mechanism of how acids affects the corrosion of mild steel was well understood in the metallurgical literature (Shreir, 1963). The kinds and amounts of acids produced depend on the type of microorganisms and the available substrate molecules. Inorganic acid-producing bacteria can oxidize elemental sulfur, thiosulfates, metal sulfides and H_2S to sulfuric acid (corrosive). These microorganisms are generically referred to as *thiobacilli* or sulfur oxidizing bacteria (SOB). The color of the corrosion products is reported to be yellow (Scott, 2004; Hu, 2004).

2.1.3. MIC Diagnosis

Diagnosing and evaluation of MIC requires a combination of microbiological, metallurgical, and chemical analyses. The first step in the diagnosis is to identify relevant microorganisms in the bulk medium (planktonic cells) or associated with corrosion products (sessile cells), as well as information about pit morphology consistent with an MIC mechanism (Little and Lee, 2009). To identify the microorganisms in each particular environment is very important for the understanding of the MIC mechanism. The microorganisms can be classified based on the corrosion product chemistry. The next step is to identify the chemical/physical characteristics of

the environment, which supports the growth and activity of bacteria. The chemical composition of the water must have sufficient specific nutrients and the physical properties of the site must comply with attachment of these organism. Different conditions supporting MIC will be explained in the following section.

2.1.3.1. Chemical and Environmental Factors

The chemical effect and features of the environment include those of the metallic substrate (the existence and/or absence of some alloying elements than can encourage the growth/attachment of the bacteria) and those of the bulk water. The chemical aspects related to the bulk water are the water temperature, the water nutrients, anions (sulfate, chloride), cations/metal, pH, the oxygen concentration, the alkalinity, dissolved gases (carbon dioxide, hydrogen sulfide, oxygen), TOC (total organic carbon), the turbidity, the conductivity, the redox potential, as well as TDS (total dissolved solid) and TSS (total suspended solid) content. Redox potential (Eh) of water samples is also another important factor in MIC. Rim-Rukeh, 2012 reported Eh values of studied water samples, which ranged from -450 mV to +850mV. The negative side of the spectrum favors methanogenic bacteria and the positive one correspond to iron bacteria (Newman *et al.*, 1991). Negative Eh values obtained are indicative of corrosive environments.

All these parameters are important factors for the MIC (Javaherdashti, 2008). The chemical oxygen demand (COD) is considered a very useful parameter which allows to know the concentration of electron donors available for sulfate or metal reduction, so that low COD would mean a low risk of availability of SRB or other types of reducers such as IRB (Scott *et al*., 2004). Beech, 2008 confirmed that Biochemical Oxygen Demand (BOD) and COD values were the highest where high levels of sulfur-oxidizing bacteria (SOB) were detected.
Rim-Rukeh, 2012 studied the physico-chemical and biological characteristics of a River, in order to identify MIC of the steel exposed to this natural freshwater environment. Reported turbidity values of water samples were high and within the range of 18 NTU to 31 NTU. Also, TDS and TOC values in all water samples analyzed ranged from 1908 mg/L to 2571 mg/l, and 11.7 -17.1 mg/L, respectively. The relatively high values of turbidity may be the result of both suspended and dissolved solids in the water, such as silt, finely divided organic and inorganic matters and soluble colored organic compound or erosion of sediments (Rim-Rukeh, 2012). These materials are potential sources of organic carbon, which constitute the bacteria energy source for production of new cellular material. Carbon is the most abundant cell constituent and can be obtained from organic matter (Videla, 1996). High level of turbidity promotes growth of microorganism within ecosystem (Characklis, 2009, Rim-Rukeh, 2012). The existence of halophilic (salt loving) SRB in waters with very high TDS (240,000 mg/L) has been reported (Alhashem *et al*., 2004). TDS and TOC results will determine the presence of decaying organic matter (leaves). High levels of TDS and TOC provide an excellent condition for bacteria growth (Rim-Rukeh, 2012). As one of the studies by Melchers, 2005 shows the nutrient level and chemical condition of water with pH ~8, conductivity ~47000(µS/cm), Nitrate ~0.01 mg/L Sulfate ~3000 was indicative of condition which support the high corrosion activity by microorganism.

2.1.3.1.a Nutrient Level

The availability of nutrients and water are essential for survival of microorganisms, it is also an important factor in determining whether the bacterial population will be planktonic or sessile. This would affect the spatial position of bacteria and its ability to attach to surfaces perhaps in biofilm. When the environment is poor in nutrient level, the bacteria may settle on surfaces. In contrast, in rich nutrient environments, bacteria do not need to necessarily settle, so planktonic grow (floating) takes place (Gandy, A. F. and Gandy, E. T., 1980,Enos andTaylor, 1996).

Microorganism need energy, carbon sources, nitrogen, phosphorus and trace elements to survive and grow (Thierry and Sand, 2011). Gandy, 1980 has pointed out that carbon, nitrogen, oxygen and hydrogen constitutes 90% of the dry weight of a cell. From them, hydrogen and oxygen comes from the water used by the cell, while carbon, oxygen and nitrogen are the limiting nutrition requirements of the cell (Gandy, 1980).

The water needs to have suitable forms of carbon, hydrogen, oxygen, sulfur, phosphorus, potassium, magnesium, calcium, manganese, nitrogen and traces of zinc, cobalt, etc. (Mansfeld, 2007; Little, 2014). Lin and Madida in 2015 studied the role of gram positive Bacillus sp in corrosion of steel by biofilm formation. Three nutrient media were chosen including, carbon source (fructose, galactose, or sucrose), $MgSO_4$ and nitrate source (NH_4NO_3 or $NaNO_3$). The results showed different corrosion loss in each media and corrosion retardation in media without any nutrients. Adding different nutrients could trigger different metabolic pathways resulting in acceleration or mitigation of the corrosion rates, which are strongly correlated to the level of biofilm formation by the microorganisms.

Carbon occurs in the biosphere in either the reduced (methane, fatty acid, carbohydrate) or the oxidized (alcohol, aldehyde, carbonic acid, carbon dioxide) form. Microorganisms control the carbon cycle by using CO_2 from the air for their cell carbon generation. Primary producers such as green plants, algae, cyanobacteria, and photosynthetic bacteria are responsible for this reaction(Thierry and Sand, 2011). The generated carbon cell will be degraded by other organisms with the production of carbon dioxide. Another possibility is the incomplete degradation happening in sediment, which causes high accumulations of organic matter in shallow marine areas (Thierry and Sand, 2011).

Nitrogen can be in the form of inorganic ammonium, nitrate, nitrite, and also originally bound nitrogen such as amino acid, which can be find in many compounds such as proteins, nucleic acids, amines, and urea (Thierry and Sand, 2011). Some microorganisms like bacteria and cyanobacteria can use nitrogen from the atmosphere (with the help of an enzyme called nitrogenase) and produce ammonia, which is incorporated in cell constituents. When cell constituents are degraded, ammonia is liberated and may be used for the synthesis of other nitrogenous compounds or become available for the process called nitrification. Nitrifying bacteria oxidize ammonia via nitrites to nitrate. The nitrifying bacteria consist of two groups: the

ammonia oxidizers, which are responsible for the oxidation of ammonia to nitrite, and the nitrite oxidizers, which are responsible for converting nitrite to nitrate (acidification). Nitrate may act as electron acceptors and be reduced to nitrite, NO, N_2O, and finally N_2 (Baumgärtner, 1990). Dissolved inorganic nitrogen (DIN) has been proposed to be important for MIC (Melchers, 2014; Melcher and Jeffrey, 2013). Recent studies by Melchers have evaluated experimental data from several marine sites in the world, in order to quantify the effect of DIN on long-term seawater immersion corrosion loss of structural steels. Results have shown that DIN concentrations from 0.01 mg/L to 0.4 mg/L (in sea and brackish waters) seem to have influence in the MIC of steel piling below the water tide for all sea water temperatures studied (Melcher and Jeffrey, 2013). For aerated seawaters, the major component of DIN is nitrate, since nitrites and ammonia rapidly oxidize to nitrate (Little, 2007).

Phosphorus are typically available in waters as inorganic phosphates and orthophosphates or as (organically bound) phosphorylated compounds such as phosphorus-containing sugars and lipids. Phosphate plays an important role as main energy storage in biological life as a backbone of DNA and RNA, and as an important component of Adenosine Triphosphate (ATP) (Thierry and Sand, 2011). Phosphate has been implicated in the accelerated corrosion of steel under pure bacterial culture laboratory conditions (Odom, 1993).

Sulfur is presented in the biosphere in many compounds and it is essential for the formation of the sulfurylated amino acids, methionine and cysteine/cystine. Other important compounds are those containing reactive thiol (organosulfur compound that contains a carbon-bonded sulfhydryl or sulphydryl) groups; such as coenzyme A or iron-sulfur redox centers involved in electron transfer reactions (Thierry and Sand, 2011). The most important sources are deposits of metal sulfide and sulfur. Metal sulfides can be attacked and degraded microbiologically by the action of specialized bacteria, which oxidize the metal sulfide to a metal sulfate (Schippers *et al.*, 1999). This is accompanied by sulfuric acid production, which keeps the metal ions solubilized. The microorganisms active in this process tolerate high heavy metal concentrations (up to several grams per liter) and low pH values (pH 1.5 and below). They may grow at temperatures from 4°C up to 90°C.

Once sulfate has been produced, a process similar to denitrification may take place. If sufficient organic matter is available and anaerobic conditions exist, sulfate will act as an electron acceptor, being reduced to sulfide (Dilling and Cypionka, 1990) by SRB. This is a physiologically diverse group of microorganisms including photosynthetically active bacteria. It contains archaea and bacteria, which are able to live at 110°C by sulfate reduction. If sulfide accumulates, two different pathways are selected depending on the oxygen availability. Under aerobic conditions, oxidation to sulfate occurs. Under anaerobic conditions in the light, photosynthetic microorganisms oxidize sulfide to sulfur and sulfate using the electrons liberated to fill up their photosynthetic system. Without light, sulfide oxidation coupled to nitrate reduction can take place. Thus, biologically, sulfur and its compounds may be oxidized and reduced by many reactions. Deposits of sulfur compounds resulting from this activity may include elemental sulfur, metal sulfides, and sulfate-like barites (Thierry and Sand, 2011).

Trace elements are needed for many metabolic purposes. They constitute only a negligible amount of the total cell weight, but they support vital functions. Iron as Fe^{2+} or Fe^{3+} is necessary for the electron transport system. It functions as an oxidizable/reducible central atom in cytochromes or in non-heme iron–sulfur proteins. Magnesium plays a role in the chlorophyll molecule. Cobalt functions in the transfer of methyl groups from/to organic or inorganic molecules (vitamin B_{12}-cobalamine- involved in the methylation of heavy metals such as Hg). Copper is an integral part of a cytochrome, which at the terminal end of the electron transport system mediates the reduction of oxygen to water (cytochrome oxidase) (Thierry and Sand, 2011).

Oxygen concentration may not always be useful, as biofilms are capable of forming anaerobic patches in aerobic bulk solution. It has been reported that biofilm with thickness of only 12 micrometer may be sufficient to create totally anaerobic regions.

2.1.3.1.b Temperature and pH

Both biological and electrochemical events depend on the pH and temperature at the metal water interface (Dexter,1993). Hydrogen ion concentration is an important factor in microbial growth. Microorganisms may be distinguished by their ability to grow under acidic, neutral, or alkaline conditions. Hence, they are called acidophiles, neutrophiles, or alkaliphiles (Thierry and Sand, 2011). The bacterium *A thiooxidans* has been detected in samples exhibiting a negative pH value, whereas in soda lakes, life has been detected at pH values of 12 and above. Fungi are able to grow over a large range of pH values. Species of *Penicillium* have been found at pH 2 and up to pH 12 (Thierry and Sand, 2011). However, most of the microorganisms live in the neutral pH range from 6 to 8. As Rim-Rukeh (2012), reported, acidic environment with pH<6 and alkaline environment with pH>8 are more corrosive than an environment with pH ranges from 6 to 8 (Bradford, 1993).

Microbial life is possible between −5°C and +114°C and microorganisms can be classified base on the temperature they need, as can be seen in Table 2.1. Most organisms live in the mesophilic range (20°C to 45°C), corresponding to the usual temperature on the surface of the earth. Only a special group of bacteria, called archaea bacteria, are able to grow at elevated temperatures (above 70°C). (Thierry and Sand, 201)

Table 2.1. Microbial Classification Base on Temperature.

Temperature	Microbial classification
−5°C to 20°C	Psychrophiles
5°C to 30°C	Psychotrophs
20°C to 45°C	Mesophiles
55°C to 85°C	Moderate thermophiles
Up to 120°C and Above	Extreme thermophiles

2.1.3.1.c Roughness

Surface roughness influence microbial cell attachment and transport rate by increasing connective mass transport near the surface, providing shelter from shear forces for small particles and increase surface area for attachment. (Characklis, 2009; Flemming *et al.*, 2009). Roughness role in MIC has been studied in the pitting and weight loss of carbon steel coupons due to corrosion by SRB culture. Roughness played an important role on the pitting corrosion. The pit density on the rough unpolished coupon surface was much higher than that on the polished surface (Chen *et al*., 2013).

2.1.3.1.d Hydrodynamics

The physical stability of the biofilm is affected by the fluid flow velocity. Generally, lower fluid flow velocity will not disturb the formation of biofilm and MIC will increase, in part due to the absence of mechanical sheer forces (Stoodley *et al*., 1998; Wen *et al*., 2006; Wen *et al*., 2007; Javaherdashti, 2008). Also, flow rate affects the thickness of the biofilm. In turbulent flow system, wet biofilm thickness rarely exceeds 1.000 mm (Characklis, 2009). Stoodley, 1998 reported that fluid flow can enhance mass transfer, but it may also produce a high shear that inhibits cell attachment and causes even detachment of an established biofilm. Wen, 2006 research showed that the fluid flow rate had a considerable impact on MIC corrosion rates of carbon steels. In 2007, his experimental results in the glass cell inoculated with *D. desulfuricans* indicated, that at 3,000 rpm (roughly equivalent to 3.5 m/s in pipe flow) sessile SRB cells could not adhere on the coupon surface to form an SRB biofilm. The results confirmed that a high linear flow velocity could indeed prevent SRB biofilm formation. Some researchers suggested that stagnant water conditions can provide less severe conditions and do not enhance corrosive attack (Borenstein, 1994).

2.1.4. Accelerated Low Water Corrosion (ALWC) and MIC

Accelerated low water corrosion (ALWC) of carbon steel pilings in estuarine and marine harbors is a phenomenon of great concern. (R. Ray *et al*., 2009; Melchers and Jeffrey, 2013; Beech and Campbell, 2008; Gehrke and Sand, 2003) It is considered a particular aggressive form of localized corrosion, sometimes called “LAT (lowest astronomical tide) corrosion. The British Standard for Marine Structures (BS 6349, 2000) has defined ALWC as a type of low water “concentrated corrosion”, characterized by severe attack leading to premature perforation of steel sheet piling at the low water level (BS 6349 standard, 2000). Even though the actual ALWC mechanism are not yet fully understood and continues being a topic of debate, some authors agree that it is a form of MIC (Beech *et al*., 2001; Melchers and Jeffrey, 2013; Beech and Campbell, 2008; Gehrke and Sand, 2003). SRB and SOB bacteria have been associated with ALWC (Gehrke and Sand, 2003). A three-year investigation of steel pilings in German marine harbors concluded that ALWC took place due to a combination of SRB and *Thiobacillus* bacteria in the fouling layers on the pilings. The contribution of sediment SRB and SOB populations to ALWC attack on the piling steel in a harbor of Southern England have been recently demonstrated (Gehrke and Sand, 2003).

The damages produced by this phenomenon have the potential to cause structural failures of the sheet pilings, failure of docks and quays constructed with steel sheet or other steel piling and may cause severe disruption of port services. The term “Accelerated Low Water Corrosion” is descriptive of the fast corrosion rates reported to be 1.0 mm/year or more, well exceeding typical steel design allowance metal loss of 0.1–0.5 mm/year (Melchers and Jeffrey, 2013). The formation of sulfides and sulfuric acid from the SRB (anaerobic region) and the *Thiobacillus* (aerobic regions), respectively, can produce a very aggressive corrosive environment (Gehrke and Sand, 2003).

Ability to predict whether a particular structure will suffer ALWC and at what stage in the structure’s life the problem can initiate is still a very difficult task. Currently, the only method for detecting ALWC is by visual inspection. Visual inspection have depicted common characteristic of ALWC, such as the presence of poorly adherent thick corrosion products of varying morphology, often seen as large blisters randomly located on sections of the structure at the low water mark. External signs of ALWC are poorly-adherent orange corrosion products over a black “sludge” underlayer covering a bright and extensively pitted steel surface upon the removal of blisters, a bright surface covered with shallow pits was exposed. Both, linear polarization resistance and weight loss measurements have confirmed increased corrosion rates for samples exposed to the electrolytes containing SRB and SOB populations isolated (Beech and Campbell, 2008).

ALWC can take place in tidal waters on inshore and marine steel structures, at or around the low water level, and in clear waters. It will normally influence a small percentage of the surface area on unprotected steel in the low water zone (Beech and Campbell, 2008). A European study documenting corrosion of steel in different harbors identified several factors which could serve as indicators when evaluating ALWC risk in steel pilings (Gubner and Beech, 1999; Moulin *et al*., 2001). The thickness and morphology of corrosion products, the pH values underneath corrosion products, the presence of algae and invertebrates, the organic carbon content, the hydrogen and oxygen levels in fouling layers and the high viable numbers of SOB in corrosion products combined with the presence of SRB were all considered parameters involved in ALWC. It is important to mention that a range of these parameters have differed significantly (i.e. were significantly higher) between ALWC sites and non-affected sites within the same harbor. Also, mean tidal range and total organic carbon of seawater, both showing statistically higher values in harbors experiencing ALWC attack than in unaffected harbors, were identified as useful ALWC risk indicators.

The influence of other parameters in ALWC such as the pollution of the environment, related to MIC, have been mentioned in other studies. There is a substantial body of evidence that the biofilm component contributes to ALWC and that the damages caused in harbor installations represents a form of MIC (Beech *et al*; 2001). Melchers and Jeffrey (Melchers and Jeffrey, 2013) have recently concluded that ALWC of steel piling in sea water harbors in the UK, Europe and elsewhere is the result primarily of anthropological water pollution. Elevated levels of DIN in sea and brackish waters are responsible for MIC of steel piling below the low water

tide level, in accordance with a wide study including field data from 13 Australian experimental sites, 9 US naval sites and some severe sites in Australia, Norway, Japan and the UK (Melchers and Jeffrey, 2013). The highest values of biological oxygen demand (BOD) and chemical oxygen demand (COD) were found at harbor entrances where high levels of SOB were detected in the gravel of the seabed (Beech and Campbell, 2008).

2.2. Biofouling and Corrosion

Any structure placed in natural marine environments is susceptible to physical, chemical and biological events that can result in the accumulation of microorganisms such as bacteria, archaea and macroorganism such as barnacles, macroalgae, mussels, bryozoans and tube worms (Hellio and Yebra, 2009).

It is known that a film of microscopic fouling organisms start forming on structural metals within a few hours of their immersion in natural waters (Dexter, 1993). The sequence of events related to the biofouling process is shown in figure 2.1 (Lehaitre, 2008; Dexter, 1993). The numerous fouling organisms may be divided into micro-organisms (or so-called biofilm, slime, micro-fouling) and macroorganism (or macro-fouling), according to their size (Lehaitre, 2008). Microfouling is defined as a result of adhesion and growth of microorganism at the metal water interface, and macrofouling is due to the attachment of macroorganism. Macrofouling organisms are found at all depths and in all natural bodies of water (Little, 2008).

Biofouling has a negative economic impact in the industry. For the global shipping industry alone, biofouling costs billions of dollars per year in prevention, maintenance, and fuel consumption (Alliance for Coastal Technologies, 2004). In 1999, a report by the naval research laboratory indicated that the use of antifouling paints could save up to 10% of the US Navy's annual fuel bill (Jones-Meehan, 1999). A heavy layer of macroorganisms also have a number of undesirable physical effects on marine structures. The fouling layer will increase both weight and hydrodynamic drag on the structure. Interference with moving parts may also occur (Little, 2008).

In addition to the macrofouling of marine steel structures where damage can result in the loss in tensile strength (Subramanian et al.,2013). Surface fouling also can enhance corrosion (Javaherdashti at al.,2013; VR de Messano et al.,2014), but its effects can be diverse, and studies are relatively limited (Neville,1998; LaQue,1982; Eashwar et al.,1990; Palraj et al.,2002,2003; de Rincon et al.,2003; De Brito,2007; VR. de Messano et al.,2009; Sangeetha et al., 2010; Palanichamy et al.,2014). Non-uniform macrofouling of such organisms may initiate localized corrosion by creating crevice conditions and oxygen concentration cells (Little,2007) as well as producing local changes in pH and anaerobic environments (Pipe,1981; Zhang et al.,1995; Newman et al.,1989; Salvago et al.,1987).Barnacles are considered as the dominant biofoulers and are the primary target of anti-fouling industries and technologies (VR de Messano et al.,2014; De Brito,2007; Eashwar et al.,1992). It has been reported that barnacles must reach to critical size to initiate crevice corrosion (Eashwar et al.,1992; Hodgkiess et al.,1998). It was suggested that the extent of the corrosion under the remnants of barnacles can be more severe

than under the living ones, suggesting that the acidic chemicals produced during the decay of the barnacles can accelerate the corrosion rate (Hodgkiess et al.,1998; Blackwood et al.,2017).

Therefore, both microfouling and macrofouling influence the corrosion process (Javaherdashti, 2013; VR de Messano, 2014). The effects of marine biofilm on corrosion have been well disseminated in the literature. Biofilm creates oxygen heterogeneities and increases mass transport resistance near a metal surface. Also, metabolic reactions in biofilms generate corrosive substances (such as an acid), and other substances that serve as cathodic reactants (Flemming, 2009). However, limit information available on the role of macrofouling and corrosion. (LaQue, 1982; Eashwar *et al.*, 1990; Neville and Hodgkiess, 1998; Palraj *et al.*, 2002; Rincon and Morris, 2003; Palraj and Venkatachari, 2006; de Brito *et al.*, 2007; de Messano *et al.*, 2009; Sangeetha *et al.*, 2010; Palanichamy,2014).

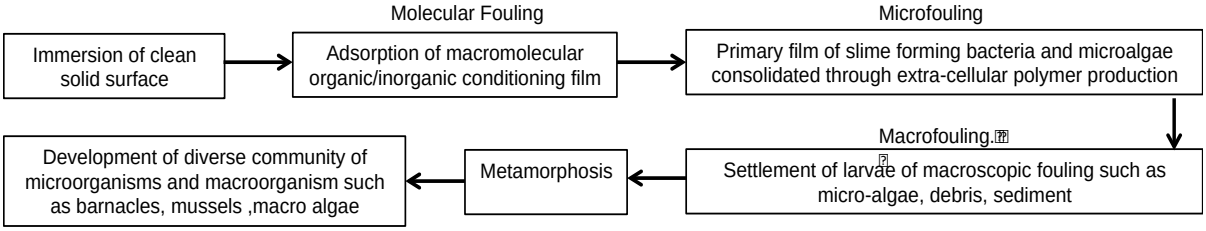

Figure 2.1. Sequence of Events in Marine Biofouling.

2.2.1. Macrofouling Characteristics

Macrofouling can occur by two groups of macroorganisms such as plants (e.g. seaweed) and animals (e.g. barnacles and mussels) (Javaherdashti, 2013), generally classified into “soft ” and “ hard ” fouling as visualized in table 2.2. The hard species present a solid skeleton such as a shell or a calcareous tube (calcareous algae, barnacles, mussels, tubiculous worms), which protects the body within, whereas the soft species have no such protection (sponges, anemones, bryozoa) (Lehaitre, 2008).

The settlement of fouling organisms can be influenced by the surface water temperature, salinity, water motion, and light (Palraj et al.,2006). The literature suggests different mechanisms for marine fouling settlement where some suggest the prerequisite of biofilms (Javaherdashti et al.,2013; Neville et al.,1998; Crisp,1974; Walters et al.,1996; Egan et al.,2002; Keough et al.,1995) while others provide other ideas on larval site selection (Lehaitre et al.,2008;Roberts et al.,1991). Surface roughness influence larval cell attachment and transport rate by increasing connective mass transport near the surface, providing shelter from shear forces and increase surface area for attachment (Flemming et al.,2009; Characklis,2009) as the shape and size of different fouling organisms can be very different: ~1µm for bacteria, 3-15µm for diatoms, and 120-500 µm for macrofouling organisms (Hellio et al.,2009).

Table 2.2. Main Hard and Soft Marine Growths. (Lehaitre, 2008; Clapp, 1948).

Sessile Organisms	
Hard fouling (calcareous or chitinous shells)	**Soft fouling**
Mollusks: Mussel, oysters Barnacle: which built cone-shaped shells built up of laminated plates Corals Annelids :which form coiled or twisted tubes like tubeworm Encrusting sponge and Bryozoa : colonial animals which form flat, spreading, multi-cellular	Seaweed Coelenterates or Hydroid such as “Tubularia” with stalk-like or branching growths, each branch terminating in an expanded tip; also “Bougainvillia” And “Campanularia” Marine algae : “Ceramium”, “Fucus” “Polysiphonia” ,“Ulva” Soft coral Calcareous and siliceous Sponge Sea Anemone

Larvae exhibit different settlement behaviors in response to flow, pressure, light, surface texture and color (Roberts *et al.*, 1991). The effect of the surface texture was evaluated trough laboratory tests in the presence of *Balanus improvisus* cyprids macrofouler. Results concluded that this macrofouler attached in much higher numbers to the control polystyrene than to control glass surfaces (O'Connor, 1996). A hard, smooth surface generally provides a more secure footing for fouling organisms than a soft material. Fouling organisms must become attached to some base which is stable with no motion. Many of the fouling organisms are affected by light, that’s why most of them settle on shaded, or dark surfaces. On the other hand, the heaviest fouling is generally found on the northern side of stationary objects in the northern hemispheres. This is true for mussels, hydroids, and many of the algae. Corrosion products also have an effect on these organisms settling. When corrosion products form very quickly (on ordinary steel) and the character of the surface is changed; the organisms are fastened not to the metal, but to the surface of the film of corrosion products.

The growth of macroorganism can enlarge the corrosion spot on either cementitious material or steel. If the fouling is equally adherent to a metal over the entire area, this may protect the steel against corrosion. If the surface is uneven, and water penetrates, there will be different oxygen concentrations at points under the fouling and elsewhere on the surface of the metal. Oxygen concentrations cells may then accelerate corrosion. While these macroorganism grow and expand through the surface, they can cover smaller organism. The covered organism quickly dies, and degeneration sets in, followed by the production of hydrogen sulfide, which can promote accelerated corrosion. Table 2.3 provides further information on the macrofoulers relating to life cycle, nutrient, reproduction, metamorphosis and settlement process

Table 2.3. Life Cycle, Reproduction Type, Food and Metamorphosis/Settlement of Macrofoulers Identified During Field Testings. (1. Fofonoff *et al*.,2003; 2010 ; 3.Bouillon et al.,2003; 4.Linda Z,2016 ; 5.Fritsch,2009 ; 6.Hellio,2009 ; 7.Thiyagarajan,2010).

Suspicious macrofouler/ Sites	Life cycle	Reproduction type	Food	Metamorphosis/ settlement
Colonial tunicates (site1)/ [1-2,4]	1, Fertilized eggs are brooded within the tunic 2, Hatching into lecithotrophic(non-feeding, yolk-dependent) tadpole larvae with muscular tail, a notochord, eyespots, and a set of adhesive papillae 3, Being expelled upon hatching and swim briefly before settlement	1, Asexually by budding 2, Sexually from fertilized eggs	Phytoplankton & other small particles	1, Larva swims for a few days until find a suitable substratum and attaches by anterior adhesive papillae 2, Larva tail is resorbed 3, After settlement, larva completes metamorphosis into a juvenile, with incurrent and excurrent siphons and two gill slits.
Hydroids (Site1)/ [2-3]	1, Reproductive polyps bud off medusas 2, After medusas mature, Eggs are released and fertilized by sperm, and then planula larva settles and metamorphoses to juvenile polyp 3, Asexual budding of hydranths contributes to colony formation and growth	1, Asexually by budding 2, Sexually from fertilized eggs		1, Planula larva settles and metamorphoses into polyp stage 2, Polyp liberates a gamete-producing male or female medusa 3, On hard substrates, solitary hydroids have a basal disc fixing them to their substrates; on soft substrates, hydroids have a pointed base and filamentous rootlets.
Barnacle (Site3&4)/ [2,6-7]	1, Nauplius stage 2, Cyprid stage 3, Adult Stage	Sexual	Small organic particles, plankton (phytoplankton and zooplankton), microscopic plants, and animal	1, Energy reserve during nauplius stages 2, During cyprid stage, cyprids using their pair of sensory antennules explore and attach to suitable substrates, and then they metamorphose into adult
Algae (Site3&4)/[5-6]	Type 1, haplontic life cycle Type 2, diplontic life cycle Type 3, three multicellular phases	1, Vegetative 2, Asexual 3, Sexual		Microalgae 1) Location of the surface;2) Initial contact; 3) Secondary adhesion Macroalgae 1) pelagic phase 2) benthic phase

2.2.2. Macrofouling and Biofilm

There is uncertainty about g how adhesion of settling invertebrates is influenced by microbial films. Generally, biofilm formation is an important factor in macrofouling (Neville and Hodgkiess, 1998). When a biofilm is formed, it becomes a suitable environment to allow the mussels and barnacles (larvae) to attach themselves onto it. These larvae then use this opportunity for growing and transforming into adults (Javaherdashti, 2013). It was shown in the literatures, that water soluble pigments (serve as positive or negative cues) produced by biofilms provide chemical and physical conditions to support larval settlement and metamorphosis (Walters *et al*., 1996; Egan *et al*., 2002). Also, the composition of microbial communities on surfaces strongly influences the rates of larval settlement of some invertebrate species (Keough and Raimondi, 1995). Therefore, biofilm often have the determining role in initiating macrofouling for some macroorganisms and any factor supporting the biofilm formation can also be related to macrofouling.

Contrarily, some marine invertebrate larvae can settle on clean surfaces (Crisp and Ryland 1960). Settling condition of a wide variety of macroorganism has been investigated by different researchers. According to available data, some macroorganism do not necessarily need the presence of a biofilm on a surface to settle (Roberts *et al*., 1991; Lehaitre, 2008). However, most of studies have concluded that the settlement of many larval species on hard surfaces is enhanced by the presence of biofilm (of certain individual bacterial isolates) (Crisp 1974).

Biofilms can also modify physical surface properties such as wettability or texture, which are important to settling larvae. The presence of a thick and slimy organic layer, underlying the relatively small attachment organs of settling larvae, would be expected to inhibit the ability of larvae to adhere tightly to a substratum (Zardus, 2008). Overall, surface-associated bacteria have important influences over the settlement of many invertebrate larvae. Bacteria may stimulate, inhibit or not affect the settlement of invertebrate larvae (Lau, 2002; Brancato & Woollacott, 1982). In 1988, Maki studied the effects of marine bacteria on the attachment of cyprid larvae of the barnacle *Balanus Amphitrite.* The author reported that most of bacteria either inhibited or did not influence on larval attachment compared to clean surfaces. Hence, larval settlement will depend on the species of invertebrates and bacteria of concern. In summary, bacterial biofilms have been found to be important in the settlement process of representatives of most marine invertebrate groups including sponges, tubeworms, cnidarians, annelids, echinoderms, phoronids, bryozoans, ascidians, and algae (Unabia and Hadfield,1999; O'Connor and Richardson,1998; Lau *et al*., 2002)

O'Connor (1996), investigation showed that barnacle settlement was different from bryozoans. Barnacles were settled in control condition and the higher numbers of settlement were observed in presence of bacterial cells. However, in the case of bryozoans, negligible number were succeed to settle in control condition.

On the other hand, Zardus, 2008 tested four species of common marine fouling organisms (a polychaete worm, an ascidian, a barnacle, and a bryozoan), which differed according to their responsiveness to biofilms at settlement. Larvae of four species of biofouling invertebrate were allowed to attach to tested surfaces that were either clean or coated with a natural biofilm. Measuring larval removal under precisely controlled flow forces, indicated that biofilms significantly increased adhesion strength in the ascidian *Phallusia nigra,* the polychaete tubeworm *Hydroides elegans,* and the barnacle *Balanus amphitrite,* at one or more developmental stages. In addition, the attachment strength in the bryozoan *Bugula neritina,* was neither facilitated nor inhibited by the presence of a biofilm. These results suggest that adhesive strength and perhaps composition may vary across different invertebrate taxa at various recruitment stages and mark a new path of inquiry for biofouling research.

Several authors have suggested that the effect of surface-associated bacterial communities on larval settlement is a function of bacterial species composition (Keough & Raimondi 1996, Lau & Qian 1997). Lau, 2002 has studied the effect of different bacterial strains (isolated from marine biofilms) on the settlement of the tubeworm Hydroides elegans. Results showed 20% settlement for clean surfaces, over 60% settlement for natural biofilm condition (bacterial strains of different species) and 0 to 60 % settlement for different bacterial strains isolated from marine biofilms.

Unabia, 1999 studied the role of bacteria in larval settlement and metamorphosis of the polychaete Hydroides elegans. His investigation showed that the settlement of Hydroides was prompted by specific bacteria up to 60%. However, one bacteria strain showed settlement less than 20%. As high as 80% settlement was achieved on multi-strain water-table biofilm. Hydroides was also succeeded to grow (settlement ~20%) on the clean surface without presence of bacteria.

2.2.3. Macroorganism and Biocorrosion

The role of macrofoulers in marine environment is unclear. There are some studies showing inhibition or acceleration of corrosion, resulting from marine biological activity. A heavy deposit of macrofouling organisms on structural steel immersed in seawater will often decrease the corrosion rate of the steel, as long as the cover of organisms remains complete and relatively uniform (Little, 2008). The heavy fouling layer acts as a barrier, limiting the dissolved oxygen at the metal surface. A layer of hard-shelled organisms (barnacles or mussels) on steel in the splash zone also shields the metal from the damaging effect of wave action. If fouling layers are incomplete, the fouling is more likely to cause initiation of localized corrosion by creating oxygen concentration cells. A report prepared by the Electric Power Research Institute (EPRI) noted that more than 75% of condenser loss in fossil-fueled power plants (with a capacity of more than 600 MW) is due to biological factors, of which 30% were due to macrofouling. This research indicates that barnacles are indeed capable of inducing localized corrosion (De Brito, 2007).

A scatter of individual barnacles on a stainless-steel surface can create oxygen concentration cells. The portion of the metal surface covered by the barnacle shell is shielded from dissolved oxygen in the water and thus becomes the anode. The result is crevice corrosion under the base of the barnacle (Little, 2008).

Most researchers agree that Balanoid barnacle growth is a primary cause of biocorrosion, especially on passive alloys (VR de Messano, 2014). VR de Messano (2014), has studied the effect of *amphibalanus amphitrite* barnacle on the corrosion behavior of three stainless steels. Open Circuit Potential (OCP) measurements demonstrated the stainless-steel corrosion by these organisms and the crevice corrosion caused by the lack of oxygen around the base of the barnacles (detected during visual inspections), despite the small size of the barnacles and the short duration of the experiments.

De Brito (2007), has conducted field experiment to evaluate the influence of macrofouling on the corrosion of carbon steel panels over a 6-month period. Three treatment conditions were applied, including a ‘Control’ treatment (absence of macrofouling), a ‘Community’ treatment (in presence of macroalgae, barnacles, hydroids and encrusting bryozoans) and a ‘Barnacle’ treatment. In the 'Control’ treatment the corrosion (uniform) rate was higher than other cases, indicating that the presence of macrofoulers provides a protection against mass loss. On the other hand, the highest percentages of localized attacks were found in the ‘Community’ and the ‘Barnacle’ treatments, showing that not only barnacles, but also other organisms induce localized corrosion.

Eashwar (1990), also investigated the role of marine fouling (algae and barnacles) on the corrosion process of the steel in the coastal water of India. As it was shown, higher corrosion rate of steel was observed in presence on heavy algae, which was accelerated during certain season. In the case of barnacles, lower corrosion rate of steel was visualized in comparison with the absence of any macroorganism and they found to be effective in inhibiting the corrosion of steel. However, stainless steel was heavily attacked by barnacles, leading to sever pitting and crevice corrosion. Marine grown life was found to affect significantly the performance of the cathodically protected steel. In 1992, Eashwar et al., investigate the mechanism of barnacle induce crevice corrosion in stainless steel. Based on his result, corrosion would occur only under dead barnacles (flesh remained inside the shell). Aerobic microorganism and oxygen must present to initiate crevice corrosion at barnacle sites. At first the decomposition of organic matter (barnacle flesh) start the acid production, which is associate with sulfur oxidizing bacteria (SOB). Corrosion cell establish between crevice area and exposed surface of stainless steel to the sub stream, followed by crevice corrosion starting from the edges and propagate inward and possibly creating a deep pit at the center in anaerobic condition.

2.3. MIC and Fouling Remediation

Generally coating and cathodic protection have been employed to protect against MIC. In the following the application of antifouling and polyurea coating and use of sacrificial zinc anode in MIC and fouling suspected environment has been investigated.

2.3.1. Coating Application

Coatings have been developed to prevent MIC in biologically active environments (Al-Darbi et al.,2002; Jack et al.,1998; Jones et al.,1992), however the long-term durability of the coatings can be affected by many factors including microbial activity. Certain bacteria are preferentially attracted to iron corrosion products and colonize in scratches and holiday coating defects allowing for localized corrosion (Mansfield et al.,1998). Furthermore, studies have shown that coating blistering and disbondment can occur as a result of microbial attack due to the production of metabolites that degrade coating chemical and physical properties (Muntasser et al.,2002).

Antifouling coatings have a long history and has an important impact on managing macrofouling (Wells et la.,2009; Yebra et al.,2004; Brady, 2005; Chambers et la.,2006). Antifouling coatings with biocides have been traditionally employed for fouling control for organisms such as bacteria, fungi, algae, plants and molluscs (Videla et la.,2005). Antifouling coatings utilizing copper as a biocide have been widely used for the last 200 years; however, due the concerns about their negative environmental impacts, biocides are subject to regulatory restrictions (Trejo et la.,2008; Wei et al.,2010). Polyurea coatings have garnered interest in industry due to some of their advantageous properties. Polyurea a has short curing time, excellent adhesion strength, chemical resistance (to mild hydrogen sulfide concentrations, carbon dioxide and sulfuric acid) and corrosion resistance which makes it a favorable candidate for wet environments (Broekaert et la., ,2002) Polyurea coatings have been used for corrosion mitigation for steel and concrete in wastewater infrastructure, water pipelines, marine structures, fuel storage tanks and fuel pipelines.

2.3.2. Cathodic Protection

Cathodic protection can be afforded on steel structures submerged in natural waters, but complications arise in the presence of microbial influenced corrosion (MIC) and marine fouling organisms. The current demand for cathodic protection depends on the chemical changes in the environment (e.g. oxygen concentration, pH and temperature) as well as physical and chemical characteristic of the metal surface (e.g.corrosion products, calcareous deposits, and biofilms (Little 1993).

Reported research described the negative role of microorganisms on cathodic protection (Little 1993; Olivares et la.,2003). Cathodic polarization to -850 mV_{CSE} has been reported to be inadequate in presence of MIC and levels more active than -950 mV_{CSE} have been suggested (Horvath et la.,1964; Barlo and Berry ,1984; Fischer,1981; Jack et al.,1996). However there remains uncertainty about the effectiveness of this value in presence of SRB. Olivares, 2003

reported polarization as negative as ~-925 mV_{CSE} led to lower corrosion rates and reduced mass loss, but SRB population was shown to continue to proliferate due to an electrostatic attraction between the bacteria and the electric charges created by cathodic protection as well as a supporting role of calcareous deposits that contained sulfates (Olivares, et al.,2003). Although total mass loss was reduced, the proliferation of SRB may still allow some level of localized corrosion to develop. Later studies by Olivares showed that -950 mV_{CSE} was not enough to control the MIC and localized corrosion developed (Olivares, et al.,2006). Research by de Romero, 2006 and 2008 showed that polarization up to -950 mV_{CSE} in laboratory and field conditions was not sufficient to prevent corrosion development and sessile bacterial growth remained high in conditions up to -1.3 V_{CSE} (de Romero, 2006;2008).

There are different views on how these microorganisms affect the cathodic protection efficiency. Bacteria may have an effect by acting as depolarizing agent and increasing the required current for cathodic protection (de Romero, 2009; Booth et al.,1960). It is also considered that biofilm formation by bacteria electrically insulates the metal from cathodic protection (Booth et al.,1960; Bryant et al.,1990). Also, extracellular polymeric substances in biofilm can generate an effect of ohmic drop (de Romero, 2009).

The presence of macro-marine fouling organisms with encrustation, such as marine sedentary fauna and flora, on steel elements can create aggressive crevice environments and inhibit effective cathodic current distribution on the steel surface. Results from studies by Swain and Maxwell,1990 showed that biofouling on aluminum anodes increase the resistance value and reduces anode current output (Swain et al.,1990). Blackwood, 2010 reported that sacrificial anodes such as zinc and aluminum remained effective even after being completely coated with biofouling in maintaining a galvanic current to reduce and control corrosion (Blackwood.2010).

Eshware, 1995 showed that SRB activity on cathodically protected steel persisted due to shielding provided by of barnacles and development of anaerobic conditions (Eashwar et al.,1995). Eshware also showed that interfacial alkalinity generated by cathodic protection might enhance shell growth in the organism. However, information in the literature on the role of fouling on CP remain inconclusive (Blackwood.2010; Eashwar et al.,1995; Houghton,1978; Edyvean,1985; Maruthamuthu et al.,1990; Pipe 1981). Littauer and Jennings showed indication of reduced biofouling in seawater using pulsed cathodic polarization of steel (Littauer et la.,1968). Sander and Maxwell,1983 found that cathodic protection doesn't alter the rate of attachment of fouling, but it inhibits the activity of biofilm (Sanders et al.,1983).

2.4. Microbiologically Influenced Deterioration (MID)

Concrete is a common construction material used for bridge infrastructure. Concrete durability has been well studied and damage mechanisms can include concrete cracking, freeze-thaw damage, alkali-silica and alkali-carbonate reaction (ASR and ACR), chemical/sulfate attack, delayed ettringite formation (DEF) and carbonation. Also, concrete can be damaged due to scouring, restraint to volume changes, fire/heat, overloading, and impact loading. Also, in certain aggressive aqueous environments, concrete deterioration by biological factors can occur.

Concrete deterioration due to interaction with microorganisms is labeled here as Microbial Induced Deterioration (MID). Researchers often refer to MID as microbially induced concrete deterioration (MICD) or microbially induced concrete corrosion (MICC) (Gutierrez-Padilla et al., 2007; Marquez et al., 2013; Vupputuri et al., 2013; Eštokov, et al., 2012; Ling, et al., 2014; Soleimani, 2012). Microbial induced deterioration of concrete has been identified as early as 1900 (Eštokov et al., 2012; Olmstead and Hamlin,1900) and has often been attributed with acid and biogenic sulfate attack when microorganisms present in the environment generate mineral or organic acids (such as sulfuric acid) that dissolve or decompose the concrete matrix. This phenomenon shares many of the physical and chemical degradation processes and makes diagnosis of the degradation by biotic factors difficult (Cwalina, 2008; Trejo et al., 2008). According to an estimate in the United States, the contribution of microorganisms in the deterioration of concrete may be within the range of 30% (Sand, 2008). It has been estimated that MID problems cost billions of dollars a year in infrastructure maintenance and repair (Sanchez-Silva and Rosowsky, 2008). MID of concrete may be responsible for deterioration of more than 150,000 bridges in the United States, especially in southern states such as Alabama, Georgia, Mississippi, and Texas. (Vupputuri et al., 2013). Also, MID represents a significant problem in several other industries including the wastewater treatment, underground structures, sewage systems, transportation industries, chemical plants, agricultural structures, marine environments and any liquid-containing structures (Eštokov, et al., 2012).

Concrete is a heterogeneous material typically consisting of the Portland cement, aggregates (coarse and fine), water and admixtures. Portland cement has a chemical composition consisting of Dicalcium Silicate ($2CaOSi_2$), Tricalcium Silicate ($3CaOSi_2$), Tricalcium Aluminate ($3CaOAl_2O_2$), Tetracalcium Aluminoferrite ($4CaOAl_2O_3Fe_2O_3$), Calcium Sulfate or Gypsum ($CaSO_4 \cdot 2H_2O$) and others (Monteiro, 2006). In aggressive environments, various physical, chemical and biological factors can attribute to degradation of the cement paste and aggregates (PCA, 2002) resulting in material degradation and loss of strength. Therefore it is important to have an understanding different kind of deteriorations in concrete.

2.4.1. Concrete Degradation by Chemical Attack

Sulfate attack sometimes called sulfate corrosion is a severe type of deterioration resulting from chemical reactions occurring when concrete components react with sulfate ions present in solution from internal and external sources. Sulfate attack can cause expansion, cracking and loss of cohesion and strength in the cement paste. The cracks may remain empty or later be partly or even completely filled with ettringite. Internal sulfate corrosion is categorized as either a) composition induced internal sulfate attack, caused by an excess of sulfate ions in the concrete itself (from clinker, aggregate, admixture, and rare excessive addition of calcium sulfate) or b) heat-induced internal sulfate attack (also referred to as delayed ettringite formation DEF), caused by thermal decomposition and subsequent reformation of ettringite due thermal conditions during concrete processing. DEF involves only monosulfate and ettringite (tri-sulfate) (Lamond, 2006).

External sulfate attack occurs when sulfate ions from an external source such as seawater, swamp water, ground water or sewage water attack components of the cement paste. Similar to internal sulfate attack, it will result in formation of gypsum and ettringite that may cause concrete to crack and scale. Deterioration of concrete through adverse chemical reaction with its surrounding environment can affect the cement paste, coarse aggregate, or embedded steel reinforcement. High quality concrete is expected to show enhanced resistance to the exposure of various atmospheric, water, soil, and chemical conditions. However harsh environments containing aggressive soluble chemicals can cause concrete deterioration (ACI 201.2R-92). In general, Portland cement concrete does not have good resistance to acids due to its high alkalinity. Cement are highly susceptible to a solution with pH less than 3. However, some weak acids can be tolerated based on the time of exposure (PCA, 2002). Acids react with the calcium hydroxide of the hydrated Portland cement. In most cases, the chemical reaction forms water-soluble calcium compounds, which are then leached away by aqueous solutions (ACI 201.2R-92). Acids such as nitric acid, hydrochloric acid, and acetic acid are very aggressive and generate highly soluble calcium salt. Other acids such as phosphoric acid is less harmful, due to their low solubility product and can inhibit the attack by blocking the pathways within the concrete. Biogenic acid can also be harmful. Almost all microorganisms either temporarily or permanently excrete organic acids such as acetic, gluconic, oxalic, citric, malic, succinic acid. An attack of biogenic acids on materials may be difficult to detect due to their metabolic origin. Their reaction with calcium results in formation of calcium oxalate and may be used as a marker of an attack by biogenic organic acids (Sand et al., 1987). Sulfuric acid is very damaging to concrete as it is associated with the combination of acid attack and a sulfate attack. Sulfur element or hydrogen sulfide can be presence on concrete surface/pores by different mechanism such as the products of combustion of many fuels that can mix with moisture and form sulfuric acid. Also, certain bacteria assist the S/HS conversion to sulfuric acid. The calcium sulfate formed from the acid reaction will also deteriorate concrete via sulfate attack (ettringite formation). In addition to individual organic and mineral acids, acid-containing or acid-producing substances, such as acidic industrial wastes, silage, fruit juices, sour milk and animal wastes will also cause damage. (ACI 201.2R-92.). Protecting Portland cement concrete from acid attack can be approach by using chemical-resistant cement and applying surface protective treatments. Siliceous aggregates in the cement are acid-resistant and are sometimes specified to improve the chemical resistance of concrete unlike limestone and dolomitic aggregates which easily decomposing by acid attack. Properly cured concrete with reduced permeability happen to have lower rate of attack from acids. (PCA, 2012)

2.4.2. Microorganism Associated with MID

According to the available literatures, a wide variety of microorganism can take part in concrete deterioration, including, bacteria and cyanobacteria as prokaryota, algae (green, red, brown), lichens, yeasts, and fungi as eukaryotes (Sand et al., 1987). These microorganisms can be classified based on their effects on concrete surfaces, concrete matrixes, and on cracking and crack growth (Aviam et al., 2004)

Table 2.4. Characteristics of *Desulfovibrio* and Five Main Acid-producing *Thiobacillus* Species. (Vupputuri et al., 2013; Islander et al., 1991; Sanchez-Silva, 2008).

Organism	**Mechanism of degradation**	**pH range**	**Life style**
Desulfovibrio	Use sulfate ion as an oxygen source and produce the sulfide ion (S^{2-})	6.9-9.9	Mixotrophic
T.Thioparus	Production of sulfuric acid	5 -7.5	Mixotrophic
T.neapolitanus	Production of polythionates and sulfuric acid oxidizes thiosulfate and sulfur	4.5-8.5	Autotrophic
T.novellus	Production of elemental sulfur	5-9.2	Heterotroph /Mixotrophic
T. thiooxidans	Production of sulfuric acid	0.5-4	Autotrophic
T.intermedius	Production of polythionates and sulfuric acid	1.7-9	Heterotroph /Mixotrophic

Table 2.4 shows a listing of select SOB related to MID. In 1945, experiments by Parker showed that sulfur oxidizing bacteria *Thiobacillus thiooxidans* are involved in accelerating the concrete deterioration process by utilizing inorganic sulfur compounds in the presence of oxygen and forming sulfuric acid (Parker, 1945). Islander et al. (1991) divided the various SOB involved in MID into two main groups of neutrophilic (NSOB) and acidophilic sulfur oxidizing bacteria (ASOB) based on the pH range for the growth, and the form of sulfur they use as substrate. The NSOB are capable of growth at pH levels up to 9 and can reduce the pH to 5, which becomes self-inhibitory for their growth. *T.thioparus, T.neapolitanus*, and *T.novellus* are categorized in the NSOB group (Gutierrez-Padilla et al, 2007). Sand (1987) showed that *T. novellus* and *T. neapolitanus* are dominant when thiosulfate is present, and the pH is moderate T. intermedius and *T. novellus* may benefit from their facultative heterotrophy, consuming aerosol-deposited organics and microbial waste products as they generate acid. As the pH falls to 6, *T. neapolitanus* is established. It has an advantage in its ability to resist high concentrations of inorganic salts, which are produced by the beginning of the corrosion process. As the pH reduces to 5, ASOB such as *T. thiooxidans, T.intermedius* start their activity and reduce the pH to as low as 0.5 (Islander et al., 1991; Nica et al., 2000). The ASOB, which can survive at very low pH, are responsible for the structural failure of concrete structures due to their ability to create a highly acidic environment. The aerobic autotrophic sulfur oxidizing bacteria *T. thiooxidans*, which can survive in low pH conditions. The low pH favors the formation of elemental sulfur, and *T. thiooxidans* rapidly oxidizes it directly to sulfate. Bielefeldt et al.

(2010) studied the kinetics of different SOB species and their bio-deterioration rate associated with pH decrease, calcium release, and sulfate production. They concluded that the bio-deterioration rate of concrete exposed to the mixed culture of ASOB and NSOB was faster than the concrete exposed only to NSOB. Milde et al. (1983) observed a positive correlation between the cell number of *T. thiooxidans* and the level of deterioration. As already noted, the sulfuric acid produced by *Thiobacillus* spp. can react with the hydrated cement paste to form gypsum and ettringite, causing surface deterioration.

The lithoautotrophic nitrifying bacteria (Nitrobacter, Nitrosomonas) are acid-producing microorganisms involved in deterioration of concrete structures by producing nitric acid through nitrification (Vupputuri, 2013; Gaylarde et al., 2003). As shown in Reactions 2-8, 2-9 and 2-10, Nitrosomonas oxidize ammonia to nitrous acid, and Nitrobacter convert nitrous to nitric acid. (Sand and Bock, 1991)

$2NH_4^+ + 3O_2 \rightarrow 2NO_2^- + 2H_2O + 4H^+$ (by Nitrosomonas) (2-8)

$2NO_2^- + O_2 \rightarrow 2NO_3^-$ (by Nitrobacter) (2-9)

$Ca(OH)_2 + 2HNO_3 \rightarrow Ca(NO_3)_2 + 2H_2O$ (2-10)

Nitric acid causes solubilization of calcium and can degrade carbonate, aluminate and silicate components of concrete. However, since this type of bacteria cannot grow at pH less than 5, the severity of bio-deterioration is much less than SOB (Soleimani, 2012). Schiffers et al., 1976; Bock and Krumbein, 1989, reported the deterioration of concrete by nitrifying bacteria in a cooling tower.

All fungi produce organic acids during their metabolism and these lead to solubilization of minerals such as K, Ca and Fe from concrete and stone substrates containing silicates, feldspars and micas. Diatomaceous algae require silica for their cell wall structure and have been implicated in the removal of this substance from concrete. Mineralogical calculations have shown the reduction in silica and the presence of remains of diatoms in various concretes (Ribas, 1993; Gaylarde, et al., 2003). Gu et al. (1998) suggested that fungi are involved in the bio-deterioration of concrete and compared the MID caused by the SOB of *T.intermedins* with degradation caused by the fungus, Fusarium sp. They reported that Fusarium sp. is equally capable of biodeteriorating concrete as *T.intermedins.* attacks concrete by etching and spalling the concrete but Fusarium sp. penetrates to a deeper depth in concrete and deteriorates the concrete by organic acid production.

2.4.3. Factors that Promote MID and Mechanism

Microorganisms associated with MID require favorable environmental conditions (such as sufficient moisture, nutrients, low pH, high relative humidity (between 60 and 98%), certain temperature, long cycles of humidification and drying, freezing and defrosting, high carbon dioxide concentrations, high chloride ion concentrations, high sulfate concentrations) to grow on concrete surfaces (Wei, et al., 2013). Roughness on the concrete surface (including roughening due to scouring by wave action) can be another supporting factor in microbial colonization

(Ribas-Silva, 1995). Microorganisms can penetrate inside the concrete matrix even if there are no observable cracks in the concrete (Sanchez-Silva and Rosowsky, 2008). They can increase concrete porosity, the coefficient of diffusion, accelerating crack propagation and also facilitate chloride ion ingress. The most common mechanism for microbe ingress in the concrete is via microcracks or through the capillaries.

It was been observed that the microorganisms can promote degradation of the concrete matrix and increases concrete permeability (Sanchez-Silva and Rosowsky, 2008; Islander et al., 1991). Higher concrete permeability can lead to reduced protection from further degradation including corrosion of the reinforcement. (Trejo, et al., 2008).

The mechanism of microbiologically induced concrete deterioration by SOB can be generally associated with acid and sulfate attack. Initially, possible chemical reactions with carbon dioxide (CO_2) and other acidic gasses (if available) can cause the pH of pore moisture to drop from values of about 13-12 to below 10. This pH drop is typically the result of abiotic (physical) processes and no microorganisms have been associated with this initial stage of MID (Gutierrez-Padilla, et al., 2007; Nielsen et al., 2005). Below pH 10, colonization of sulfur-reducing and sulfur-oxidizing bacteria on concrete can occur which participates in the sulfur cycle in their environment, especially in aquatic environments that sulfate ions are widely distributed (Wei, et al., 2013).

Biogenic oxidation of sulfur on the concrete surface lowers the pH further to create condition for further microbe colonization. This step is assisted by SRB microorganism, e.g. *Desulfovibrio* (pH 6.9-9.9) (Eštokov et al., 2012), which use the sulfate ion as an oxygen source for the digestion of organic matter and release back the sulfide ion (S^{2-}). (Reaction 2-13). The sulfide ion exists either in the form of bisulfide ion (HS^-) or hydrogen sulfide gas (H_2S), based on the pH condition and the temperature (O'Dea, 2007). H_2S can also react with oxygen to produce elemental sulfur (S), sulfite (SO_2^{3-}), and thiosulfate ($S_2O_3^{2-}$) which are deposited on the surface of the concrete structures (in yellow-brown color (Islander et al., 1991) and are more digestible by sulfur oxidizing bacteria (SOB) (Nica et al., 2000). SOB converts the sulfur compounds to sulfuric acid, which is corrosive and causes concrete deterioration (Reaction 2-14). (Eštokov et al., 2012; Vupputuri, 2013; Marquez et al., 2013; Soleimani, 2012; Rajakaruna, 2010; Cwalina, 2008; Wei et al., 2013; Wei et al., 2010; Taylor, 2003). As an example, thiosulfate oxidation by *T. thioparus* may occur as (Starkey 1935; Alcantara, 2004):

$$5Na_2S_2O_3 + H_2O + 4O_2 \rightarrow 5Na_2SO_4 + H_2SO_4 + 4S \quad \text{(Limited oxygen)} \quad (2\text{-}11)$$

$$Na_2S_2O_3 + 2O_2 + H_2O \rightarrow Na_2SO_4 + H_2SO_4 \quad \text{(High oxygen)} \quad (2\text{-}12)$$

The biogenic release of acid degrades the cementitious material in the concrete, thus generating gypsum ($CaSO_4$ of various hydration states) (Reaction 15) (Mori et al., 1992). Gypsum can act as a protective layer for concrete in the same way that initial corrosion protects metals (like the oxide layer on aluminum) (Wei et al., 2013). If this “protective” coating of gypsum is removed, the concrete surface can be exposed to acid attack. The gypsum may also react with calcium aluminate hydrates to form ettringite ($C_3A\overline{S}_3H_{32}$) (Reaction 16) which

increases internal pressures caused by its rather large volume and leads to the formation of cracks concrete expansion and accompanied by the loss of strength and loss of adhesion to a greater extent leading to structural failure. (Bashir et al., 2012; Eštokov et al., 2012; Vupputuri, 2013; Marquez et al., 2013; Soleimani, 2012; Rajakaruna, 2010; Cwalina, 2008; Wei et al., 2013; Wei et al., 2010; Taylor, 2003). Deterioration worsens if the H_2S gas also reacts with the concrete reinforcement through cracks and corrodes the steel reinforcements.

$SO_4^{2-} + 2H^+ + 4H_2 \rightarrow H_2S + 4H_2O$ (Sulfate reducing bacteria) (2-13)

$H_2S + 2O_2 \rightarrow H_2SO_4$ By SOB (Sulfur oxidizing bacteria) (2-14)

$Ca(OH)_2 + Ca(OH)_2 \rightarrow CaSO_4.2H_2O$ (Gypsum formation) (2-15)

$3CaO.Al_2O_3.12\ H_2O + 3(CaSO_4.\ 2\ H_2O) + 13\ H_2O \rightarrow 3CaO.Al_2O_3.3CaSO_4.31H_2O$ (Ettringite formation) (2-16)

2.4.4. Case studies Related to MID

Microbiologically induced concrete corrosion has been studied in the United States, Germany, Belgium, Denmark, Lebanon, Japan, and Australia. (Santo Domingo, et al., 2011; Sand and Bock 1984; Vincke et al., 2001; Nielsen et al., 2008; Ayoub et al., 2004; Okabe et al., 2007; Mori et al.,1992; Cayford et al., 2012)

The U.S. Department of Energy (DOE) in 1995 conducted a study on material resistance to attack by chemical, physical and biological agents for condition related to the Yucca Mountain nuclear waste repository. Laboratory tests in the study included exposing various concrete mixes at a test site in a cooling tower in New Zealand that had similar environmental and exposure conditions as the Yucca Mountain site including elevated temperatures, moisture and presence of reduced chemical species. It was confirmed that concrete mix designs used in Yucca Mountain can be susceptible to MID attack. SEM micrographs and selective isolation methods detected *Thiobacillus* and nitrifying bacteria actively growing at sampling sites in the cooling tower. (Rogers, 1995).

Texas Department of Transportation (TxDOT) in 2008, reported surface deterioration of reinforced concrete columns possibly due to microbial attack. The pH of the water body was slightly acidic and near neutral. Testing indicated that the number of microbe's present was correlated with the degree of damage. Active sulfur oxidizing bacteria was also identified using FISH analysis; total counts of microbial cells indicated a range from $5.27\pm0.88\times10^{6}$/g (slight deterioration) to $3.60\pm0.31\times10^{7}$/g (severely deteriorated). The research identified five genera: these included *Bacillus, Brachybacterium, Flavobacterium, Lysinibacillus* and *Thiomonas*. (Trejo et al., 2008). The Oklahoma Transportation Center in 2013, performed detail analysis on samples from the Texas deteriorated concrete bridge structure. Acid-producing microbes were present in the deteriorated bridge columns. Genetic analysis tools revealed that these microbes were closely related to microbes found in sewer systems and appeared to work in a similar manner. Similar to the results from the TXDOT report, the cultures showed a major decrease in pH and oxidation of thiosulfate present in the medium and the release of calcium from concrete.

The availability of sulfur compounds such as H_2S, $S_2O_3^{2-}$ and other reduced sulfur compounds led to the increased growth of sulfur oxidizing acid producers. During active corrosion (at low pH) more than 60% of the microbe population included sulfur oxidizing bacteria such as Thiobacillus *thioparas*, *Alicyclobacillus* spp., *Alicyclobacillus acidocaldarius*, *Alicyclobacillus pomorum*, and *Bacillus* spp. These results were consistent with other studies dealing with corrosion of sewer pipes and wastewater treatment facilities suggesting that sulfur oxidizers are mainly responsible for concrete corrosion. (Vupputuri, 2013).

In 2014, the US Army Corps of Engineer reported that deterioration of the cement pastes and coarse aggregate in a south Florida reinforced concrete navigation structure was not due to sulfate attack, acid attack, or Cl^- induced corrosion of reinforcing steel (Moser et al., 2014). The concrete distress was thought to be caused by dissolution of soluble phases and bio-deterioration which can result in localized acidification at the surface and direct or chemical consumption of mineral phases present in concrete. Negligible concentrations of SO_4^{2-} and Cl^- was identified in the water and the pH was near neutral. XRF and petrographic analysis of extracted concrete cores showed minor carbonation and leaching of soluble phases from the surface of the concrete but no evidence of deterioration resulting from sulfate attack. SEM shows significant loss of limestone, while the siliceous, fine aggregates were unaffected.

Figure 2.2. Microbial-induced Bio-deterioration of Concrete. (Trejo et al., 2008).

2.4.5. Methods for Estimating and Measuring Microorganism related to MID

Biodeterioration of concrete requires the availability of water and nutrients. Parameters such as porosity, permeability, and environmental conditions, can help to determine the rate of bio corrosive attacks. Qualitative and quantitative methods are utilized to identify the microorganisms as well as their metabolic activity. Several methods for studying MID such as characterization of the population structure and molecular techniques have been developed (Minteny et al., 2000; Wei et al., 2013). Traditional cultivation methods for enrichment and isolation of microorganisms have been used to characterize the population structure of microbial communities on deteriorated concrete, (Islander et al., 1991; Diercks et al., 1991) but may fail to provide a complete portrait of all the bacteria that are associated deteriorated concrete (Wei et al., 2013). Molecular techniques including analysis of the 16S rRNA gene sequence and analysis by denaturing gradient gel electrophoresis (DGGE) have proven to be useful for precisely describing the microbial communities in environmental samples but are not definitive

methods for quantitative population analysis, (Vincke et al., 2001). Fluorescent in situ hybridization (FISH) provides an alternative approach towards quantitative population analysis in these environments (Wei et al., 2013).

2.4.6. Biodeterioration Prevention Methods and Concrete Protection

MID is the result of attack of biogenic substances, which are the products of the metabolic activity (Cwalina, 2008). Microorganisms can initiation and accelerate the corrosion process. Cleaning the bacterial biofilm and corrosive deposits on the surfaces can be an effective way to prevent or control bio-corrosion (Videla, 2002). Effective protection against MID can be named as including chemical or antimicrobial coating, treatments with biocides, apply modifications of concrete mix design, and coating with beneficial biofilm.

2.4.6.1. Chemical or Antimicrobial Coating

Protective coatings create a physical barrier between corrosion susceptible concrete and the biologically active environment. Chemical coating is a common approach to protect from any type of corrosion. Generally, coating is achieved through nontoxic products consisting of silicone, epoxy-resins, and fluorinated compounds (Videla and Herrera, 2005). The coating for concrete structures in marine environment should resist the permeation of H_2S and sulfuric acid. In addition, it should not release the corrosive substances or be altered by bacterial attack (O'Dea, 2007). Shook and Bell (2003) concluded that the antimicrobial coating was capable of 100% removal of *thiobacillus thiooxidans* from the concrete surface. Haile et al. (2008, 2009) mixed silver loaded zeolite in an epoxy resin resulting in the reduction of MID. De Muynck et al. (2009) studied two types of antimicrobial admixtures (i.e., copper/silver zeolite or antimicrobial fiber) and four types of surface coatings (i.e., polyurea coating, epoxy coating, cementitious coating and silicate coating) regarding their effectiveness to prevent biogenic sulfuric acid deterioration by means of chemical and microbiological tests. They observed the best resistance to both chemical and microbiological tests in epoxy coating and the worst performance in the cementitious coatings.

Coatings can delaminate over time because of either improper preparation of the concrete surface or inadequate and improper application in the field. Any discontinuity (e.g. cracks and defects) in coating can make a preferential pathway for localized deterioration. Furthermore, bacteria can penetrate inadequate coatings and proliferate on the underlying concrete surface, and thereby further destroy the bond between the coating and the concrete (Soleimani, 2012).

2.4.6.2. Use of Supplementary Cementitious Materials in Concrete

Concrete mixes promoting high alkalinity and low permeability can inhibit SOB attachment (Vincke et al., 2002; De Muynck et al., 2009). Silica fume or fly ash reduces permeability and diffusivity of concrete, (Yilmaz, 2010; Kazuyuki and Kawamura, 1994). Polymer addition improves the durability of concrete to sulfuric acid by preventing the expansive

ettringite formation due to interaction of the cement hydrate with the polymer particles (Beeldens et al., 2001). Vincke et al. (2002) evaluated the influence of four different types of polymer and silica fume. No enhanced improvement on MID mitigation by addition of the acrylic polymer or silica fume was observed. The addition of the styrene acrylic ester showed better performance in terms of the weight loss, pH reduction and calcium release. Kazuyuki and Kawamura (1993) studied the effect of fly ash and silica fume on resistance of concrete. The results of their experiments showed that the effectiveness of fly ash and silica fume to sulfate solution varies depending on the type of cation involved in sulfate solution (Mg^{2+} or Na^{+}) and the percentage of pozzolan used. They also concluded that fly ash and silica fume could not prevent the more severe deterioration caused by sulfuric acid which results in the softening of the mortar by dissolution of calcium silicate hydrate (Soleimani, 2012).

2.4.6.3. Biocide Treatment

The most common chemical method for controlling biofouling is biocide addition (Videla and Herrera, 2005). Biocides are oxidizing or non-oxidizing compounds capable of killing microorganisms or inhibition of their growth (Videla, 2002; Videla and Herrera, 2005). Biocides are inorganic oxidizing agents such as chlorine, ozone and bromine, or organic non-oxidizing agents such as isothiazolones, ammonium compounds, and aldehydes. The combination of oxidizing and non-oxidizing biocides or two non-oxidizing biocides may be used to increase the efficiency of the biocide treatment (Videla and Herrera, 2005). Non-oxidizing biocides are more effective to control bacteria, algae and fungi (Videla and Herrera, 2005). Oxidizing biocides are less persistent because of their dependence to pH of solution. Their negative effects include interaction with other chemicals used in the treatment, which reduces their effectiveness. Biocides can be toxic to humans and the environment and are subject to regulatory inspection and restrictions (Wei, 2013; Trejo et al., 2008).

Biocides selection depends on the microorganisms that will settle the concrete stone Microorganisms in the biofilm are more resistant to biocides because of their protection by EPS. Hence higher concentration of biocides will be needed to prevent the biofilm induce corrosion, and that make this treatment method very cost ineffective. Simultaneous usage of the biocide and the protective coating as well as the biocides addition to the coating is more frequently recommended (Soleimani, 2012).

3. FLORIDA NATURAL WATER ENVIRONMENTS

3.1. S.R. 312 over Matanzas River

3.1.1. Background

Sampling of water near the bridge was tested to characterize water pH, chloride and sulfate content, mineral content, and microbe content. This information was compared to earlier testing and available environmental databases and used to help identify other locations that may be susceptible to MIC.

Florida State Road 312 (SR-312) bridge over Matanzas River (Saint Augustine, Florida) was constructed in 1976 (Figure 3.1). FDOT coordinates routine bridge inspections. In the earliest underwater inspection records reviewed by the researchers (dated on 5/12/2004), significant corrosion of some of the submerged H-piles were detected. This corrosion advanced upon subsequent inspections and was suspected to be MIC. A level III inspection in 2006 and further subsequent inspections in 2008-2016 showed and verified severe metal section loss in increasing number of H-piles. A summary of the FDOT inspection reports from 2004 to 2016 is shown in Table 3.1.

Figure 3.1. View of the State Road 312 Bridge.

The locations with suspected MIC often had heavy marine growth. An example of a corrosion hole in a steel pile suspected to be due to MIC is shown in Figure 3.2. Figure 3.3 shows the cumulative fraction of reported H-pile corrosion deficiencies for the bridge. The depths of corrosion pitting, or holes ranged from ~1 to 30 ft below the pile cap. The median value of the depths where corrosion deficiencies were observed was 2.5 ft indicating that a large fraction of the deficiencies occurred close to the water surface. Most of the corrosion pits were 1/8 inch in diameter but pits up to ½ inch were recorded and corrosion holes were as large as 3 inch in diameter.

Figure 3.2. Underwater Image of a Hole on a Steel Pile due to Corrosion. Photo courtesy of FDOT.

Table 3.1. Bridge Inspection Findings of Steel Piles

Inspection Date	Description
2004, 2006	Steel H-pile with metal loss due to corrosion. Higher level of inspection revealed greater number of H-piles with severe corrosion.
2008, 2010	H-pile locations showed random areas of corrosion cells/pits of up to 3" in diameter and varied up to full depth. The corrosion cells/pits were covered with a bright orange plume, which when removed revealed flakey grey, black corrosion product. The localized corrosion in these areas was presumed to be due to MIC.
2011	Steel H-piles typically revealed pitting from 1/8" up to 2". Also, 28 steel piles had corrosion.
2014-2016	The H-pile pilings, two per footing for a total of 28, were in poor condition. They depicted random dense patterns of corrosion cells or pits (up to 3” diameter and vary up to full depth). Corrosion cells/pits were covered with a bright orange plume, which when removed revealed flakey grey, black corrosion product. The next layer is a bright bare metal, several with holes through the web and or flange. Some of these corrosion cells/pits were located at the flange web interface. This condition appears to be MIC.

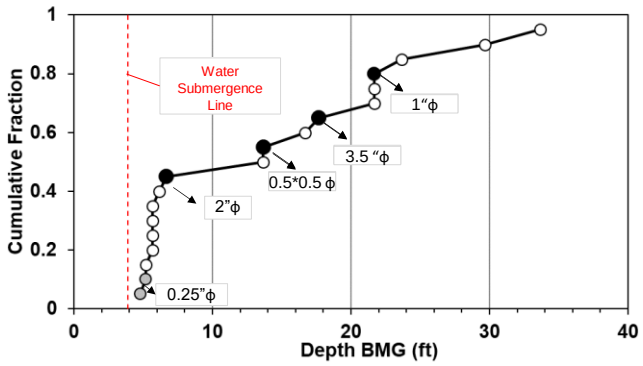

Figure 3.3. Cumulative Fraction of the Steel H-pile Corrosion.

3.1.2. Marine Fouling

Underwater visual inspection and video and photo-documentation of steel piles was performed on December 13, 2016 during a site visit. Based on inspection records of severe steel corrosion, Piers 22-4 and 23-17 were selected for this survey. Figure 3.4 depicts a selection of some underwater images of the piers. Heavy marine growth and macrofoulers covering the steel surface was evident and it was difficult to see the corrosion problems (pitting corrosion) already mentioned in previous FDOT reports. From the underwater video monitor, only small areas of the H-piles appeared without marine growth.

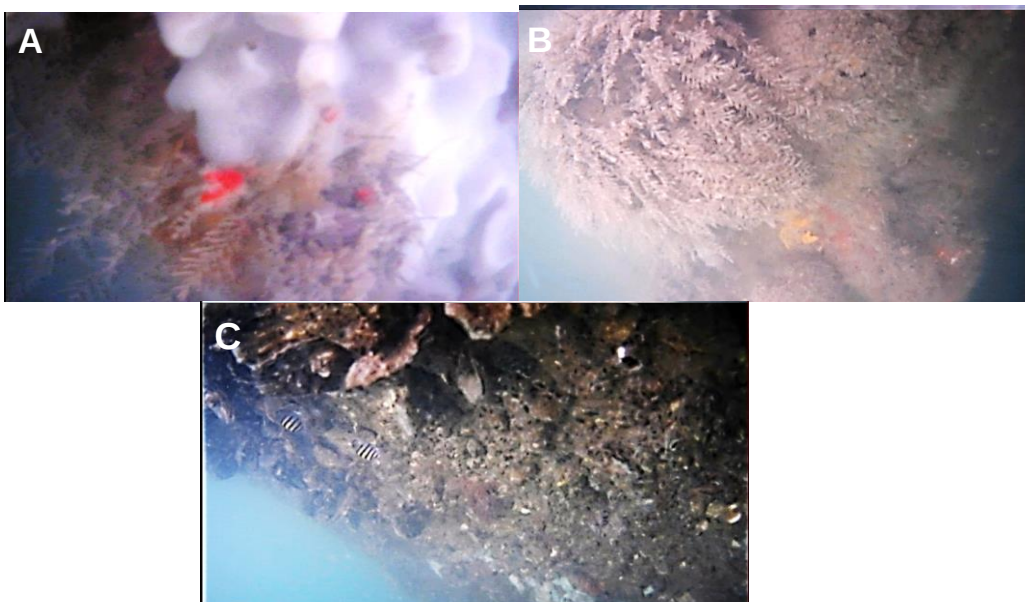

Figure 3.4. Underwater Images of Steel Piles at SR-312 Bridge over Matanzas River. A-C. View of steel piles covered by heavy marine grow.

3.1.3. Water Quality

3.1.3.1. Field Testing

FDOT preliminary assessments of steel coupons and water samples in 2013 have revealed the presence of bacteria often associated with MIC (FDOT, 2013, 2016). Laboratory results of steel coupons using swabs have revealed aerobic organisms (>1,000 per swab). Anaerobic SRB were present >100,000 colony forming units CFU/mL. Acid producing bacteria (*Bacillus sp.*) were present >100 CFU/mL. Slime producing bacteria including *Pseudomonas luteola, Sphingomonsa paucimobilis* and *Brevundimonas vesicularis* were also recovered. Analysis of water samples revealed the existence of anaerobic SRB ranging from ~100 to 10,000 CFU/mL, acid producing bacteria (*Bacillus sp.*) >100 CFU/mL and recovery of slime producing bacteria including *Brevundimonas diminuta* and *Pseudomonas oryzihabitans*.

Additional testing was conducted by the researchers in June 2016 to verify microorganism presence as well as to characterize the water environmental conditions (including dissolved oxygen, pH, conductivity, sulfate, chloride, phosphorus, nitrate, total organic nitrogen, total nitrogen, ammonia, and iron content) that may support the microorganisms related to MIC. Water samples were collected from two locations at the bridge site as well as at two depths reported in feet below high tide (BHT) (Table 3.2).

Table 3.2. Water Sampling Locations.

Bridge Location		Depth (ft BHT[1])
A	A1	~10
	A2	~20
B	B1	~10

1. Below High Tide

Microbiological analysis of the water samples is presented in Table 3.3. Similar to earlier testing, slime-forming bacteria, SRB and acid producing bacteria were identified in all the water samples. Iron-reducing bacteria were also identified. It is uncertain if iron-reducing bacteria were considered in the earlier analysis. It is noted that there was high accumulation of SRB (~27,000 CFU/ml) in both assessments. Although it is understood that the quantity of bacteria in the analysis of water samples cannot directly correlate to MIC risk, the high resolved concentrations are indicators that there is greater possibility for the bacteria to proliferate and contribute to MIC. Furthermore, analysis of the water samples showed the presence of important nutrients (such as sulfate, phosphorus, nitrogen and iron) that can support microorganism activity (Table 3.4). Data presented in Tables 3.4, 3.5 and 3.6 show results of pH, DO, temperature, and conductivity for water samples.

Table 3.3. Microbiological Analysis of Water Samples.

Sample ID	Iron-Reducing Bacteria (IRB) CFU.mL^{-1}	Slime-Forming Bacteria (SFB) CFU.mL^{-1}	Sulfate Reducing Bacteria (SRB) CFU.mL^{-1}	Acid Producing Bacteria (APB) CFU.mL^{-1}
A1	150	13,000	27,000	450
A2	500	13,000	27,000	450
B1	500	13,000	27,000	450

Table 3.4. Chemical Analysis Results of Water Samples.

Parameters	Sample ID		
	A1	A2	B1
Sulfate/mg.L^{-1}	2,700	2,700	2,700
Chloride/mg.L^{-1}	20,000	19,000	20,000
Phosphorus/mg.L^{-1}	0.11	0.12	0.1
Ammonia/mg.L^{-1}	0.03	0.03	0.05
Iron/mg.L^{-1}	0.58	0.08	0.08
Nitrate/mg.L^{-1}	0.5	0.5	0.5
Total Organic Nitrogen/mg.L^{-1}	0.29	0.41	0.51
Total Nitrogen/mg.L^{-1}	0.81	0.93	1.06

Table 3.5. Field Dissolved Oxygen, pH and Water Temperature.

Location	Depth / ft	pH	Temp. / ^{o}C	DO / mg.L^{-1}	DO / %	pH	Temp. / ^{o}C	DO / mg.L^{-1}	DO / %
		Time 11:00				Time 13:00			
A	10	8.3	30.7	4.13	67	8.1	30	3.75	60
	20	8.3	29.9	4.29	69	8.1	30	3.63	60
	30	8.1	29.9	4.27	68.4	8.1	30	3.25	54
	40	8.1	29.9	4.18	67	na	na	na	na
	50	8.1	29.9	4.13	65.3	na	na	na	na
		Time 12:00				Time 13:00			
B	10	7.96	31.7	4.13	67	7.96	30	3.7	61.5

Table 3.6. Water Sample Conductivity.

Sample ID	Conductivity / μs.cm^{-1}
A1	33.9 T=16.9 °C
A2	38.2 T=12.8 °C
B1	38.7 T=13.8 °C

It is noted that the bacteria concentration of the water samples collected at 10 feet BHT and 20 feet BHT were generally similar. At the same depths, the sulfate, chloride, phosphorus, ammonia, iron, nitrate, total organic nitrogen, total nitrogen, DO, temperature, pH, and conductivity were similar. DO, temperature, and pH measurements at depths down to 50 feet BHT were also comparable. It is remarked that water movement can be fast during tides. Table 5 shows results of field water environmental conditions during an incoming high tide. Although the convection of the water during the tide event seemed significant from the surface, DO measurements did not increase as expected and indeed diminished after 2 hours.
Further evaluations on the influence on microorganism activity especially anaerobic SRB will need to be considered.

3.1.3.2. Review of Florida Environmental Database

The possible contribution of water nutrient concentrations to bacterial proliferation was considered as a first approach to identify locations with similar environments and that may also support microbial activity. The water chemistry data from the case study was reviewed and compared with available databases from water management districts in Florida. Florida has five water management districts: Northwest Florida, St. Johns River, Suwannee River, Southwest Florida and South Florida. Water quality data of the Florida bridge case study for the last 20 years (1996-2016) is presented in Table 3.7. It can be seen from the table that this site has high concentration of sulfate, chloride, calcium, sodium, potassium, and magnesium. Also, the amount of total nitrogen and phosphorus is low to medium and the pH and dissolved oxygen (DO) are in the intermediate level. Chemical analysis data (sulfate, chloride, iron, phosphorus, NOx, pH, temperature, alkalinity, etc.), as well as salinity, conductivity and dissolved oxygen are depicted in Figure 3.5 and 3.6, respectively. For comparison, the recent field data were also plotted and are highlighted in red.

Table 3.7. Water Quality data of the Case Study Site from 1996 to 2016.

Analytes	N Data	Min	Median	Max	Range
Water temperature/°C	151	10.90	22.62	30.80	Mid
Specific conductance/ µmhos.cm^{-1} @ 25 °C	152	28640.00	49770.00	55937.00	High
Sample collection depth/ meters	155	0.50	0.50	2.93	Mid-High
Dissolved oxygen analysis by probe/mg.L^{-1}	154	4.28	6.42	9.89	Mid
pH/standard units	153	6.77	7.85	9.78	Mid
Total alkalinity/mg.L^{-1} as $CaCO_3$	86	69.58	115.91	125.70	High
Total nitrogen/mg.L^{-1} as N	150	0.01	0.43	1.01	Low
Total phosphorus/mg.L^{-1} as P)	152	0.02	0.08	0.61	Mid
Total organic carbon/mg.L^{-1} as C	87	1.25	3.05	27.40	Low
Total calcium/mg.L^{-1} as Ca	87	140.36	373.80	811.00	High
Total magnesium/mg.L^{-1} as Mg	87	1.14	1227.00	6490.00	High
Total sodium/mg.L^{-1} as Na	86	2820.00	10265.00	17500.00	High
Total potassium/mg.L^{-1} as K	86	152.77	416.50	3640.00	High
Total chloride/mg.L^{-1}	87	5973.67	19300.00	44352.60	High
Total sulfate/mg.L^{-1} as SO_4	86	164.00	2642.34	6170.64	High
Hardness/mg.L^{-1} Ca+Mg	85	1790.00	5957.62	7380.00	High
Lab turbidity/NTU	156	1.09	5.63	23.60	Mid-High
Sample site depth/meters	155	1.50	6.20	14.10	High

N data. number of data, Min. minimum, Max: maximum((http://www.sjrwmd.com/watershedfacts/factPages/MR312.html))

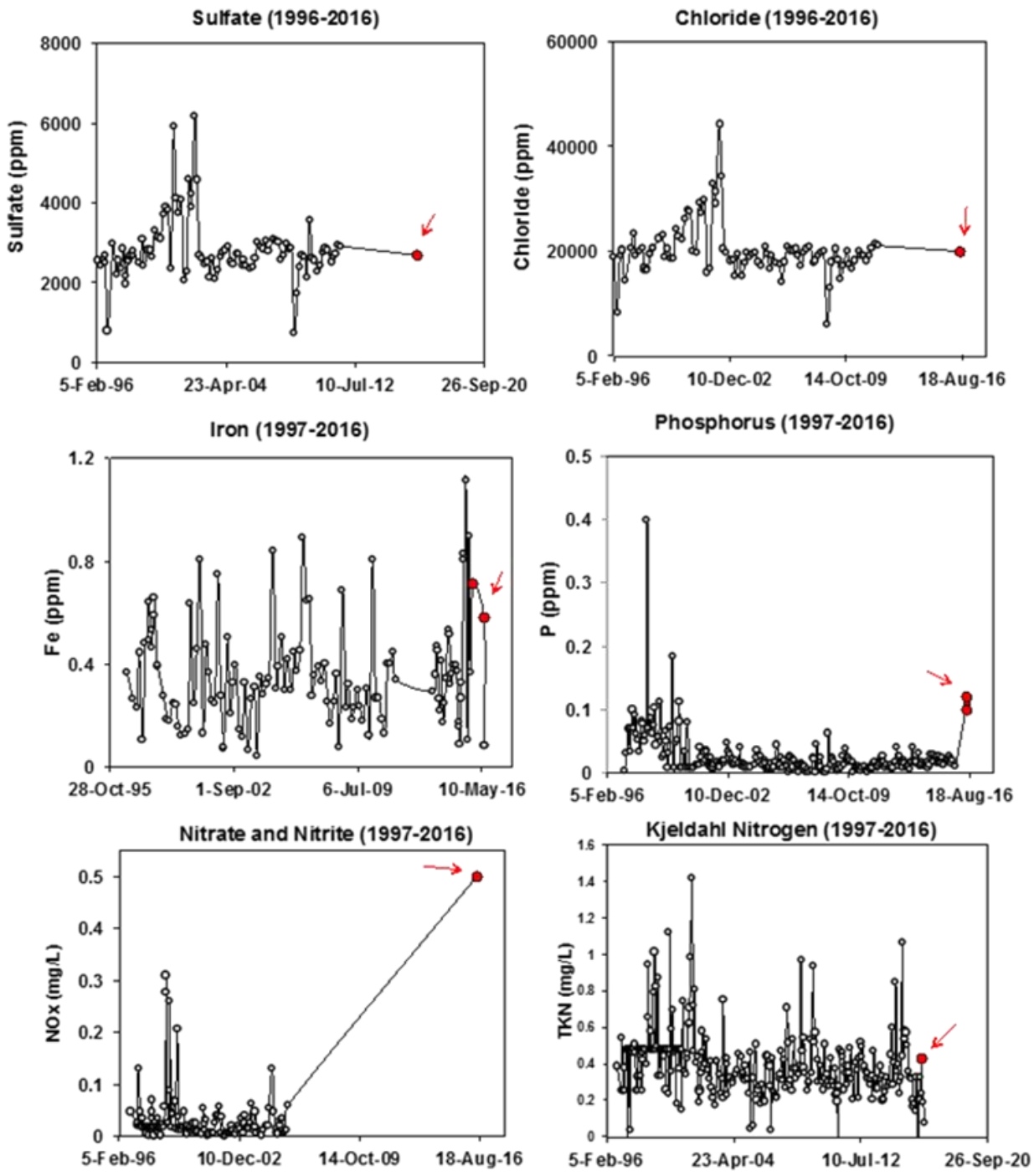

Figure 3.5. Chemical Analysis of Water Samples.
Red full point: recent measurements during site visit. (Continues).

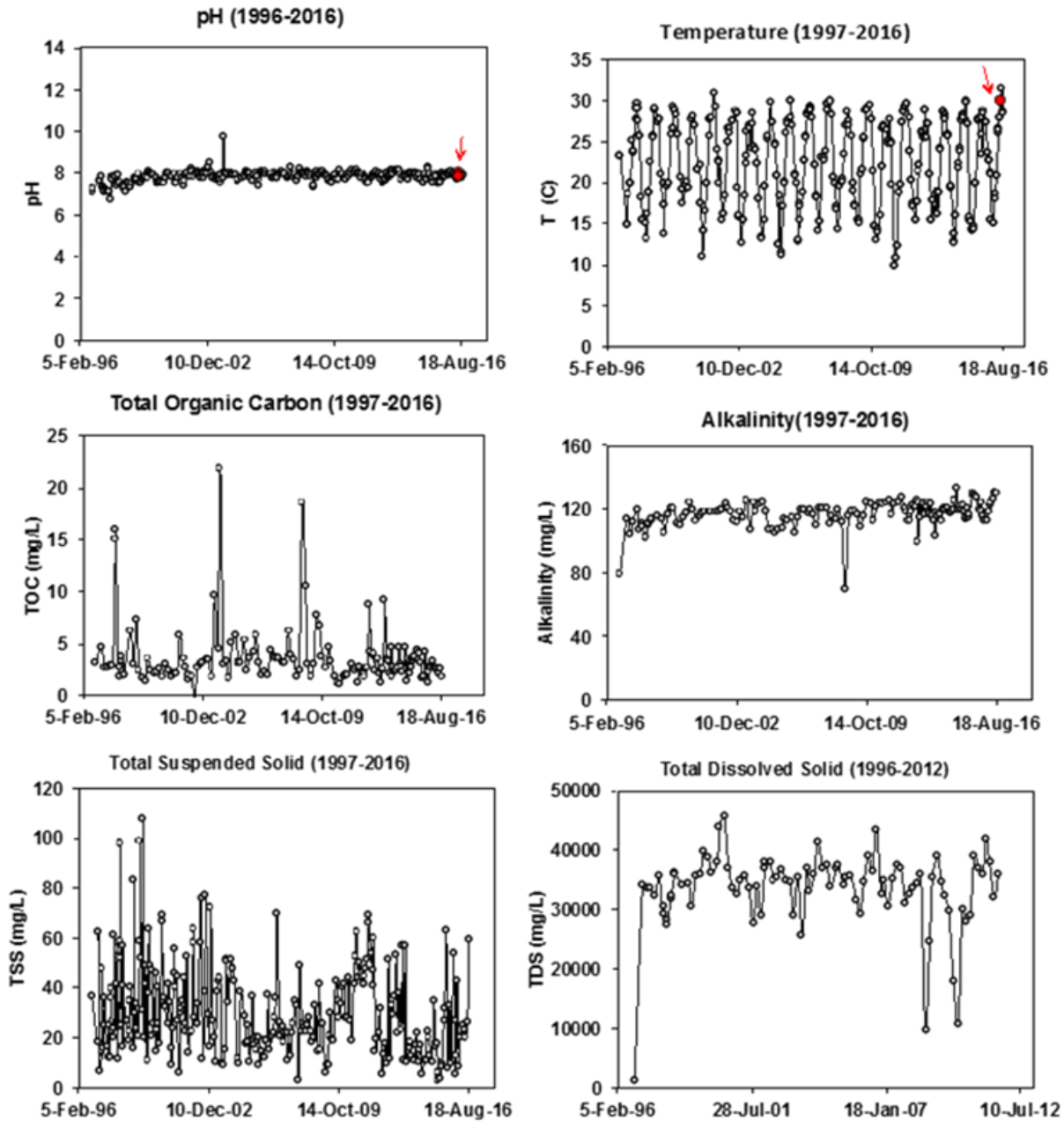

Figure 3.5. (Continued). Chemical Analysis of Water Samples.
Red full point: recent measurements during site visit.

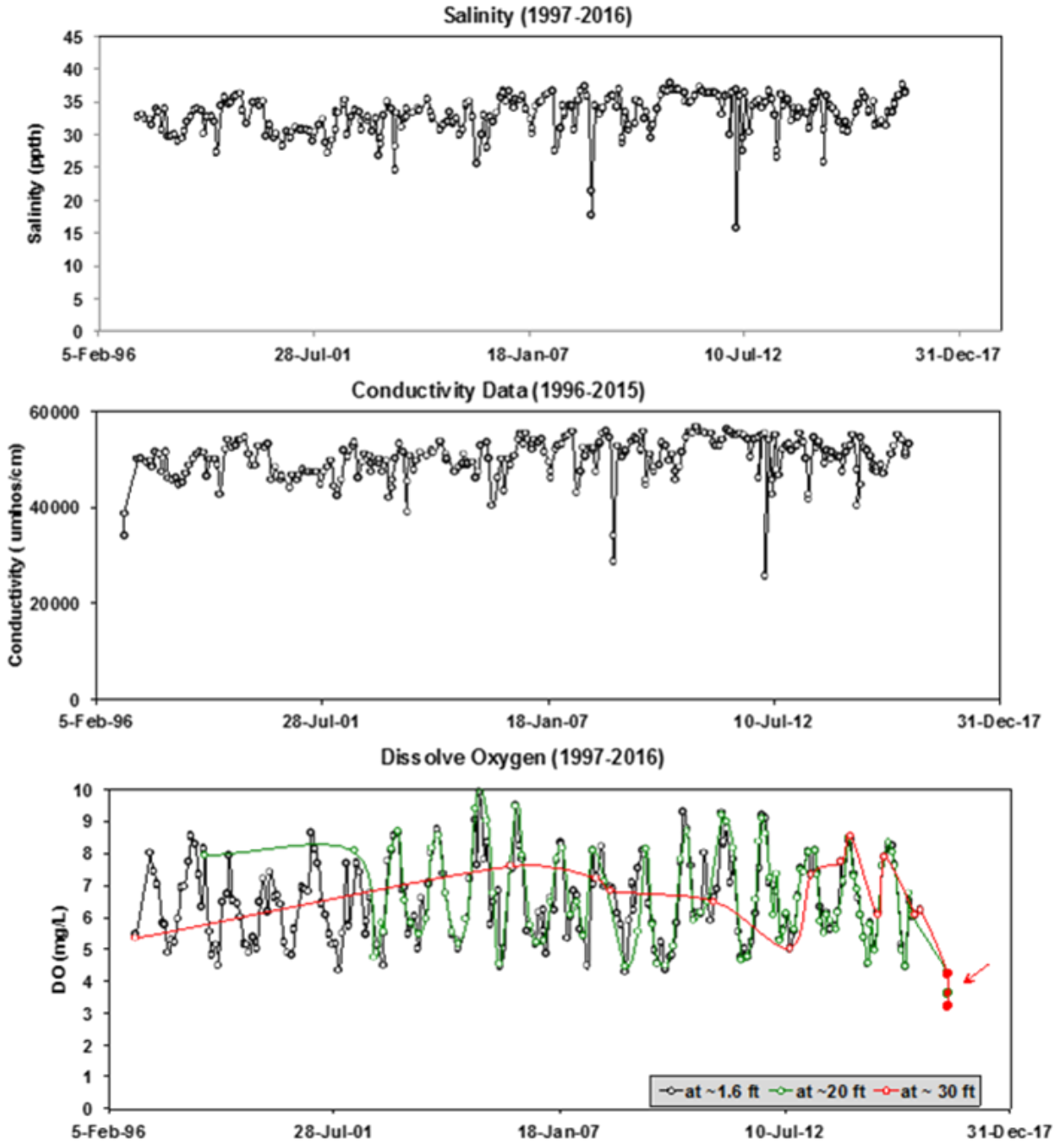

Figure 3.6. Salinity, Conductivity, and Dissolved Oxygen of Water Samples.
Red full point: recent measurements during site visit.

3.1.4 Comparative Florida Natural Waters

As shown in Figures 3.5 and 3.6, most of the recent measurements are in agreement with previous historical data. From the recent and historical environmental field data, concentrations of carbon (1.25<C<27.40 mg/L), sulfate (>2500 mg/L), nitrogen (0.01<N<1.01 mg/L), phosphorus (0.02<P<0.6 mg/L), as well as high concentration of Ca, K, Na, Mg in water samples were coincident with the MIC development. This is consistent with previous studies that have reported that carbon, oxygen and nitrogen are considered as important nutrients for sustained microbial activity related to MIC (Gaudy, A.F. and Gaudy, E.T., 1980). Environmental parameters such as high alkalinity, high chloride concentration (>20,000 mg/L), water temperature (around 30°C) and pH (from 6 to 9.5) could also contribute to the biocorrosion of steel piles. The available databases from the water management district of Florida were reviewed to identify marine environments that were similar to the case study. It was apparent that there are many sites that have similar conditions as the case study. Select sites with similar environmental conditions are shown in Figure 3.7.

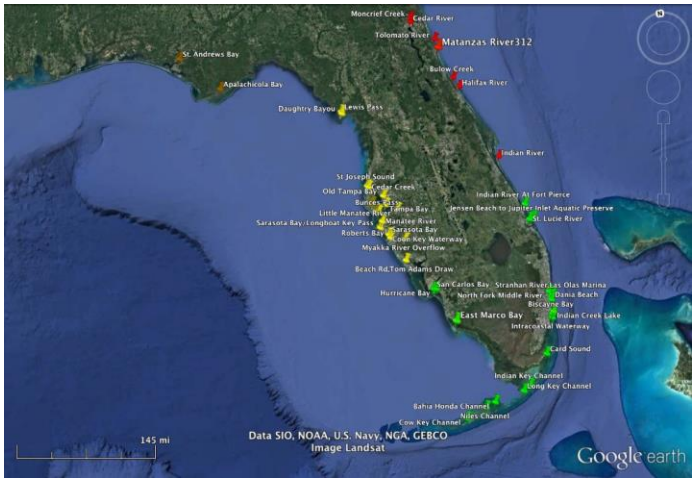

Figure 3.7. Examples of Florida Water Bodies that May Support MIC.
Red: St. Johns River Water Management District, Yellow: Southwest Florida Water Management District, Green: South Florida Water Management District, Brown: Northwest Florida Water Management District. Image captured from Google Earth.

In light of the findings from the case study, review of the technical literature and available environmental databases; there may be locations in Florida that meet environmental conditions and nutrients requirements for microorganism colonization and sustained activity. Verifying microbial activity at other sites and importantly identifying possible MIC is of interest and further laboratory and field testing is ongoing.

After survey and testing of State Road 312 (SR-312) Bridge over Matanzas River (presented in Task 2), four additional test sites were surveyed (Figure 3.8, Table 3.8). The selection of the four locations were made in consideration of information on presence of steel corrosion and history of enhanced water nutrient levels, as well as to determine possible localization and differentiation of water conditions at upstream/downstream locations of water bodies. Water samples close to the bridges were collected and analyzed for chemical makeup and microbial content. Also, visual inspections of steel/concrete piles were carried out by means of photo-documentation and underwater videos recorded during site visits. Site visit results, including the case study site, are compiled and presented in this report.

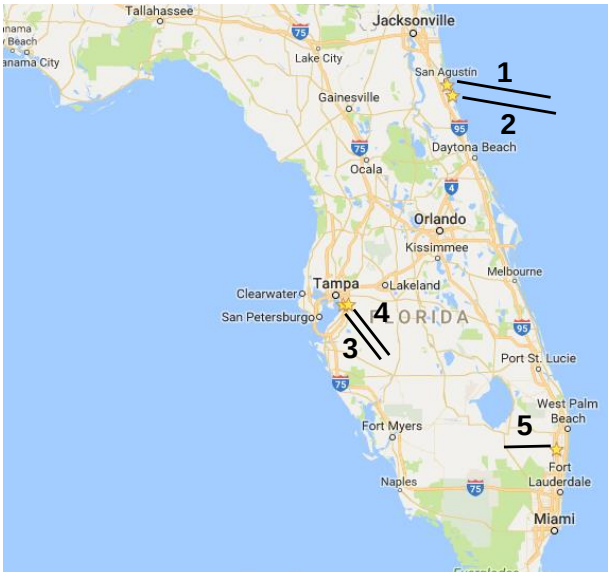

Figure 3.8. Test Locations. Image from Google Maps.

Table 3.8. Test Locations.

Test Site	Water Body	Chloride Content (ppm)
SR-312 over Matanzas R.	Matanzas R.	21,584[1]
SR-206 at Crescent B.	Matanzas R.	23,293[1]
US-41 over Alafia R.	Alafia R.	650[1]
US-301 over Alafia R.	Alafia R.	Null[2]
FL. TP at Boynton B.	Canal west of TP and Canal east of TP	52[3]

1. FDOT environmental data. 2. Hillsborough County EPC database. 3. FDOT reports.

3.2. SR-206 at Crescent Beach over Matanzas River

SR-206 at Crescent Beach is located over Matanzas River, in St. Augustine, Florida. A view of the site is presented in figure 3.9. Sample collection and visual inspection was performed on December 13th, 2016.

Figure 3.9. Views of Crescent Beach Bridge (Site 2).

Figure 3.10a shows the presence of macrofoulers attached to the concrete footer at SR-206 at Crescent Beach. The marine macro-organisms were similar to that observed on SR-312 (Figure 9b) located approximately 8 miles further north on the Matanzas River. The types of marine macro-organisms attached to the substructure are expected to be similar for both sites.

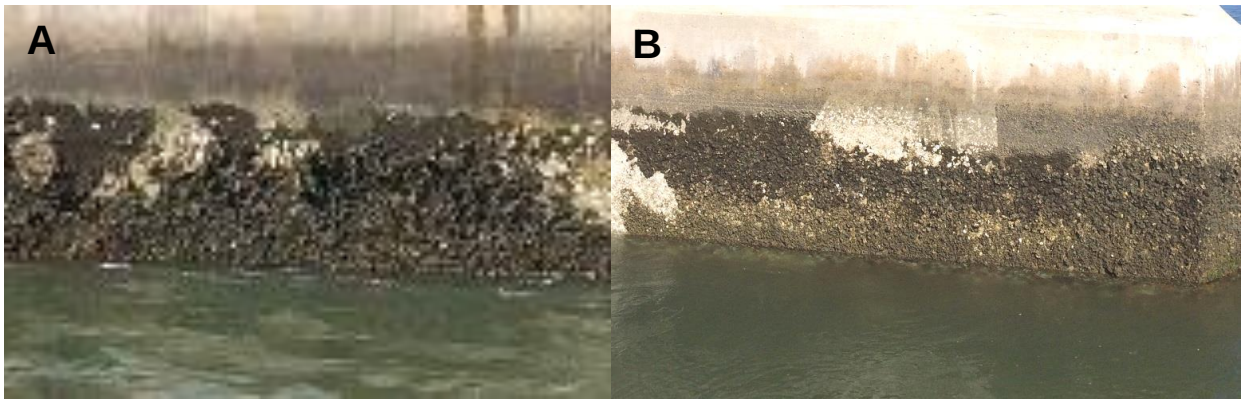

Figure 3.10. Macrofoulers on Concrete Footer (Site 2).

Water samples were collected at different depths reported in feet below high tide (BHT). Water collection was carried out when water line was 2 feet BHT. Samples for water chemistry and microbe assessment were collected at a depth of 3 feet below the water line. The water chemistry and microbiological content results of the water samples tested are summarized in Tables 3.9, 3.10 and 3.11 presented below.

Table 3.9. Microbiological Analysis Results (Site 2).

Bacteria Type	**Values/CFU.mL^{-1}**
Iron-Reducing Bacteria (IRB)	35,000.00
Slime-Forming Bacteria (SFB)	440,000.00
Sulfate Reducing Bacteria (SRB)	115,000.00
Acid Producing Bacteria (APB)	82,000.00

Table 3.10. Chemical Analysis Results (Site 2).

Parameters	**Values**
Sulfate/mg.L^{-1}	2,900.00
Chloride/mg.L^{-1}	20,000.00
Phosphorus/mg.L^{-1}	0.14
Ammonia/mg.L^{-1}	0.03
Iron/mg.L^{-1}	0.55
Nitrate/mg.L^{-1}	0.05
Total Organic Nitrogen/mg.L^{-1}	0.17
Total Nitrogen/mg.L^{-1}	0.20

Table 3.11. Field Dissolved Oxygen, pH, Resistivity, Conductivity, and Water Temperature at Different Depths (Site 2).

Depth/ft	**pH**	**DO %**	**Temp./ C^{o}**	**Resistivity/ ohm-cm**	**Conductivity /mS.cm^{-1}**
5	7.76	93.33	19.00	121.73	46.07
10	7.75	92.27	19.00	123.73	46.10
15	7.71	92.23	19.00	74.04	46.27
20	7.71	92.47	19.00	131.40	46.23

The results of the water chemistry analysis obtained of the site visit were compared with database information of St. Johns River Water Management District in Florida. Chemical analysis (phosphorus, nitrate, salinity, nitrogen, pH, and Temperature) and dissolved oxygen were plotted with time and are presented in Figure 3.11 and 3.12, respectively. For comparison purpose, the recent field data were also plotted and are highlighted.

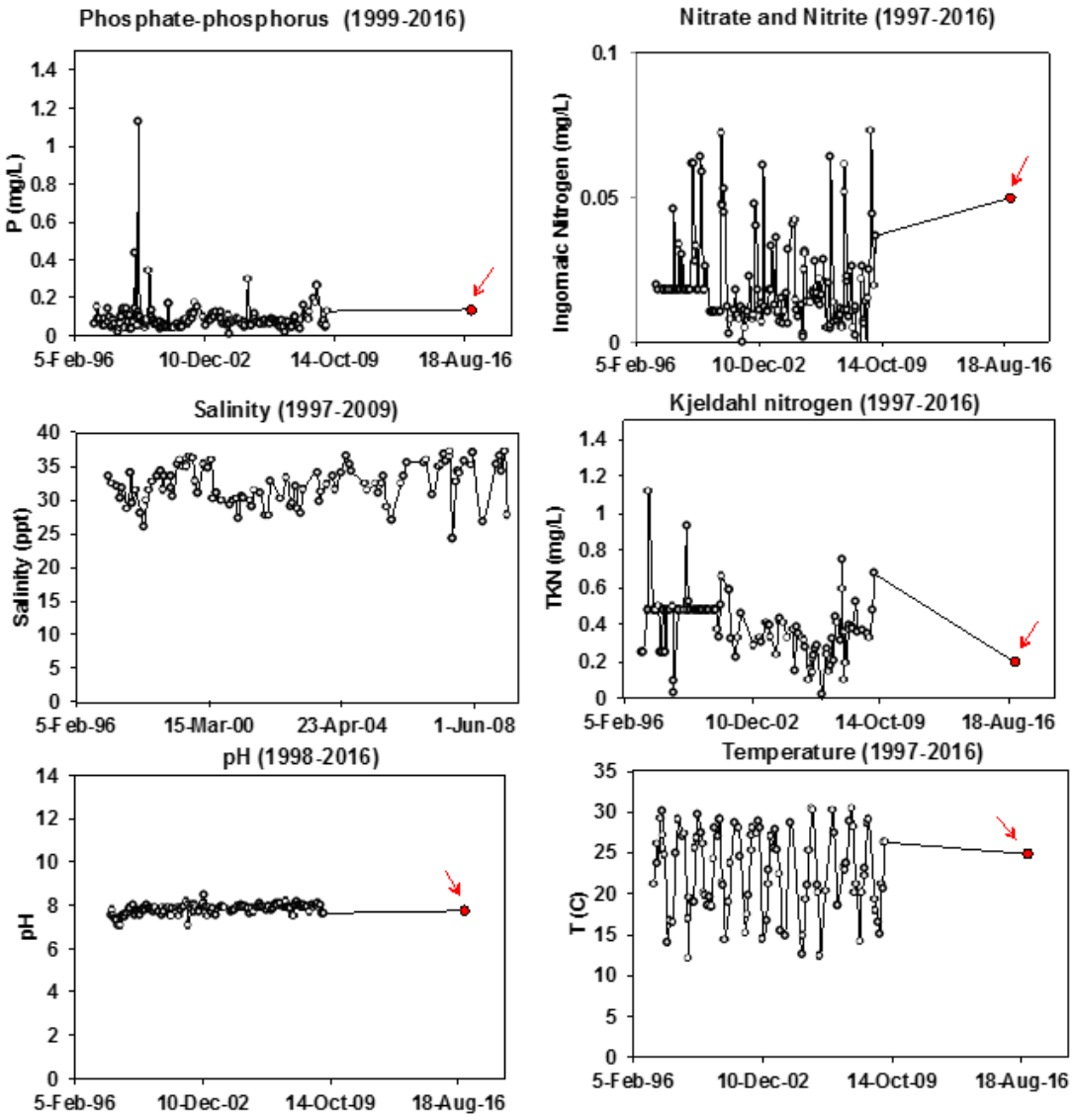

Figure 3.11. Water Chemistry Data of the Site (Site 2).
Red full points: recent measurements during site visit.

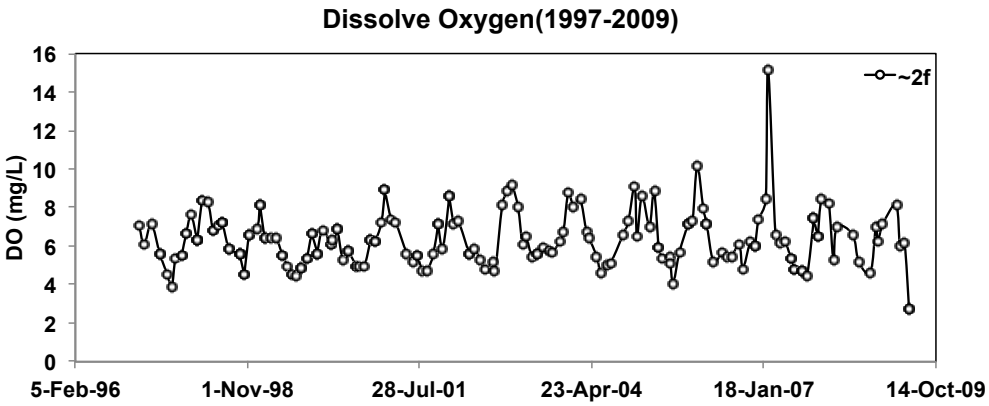

Figure 3.12. Dissolved Oxygen Data (Site 2).

3.3. US-41 over Alafia River

US-41 Bridge over Alafia River was also selected for the investigation. This bridge is very close to the river mouth and next to phosphate mining facilities. Some pictures of the site were taken during the site visit on January 9, 2017 and are presented in Figure 3.13. This bridge has concrete piles.

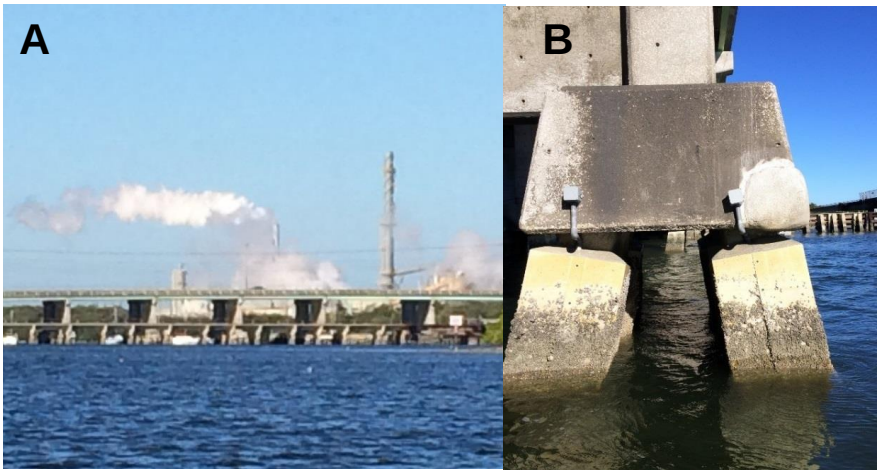

Figure 3.13. Images of the US-41 Bridge over Alafia River (Site 3).
A. View of the bridge and a Mosaic factory in the back. B. View of concrete piles.

Visual analysis of the concrete piles had marine macrofoulers attached to the surface, as observed in Figure 3.14. Images captured from underwater videos performed (Figure 3.15) reaffirms heavy marine growth throughout the submerged portions of the structural element.

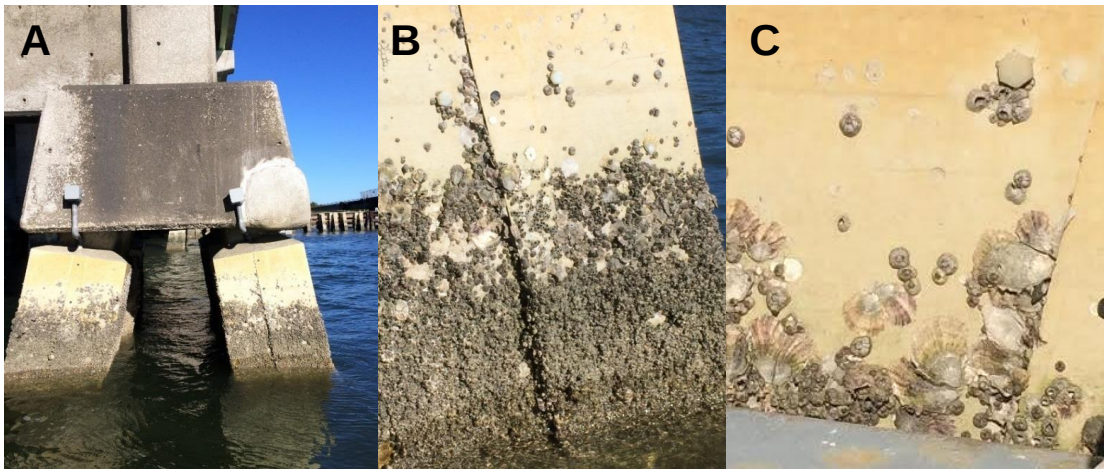

Figure 3.14. Presence of Macrofoulers Attached to Concrete Piles (Site 3).

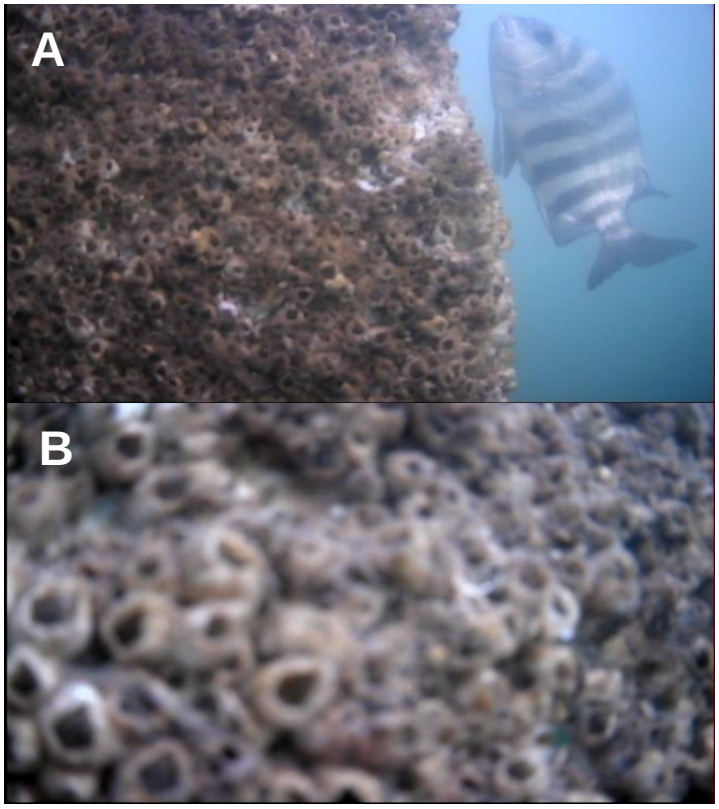

Figure 3.15. Underwater Images of Concrete Piles (Site 3).
A – B. View of marine grow and macrofoulers attached to the surface. B. Zoom of the marine macro-organisms.

Water samples were collected at different depths reported in feet BHT. Water collection was carried out when water line was 2 feet BHT. Results of water chemistry and microbial content determined in the water sample collected during the site visit are summarized in Tables 3.12, 3.13 and3. 14.

Table 3.12. Microbiological Analysis Results (Site 3).

Bacteria	**Values/CFU.mL^{-1}**
Iron-Reducing Bacteria (IRB)	9,000.00
Slime-Forming Bacteria (SFB)	1,750,000.00
Sulfate Reducing Bacteria (SRB)	325.00
Acid Producing Bacteria (APB)	82,000.00

Table 3.13. Chemical Analysis Results (Site 3).

Parameters	**Values**
Sulfate/mg.L^{-1}	620.00
Chloride/mg/L^{-1}	3,800.00
Phosphorus/mg/L^{-1}	0.28
Ammonia/mg/L^{-1}	0.08
Iron/mg/L^{-1}	3.5
Nitrate/mg/L^{-1}	0.65
Total Organic Nitrogen/mg.L^{-1}	0.48
Total Nitrogen/mg.L^{-1}	1.1

Table 3.14. Field Dissolved Oxygen, pH, Resistivity, Conductivity, and Water Temperature at Different Depths (Site 3).

Parameters	**Values**
Depth/ft	5
pH	7.80
DO/mg.L^{-1}	7.90
DO/%	95.40
Temp./C^{o}	16.60
Resistivity/ohm-cm	197.43
Conductivity/mS.cm^{-1}	36.55

The water chemistry data of the site was reviewed and compared with available database information obtained from the Southwest Florida Water Management District. Selected water chemistry database parameters such as phosphate, total suspended solids, total nitrogen, organic carbon, etc. were plotted with time and are visualized in Figure 3.16. Temperature, pH, salinity and biochemical oxygen demand, as well as dissolved oxygen and dissolved oxygen

saturation were also represented with time in Figures 3.17 and 3.18, respectively. For comparative purposes, the water chemistry results of the site visit were also represented in the same graph and are highlighted.

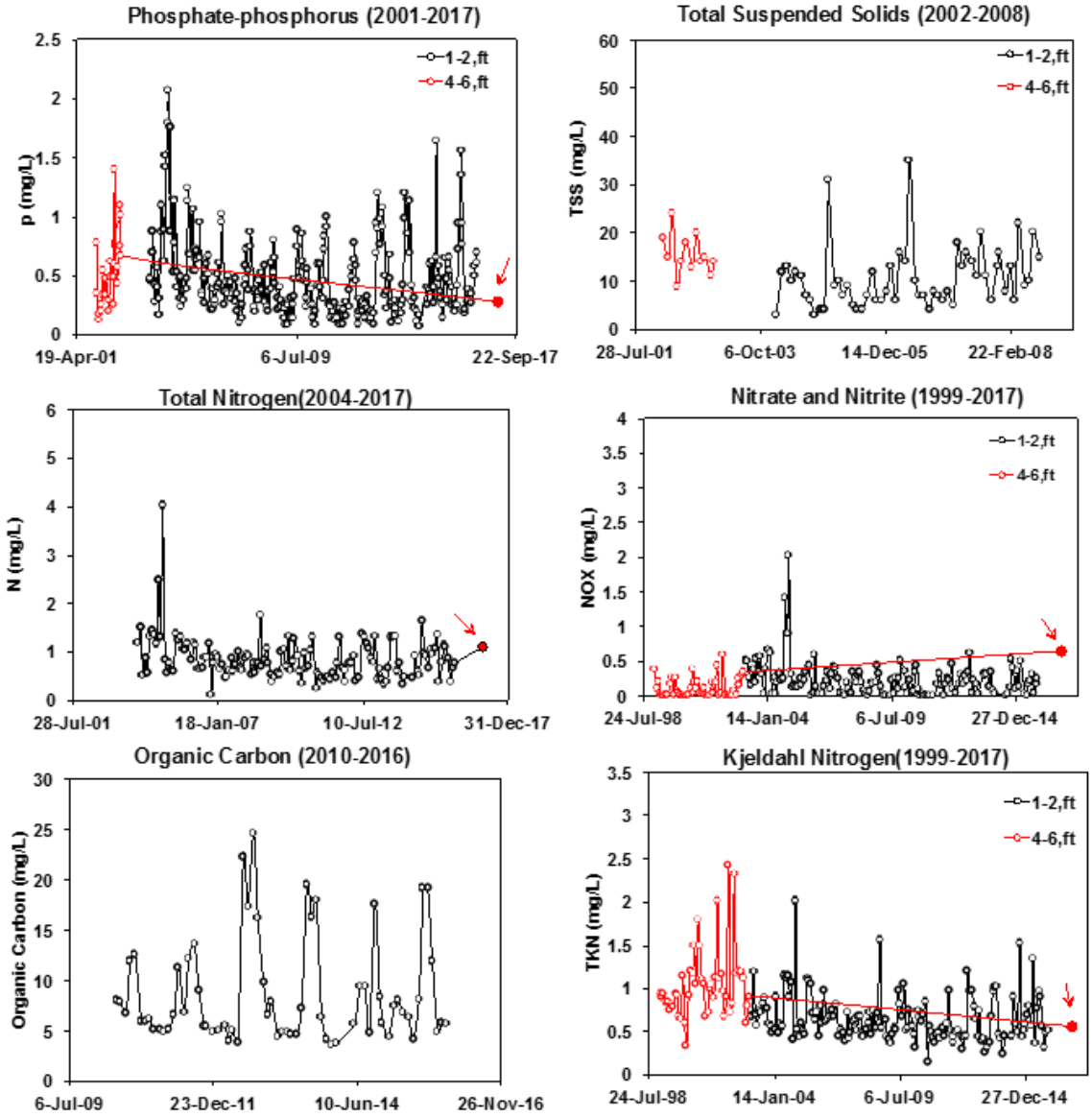

Figure 3.16. Water Quality Data of the Site (Site 3).
Red full points: recent measurements during the site visit.

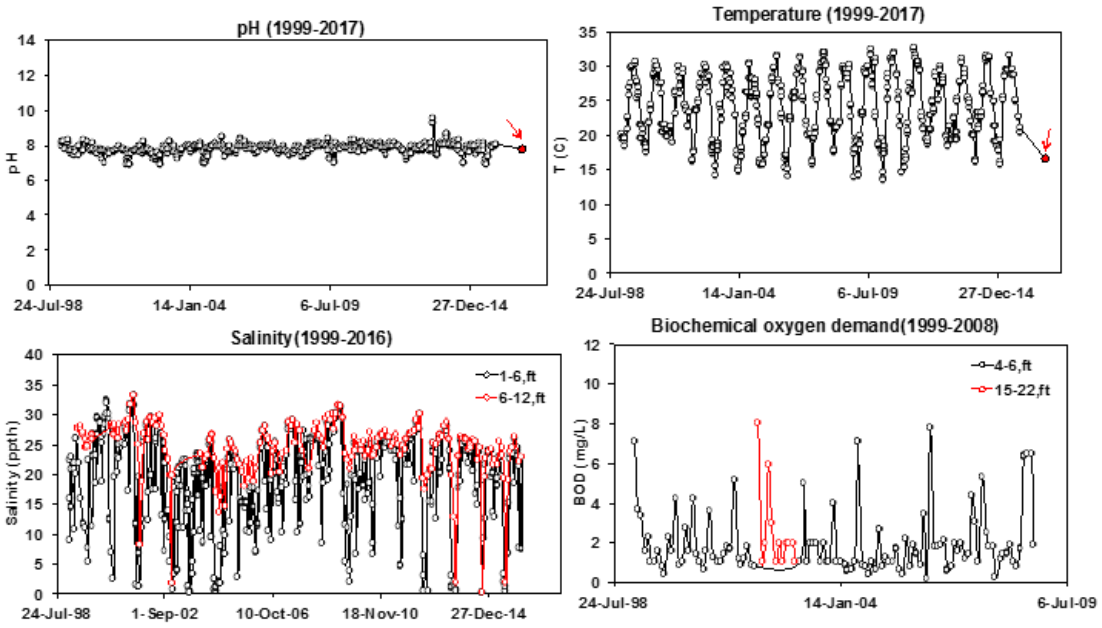

Figure 3.17. Temperature, pH, Salinity, and Biochemical Oxygen Demand with Time (Site 3). Red full point: recent measurements during site visit.

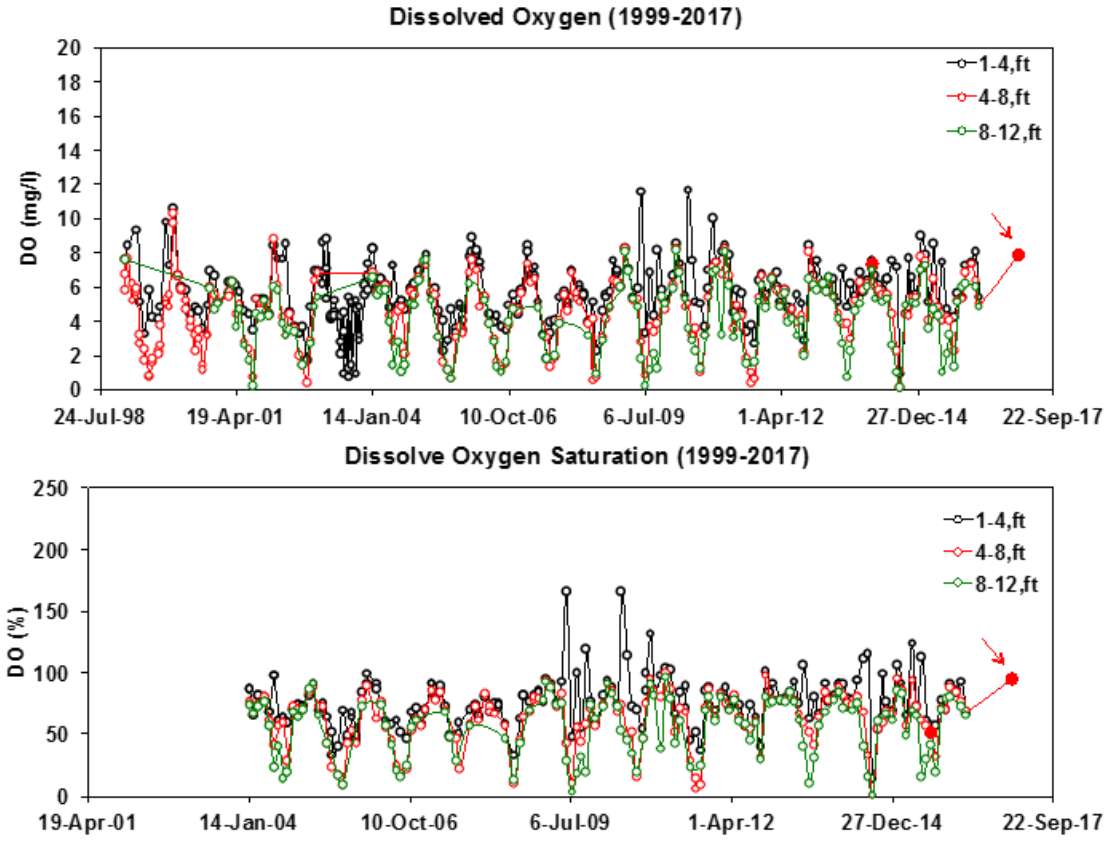

Figure 3.18. Dissolved Oxygen and Dissolved Oxygen Saturation by Time (Site 3). Red full point: recent measurements during the site visit.

3.4. US-301 Over Alafia River

US-301 Bridge over Alafia River was surveyed on January 9th, 2017. The test site location was approximately 8 miles upstream from the US-41 Bridge. It has concrete piles, as depicted in Figure 3.19.

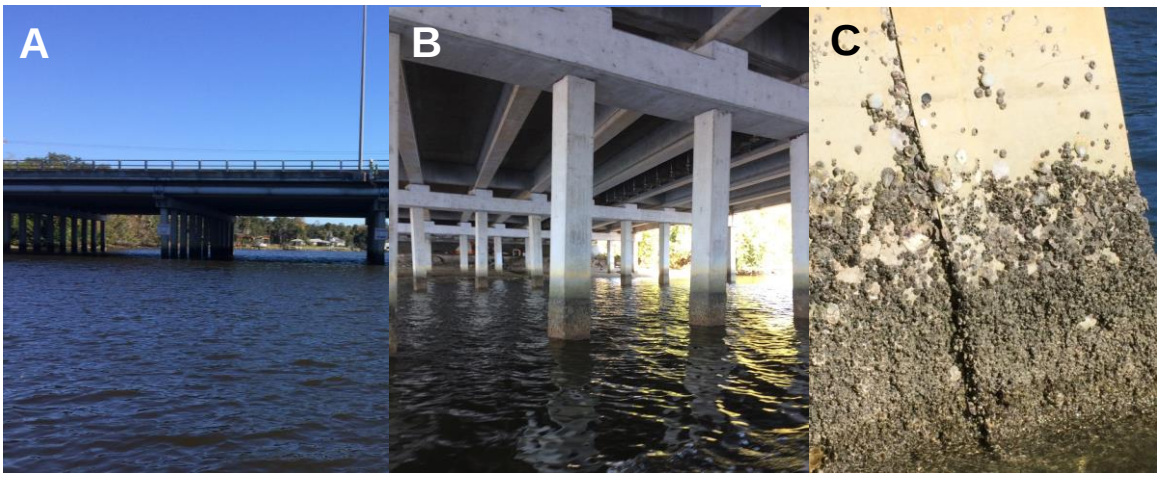

Figure 3.19. Images of US-301 Bridge over Alafia River (Site 4).
A. Bridge view. B. View of the concrete piles. C. Concrete piles with attached macrofoulers.

Visual inspection of the concrete piles was carried out during the site visit. The tidal region of concrete piles showed existence of marine macrofoulers (Figure 3.20). Images obtained from underwater videos (Figure 3.21) reaffirm the presence of marine macro-organisms throughout the submerged portions of the concrete piles due to macrofouling process.

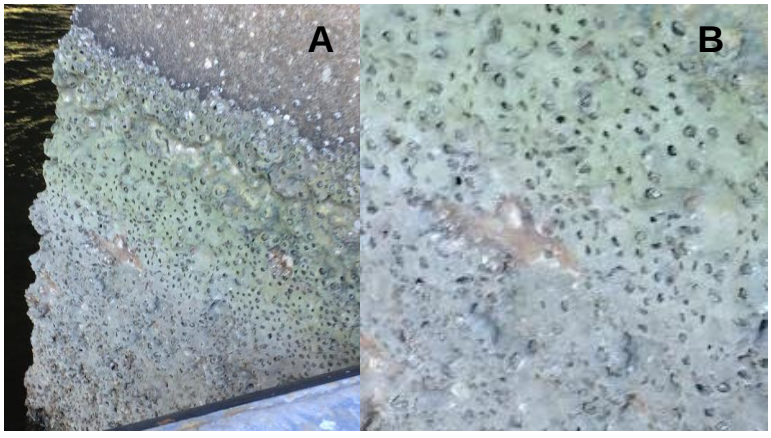

Figure 3.20. Presence of Macrofoulers Attached to Concrete Piles (Site 4).

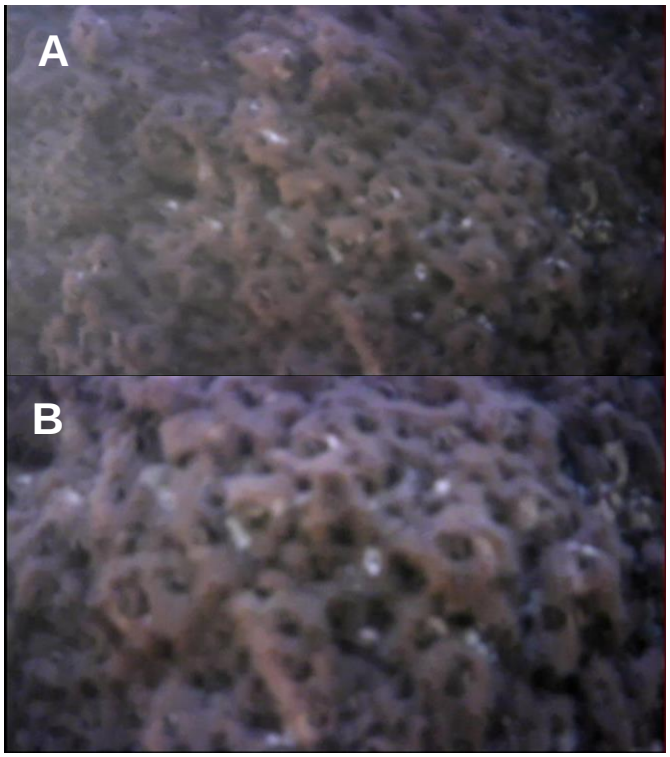

Figure 3.21. Underwater Images of Concrete Piles in US-301 Bridge over Alafia River (Site 4). A. Concrete surface covered with macrofoulers. B. Zoom of the macrofoulers.

Water samples were collected at different depths reported in feet BHT. Water collection was carried out when water line was 2 feet BHT. Results of water chemistry and microbial content determined in the water sample collected during the site visit are summarized in Tables 3.15, 3.16 and 3.17.

Table 3.15. Microbiological Analysis Results (Site 4).

Bacteria CFU/mL	**Values / CFU.mL^{-1}**
Iron-Reducing Bacteria (IRB)	9,000.00
Slime-Forming Bacteria (SFB)	1,750,000.00
Sulfate Reducing Bacteria (SRB)	500,000.00
Acid Producing Bacteria (APB)	82,000.00

Table 3.16. Chemical Analysis Results (Site 4).

Parameters	Values
Sulfate/mg.L^{-1}	2,200.00
Chloride/mg.L^{-1}	16,000.00
Phosphorus/mg.L^{-1}	0.71
Ammonia/mg.L^{-1}	0.04
Iron/mg.L^{-1}	0.15
Nitrate/mg.L^{-1}	0.5
Total Organic Nitrogen/mg.L^{-1}	0.52
Total Nitrogen/mg.L^{-1}	0.56

Table 3.17. Field Dissolved Oxygen, pH, Resistivity, Conductivity, and Water Temperature at Different Depths (Site 4).

Parameters	Values
Depth/ft	5
pH	7.78
DO/mg.L^{-1}	6.53
DO/%	73.37
Temp./C^{o}	16.57
Resistivity/ohm-cm	825.08
Conductivity /mS.cm^{-1}	10.73

The water chemistry data of the site was reviewed and compared with available database information obtained from the Southwest Florida Water Management District. Selected water chemistry database parameters were plotted with time and are visualized in Figures 3.22, 3.23 and 3.24. For comparative purposes, the water chemistry results of the site visit were also represented in the same graph and are highlighted.

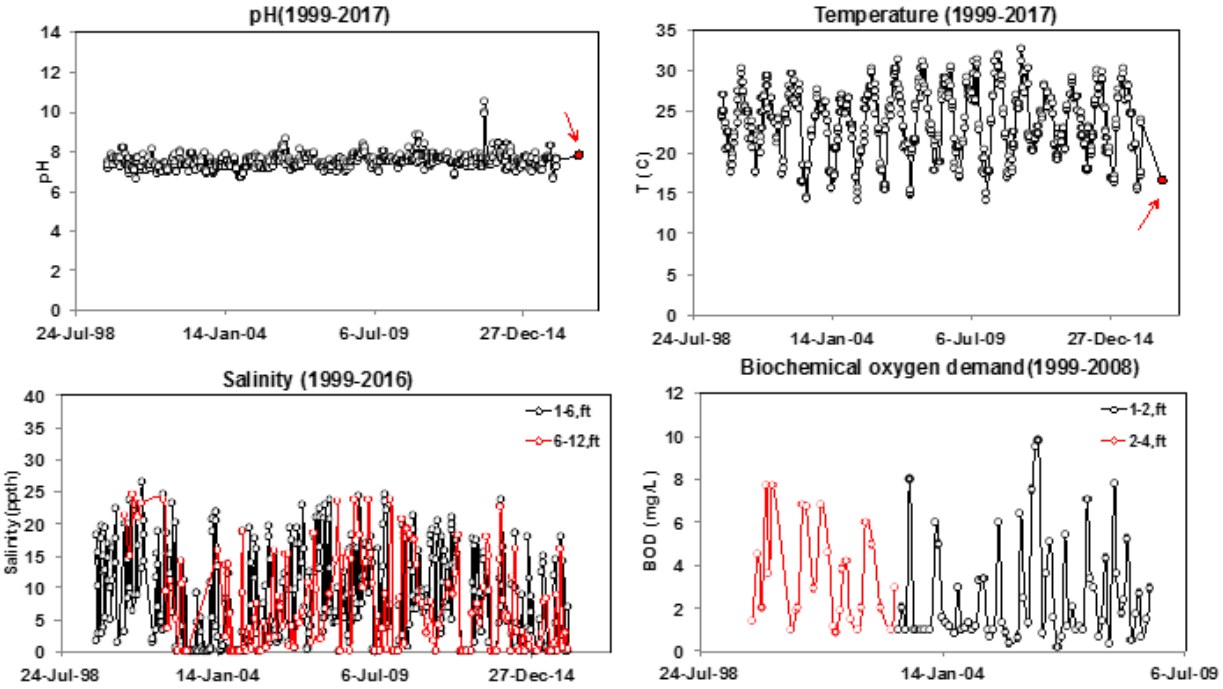

Figure 3.22. Temperature, pH, Salinity, and Biochemical Oxygen Demand with Time (Site 4). Red full point: recent measurement during the site visit.

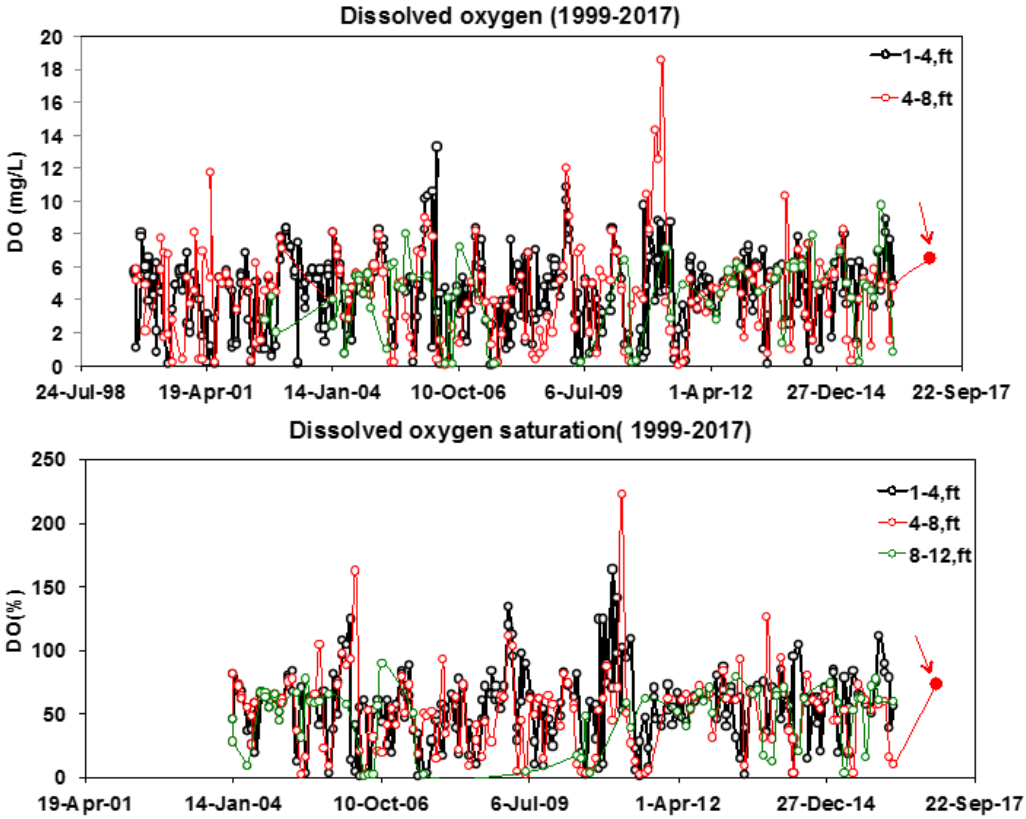

Figure 3.23. Dissolved Oxygen and Dissolved Oxygen Saturation by Time (Site 4). Red full point: recent measurements during the site visit.

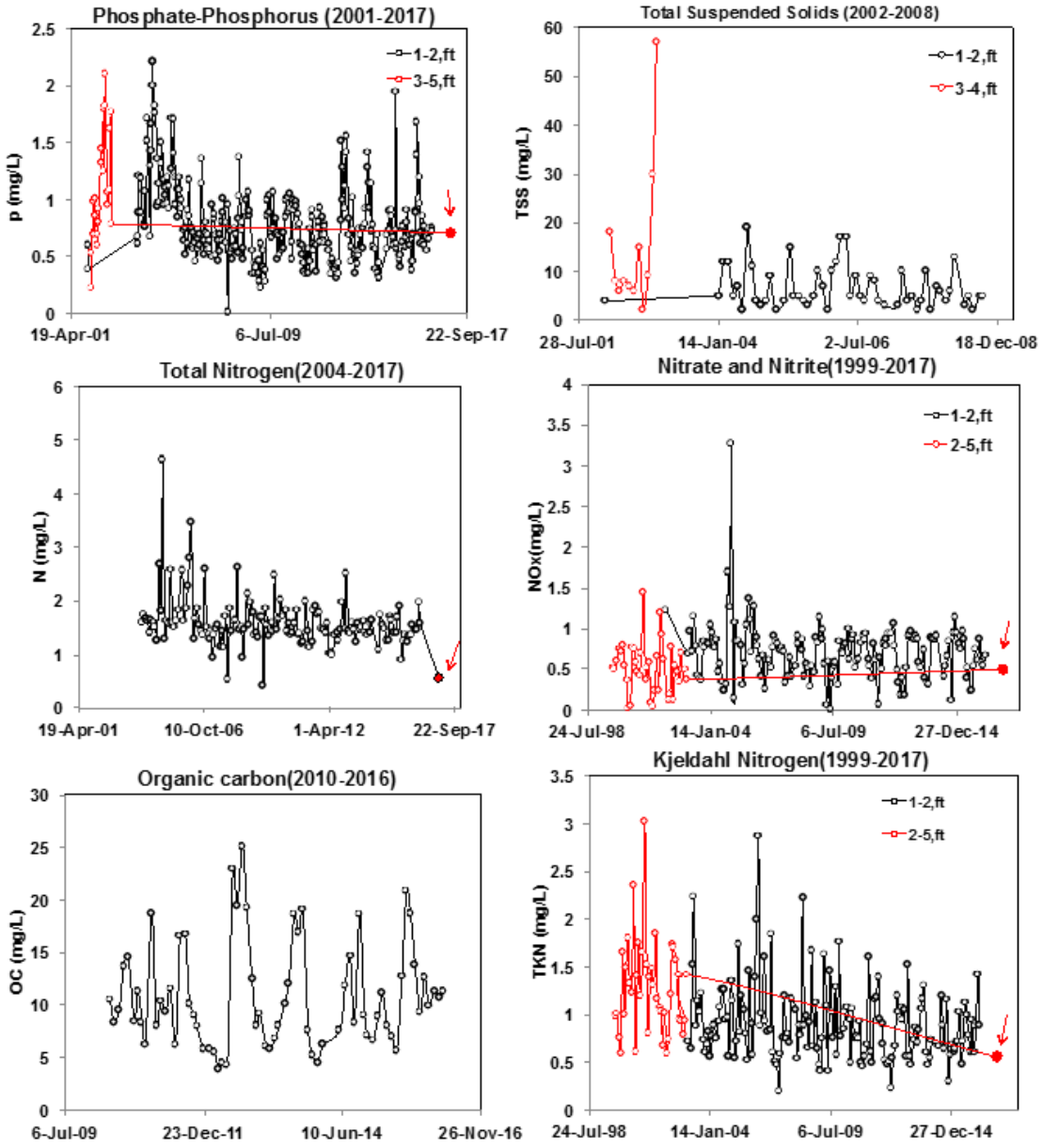

Figure 3.24. Water Chemistry Data with Time (Site 4).
Red full point. Recent measurements during the site visit.

3.5. Florida Turnpike at Boynton Beach

Steel sheet piles on the abutments of canals located on both sides (west and east) of the Florida Turnpike at Boynton Beach Boulevard were investigated on October 31, 2016. Figure 3.25 depicts a view of the selected area (west side).

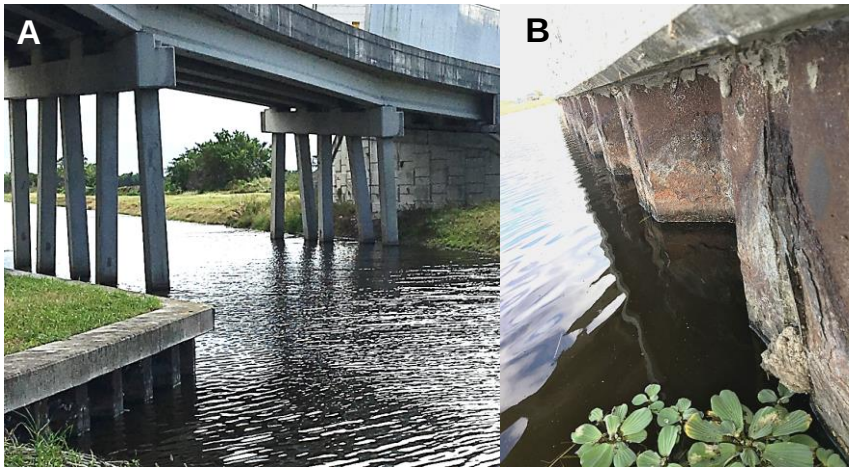

Figure 3.25. Images of Turnpike/Boynton Beach Site (west side) (Site 5).
A. View of the site. B. View of corroded steel piles.

Visual analysis of the steel piles show corrosion deterioration with loss of material, as can be seen in Figure 3.25B. It is depicted the absence of marine growth attached to the steel surface.

In accordance with previous FDOT results, the west side of the canal may have higher pollution level than the east side due to the presence of agricultural land uses adjacent to the canal. Only water samples taken at the west side of the canal were analyzed for water chemistry and microbiological content. However, other physico-chemical parameters such as pH, resistivity, conductivity, dissolved oxygen and temperature were also measured for both sides. The experimental data are presented in Tables 3.18, 3.19 and 23.0. Water samples were collected at different depths reported in feet BHT. Water collection was carried out when water line was 3 feet BHT.

Table 3.18. Microbiological Analysis Results (Site 5).

Bacteria CFU/mL	**Values/CFU.mL^{-1}**
Iron-Reducing Bacteria (IRB)	9,000.00
Slime-Forming Bacteria (SFB)	1,750,000.00
Sulfate Reducing Bacteria (SRB)	500,000.00
Acid Producing Bacteria (APB)	82,000.00

Table 3.19. Chemical Analysis Results (Site 5).

Parameters	Values
Sulfate/mg.L^{-1}	48.00
Chloride/mg.L^{-1}	94.00
Phosphorus/mg.L^{-1}	0.11
Ammonia/mg.L^{-1}	0.16
Iron/mg.L^{-1}	0.14
Nitrate/mg.L^{-1}	0.53
Total Organic Nitrogen/mg.L^{-1}	1.40
Total Nitrogen/mg.L^{-1}	2.20

Table 3.20. Field Dissolved Oxygen, pH, Resistivity, Conductivity, and Water Temperature at Different Depths (Site 5).

Location	Depth /ft	pH	DO/%	Temp./ C^{o}	Resistivity/ ohm-cm	Conductivity/ MicroS.cm^{-1}
TP-Boynton Beach ***(West side)***	1	7.71	68.70	24.30	8587.63	756.00
	3	7.63	65.87	24.23	9164.58	759.00
TP-Boynton beach ***(East side)***	1	7.65	76.43	24.53	9531.43	754.33
	3	7.62	70.58	24.63	9114.56	756.00
	8	7.64	56.98	24.00	8844.42	752.75

TP. Turnpike

In this section, the water chemistry results of the site visit to canals were reviewed and compared with database information from the South Florida Water Management District were the canals are located. Selected water chemistry database parameters were plotted with time and are presented in Figure 3.26, 3.27 and 3.28. For comparative purposes, the water chemistry results of the site visit were also represented in the same graph and are highlighted.

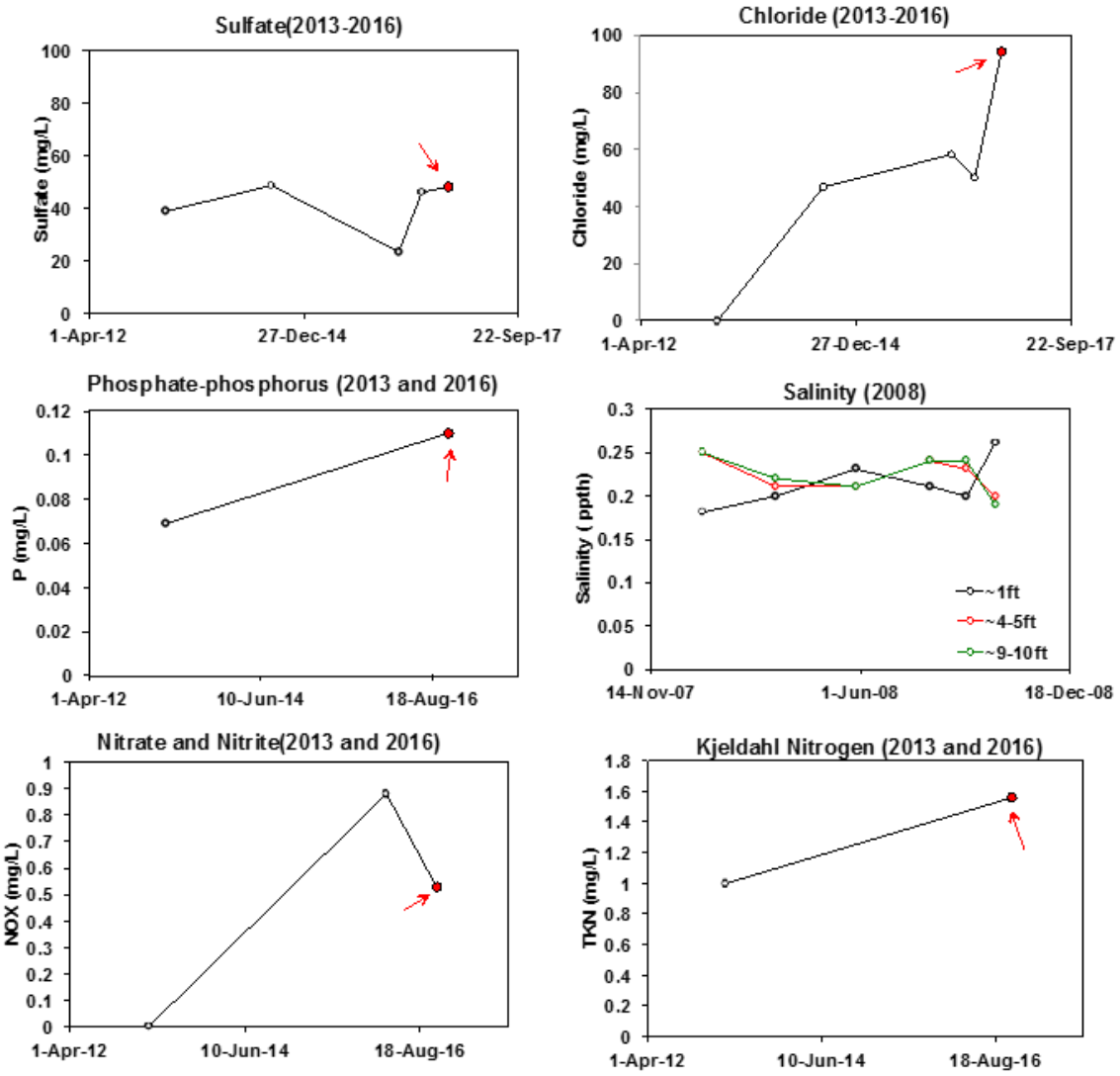

Figure 3.26. Water Chemistry Data of the Site (Site 5).
Red full point: recent measurements during site visit.

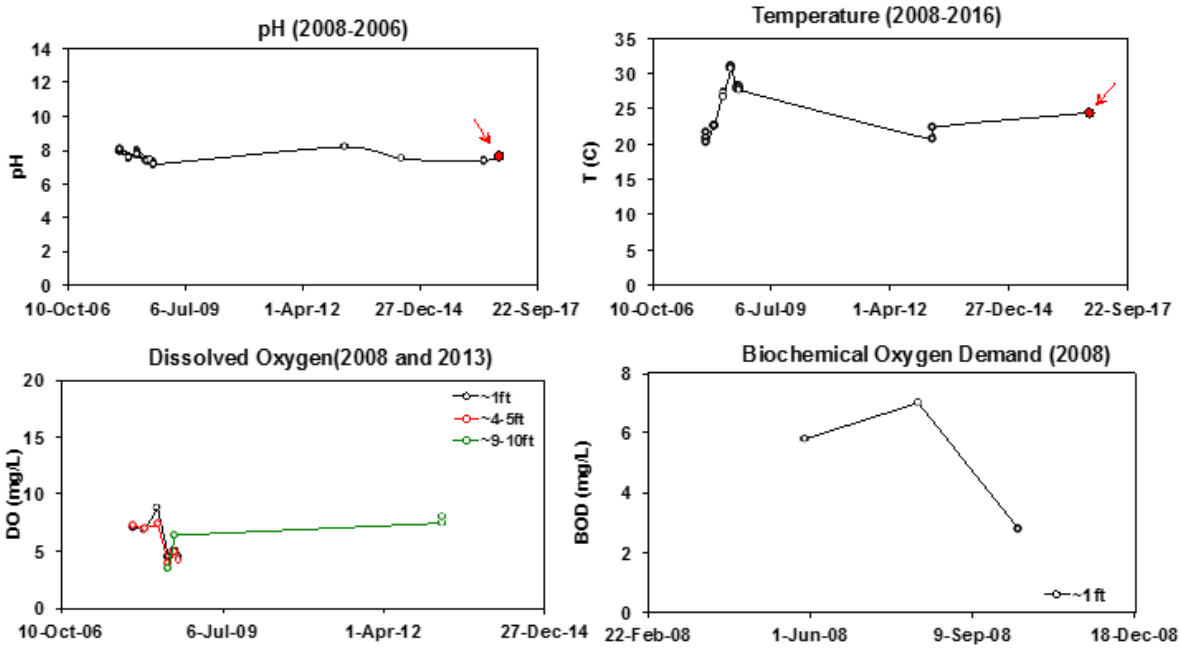

Figure 3.27. Temperature, pH, Biochemical Oxygen Demand, and Dissolved Oxygen Data (Site 5). Red full point: recent measurements during site visit.

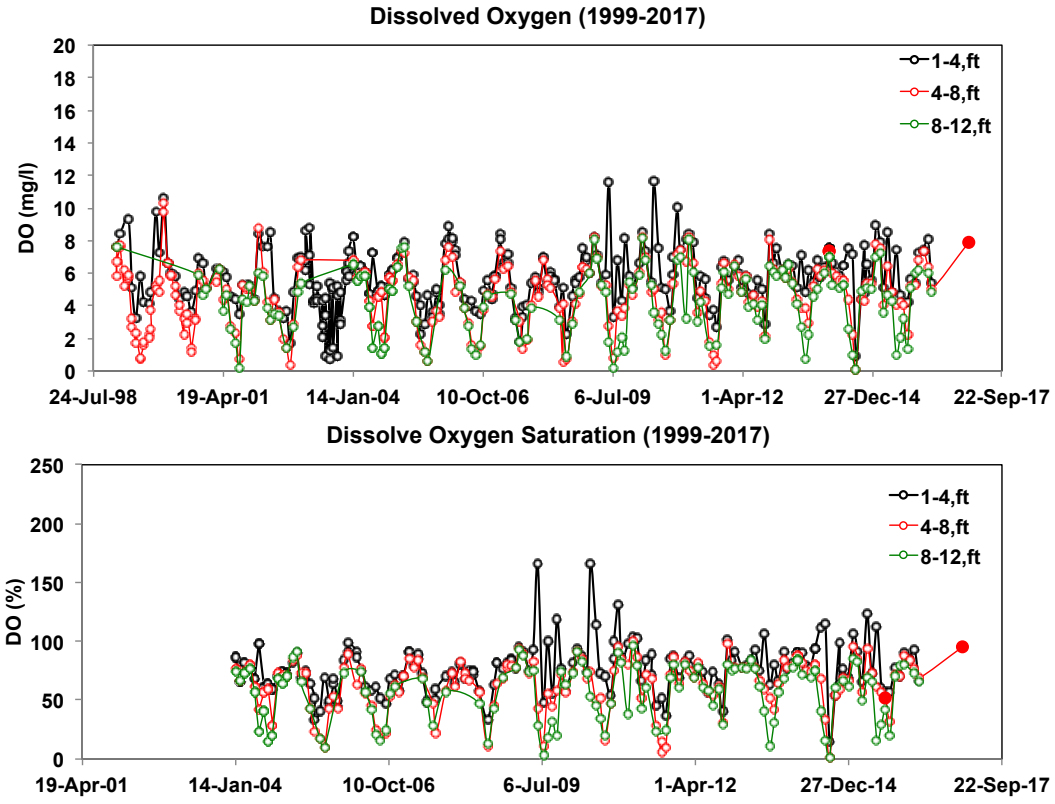

Figure 3.28. Dissolved Oxygen and Dissolved Oxygen Saturation by Time (Site 5). Red full point: recent measurements during the site visit.

3.6. Macrofouler Characteristics

Pictures taken from four selected sites in this study show different types of macrofoulers (varying from site to site), which were attached to the submerged steel/concrete piles (Table 3.21). These macrofoulers included hydroids, tunicates, diatoms, algae, and barnacles. Comparison between stock reference photos of identified species (reference picture) and photos from the sites is made in table 3.21.

Table 3.21. Comparison Between Reference Photos and Photos of Macrofoulers Attached to the Submerged Steel and Concrete Piles from the Sites. (Continues).

Pictures from site visit	**Suspected macrofoulers (Reference pictures)**	
Site 1		
 Tunicates	 *Didemnum perlucidum*[1]	 *Didemnum vexillum*[2]
 Hydroids	 *Plumularia*[3]	 *Aglaophenia*[3]
		
Acorn Barnacle	*Megabalanus coccopoma*	

Table 3.21. (Continued). Comparison Between Reference Photos and Photos of Macrofoulers Attached to the Submerged Steel and Concrete Piles from the Sites.

Site 3		
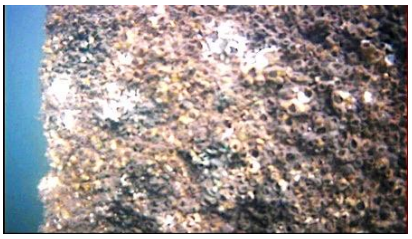		
Bay Barnacles	*Amphibalanus improvisus*,	
Site 4		
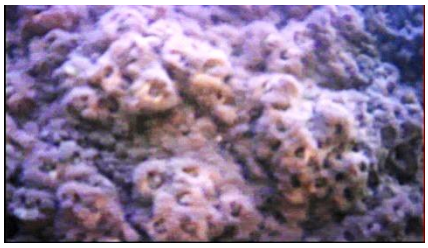		
Bay Barnacles	*Semibalanus balanoides*[5]	
Site 5		
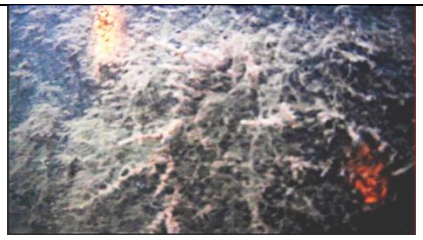		
Macroalgae		

(1.Fofonoff PW, 2003; 2. Alaska Department of Fish and Game; 3. SeaNet; 4.Wikipedia; 5.VISINDAVEFURINN)

3.7. Field Survey Checklist for Corrosion Assessment

A field survey checklist is proposed in this section with the aim of evaluating (quantitative and qualitative) the different stages of corrosion and deterioration of steel/concrete samples exposed to field conditions. Quantitative parameters will include microbiological and water chemistry analysis (water samples), as well as corrosion measurements (linear polarization resistance-LPR, OCP, etc.) and corrosion products analysis, etc. Qualitative evaluations of coupons will consider visual inspection of samples as well as general information about environmental conditions of each location under study. This will also include parameters that will measure the performance of different surfaces over time. The lists of parameters considered for the field survey checklist are presented in table 3.22.
The checklist parameters for the field survey are organized in three different categories, which are explained below:

Category 1: Essential parameters that support microbial activity
Category 2: Primary conditions related to MIC
Category 3: Indirect environmental factors supporting microbial activity and MIC
Category A: Parameter for measuring bacteria
Category B: Parameters for measuring deteriorationTable 15: Field survey checklist and parameter categories for each selected site.

Table 3.22. Field Survey Checklist and Parameter Categories for Each Selected Site (Continues).

	Category
Structure	Concrete/ Steel
Seasonal effects/General	
Tide levels	3
Air temperature	3
Sunshine	3
Water depth	3
Fluid flow (hydrodynamic)	3

Table 3.22. (Continued). Field Survey Checklist and Parameter Categories for Each Selected Site.

Seawater analysis	
Temperature	2
pH	2
Conductivity	3
Dissolved oxygen	2
Sulfate	2
Chloride	2
Phosphorus	1
Ammonia	1
Iron	2
Nitrate	1
TON	1
Total N	1
COD or BOD	A
Optical density=turbidity	3
SRB	2
IRB	2
APB	2
SFB	2
Surface condition (samples and piles)	
Coloration (corrosion products)	2
Corrosion progress	2
Corrosion products characteristics	2
Corrosion products morphology	2
OCP, LPR,	B
Deterioration progress (concrete surfaces)	B
Morphology of concrete deterioration	B
Microbial growth/Macrofoulers	2
Thickness loss (piles and samples)	B

4. FIELD CORROSION TESTING

4.1. Methodology

Steel samples were installed at three Florida sites (Table 4.1). These sites included SR-312 Bridge over Matanzas river (St. Augustine), US-41 bridge downstream over Alafia river (Tampa Bay) and US-301 bridge upstream over Alafia river (Tampa Bay). The selected sites comprised of different types of water bodies (estuarial/brackish and fresh water) with environmental conditions that support MIC. Table A1 shows environmental, chemical, and microbial characteristics of the test sites.

The 5X3X1/8" steel coupons (composition of 0.02%C, 0.16 % Mn, 0.006% S and 0.03% Si) were installed on test racks made up of a polypropylene sheet attached to an aluminum frame secured to a bridge pier. For all three test sites, three surface roughness were prepared for the steel coupon samples: as-received, 60 grit, and 400 grit. The test steel coupons placed in three Florida natural waters (Table A1) had heavy marine fouling shortly after initial immersion and continued to accumulate encrustation up to the time of retrieval.

Figure 4.1 shows an example test rack with marine growth. Sample placement was measured relative to the marine growth line, identified as distance below the marine growth line (BMG). The position of the test racks of each test site relative to the water surface varied due to the variation in the geometry of the test site bridge substructure where the test racks were installed as well as due to variation in tidal levels.

Generally, the test sites had some samples exposed in atmospheric conditions but were subjected to spray and tidal action as well as samples permanently submerged in water. Table 4.2 shows the depth locations of test sample and test condition at each test site. At site I, barnacles were predominant in the tidal region. Hydroids and marine flora amassed below low tide levels. At the site II and III, barnacles were the predominant macrofouler down to the depth of the test frame. The barnacles were more prolific at the Site II.

Figure 4.1. Typical Outdoor Exposure Test Rack at Three Sites.

Table 4.1. Field Test Sites.

Test Sites	Samples Installation Date	Samples Retrieval Date	Time of Exposure (Days)
Matanzas R. (Site I)	07/18/2017	04/25/2018	281
Alafia R. (Downstream) (Site II)	11/12/2017	07/18/2018	248
Alafia R. (Upstream) (Site III)	01/30/2018	07/17/2018	168

Table 4.2. Experimental Test Condition.

Test Sites	Steel Condition	No. of Coupons	Distance BMG (ft)
Matanzas R. (Site I)	As-received	14	~2 to 8
	400 Grit surface roughness	14	~2 to 8
	60 Grit surface roughness	14	~2 to 8
Alafia R. (Downstream) (Site II)	As-received	14	~ -0.5* to 6
	400 Grit surface roughness	14	~ -0.5* to 6
	60 Grit surface roughness	14	~ -0.5* to 6
Alafia R. (Upstream) (Site III)	As-received	14	~0 to 6
	400 Grit surface roughness	14	~0 to 6
	60 Grit surface roughness	14	~0 to 6

* Minus sign denotes distance above the marine growth line.

Interim verification tests to identify marine fouling and surface bacterial growth were made 1-2 months after initial installation for site I and II sites. Project delays prohibited interim testing at the site IIII site. Those interim tests included visual photo-documentation of steel coupon surface conditions and analysis of developed surface bacteria population. The test racks were temporarily removed from the bridge pier to allow closer onsite inspection. The surface fouling was left intact for the photo-documentation, but marine growth was removed on small portions (~1 in^2) of the coupons where swabs were collected for the microbiological analysis. Biological Activity Reaction Test (BART) kits were used to assess the population and the activity of the four common MIC related bacteria (SRB, IRB, SLYM and APB) on the steel coupon surface below the layers of marine growth.

Corrosion potentials were measured upon installation, during the interim testing and just prior to test rack decommissioning. A copper/copper-sulfate electrode dipped in the river was used as the reference electrode.

The test racks were decommissioned after ~280 days for site I, ~248 days for site II, and ~168 days for site III. The test samples were removed from the test rack and stored in sealed containers containing river water for transport back to the laboratory. In the laboratory, individual coupons were immersed in collected river water only immersing 3.5 inch of the coupon in solution. The immersed surface area was ~52 in^2. Additional electrochemical tests were made in the laboratory. Corrosion measurement consisted of measurements of the open circuit potential (OCP), linear polarization resistance (LPR), and electrochemical impedance spectroscopy (EIS). A saturated calomel electrode (SCE) was used as a reference electrode for all tests. An activated titanium mesh was used as the counter electrode. The scanned potentials for the LPR testing was made from the open-circuit potential and cathodically polarized 25 mV at a scan rate of 0.1 mV/s. The corrosion current density was calculated with from the polarization resistance, Rp, following the equation icorr=B/(RpxA) where B was assumed to be 26 mV and A was the nominal surface area of steel coupon immersed in the solution. EIS testing was made at the OCP condition with 10 mV AC perturbation voltage from frequencies 1MHz > f >1Hz. Figure 2 shows an example of the electrochemical testing in the laboratory.

All retrieved samples were hand cleaned to remove surface fouling and photo documentation of surface corrosion was made under magnification with a stereo microscope. Remnant traces of barnacle attachment as well as maximum corrosion pit diameter and pit depths were documented. Select samples from various immersion depths were further cleaned following ASTM G1-03 but immersed in cleaning solution for up to 2 hours. The difference in mass before and after outdoor exposure was used to calculate the apparent corrosion rate.

4.2. Visual Observation (Marine Biofouling)

4.2.1. Site I

Heavy fouling occurred during the 281 days of exposure (Figure 4.2). The general fouling organism of SR-312 (Matanzas River) were hydroids, bryozoans, barnacles, and oysters. During the period of exposure, fouling organisms consisted mostly of clustered acorn barnacles at 3-4 ft below marine growth (BMG) and soft marine masses (hydroids) at 4-8ft BMG along with isolated acorn barnacles at deeper depths. The species of the acorn barnacle at the intertidal zone can be recognized as *Amphibalanus Amphitrite* (diameters less <10 mm) and *Megabalanus coccopoma* in the immersion zone (diameters > 10 mm diameter) at immersion zone. Both species are common coastal and estuarine organisms. Settlement of fouling organisms on steel substrates typically included initial bacteria biofilm formation, preferential settlement of diatoms, colonization of bryozoans, and growth of barnacles and oysters. Figure 4.5 shows exposed samples before and after cleaning with three surface conditions at various depth (2-8ft BMG).

Figure 4.2. Example of Marine Fouling on Outdoor Test Racks.

4.2.2. Site II

Steel coupons were exposed for 248 days at US-41 which resulted in a very dense coverage of macrofouling organism (Figure 4.3), primarily bay barnacles, *Amphibalanus improvisus*, occurring in the brackish water environment at the mouth of the Alafia River emptying into the Gulf of Mexico. Barnacle diameters ranged from 5 to 16 mm. Clustered and interlayered populations of barnacles were observed from 2-5.5 ft. BMG. One sample in each surface condition was placed at 0.5 ft above the marine growth line (and as expected no marine fouling occurred there). Samples at 0.5 to 1 ft BMG developed a thick iron oxide layer even after hand cleaning. Fouling and oxide layers could be easily hand cleaned on samples from 2 to 5.5 ft BMG and revealed non-uniform sinuous texture. It was observed that the attachment of macrofouler on samples with 60 and 400 grit surface roughness were not as strong as samples in the as-received condition. Figure 4.6 shows exposed samples before and after cleaning with three surface conditions at various depth (-0.5-5.5ft BMG).

Figure 4.3. Example of Marine Fouling on Outdoor Test Racks.

4.2.3. Site III

Steel coupons were exposed in Alafia River at US-301 for 168 days (Figure 4.4). Similar fouling organisms as the US-41 site were observed but the barnacle population was significantly lower due to the lower salinity and nutrient levels upstream. The barnacles were clustered at 2-4.5 ft BMG but in less dense communities as compared to the US-41 site. Barnacle diameters were from 5 to 15 mm. Samples at 0.5 to 2ft BMG (intertidal zone) had thick outer oxide film with rough surface after cleaning. Figure 4.7 shows exposed samples before and after cleaning with three surface conditions at various depth (0.5-6ft BMG).

Figure 4.4. Example of Marine Fouling on Outdoor Test Racks.

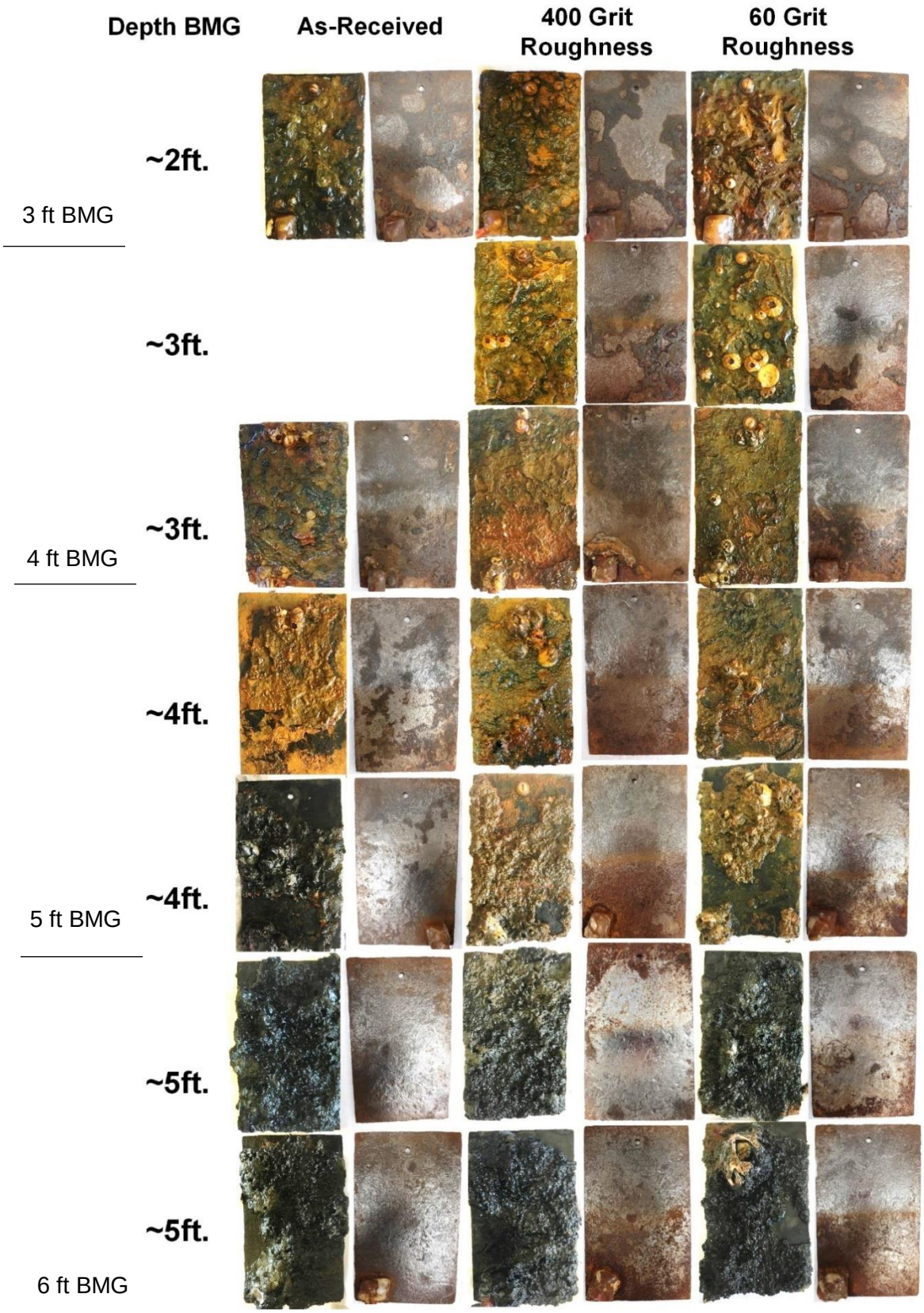

Figure 4.5. Test Coupons Exposed in Matanzas River at SR-312. (Continues).

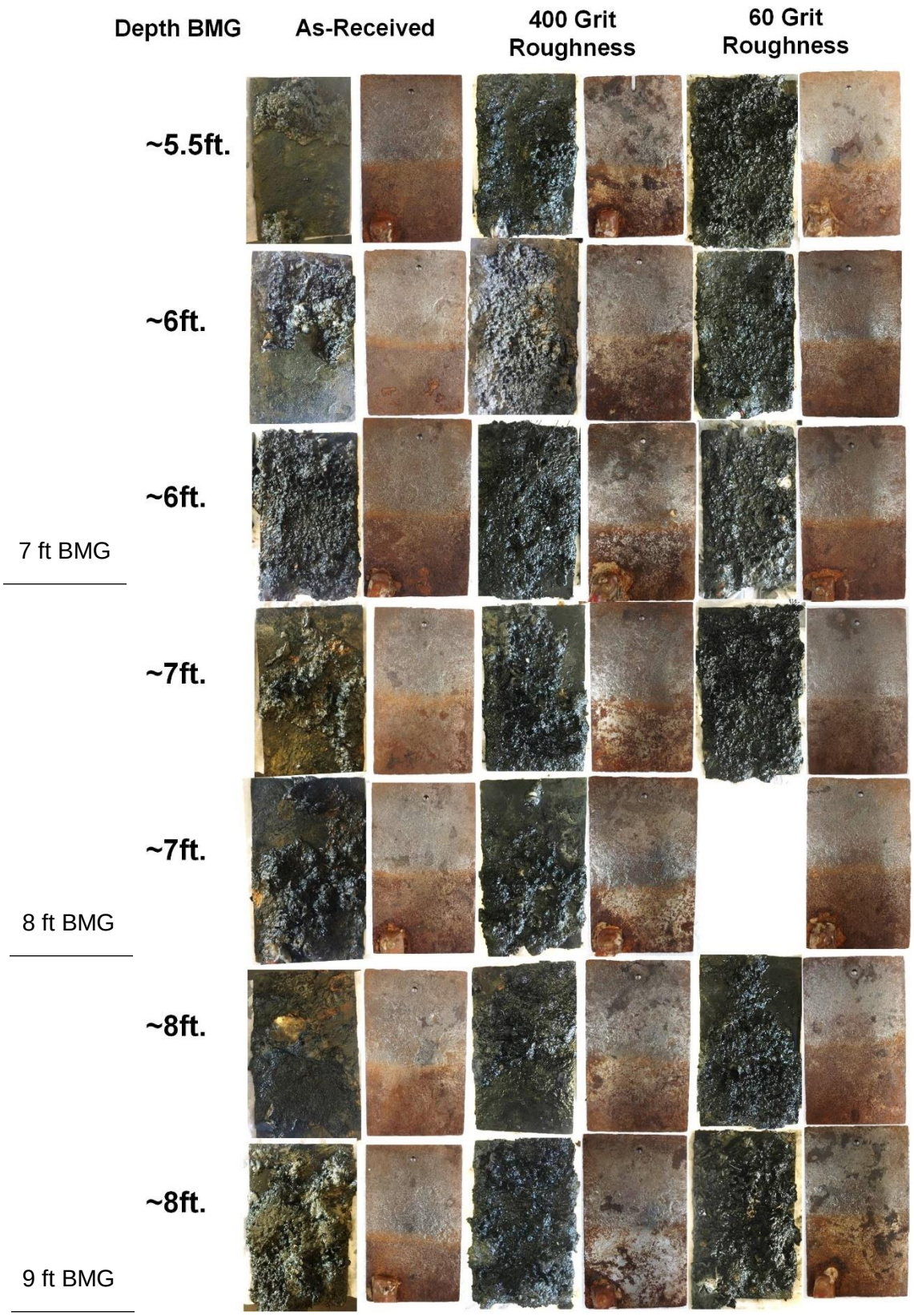

Figure 4.5. (Continued). Test Coupons Exposed in Matanzas River at SR-312.

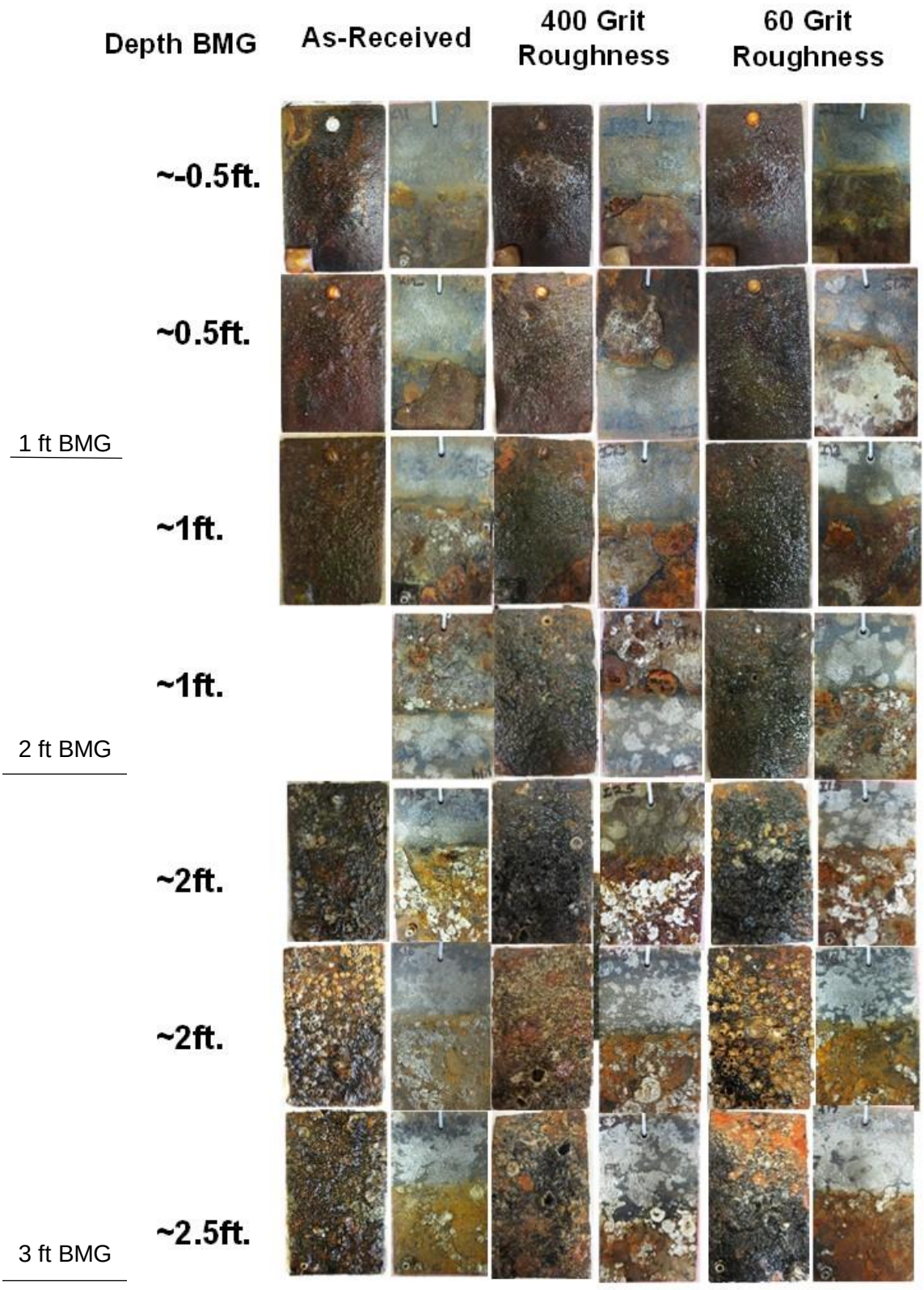

Figure 4.6. Test Coupons Exposed in Alafia River at US-41. (Continues).

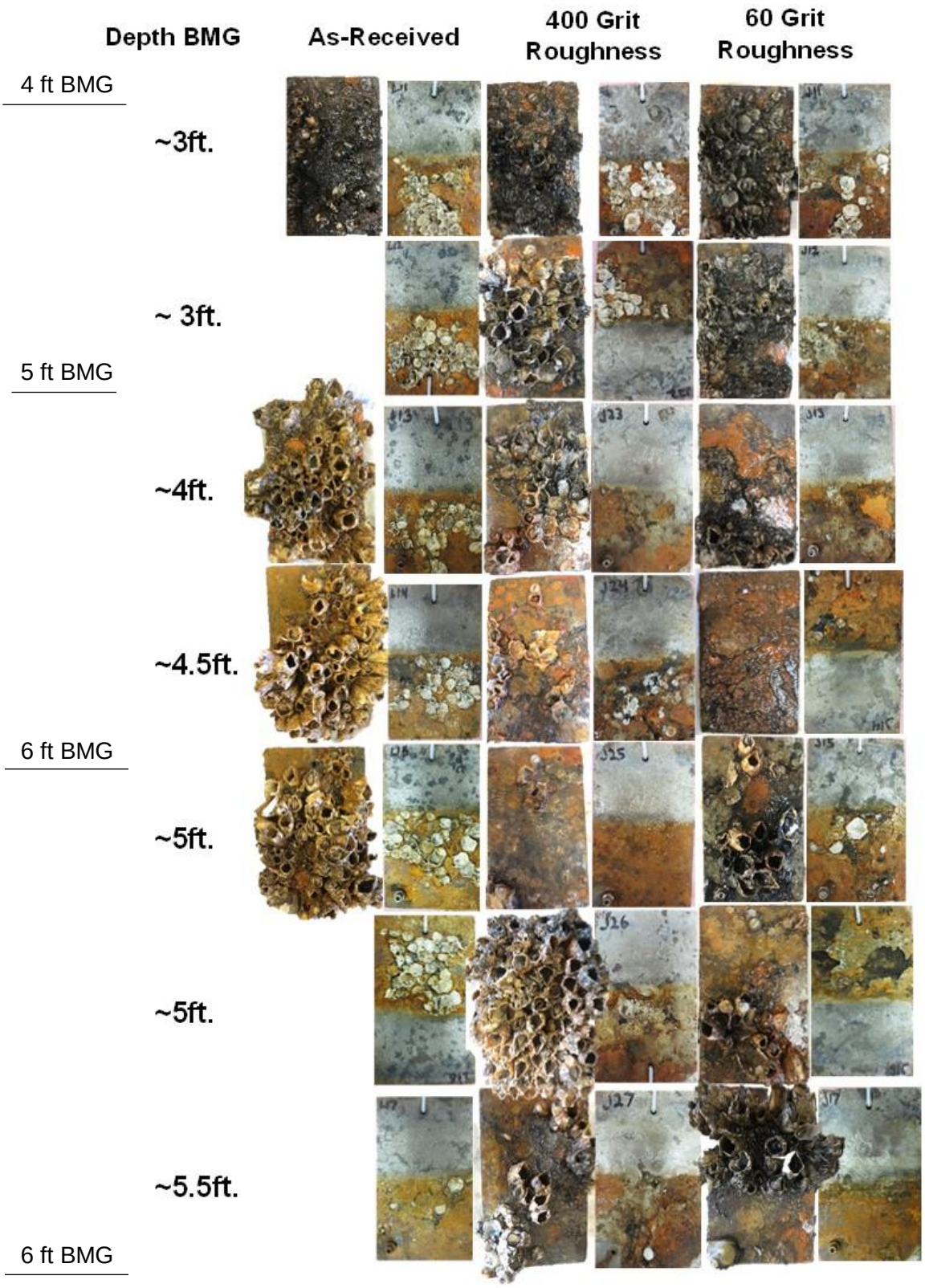

Figure 4.6. (Continued). Test Coupons Exposed in Alafia River at US-41.

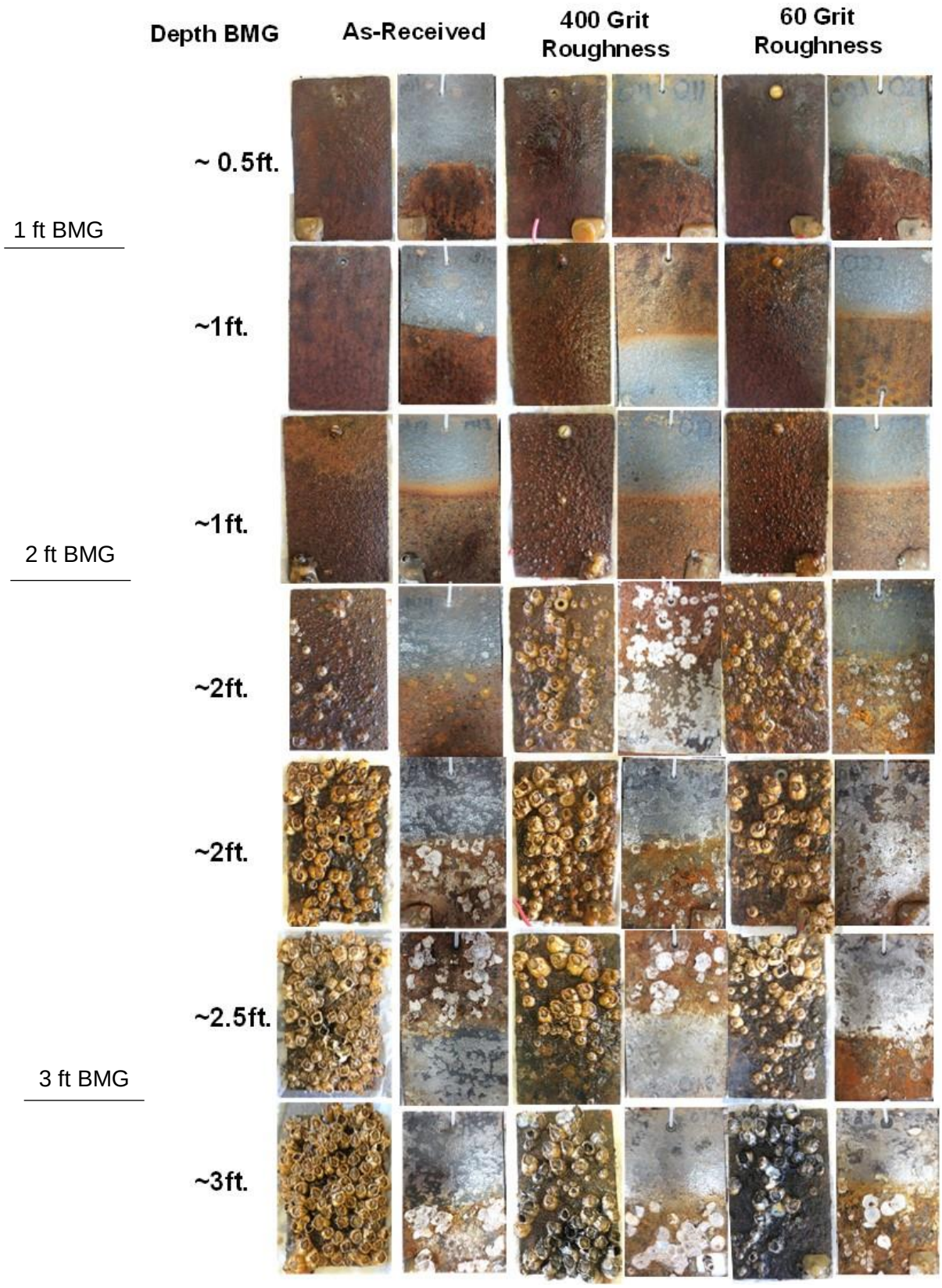

Figure 4.7. Test Coupons Exposed in Alafia River at US-301. (Continues).

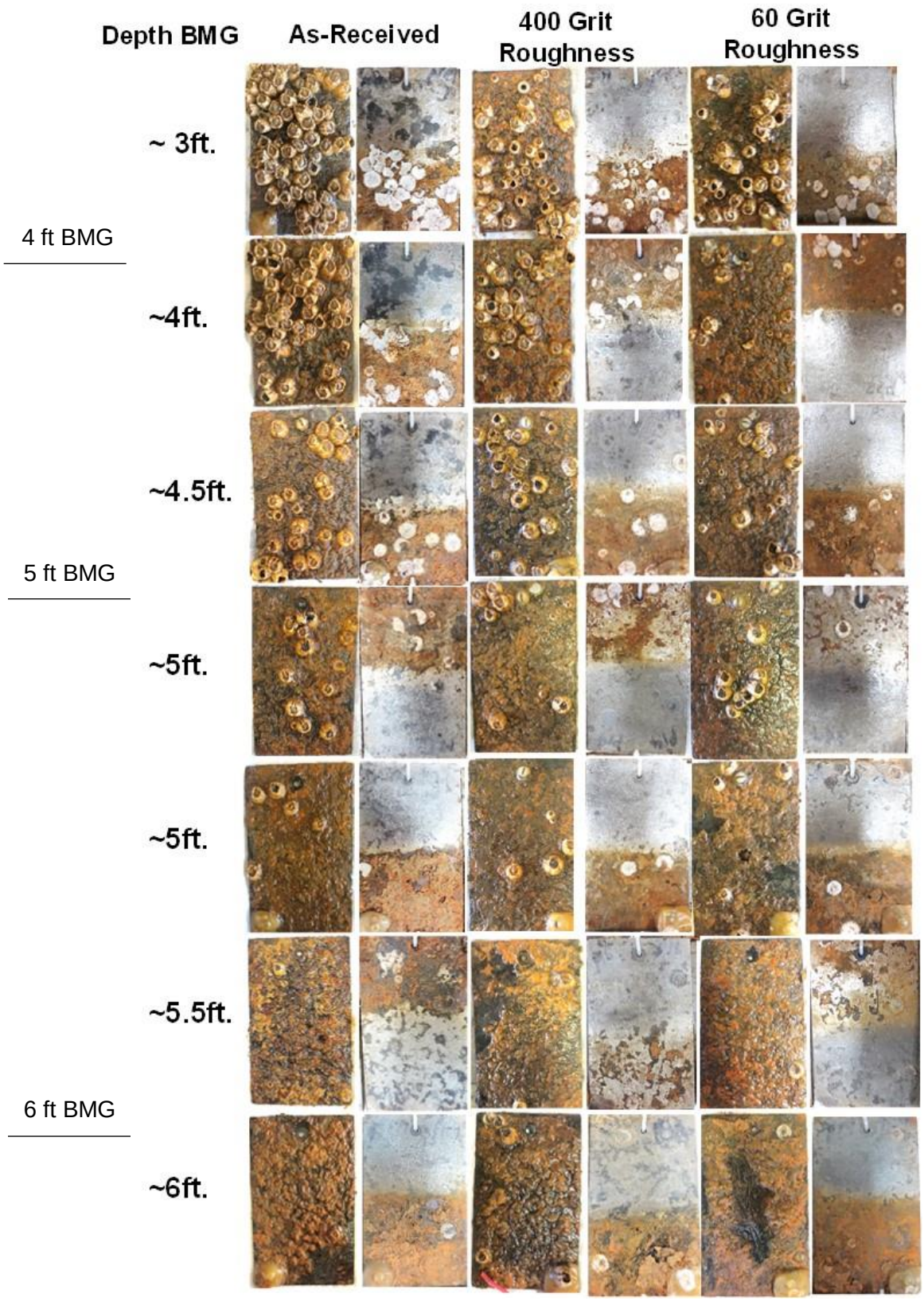

Figure 4.7. (Continued). Test Coupons Exposed in Alafia River at US-301.

4.3. Microbiological Analysis

Anaerobic environments can be created beneath the fouling organisms (such as barnacles) which can host sulfate reducing bacteria. MIC due to SRB typically develop surface biofilm and black deposits of iron corrosion products such as iron sulfide (Figure 4.8). In addition to SRB, three other types of corrosion related bacteria (IRB, APB and SFB) was meaured under fouling surfaces for selected samples. Marine growth was removed, and ~1 in^2 of steel samples was swabbed. That swabbed material (often surface films) was suspended in deionized water in a sterile container. That solution was then tested with a BART test kit. This test was done during the interim testing and the final day for each site exposure. All results showed some level of bacteria development. The results of the final test (and maximum values from interim testing) are reported here (Table 4.3 and 4.4). All three site had high population of IRB, APB and SFB indicating aggressive condition. SR-312 and US-41 had highest populationd of SRB comparing to US-310 which has much less SRB presence. SR-312 and US-41 also had dense coverage of macroufoulers such as barnacle and soft marine massed.

Figure 4.8. Example of Under Fouling Surface Condition.

Table 4.3. Bacteria Content in Field Corrosion Testing at Site I at Day 290 (Continues)

Bacteria (CFU.mL^{-1})	**As-Received (Site I)**			
	~4.3 ft.	**~5.1ft.**	**~7.6ft.**	**~8ft.**
Sulfate Reducing Bacteria (SRB)	6,000(A)	75(M), 500,000(A)*	1,400(M)	75(M), 115,000 (A) *
Iron-Reducing Bacteria (IRB)	2,200(M)	2,200(M), 150(M)*	9,000(A)	35,000(A), 2,200(M)*
Acid Producing Bacteria (APB)	82,000(A)	82,000(A), 14,000(A)*	82,000(A)	82,000(A), 475,000(A)*
Slime-Forming Bacteria (SFB)	1,750,000(A)	1,750,000(A), 1,750,000(A)*	1,750,000(A)	1,750,000(A). 440,000(A)*

*Values from interim testing at 30 -90 Days

Table 4.3. (Continued). Bacteria content in field corrosion testing at Site I at day 290.

Bacteria (CFU.mL$^{-1)}$	P400 Surface Roughness (Site I)		
	~4.3 ft.	~5.1ft.	~7.6ft.
Sulfate Reducing Bacteria (SRB)	6,000(A)	1400(M)	27,000(A)
Iron-Reducing Bacteria (IRB)	2,200(M)	2,200(M)	35,000(A)
Acid Producing Bacteria (APB)	82,000(A)	82,000(A)	82,000(A)
Slime-Forming Bacteria (SFB)	1,750,000(A)	1,750,000(A)	1,750,000(A)

Bacteria (CFU.mL$^{-1)}$	P60 Surface Roughness (Site I)		
	~4.3 ft.	~5.1ft.	~7.6ft.
Sulfate Reducing Bacteria (SRB)	6,000(A)	6,000(A)	6,000(A)
Iron-Reducing Bacteria (IRB)	2,200(M)	9,000(A)	35,000(A)
Acid Producing Bacteria (APB)	8,2000(A)	82,000(A)	82,000(A)
Slime-Forming Bacteria (SFB)	1,750,000(A)	1,750,000(A)	1,750,000(A)

Aggressivity. (NA) Not Aggressive, (M) Moderately Aggressive, (A) Aggressive. General guidelines for BART test for corrosion

Table 4.4. Bacteria content in Field Corrosion Testing at Site II and III at Day 170-245.

Bacteria (CFU.mL-1)	Site II		Site III	
	As- Received (~5.5 ft)	60 Grit (~5.5 ft)	As- Received (~6 ft)	60 Grit (~6 ft)
Sulfate Reducing Bacteria (SRB)	27,000 (A), 5(NA)*	1,400(M), 20 (NA)*	20(NA)	1,400(M)
Iron-Reducing Bacteria (IRB)	9,000(A), 150(M)*	9,000(A), 150 (M)*	35,000(A)	140,000(A)
Acid Producing Bacteria (APB)	475,000(A), 82,000(A)*	82,000(A), 82,000(A)*	475,000(A)	475,000(A)
Slime-Forming Bacteria (SFB)	1,750,000(A), 440,000(A)*	1,750,000(A), 440,000(A)*	1,750,000(A)	1,750,000(A)

*Values from interim testing at 30 Days. Aggressivity. (NA) Not Aggressive, (M) Moderately Aggressive, (A) Aggressive.

4.4. Corrosion Development

Marine organisms can enhance corrosion, but its effects can be diverse, and studies are relatively limited (Neville,1998; Eashwar,1990; Palraj,2002; Rincon,2003; De Brito,2007; VR. de Messano,2009). Balanoid barnacle growth is considered a major cause of biocorrosion on passive alloys in marine environments (Eashwar,1992; VR de Messano,2014; De Brito,2007). The specific mechanism of adhesion of the organisms, their metabolism, and distribution on the metal influence the corrosion processes. In general, the level of adherence of organisms to the steel substrate has a major effect. When the adhesion of the fouling organism is strong and fouling is uniformly covered on the steel, the steel surface may provide some level of barrier protection. The dense coverage of the substrates reduces the access of diffusion of oxygen thereby leading to overall reduction in corrosion rate. Loose attachment and non-uniform macrofouling of organisms may initiate localized corrosion by creating oxygen concentration cells resulting in crevice corrosion under the base of the barnacle. Furthermore, these organism shelter the underlying metal from access by dissolved oxygen and create de-aerated environment supporting the SRB growth and activity. Therefore, crevice corrosion along with MIC can enhance the corrosion of steel structure in natural water.

4.4.1.OCP and LPR

Field test coupons were removed from the outdoor test site and stored in river water for additional testing in the laboratory. The OCP and corrosion rates measured in the laboratory would not necessarily be representative of in-situ field conditions as oxygen levels and other steel surface parameters could be different. Nevertheless, the lab testing would ideally identify differing surface characteristics that developed in the field including the effects of fouling and film development.

Figure 15 shows the measured potentials plotted by original placement of the steel coupons at various submersion depths along with the corresponding in-situ field measurements. In the laboratory testing, oxygen may abound in the open shallow test solutions, especially since the test samples had to be decommissioned from the field test rack, transported, and re-instrumented for testing in the lab. Nevertheless, lab-measured potentials of the freely corroding samples were not dissimilar to in-situ field measurements indicating that the effects of changes in the steel electrode were minimal.

The lab and field in-situ measured potentials showed more negative values for the freely-corroded samples originally placed at depths with permanent submersion (>5 ft BMG for Site I, >3 ft BMG for site II and III). This can be in part reflective of greater coverage of the substrate by biofouling. For example, marine flora amassed at depths greater than 5 ft BMG at Site I and interlayers of clustered barnacles formed at depths greater than 3 ft BMG for Site II and III. The presence of the marine fouling could possibly reduce surface area for oxygen reduction or possibly create local anodes below the occluded regions. These regions could develop local differential aeration cells and support MIC.

Lab LPR measurements for samples at permanent submersion depths showed greater instantaneous corrosion rates at Site I than Site II and III (i_{corr}(site I) > i_{corr}(site II)> i_{corr}(site III)) (Figure 16). This trend was similar to that identified from the average corrosion rates calculated from mass loss measurements (described later). However, even though similar trends in corrosion aggressivity of submerged water conditions in the field test sites were identifiable, the instantaneous rates determined in the lab testing were consistently greater than the largest average corrosion rates calculated by mass loss, reflecting test errors (such as oxygen levels) in the test setup. Furthermore, the instantaneous corrosion rates for samples collected from tidal regions (measured in a static lab test solution) did not capture the aggressive conditions (such as cyclic wetting) at the field site. A simplified analysis approach for the EIS test data (assuming that the total impedance magnitude at 1 Hz would capture trends of the interface activity) showed supporting trends for the measured instantaneous corrosion rates (Figure 17).

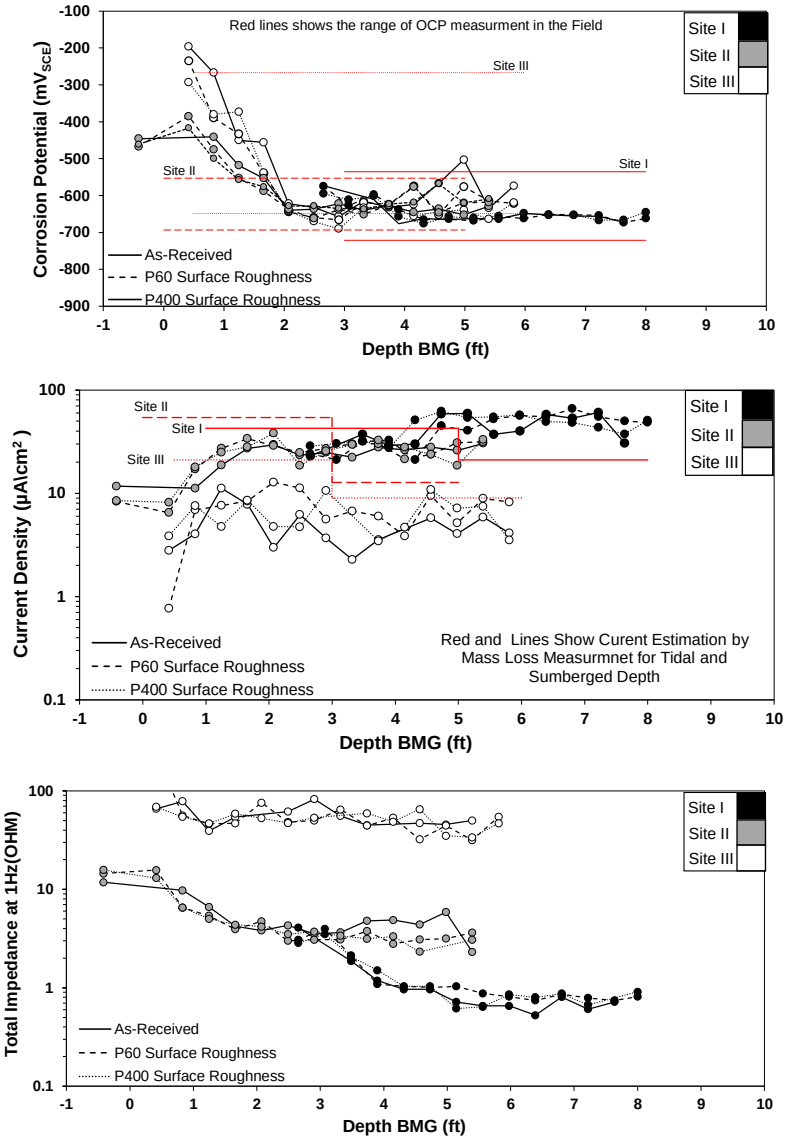

Figure 4.9. OCP, LPR, and EIS results for Field Samples.

4.4.2. Surface Corrosion Characteristic

The selected exposed steel coupons at the three field sites were hand cleaned to remove marine growth and then chemically cleaned to remove remaining surface deposits. After cleaning, visual examination was made to identify the level of steel substrate corrosion loss and possible pitting on the steel samples. Furthermore, the samples were weighed to identify the mass loss after outdoor exposures. Figure 4.10- 4.12 shows magnified representative images of corrosion pits and surface patterns of the corroded surface on select sample after cleaning.

As Table 4.5-4.7 shows, in the case of SR-312, the observed pit diameter and depth ranged from 2 mm to 9 mm and 0.1 mm to 1.3 mm, respectively. US-41 samples had pit diameter (3.5 mm-12 mm) and depth (0.14 mm-0.74 mm) and US-301 had pits diameter (2 mm-5 mm), depth (0.12 mm -0.9 mm). In many cases, corrosion pits were observed at center of the remnant barnacles on the steel. The nominal corrosion rates of steel in three test sites were calculated from the mass difference before and after exposure. Results are shown in figure 4.13-4.14.

4.4.3. Mass Loss

Tomilson,1977 made an extensive survey of the extent of corrosion on steel piling in marine structures at various sites (seawater and fresh water) and reported probable maximum corrosion loss rates by classifying it into different sections including splash, intertidal, low water and immersion zones. The values in MDD ($mg/cm^2/day$) correspond to 19.3 mdd for splash zone, 8.6 mdd for intertidal zone, 19.3 mdd for low water zone and 10.7 mdd for immersion zone. As shown in Figure 4.13 and 4.14, the corrosion loss of the selected samples at SR-312 exceeding the values significantly at different depth of submergence. For US-41 and US-301, the mass loss at immersion zone was significant but less than calculated for SR-312. US-301 samples showed some level of mass loss despite the relatively lower level of fouling (small barnacles) compared to the other two sites.

Figure 4.10. Magnified View of Surfaces of Samples from SR-312 Site. Arrows highlight notable features such as pitting, surface corrosion, remnant barnacle location. Rule at 1 mm intervals.

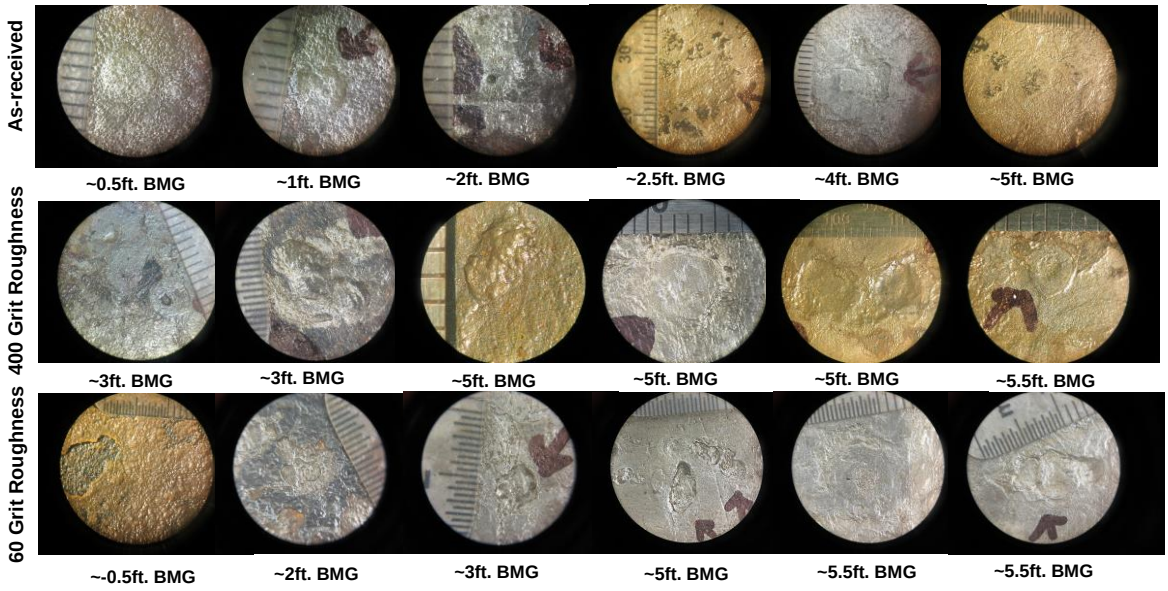

Figure 4.11. Magnified View of Surfaces of Samples from US-41 Site. Arrows highlight notable features such as pitting, surface corrosion, remnant barnacle location. Rule at 1 mm intervals.

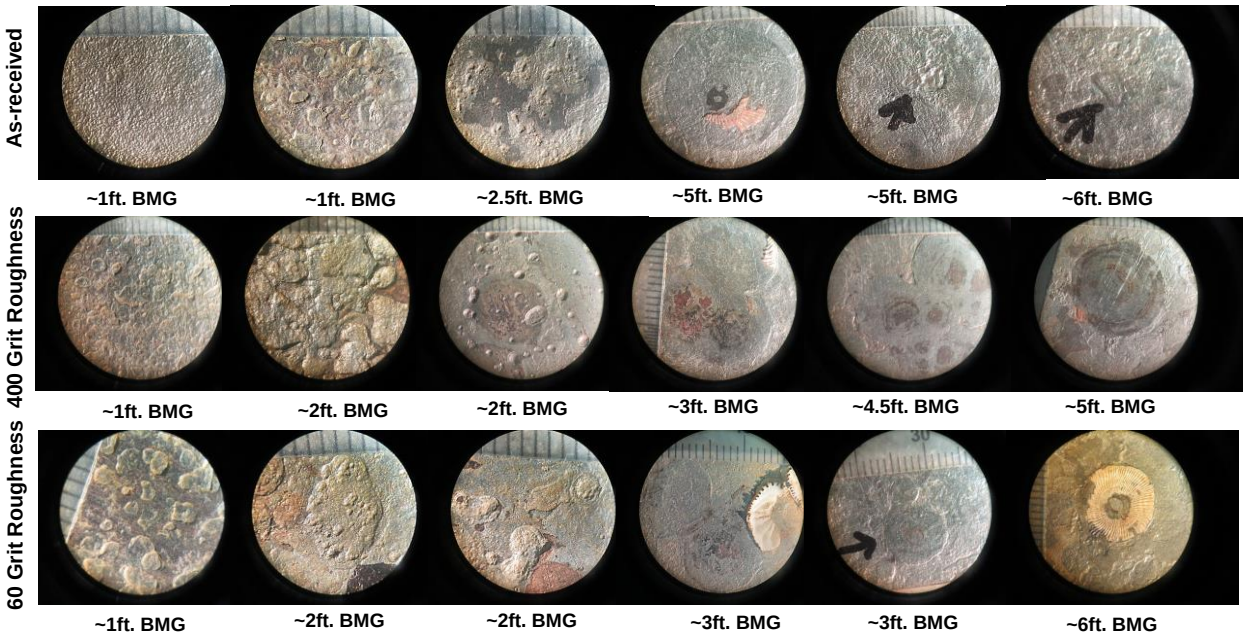

Figure 4.12. Magnified View of Surfaces of Samples from US-301 Site. Arrows highlight notable features such as pitting, surface corrosion, remnant barnacle location. Rule at 1 mm intervals.

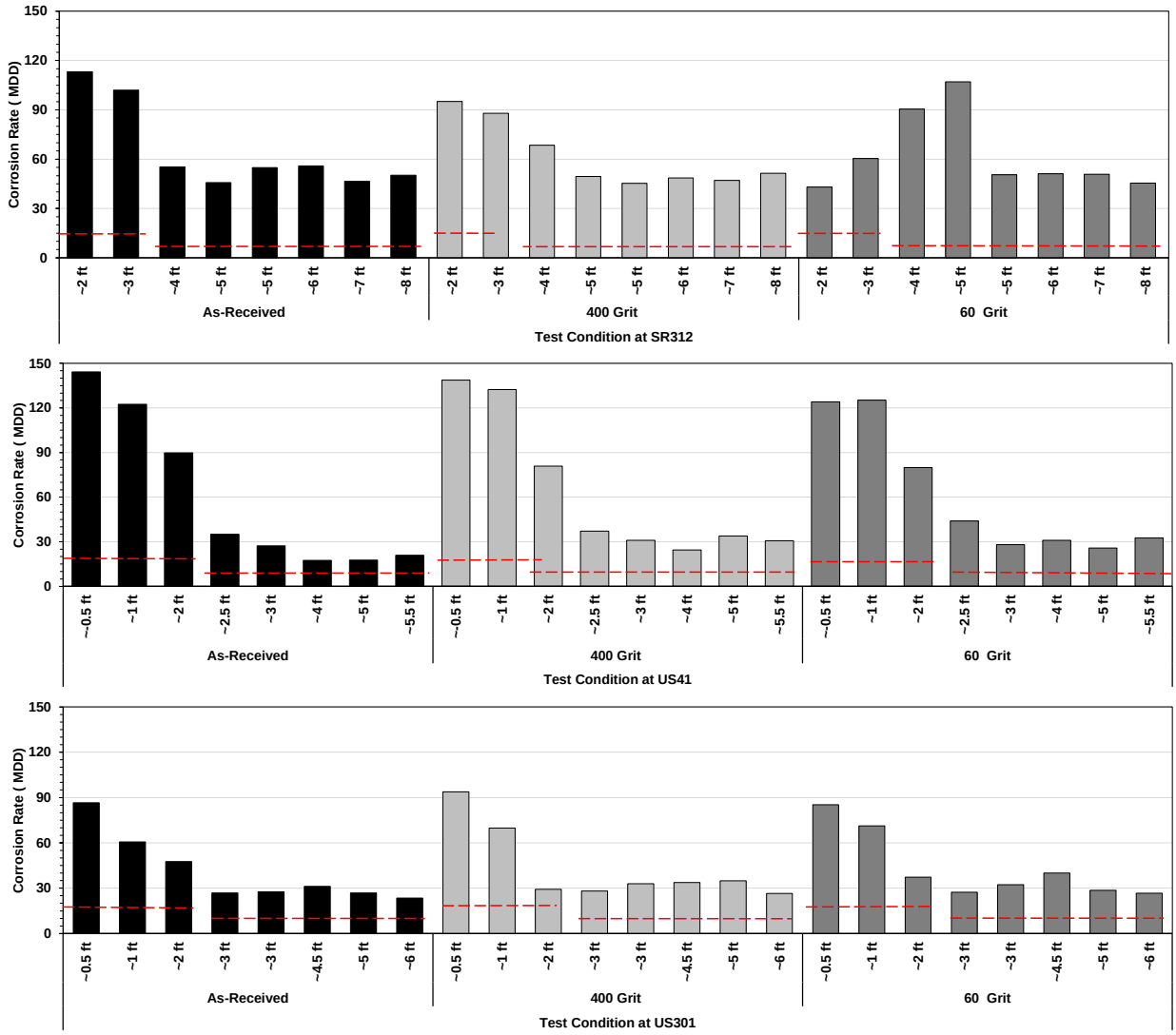

Figure 4.13. Calculated Nominal Corrosion Rates of Steel with Varying Surface Conditions in Florida Natural Waters. (Red Dash line are representative of average corrosion at intertidal and immersion zone (Tomilson,2014))

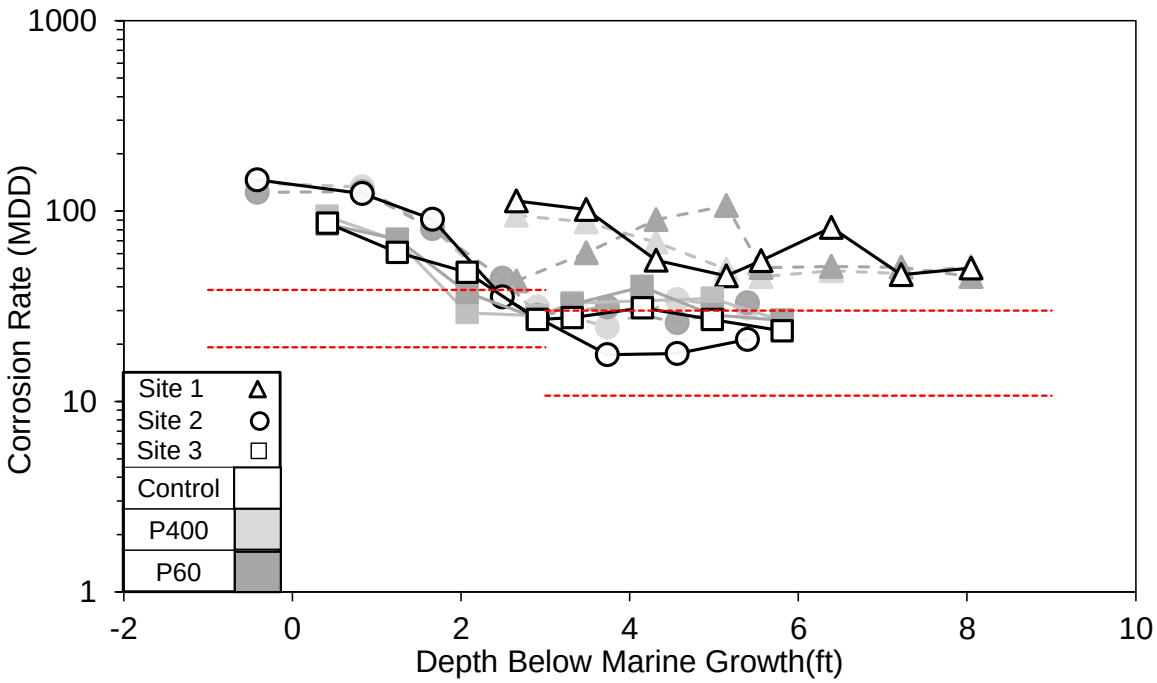

Figure 4.14. Calculated Nominal Corrosion as Function of Immersion Depth.

Table 4.5. Characteristics of Steel Surface after Outdoor Exposure (SR-312). (Continues).

Sample ID	Depth BMG (ft)	Appearance			Pits				Remnant Barnacle on Steel, ϕ(mm)	Barnacle on Orange Surface ϕ (mm)	Barnacle Pattern
		Thick Outer Oxide	Remnant Mill Scale	Bright Surface Luster after Hand Cleaning	Rough	Small Circular Pits~ ϕ≤1mm	Med. Irregular Pits (ϕ(mm), D(mm))	Sinuous Surface Corrosion Texture.			
As-Received											
A1EO01-1	~2	✓	✓	-	✓	-	-	-	-	NA	Isolated
A1EO02-1	~3	-	✓	-	✓	-	-	-	-	NA	Isolated
A1EO03-1	~3	✓	✓	-	✓	-	-	-	-	NA	Clustered
A1EO04-1	~4	-	✓	✓	✓	-	-	-	-	NA	Clustered
A1EO05-1	~4	-	✓	✓	✓	-	✓ (6,0.45)	✓(A)†	-	NA	Clustered
A1EO06-1	~5	-	-	✓	✓	-	✓ (5,0.41)	✓	-	NA	Isolated
A1EO07-1	~5	-	-	✓	✓	-	✓ (6,0.25)	✓	✓,10	NA	Isolated
A1EO08-1	~5.5	-	-	✓	-	-	✓ (4,0.45)	✓(A)†	✓,6	NA	-
A1EO09-1	~6	-	-	✓	✓	-	✓ (4,0.3)	✓	✓	NA	-
A1EO10-1	~6	-	-	✓	✓	-	✓ (4,0.1)	✓	✓,6	NA	-
A1EO11-1	~7	-	-	✓	✓	-	✓ (6,0.3)	✓	✓,6	NA	-
A1EO12-1	~7	-	-	✓	✓	-	✓ (5,0.4)	✓	✓,10	NA	-
A1EO13-1	~8	-	-	✓	-	-	✓ (8,1.3)	✓(A)†	-	NA	-
A1EO14-1	~8	-	-	✓	-	-	✓ (9,0.5)	✓	✓,8	NA	-
400 Grit											
A2EO01-1	~2	✓	✓	-	✓	-	-	-	-	NA	Isolated
A2EO02-1	~3	-	✓	-	✓	-	-	-	-	NA	Isolated
A2EO03-1	~3	✓	✓	-	✓	-	-	-	-	NA	Clustered
A2EO04-1	~4	-	✓	✓	✓	-	✓ (5,0.3)	✓	-	NA	Clustered
A2EO05-1	~4	-	-	✓	✓	-	✓ (3,0.19)	✓	-	NA	Clustered

Table 4.5. (Continued). Characteristics of Steel Surface after Outdoor Exposure (SR-312).

A2EO06-1	~5	-	-	✓	✓	-	✓	✓	-	NA	Isolated
A2EO07-1	~5	-	-	✓	-	-	✓ (4,0.2)	✓(A)†	✓,6	NA	Isolated
A2EO08-1	~5.5	-	✓	✓	-	-	✓ (4,0.26)	✓	✓,5	NA	-
A2EO09-1	~6	-	-	✓	-	-	✓ (3,0.3)	✓	✓,4	NA	-
A2EO10-1	~6	-	✓	✓	✓	-	-	✓	✓,6	NA	-
A2EO11-1	~7	-	-	✓	-	-	✓ (5,0.1)	✓	✓,9	NA	-
A2EO12-1	~7	-	-	✓	-	-	✓ (4,0.1)	✓	-	NA	-
A2EO13-1	~8	-	-	✓	-	-	✓ (4,0.2)	✓	-	NA	-
A2EO14-1	~8	-	-	✓	-	-	-	✓	✓,5	NA	-
60 Grit											
A3EO01-1	~2	✓	✓	-	✓	-	-	-	-	NA	Isolated
A3EO02-1	~3	✓	✓	-	✓	-	-	-	-	NA	Isolated
A3EO03-1	~3	✓	✓	-	✓	-	-	-	-	NA	Clustered
A3EO04-1	~4	-	✓	✓	✓	-	✓ (3,0.3)	-	-	NA	Clustered
A3EO05-1	~4	-	-	✓	✓	-	✓ (7,0.5)	✓	✓,6	NA	Clustered
A3EO06-1	~5	-	-	✓	✓	-	-	✓	-	NA	Isolated
A3EO07-1	~5	-	-	✓	-	-	✓ (2,0.2)	✓	-	NA	Isolated
A2EO08-1	~5.5	-	✓	✓	-	-	✓ (4,0.4)	✓	✓,5	NA	-
A3EO09-1	~6	-	-	✓	-	-	✓ (5,0.2)	✓	✓,8	NA	-
A3EO10-1	~6	-	-	✓	-	-	✓ (4,0.2)	✓	✓,6	NA	-
A3EO11-1	~7	-	-	✓	-	-	✓ (5,0.3)	✓	✓,6	NA	-
A3EO12-1	~7	-	-	✓	✓	-	✓ (4,0.2)	✓	✓,5	NA	-
A3EO13-1	~8	-	-	✓	-	-	✓ (4,0.2)	✓	✓,5	NA	-
A3EO14-1	~8	-	✓	✓	-	-	-	✓	✓,10	NA	-

†(A). Deep Localized mass loss

Table 4.6. Characteristics of Steel Surface after Outdoor Exposure (US-41). (Continues)

Sample ID	Depth BMG (ft)	Appearance			Pits				Remnant Barnacle on Steel, ϕ(mm)	Barnacle on Orange Surface ϕ (mm)	Barnacle Pattern
		Thick Outer Oxide	Remnant Mill Scale	Bright Surface Luster after Hand Cleaning	Rough	Small Circular Pits~ ϕ≤1mm	Med. Irregular Pits (ϕ(mm), D(mm))	Sinuous Surface Corrosion Texture.			
As-Received											
B1EO01-1	~-0.5	✓	-	-	✓	-	-	-	-	-	-
B1EO02-1	~0.5	✓	-	-	✓	-	-	-	-	-	-
B1EO03-1	~1	✓	-	-	✓	-	-	-	-	-	-
B1EO04-1	~1	✓	✓	✓	✓	-	✓ (5, NA)	-	-	✓, 7	-
B1EO05-1	~2	✓	✓	✓	✓	-	-	-	-	✓, 10	Clustered
B1EO06-1	~2	-	✓	✓	-	✓	-	✓	-	✓, 8	Clustered
B1EO07-1	~2.5	-	✓	✓	-	-	✓ (4,0.36)	✓	✓,12	✓, 12	Clustered
B1EO08-1	~3	-	✓	✓	-	-	✓ (10,0.25)	✓	✓,7	✓, 10	Clustered
B1EO09-1	~3	-	✓	✓	-	-	✓ (6,0.28)	✓	✓,10	✓, 14	Clustered
B1EO10-1	~4	-	✓	✓	-	-	✓ (4,0.25)	✓	✓,10	✓, 14	Clustered
B1EO11-1	~4.5	-	-	✓	-	-	✓ (7,0.44)	✓	-	✓, 14	Clustered
B1EO12-1	~5	-	✓	✓	-	-	✓ (4,0.34)	✓	✓,8	✓, 10	Clustered
B1EO13-1	~5	-	✓	✓	-	-	-	✓	✓,10	✓, 10	Clustered
B1EO14-1	~5.5	-	-	✓	-	-	-	✓	✓,5	✓, 10	Clustered
400 Grit											
B2EO01-1	~-0.5	✓	-	-	✓	-	-	-	-	-	-
B2EO02-1	~0.5	✓	-	-	✓	-	-	-	-	-	-
B2EO03-1	~1	✓	-	-	✓	-	-	-	-	-	-
B2EO04-1	~1	✓	✓	✓	✓	-	-	-	-	✓, 10	-
B2EO05-1	~2	✓	✓	✓	✓	-	-	-	-	✓, 10	Clustered

Table 4.6. (Continued). Characteristics of Steel Surface after Outdoor Exposure (US-41).

B2EO06-1	~2	-	✓	✓	✓	-	✓ (6,0.72)	-	-	✓, 20	Clustered
B2EO07-1	~2.5	-	✓	✓	-	-	✓ (3.5,0.25)	✓	✓,14	✓, 13	Clustered
B2EO08-1	~3	-	✓	✓	-	-	✓ (7,0.3)	✓	✓,7(B)‡	✓, 16	Clustered
B2EO09-1	~3	-	✓	✓	-	-	✓ (9,0.4)	✓	✓,14	✓, 10	Clustered
B2EO10-1	~4	-	-	✓	-	-	✓ (2,0.2)	✓	✓,13	✓, 14	Clustered
B2EO11-1	~4.5	-	-	✓	✓	-	✓ (12,0.27)	✓	✓,10(B)‡	✓, 8	Clustered
B2EO12-1	~5	-	-	✓	-	-	✓ (10,0.45)	✓	✓,6(B)‡	✓, 6	Clustered
B2EO13-1	~5	-	-	✓	-	-	✓ (10,0.46)	✓	✓,14(B)‡	✓, 6	Clustered
B2EO14-1	~5.5	-	-	✓	-	-	✓ (4,0.40)	✓	✓,10(B)‡	✓, 10	Clustered
60 Grit											
B3EO01-1	~-0.5	✓	-	-	✓	-	-	-	-	-	-
B3EO02-1	~0.5	✓	-	-	✓	-	-	-	-	-	-
B3EO03-1	~1	✓	-	-	✓	-	-	-	-	-	-
B3EO04-1	~1	✓	✓	✓	✓	-	-	-	-	✓, 7	-
B3EO05-1	~2	✓	✓	✓	✓	-	-	-	-	✓, 12	Clustered
B3EO06-1	~2	-	✓	✓	-	-	✓ (10,0.5)	✓	-	✓, 6	Clustered
B3EO07-1	~2.5	-	✓	✓	-	-	✓ (5,0.30)	✓	✓,8	✓, 15	Clustered
B2EO08-1	~3	-	✓	✓	-	-	✓ (5,0.26)	✓	✓,10	✓, 15	Clustered
B3EO09-1	~3	-	-	✓	-	-	✓ (5,0.37)	✓	✓,15(B)‡	✓, 10	Clustered
B3EO10-1	~4	-	-	✓	-	-	✓ (5,0.14)	✓	✓,10	✓, 15	Clustered
B3EO11-1	~4.5	-	-	✓	-	-	✓ (10,0.41)	✓	✓,5	✓, 6	Clustered
B3EO12-1	~5	-	-	✓	-	-	✓ (5,0.16)	✓	✓,6	✓, 15	Clustered
B3EO13-1	~5	-	-	✓	-	-	✓ (7,0.30)	✓	✓,6(B)‡	✓, 6	Clustered
B3EO14-1	~5.5	-	-	✓	-	-	✓ (10,0.30)	✓	✓,10(B)‡	✓, 10	Clustered

‡ (B). Local Inter Circumcentric Basal Plate Corrosion

Table 4.7. Characteristics of Steel Surface after Outdoor Exposure (US-301). (Continues)

Sample ID	Depth BMG (ft)	Appearance			Pits				Remnant Barnacle on Steel, ϕ(mm)	Barnacle on Orange Surface, ϕ(mm)	Barnacle Pattern
		Thick Outer Oxide	Remnant Mill Scale	Bright Surface Luster after Hand Cleaning	Rough	Small Circular Pits~ ϕ≤1mm	Med. Irregular Pits (ϕ(mm), D(mm))	Sinuous Surface Corrosion Texture.			
As-Received											
C1EO01-1	~0.5	✓	✓	-	✓	-	-	-	-	-	-
C1EO02-1	~1	✓	✓	-	✓	-	-	-	-	-	-
C1EO03-1	~1	✓	✓	-	✓	-	-	-	-	-	-
C1EO04-1	~2	-	✓	-	✓	-	-	-	-	-	-
C1EO05-1	~2	-	✓	✓	✓	✓	-	-	-	✓, 12	Clustered
C1EO06-1	~2.5	-	✓	✓	-	✓	-	-	-	✓, 15	Clustered
C1EO07-1	~3	-	✓	✓	-	✓	-	-	-	✓, 10	Clustered
C1EO08-1	~3	-	✓	✓	-	-	-	✓	✓,15	✓, 14	Clustered
C1EO09-1	~4	-	✓	✓	-	-	-	✓	✓,10	✓, 14	Clustered
C1EO10-1	~4.5	-	✓	✓	-	-	-	✓	✓,14	✓, 12	Isolated
C1EO11-1	~5	-	✓	✓	-	-	✓ (4,0.12)	✓	✓,15	✓, 15	Isolated
C1EO12-1	~5	-	✓	✓	-	-	✓ (5, NA)	✓	✓,10	✓, 11	Isolated
C1EO13-1	~5.5	-	✓	✓	-	-	✓ (2, 0.2)	✓	-	✓, 5	Isolated
C1EO14-1	~6	-	✓	✓	-	-	✓ (3, 0.12)	✓	-	✓, 10	Isolated
400 Grit											
C2EO01-1	~0.5	✓	✓	-	✓	-	-	-	-	-	-
C2EO02-1	~1	✓	✓	-	✓	-	-	-	-	-	-
C2EO03-1	~1	✓	✓	-	✓	-	-	-	-	-	-
C2EO04-1	~2	-	✓	✓	-	✓	✓ (5,0.6-0.9)	✓(A)†	✓,10	✓, 10	Clustered
C2EO05-1	~2	-	✓	✓	-	✓	✓ (5,0.3)	✓(A)†	✓,10	✓, 10	Clustered

Table 4.7. (Continued). Characteristics of Steel Surface after Outdoor Exposure (US-301).

C2EO06-1	~2.5	-	-	✓	✓	-	-	✓	✓,8	✓, 14	Clustered
C2EO07-1	~3	-	-	✓	-	-	-	✓	✓,14	✓, 14	Clustered
C2EO08-1	~3	-	-	✓	-	-	-	✓	✓,15	✓, 16	Clustered
C2EO09-1	~4	-	-	✓	-	-	-	✓	✓,12	✓, 15	Clustered
C2EO10-1	~4.5	-	-	✓	-	-	✓ (2,0.2)	✓	✓,10(B)‡	✓, 15	Isolated
C2EO11-1	~5	-	-	✓	-	-	-	✓	✓,15	✓, 10	Isolated
C2EO12-1	~5	-	-	✓	-	-	-	✓	✓,5	✓, 15	Isolated
C2EO13-1	~5.5	-	-	✓	-	-	-	✓	✓,14	✓, 10	Isolated
C2EO14-1	~6	-	-	✓	-	-	✓ (5,0.5)	✓	✓,14	✓, 10	Isolated
60 Grit											
C3EO01-1	~0.5	✓	✓	-	✓	-	-	-	-	-	-
C3EO02-1	~1	✓	✓	-	✓	-	-	-	-	-	-
C3EO03-1	~1	✓	✓	-	✓	-	-	-	-	-	-
C3EO04-1	~2	-	✓	-	✓	-	-	-	-	-	-
C3EO05-1	~2	-	✓	✓	-	✓	✓ (6,0.42)	✓	✓,10	-	Clustered
C3EO06-1	~2.5	-	✓	✓	-	-	✓ (4,0.1)	✓	✓,10	✓, 5	Clustered
C3EO07-1	~3	-	✓	✓	-	-	-	✓	✓,14	✓, 14	Clustered
C2EO08-1	~3	-	-	✓	-	-	-	✓	✓,14(B)‡	✓, 10	Clustered
C3EO09-1	~4	-	-	✓	-	-	-	✓	✓,12	✓, 12	Clustered
C3EO10-1	~4.5	-	-	✓	-	-	-	✓	✓,15	✓, 14	Isolated
C3EO11-1	~5	-	-	✓	-	-	-	✓	✓,11	✓, 14	Isolated
C3EO12-1	~5	-	-	✓	-	-	-	✓	✓,10	✓, 12	Isolated
C3EO13-1	~5.5	-	✓	✓	-	-	✓ (4,0.12)	✓	✓,12	-	Isolated
C3EO14-1	~6	-	✓	✓	-	-	-	✓	✓,10	✓, 5	Isolated

†(A). Deep Localized mass loss ,‡ (B). Local Inter Circumcentric Basal Plate Corrosion

5. LABORATORY TESTING FOR MIC

5.1. Methodology

Laboratory experiments made under test setup A varied the availability of isolated sulfate reducing bacteria and nutrient levels. Experiments in test setup B followed a modified laboratory test setup and a single inoculation of isolated sulfate reducing bacteria was initially introduced and the level of biotic and electrochemical activity was continuously monitored.

5.1.1. Test Set Up A

Testing was conducted on 40 samples for up to 70 days. Thin cylinder-shaped working electrodes (~3/4-inch length) were cut from 1/2-inch diameter low carbon steel (A36) rods. Insulated copper electrical contact wires were attached to the one axial surface of the electrodes by spot soldering, and the steel working electrode was then mounted in non-conductive resin where only the opposite axial surface was exposed. That exposed surface was wet-ground on diamond abrasive disk to a uniform 800 grit (20µ) finish.

Some samples incorporated radial crevice conditions on the exposed electrode surface. The crevice height (12 mils), radial length (7/32 inch) and center mouth (1/16-inch diameter) were made with plastic shims and a plastic cap placed on the mounted electrode as shown in figure 5.1. An activated titanium wire was used as a permanent reference electrode that was routinely calibrated with a saturated calomel (SCE) electrode. An activated titanium rod was used as the counter electrode. All test cells and equipment were cleaned with ethanol to prevent contamination.

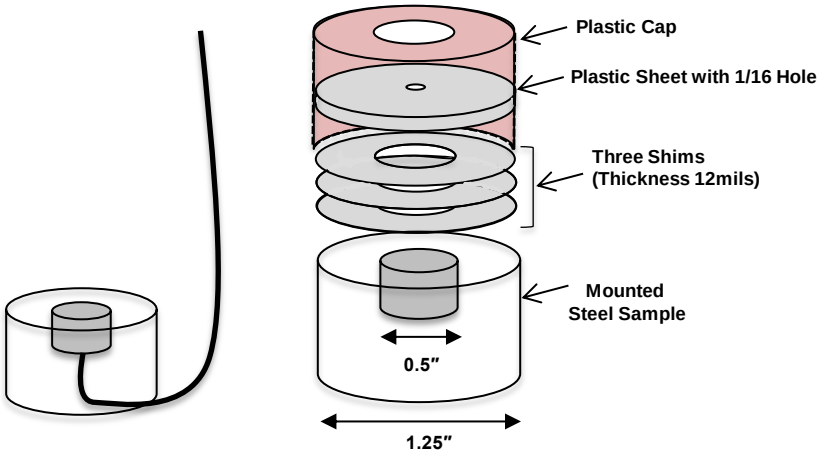

Figure 5.1. Schematic of Working Electrode in Test Setup A.

Test cells as shown in figure 5.2 were filled with 600 mL of deionized water and 10 mL of modified postage B medium solution (Postgate,1984). The growth media was chosen based on NACE standard TM0194-2014. The composition of the medium is presented in Table 5.1. In order to investigate the effect of nutrient concentration, sodium sulfate was added to the solution

as part of one test condition according to the maximum level of sulfate ion concentration in the Matanzas river (2,000 ppm). Test conditions are summarized in Table 5.2.

Figure 5.2. Test Setup A Test Cells.

Table 5.1. Composition of Modified Postgate B Medium.

Constituents	Composition (%)
Potassium Phosphate (KH_2PO_4)	0.05
Ammonium Chloride (NH_4Cl)	0.1
Sodium Sulfate (Na_2SO_4)	0.1
Sodium Chloride (NaCl)	2.5
Iron Sulfate ($FeSO_4.7H_2O$)	0.05
Sodium Lactate	0.5
Yeast extract	0.1

Table 5.2. Test Setup A Conditions

Test Condition	De-Aerated or Naturally Aerated Conditions			
Control (CTRL)	SRB*	SRB with Hard Crevice	No SRB*	No SRB with Hard Crevice
Sulfate Addition (SULF1/SULF2*)				

*An additional test set of duplicate samples, SULF2, were made for these marked test conditions. These sets showed high COD.

The pH of the test solution (pH 6.5-8.0) had been confirmed to be in a suitable range for sustained SRB growth (Barton et al.,1995). For anaerobic test conditions, the solution was de-aerated by introducing industrial nitrogen gas for five minutes every three days. A thin layer of mineral oil was added to samples in de-aerated cases to maintain the low oxygen condition. For the aerobic test condition, the solution remained naturally aerated.

Inoculated Postgate B broth containing SRB cultures that were previously isolated from water samples collected from Matanzas River at SR-312, were used in serial dilutions following NACE standard TM0194-2002. In the serial dilutions, bacterial growth was detected by the production of hydrogen sulfide or iron sulfide. Iron sulfide precipitation resulted in the blackening of the broth after ~3-5 days at 30 °C. The test cells for all SRB test conditions (Table 2) were periodically inoculated with 5 ml of the inoculated broths. The test solutions were inoculated at day 0, day 15-20, and day 30-40. Also, an additional 10ml of Postgate B (as a nutrient) was added to the cells after day 3 and after the second and third inoculation.

The level of bacterial activity in the test cell was in part assessed by measuring the chemical oxygen demand (COD), hydrogen sulfide, and bacteria population. The COD can be used as general measure of microbial activity and it may be possible to estimate the concentration of electron donors available for sulfate or metal reduction. Low COD would mean a low risk of availability to SRB (Scott,2004). COD of each samples was measured by a colorimetric COD method every 5 days (O'Dell,1993). A hydrogen sulfide color disc test kit was used for the sulfide estimation. Biological Activity Reaction Test (BART) kits were used to verify the population and the activity of the four common MIC related bacteria (SRB, IRB, SLYM and APB). Sani-Check B Dipslides test kit was used to get a quantitative interpretation for total bacteria content.

Corrosion testing consisted of periodic measurements of the open circuit potential (OCP) and linear polarization resistance (LPR). The OCP was measured using the activated titanium reference electrode and the values were periodically calibrated against a SCE reference electrode. The scanned potentials for the LPR testing was made from the open-circuit potential and cathodically polarized 25 mV at a scan rate of 0.05 mV/s. The corrosion current density was calculated from the resolved polarization resistance corrected for solution resistance, Rp,

following the equation icorr=B/(RpxA) where B was assumed to be 26 mV and A was the surface area of the working electrode. Anodic polarization scan from 0 V_{OCP} to -1000 mV_{SCE} in the forward sweep and reversed up to +600 mV_{SCE}.

After ~70 days, the steel working electrode was removed from the test solution. Coverings were removed from crevice samples. All samples were rinsed with ethanol and dried. Photodocumentation for corrosion development and remnant physical effects of microbial activity was made.

5.1.2. Test Setup B

Tests were conducted on 48 test cells for up to 15 days. Experimental parameters for test setup B are shown in table 5.3. Working electrode steel coupon fabrication and coupon mounting were made similar to that described for test setup A. In these samples, the copper electrical wire was soldered to an auxiliary steel screw attached to the steel sample. Augmentation of testing from setup A included another subset of surface roughness where the exposed electrode surface was wet-ground to either uniform P2000 grit (10µ) or 60 grit (269 µ) finish. Also (like test setup A) a crevice environment was introduced but the parameters and setup were modified as shown in figure 5.3. Testing included both representations of physical hard and porous crevice conditions characteristic of hard-shell barnacles and soft marine flora and fauna.

Hard crevices with a controlled height (3 mils), radial depth (7/32 inch) and opening (1/16-inch diameter) was made by using plastic film of known thickness. The plastic shims were affixed on the surface of the mounted samples as shown in Figure 5.3. Soft crevice conditions were replicated by placing a porous sponge on the working electrode surface. Activated titanium mesh and saturated calomel (SCE) electrodes were used as reference electrodes. Another activated titanium mesh was used as counter electrodes. All test cells and equipment were cleaned with ethanol.

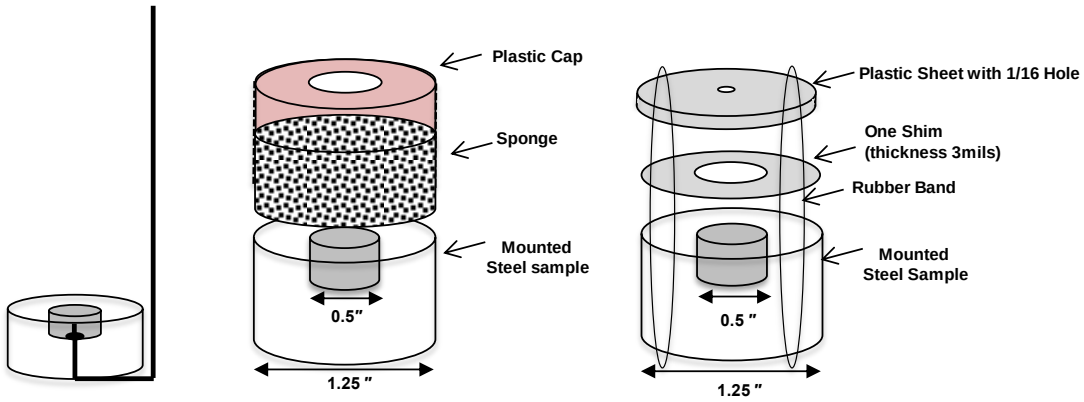

Figure 5.3. Schematic of Working Electrode in Test Setup B.

Table 5.3. Test Setup B Conditions.

Test Condition	De-Aerated or Naturally Aerated Conditions					
Control (CTRL-A/CTRL-B*)	SRB*	SRB with Hard Crevice*	SRB with Soft Crevice	No SRB*	No SRB with Hard Crevice	No SRB with Soft Crevice
Sulfate Ion Addition (SULF-A)						
60 Grit Surface Roughness (60GRT-A)						

***** Control test conditions also included a subset (CTRL-B) where 20 mL (CTRL-B20) and 40 mL (CTRLB-40) of modified Postgate medium solution was used. In this subset, a different SRB inoculation was introduced.

Test cells were filled with 300 mL deionized water and 20-40 mL of modified Postgate B medium solution (Postgate,1984). A picture of test cells for test setup B is shown in Figure 5.4. For all test conditions, 20 mL of the medium solution was used, but a control test subset at indicated in Table 3 had a higher dosage of the medium solution (40 mL).

Figure 5.4. Test Setup B Test Cells.

One test condition (SULF-A) incorporated higher initial sulfate ion concentrations in order to investigate the effect of nutrient concentration. Sodium sulfate was added to the test solution to replicate maximum sulfate concentrations in the Matanzas river (2,000 ppm). The second supplemental test condition (60GRT-A) utilized working electrodes with a coarser surface finish (60 grit) than the P2000 surface finish used for all other test conditions.

The pH of all test solutions was ~6.5-8. For de-aerated test conditions, high purity nitrogen gas was bubbled in the solution for ten minutes each day. To prevent subsequent oxygen ingress, a thin layer of mineral oil was added to the solution surface for these samples. Test cells for all test conditions to assess SRB presence (Table 3) were inoculated with10 ml of the inoculated broths.

Assessment of microbial activity was made by chemical oxygen demand (COD) and sulfide production. COD of each samples was measured by a colorimetric COD method every 5

days. A hydrogen sulfide color disc test kit was used for the sulfide estimation. Biotechnology Solutions sessile test kits were used for detection of sulfate reducing bacteria by serial dilution in Modified Postgate B (MPB) following NACE standard TM0194-2014. Sterile cotton swabs were used to gently scrape the sessile sample area (1 cm^2 area) and the slime (solid) was placed into a sterile Phosphate Buffer Solution (PBS). Serial dilution of the 1 ml PBS ranged from 4-8 times.

Corrosion testing consisted of open circuit potential (OCP) and linear polarization resistance (LPR). OCP was measured versus a saturated calomel electrode every day through a luggin capillary in the test setup. LPR testing was made from initial OCP to -25mV vs.OCP at a scan rate of 0.05mV/s. The corrosion current density was calculated from the resolved polarization resistance corrected for solution resistance, Rp, following the equation icorr=B/(RpxA) where B was assumed to be 26 mV and A was the surface area of the working electrode. Anodic polarization scan from -1 V_{SCE} to 600 mV_{SCE} in the forward sweep and reversed back to -1 V_{SCE} for the subset of control test conditions where 40mL of modified Postgate medium solution was used (CTRL-B40). Those samples were preconditioned at -1V_{SCE} for 3 minutes to reduce transient capacitive effects.

After ~15 days, the steel working electrode was removed from the test solution. Coverings were removed from crevice samples. All samples were rinsed with ethanol and dried. Photodocumentation for corrosion development and remnant physical effects of microbial activity was made.

5.2. Results and Discussion

5.2.1. Test Setup A

5.2.1.1. Microbiological Activity

5.2.1.1.a Sulfide Production

Sulfide levels were measured on select days after SRB inoculation for CTRL and SULF1/SULF2 samples as shown in Table 5.4. As an example, shown in Figure 5.5, SRB proliferation in the inoculated test solution was evident by precipitation of black iron sulfide in the test solution. Measured sulfide levels are shown in Table 5.4. As expected, some level of iron sulfide precipitation was seen in all inoculated de-aerated CTRL solutions including in crevice conditions (as evident by the higher measured sulfide content consistent with the opaqueness of the test solution). In the comparative naturally aerated open (non-crevice solution), sulfide levels were generally lower. Also, in contrast to the de-aerated condition, sulfide production levels appeared to drop after inoculation events possibly indicating less favorable environments for continued SRB activity despite the new introduction of additional bacteria and nutrients. Similarly, the crevice environments in the naturally aerated conditions did not appear to support prolonged SRB activity after inoculation events.

With sulfate additions, sulfide production was observed for both aerated and de-aerated solutions for both open (non-crevice) and crevice conditions (with the exception for the SULF2 condition after later inoculations where zero sulfide levels were measured for the naturally aerated open (non-crevice) environment), generally indicating positive effect of sulfates to promote SRB activity.

Figure 5.5. Visual Indication of Iron Sulfide Precipitation in Test Solution.
Left- Inoculation with SRB. Right- control case

Table 5.4. Sulfide Production Level mg/L (CTRL and SULF1/SULF2).

Test Condition	Time (days)	De-Aerated				Naturally Aerated			
		Open (None-Crevice)		Crevice		Open (None-Crevice)		Crevice	
CTRL	16†	2.26	1.8	1.48	1.27	0.27	-	0.4	0.16
	21	2.97	2.12	2.97	3.71	0	-	0	0
	33	0.48	0.64	1.91	2.12	0	-	0	0
	37†	7.42	7.42	7.95	8.48	2.33	-	2.97	2.6
	53	0	2.33	1.27	1.80	0	-	0	0
SULF1/ SULF2*	0†	0/0.42*	0/0.424*	0.42	0.85	0/0.42*	0.42/0.42*	2.12	1.91
	5	-/0.21*	-/1.06*	0.64	0.42	-/1.27*	-/0.85*	0.85	1.91
	23†	-/1.59*	1.7/1.77*	0.64	0.84	0.42/0*	1.48/0*	1.06	1.06

† Sulfide measurements after inoculation events.

5.2.1.1.b Chemical Oxygen Demand

Figure 5.6 shows the results of COD measurements conducted for the test solutions with and without inoculation of SRB for the CTRL, SULF1, and SULF2 Setup A test conditions shown in Table 2. Although COD levels in itself does not directly give indication of SRB populations, COD levels are considered as a metric of environmental conditions to support SRB activity. SRB activity can be associated with oxidation of organic compounds (such as in waste water systems) or cathodic depolarization of steel (such as in MIC). Changes in COD with time could ideally provide some indication on other solution conditions due to SRB population changes. The addition of sulfate ions in solutions (SULF1/SULF2 conditions) inoculated with SRB was thought to provide environments conducive for the proliferation of the SRB in reactions to enhance MIC. At this time, the effects of other bacteria that may develop in the test solution on changes in COD are not considered.

In the testing conducted here, it was posed that changes in COD with time may reflect a series of possible reactions in solution. After SRB inoculation, a drop in COD may indicate the oxidation of vestigial organic compounds as a food source for SRB (but not necessarily oxidation of the steel and hydrogen reduction in the test solution). Deviation from this drop may indicate reduced SRB activity associated with biological sulfate reduction. That same SRB activity in presence of sulfates, however, could result also in an increase in COD as sulfate is reduced to sulfide thus increasing the concentration of electron donors. In cases associated with steel corrosion or with vestigial iron ion concentrations, the enhanced iron ion content can also be reflected by higher COD; however, as SRB reduces sulfates to sulfides as just mentioned, the iron ions can allow precipitation of iron sulfides thus reducing the level of sulfides acting as electron donors thus possibly a lower COD value. In the small-scale lab cells, prolonged SRB health is not attainable. An increase in non-biotic organic material (dead microbes) was posed to also affect COD levels.

CTRL. For the CTRL inoculated case, the initial COD levels were expectedly low upon first inoculation in both naturally aerated and de-aerated solutions. The COD levels significantly

increased in the de-aerated solution up to a week after the first inoculation, presumably as the SRB population developed under anaerobic conditions and sulfide production ensued. The COD levels thereafter decreased and fluctuated as iron sulfide precipitated prior to the second inoculation where positive sulfide levels were measured. After the subsequent inoculations of isolated SRB into the test cell, similar periodic COD levels were observed.

Similar periodic behavior was observed for the naturally aerated conditions although COD levels were generally lower overall. Indeed, SRB growth was less prolific (likely due to the presence of oxygen) as indicated by the low COD levels even after both inoculations on days 0 and 15. There was a slight increase in COD after each inoculation event but not to the extent observed in the de-aerated case.

It was anticipated that local oxygen depletion within crevice environments could develop anaerobic conditions to support SRB development there. However, the results did not give strong indication of supported SRB growth in the localized occluded environments in the crevice after either inoculation events. The relatively low COD values were likely in part due to sampling from the bulk solution and not directly within the crevice itself where the SRB population can be concentrated.

The sulfide test results (Table 7) after the second inoculation were consistent with the COD indicators of SRB development in the de-aerated open and crevice CTRL solutions such as the large initial increase in COD due to sulfide production. The lower COD levels for the naturally aerated cases were comparable to the lower sulfide content measured after the second inoculation.

The high COD for non-inoculated CTRL de-aerated cases did not show the visual indication of iron sulfide formation associated with SRB and some contamination possibly due to inadvertent contamination with the isolating oil used in the test cell during the second inoculation was suspected or other microbiological activity. Modification of the test setup and test methods for Test setup B were made in part due to this consideration.

SULF1/SULF2. As shown in Figure 8, high COD levels were detected in the SULF2 tests (where additional sulfate ions were introduced) even where no SRB was introduced. The experiment was repeated with another set of duplicate samples in SULF1 tests. In the repeated experiment, measured COD levels were lower and in the order of magnitude from the control CTRL test conditions. Fewer COD measurements were made for these cases and periodic behavior of COD due to sulfide production and iron sulfide precipitation were not captured here.

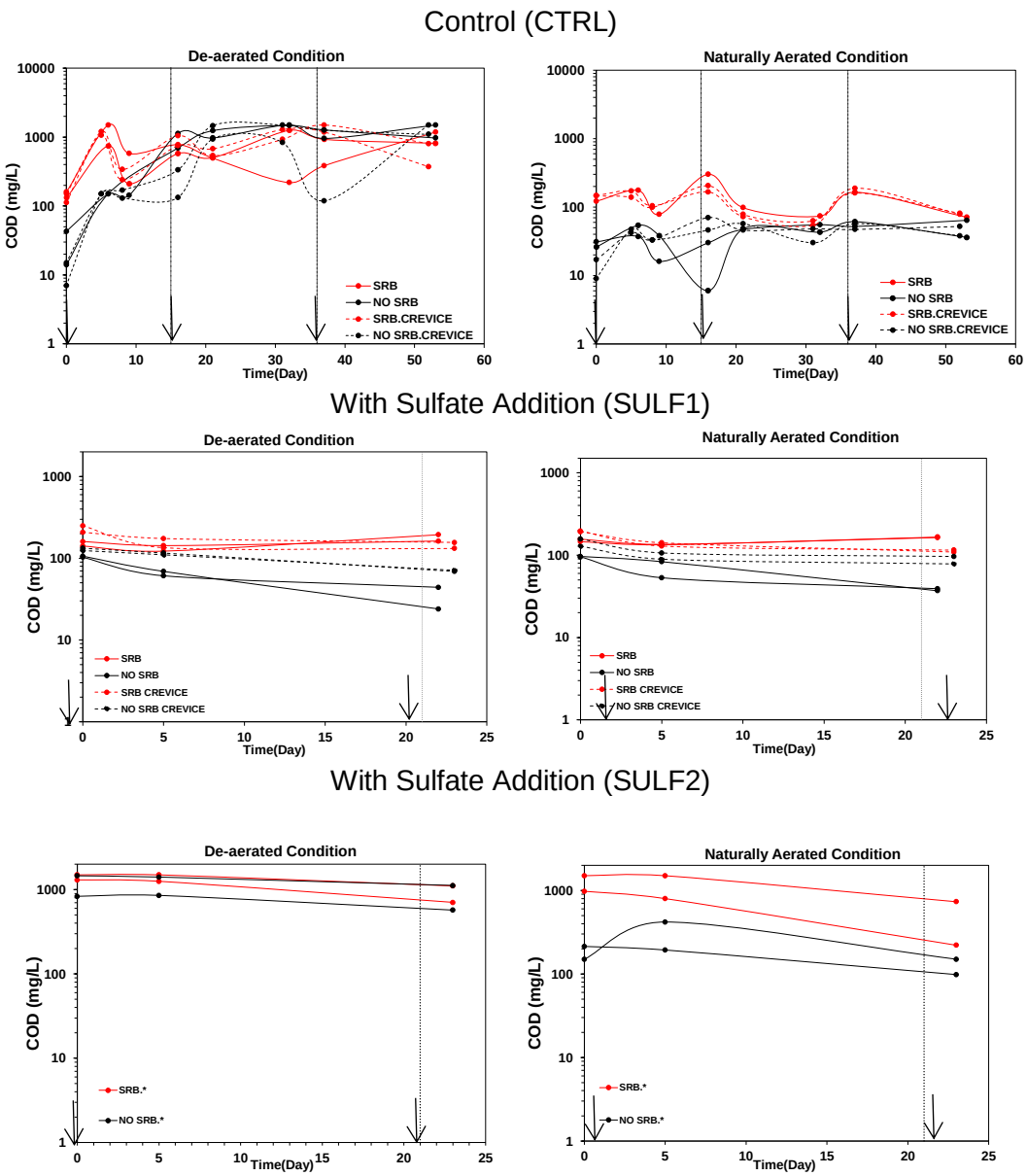

Figure 5.6. Chemical Oxygen Demand for Samples in Test Setup A.
Vertical lines represent time of inoculation.
Results from duplicate samples shown for each test condition.

5.2.1.1.c Microbiological Analysis

Samples of solution for the CTRL cases were taken for the bacteria microbiological analysis. Results are shown in Table 5.5 -5.7. The inoculated solutions all showed high concentrations of SRB as well as IRB, APB, and SFB. As expected, SRB levels were higher in the de-aerated solutions than the naturally aerated conditions. Correlating trend of higher SRB levels in crevice conditions with some level of expected de-aeration was not captured by the solution sampling methodology. Test setup B employed complementary BTS sessile test kits sampling the crevice surface.

SRB testing of non-inoculated solutions confirmed low SRB activity. The low SRB counts were consistent with low COD for the naturally aerated CTRL case and confirmed that the high COD in the de-aerated CTRL case was not associated with SRB. However, in the latter case, the total bacteria content was high (10^6-10^7 cfu/mL) in comparison to the comparable naturally aerated condition sample (10^2-10^3 cfu/mL).

Table 5.5. Bacteria Content in Test Setup A De-aerated CTRL Conditions.

Bacteria (CFU.mL^{-1})	**Inoculated**	**Non-Inoculated**	**Inoculated/Crevice**	**None-Inoculated/ Crevice**
Sulfate Reducing Bacteria (SRB)	500,000 (A), 500,000 (A)	-, -	500,000 (A), 115,000 (A)	<1 (NA), <1 (NA)
Iron-Reducing Bacteria (IRB)	35,000 (A), 35,000 (A)	-, -	35,000 (A), 35,000 (A)	<1 (NA), <1 (NA)
Acid Producing Bacteria (APB)	82,000 (A), 82,000 (A)	-, -	82,000 (A), 82,000 (A)	450 (M), 450 (M)
Slime-Forming Bacteria (SFB)	440,000 (A), 440,000 (A)	-, -	440,000 (A), 440,000 (A)	<20 (NA), <20 (NA)

Aggressivity: (NA) Not Aggressive, (M) Moderately Aggressive, (A) Aggressive. General guidelines for BART test for corrosion

Table 5.6. Bacteria Content in Test Setup A Naturally Aerated CTRL Conditions.

Bacteria (CFU.mL-1)	**Inoculated**	**Not Inoculated**	**Inoculated/Crevice**	**Not Inoculated/ Crevice**
Sulfate Reducing Bacteria (SRB)	27,000 (A), -	<1 (NA), -	27,000 (A), 6,000 (A)	<1 (NA), <1 (NA)
Iron-Reducing Bacteria (IRB)	35,000 (A), -	<1 (NA), -	9,000 (A), 9,000 (A)	<1 (NA), <1 (NA)
Acid Producing Bacteria (APB)	475,000 (A), -	<2 (NA), -	82,000 (A), 82,000 (A)	450 (M), 450 (M)
Slime-Forming Bacteria (SFB)	67,000 (A), -	67,000 (A), -	440,000 (A), 440,000 (A)	500 (M), 500 (M)

Aggressivity. (NA) Not Aggressive, (M) Moderately Aggressive, (A) Aggressive. General guidelines for BART test for corrosion

Table 5.7. Total Bacteria Content in Test Setup A Naturally Aerated CTRL Conditions.

Test Conditions			Total Bacteria (cfu/ml)
Inoculated	De-Aerated	None Crevice	10^7, 10^7
		Crevice	10^7, 10^7
	Naturally Aerated	None Crevice	-, 10^7
		Crevice	10^6, 10^4
Not Inoculated	De-Aerated	None Crevice	10^6, 10^7
		Crevice	10^5, 10^5
	Naturally Aerated	None Crevice	10^2-10^3, 10^2-10^3
		Crevice	10^2, 10^4

5.2.1.2. Electrochemical Behavior

In the conventional understanding of MIC by SRB, SRB reduces sulfate ions by biotic reactions of adsorbed hydrogen (cathodic depolarization) that results in enhanced iron oxidation. The availability of adsorbed hydrogen can be available from the disassociation of water as part of the hydrogen evolution reaction.

It was postulated in the body of work of the research here that characteristics of crevice environments can affect the oxygen and hydrogen cathodic reactions (and its rates within an isolated crevice) and the metabolic paths as part of MIC caused by SRB. In the conventional view of crevice corrosion, acidification can occur from hydrolysis of water with the autocatalytic accumulation of chlorides. Within that localized environment, hydrogen reduction may occur at more noble potentials. However, the physical characteristics of the crevice (such as that differentiated between hard and soft marine fouling) were thought to affect the rates of reaction. If limitation of hydrogen reduction were imposed within the crevice, availability of adsorbed hydrogen used in biotic reactions of the hydrogenase enzyme in SRB as part of the pathway to reduce sulfate ions would then possibly reduce the rate of that form of MIC. Limitation on hydrogen reduction was posed for conditions with tight crevices. Soft porous crevices (as later considered in test setup B) would have adequate convection that result in more noble corrosion potential but higher corrosion rates. Hydrogen and available nutrients could promote MIC by SRB. Discussion on the electrochemical characteristics here and for test setup B are presented to identify these reactions relevant to SRB and MIC development.

5.2.1.2.a Open-Circuit Potential

Figure 5.7 shows the development of the corrosion potential for the steel samples in test setup A with the test conditions shown in Table 5.8. Notably the potentials during the test were generally in the range of -650 to -750mV_{SCE} consistent with expected values for steel in open neutral pH solutions. Although hydrogen reduction is expected to be thermodynamically possible at these potential levels (at neutral pH), the reduction reaction is expected to be predominantly oxygen reduction through the developed oxide layer on the steel surfaces in open solution environments. For the laboratory tests, the solutions had generally low oxygen

levels (relative to field conditions) with the introduction of industrial nitrogen for the de-aerated conditions and limited solution convection to promote oxygen intake for the naturally aerated conditions. Due to diffusion limitation of oxygen, corrosion rates are expected to be somewhat moderated, especially for the de-aerated test conditions. Oxide film development in crevice environments, however, would not have the same effect as in open conditions and oxygen diffusion would then not limit the corrosion rate of the steel within the crevice. Hydrogen reduction may be more important in this case.

The increase in potentials was related to cathodic ennoblement due to SRB activity. Subsequent drop in potentials were thought to be due to loss of SRB activity where adsorbed hydrogen on the steel surface could redevelop due to the loss of biotic reactions as SRB colonies diminish. The time frame where potential ennoblement was first measured until the drop in potential is shown in Table 5.8.

For the de-aerated case, there was ennoblement of potential after day 1 (and for up to 1 week) for inoculated cases coinciding with the proliferation of SRB after the initial inoculation event. The potential ennoblement occurred to a lesser extent after day 15, and no observable effect after day 35. Similar to the de-aerated test conditions, potential ennoblement was measured in the naturally aerated solutions after the first inoculation event and to a lesser extent after the second inoculation event on day 15. Like the de-aerated condition, no effect was observed after the third inoculation event on day 35.

Samples in de-aerated cases had open circuit potentials similar to those in the naturally aerated solutions. This would suggest that there was sufficient oxygen in the de-aerated solutions (using industrial nitrogen) where oxygen diffusion limitation was not well differentiated between aeration levels. This may have an impact in SRB development. Indeed, in the test solution, it was apparent that microbe activity was not consistently well augmented upon subsequent inoculations. This was in part due to the test conditions including aeration levels but also may be due to the fact the test solution itself was not circulated and environmental conditions deteriorated to where it could not support further activity.

Nevertheless, the apparent positive shift in measured potentials after inoculation was generally consistent with observed increase in COD and sulfide production after inoculation events. However, the time duration of potential ennoblement did not always have perfect periodicity with sulfide production levels after inoculation. The potential ennoblement after the second inoculation on day 15 in de-aerated solution was not prolonged (typically only 1 day) even though sulfide measurements there showed sulfide production after day 33. In the naturally aerated solution, the short time of measured potential ennoblement was closer attuned to the quick drop off in sulfide production after each inoculation event. Further consideration of solubility of sulfide and its various forms as well as iron cation presence should be made to elucidate the relationship between potential ennoblement and the measurable sulfide levels at discrete times.

In some control non-inoculated case, the OCP showed more noble potentials within the first few days. This observation was not expected as the periodic bubbling of nitrogen was conducted, and the chemical indicators described earlier did not indicate SRB development.

Similar potential ennoblement behavior was observed for the SULF open (non-crevice) test conditions indicating SRB development after the initial inoculation; however, the magnitude of polarization was apparently less. The additional sulfate levels did not appear to enhance SRB development in the open test conditions even with the additional SRB inoculations.

In both de-aerated and naturally aerated solutions (both CTRL and SULF conditions), the time of observed potential ennoblement was relatively short (typically less than 10 days). As described earlier, subsequent re-inoculation (with addition of nutrients) did not always sustain SRB activity. SRB activity appeared more continuous in the de-aerated solutions in open and crevice conditions. Potential ennoblement events in inoculated crevice environments were somewhat longer suggesting beneficial conditions to support SRB growth. The time of steel potential ennoblement was longest for crevice environments with higher sulfate levels. Although experimental scatter was apparent between test conditions and during the time of experiments, there was indication of more negative potentials for the samples with crevice environments, presumable due to oxygen depletion within the occluded crevice region. Oxygen depletion would lead to favorable anaerobic conditions for SRB.

Table 5.8. Time Duration of Potential Ennoblement (Days).

Test Condition	Inoculation	De- Aerated Condition				Naturally Aerated Condition			
		Open (No Crevice)		Hard Crevice		Open (No Crevice)		Hard Crevice	
CTRL	After 1st Inoculation	7	7	15(full)	9	3	NA	7	7
	After 2nd Inoculation	1	1	1	1	1	NA	1	1
SULF1/ SULF2	After 1st Inoculation	13/14*	13/14*	21(full)	21(full)	13/7*	13/9*	21(full)	21(full)
	After 2nd Inoculation	-/-*	-/-*	10	20 (full)	-/-*	-/-*	10	20(full)

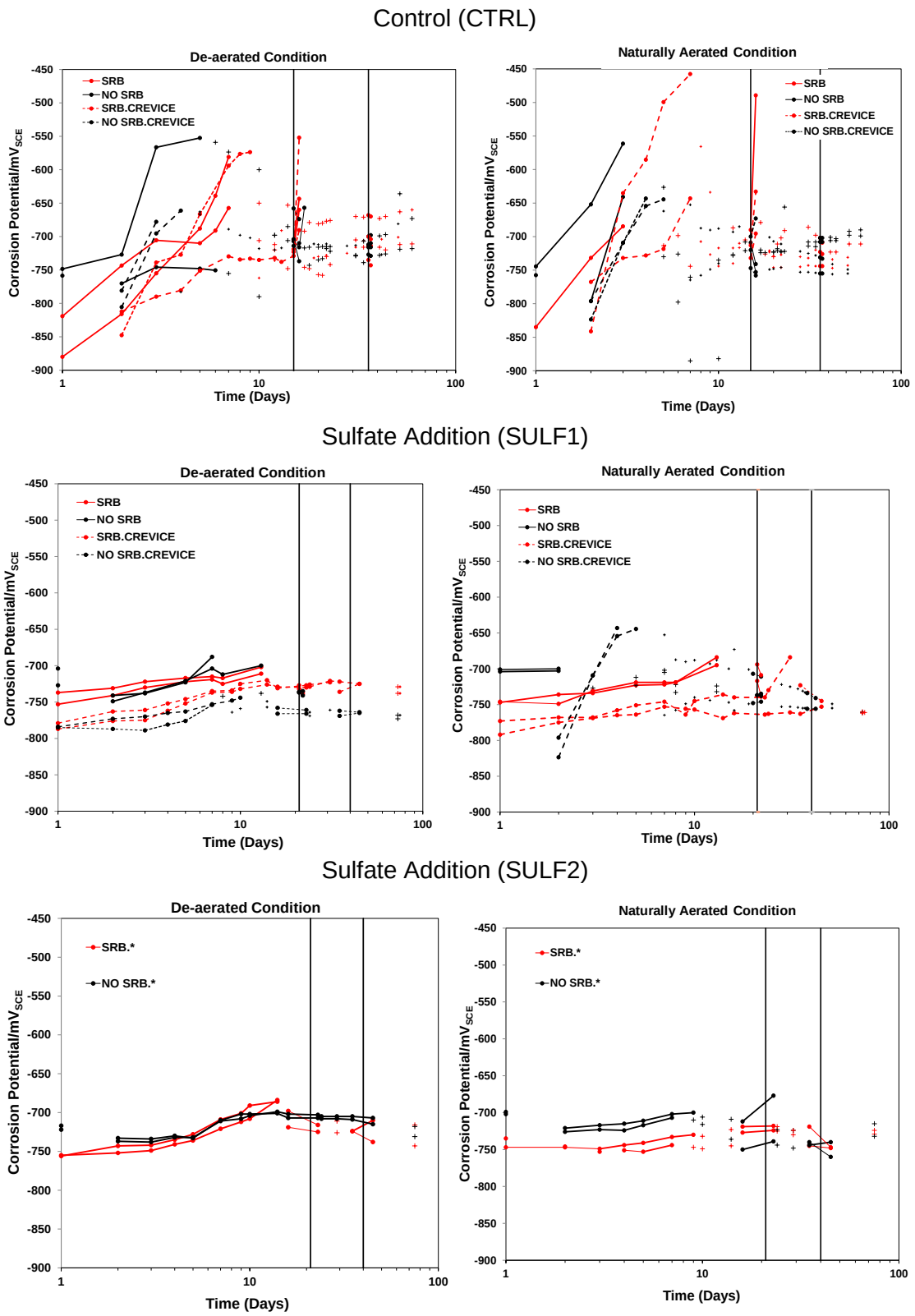

Figure 5.7. Open-Circuit Potential of Steel in Test Setup A Samples.
Vertical lines represent time of inoculation.
Results from duplicate samples shown for each test condition.

5.2.1.2.b Linear Polarization Resistance

Figure 5.8 shows the corrosion current density for the steel samples in test setup A. The trends in corrosion rates for the various test conditions were complicated and arise from the many chemical, environmental, and biotic factors in the testing. Assessment of the results is presented first by discussion of expected behavior in light of results earlier described and then with discussion of possible factors that may lead to deviations.

In de-aerated conditions, general corrosion is expected to occur at lower levels due to the less available oxygen levels to participate in oxygen reduction reactions. However, microbiological influenced corrosion was expected to be enhanced as SRB can better proliferate in anaerobic conditions. The corrosion rate for samples in the CTRL case significantly increased after the second inoculation event for both open and crevice environments. The rate was higher for the open environment than the crevice environment for the majority of the test (although high current densities for the crevice samples were measured near the end of the test exposure). The high currents were considered in part due to the higher SRB population described earlier and also due to the fact that part of the steel surface, within the crevice, had air bubbles that reduced the effective surface area. Furthermore, interpretation of corrosion current density can be complicated for localized corrosion in the crevice conditions. Conventional LPR measurements assume uniform current distribution to polarize the steel samples and assumes that the surface reaction to be homogeneous. These assumptions are likely not met for these measurements where corrosion, due to microbial activity, was expected to result in corrosion with localized anodes Corrosion current increased for one sample in the control de-aerated case with open environment after 15 days. As mentioned earlier, the control cases did exhibit higher COD not attributed to SRB during the same time period. Development of other forms of MIC cannot currently be discounted.

SRB levels were shown to be higher in the de-aerated test solutions than naturally aerated solutions and apparent potential ennoblement was observed after the first and second inoculations. LPR test results in the CTRL and SULF2 conditions showed trends consistent with these expectations. In these cases, the corrosion current densities were greater than 1 uA/cm^2. In the SULF1 condition however, the corrosion rates for the inoculated conditions was much less than the control non-inoculated solution. Review of earlier data showed that this test condition had low sulfide production after first inoculation and relatively low COD levels. Even though potential ennoblement was apparent, the shift in potential (as with the other SULF conditions) was not as great as in the CTRL condition. This would suggest that SRB development was not as strong as in the CTRL and SULF2 conditions.

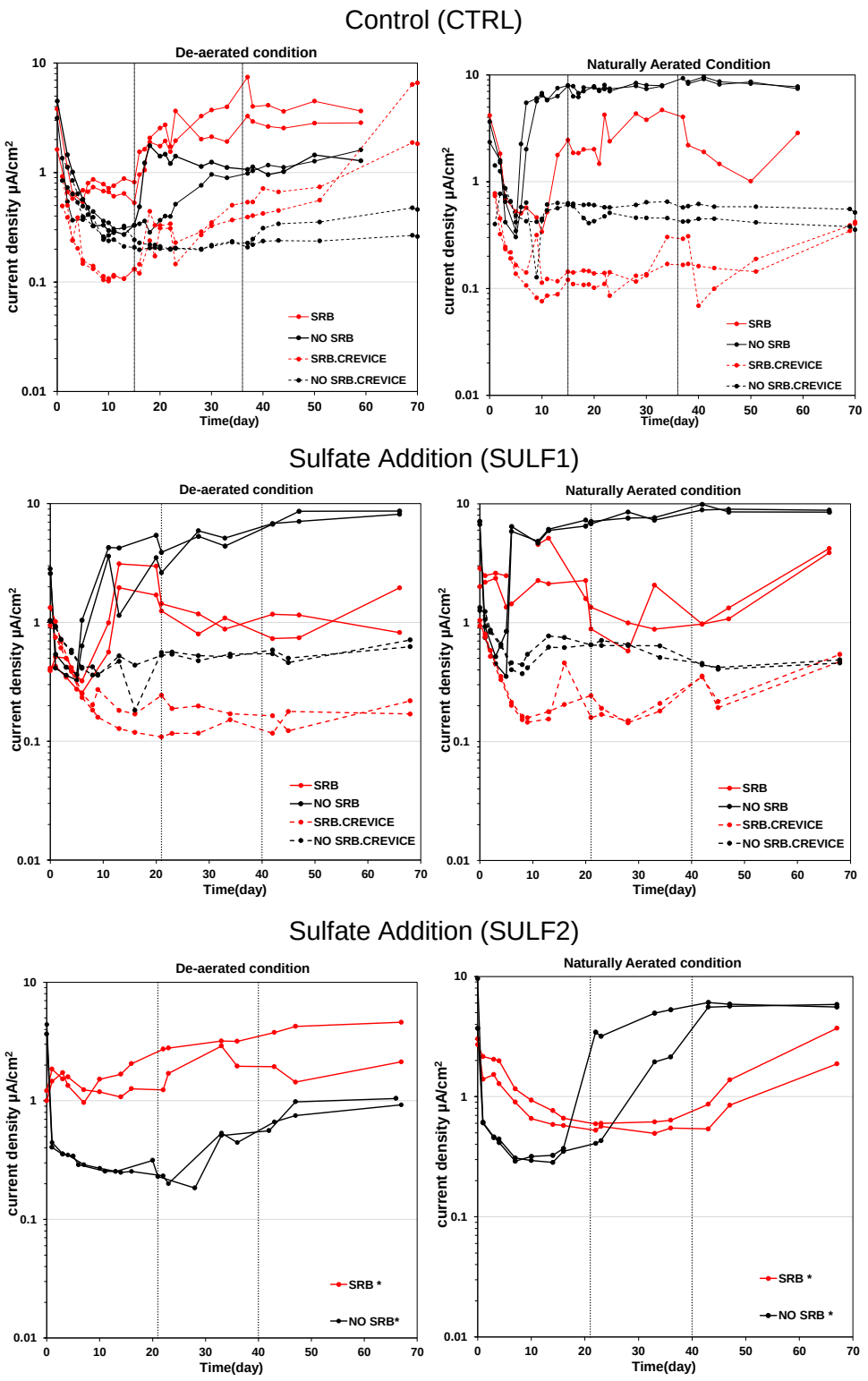

Figure 5.8. Corrosion Current Density for Test Setup A Samples.
Vertical lines represent time of inoculation.
Results from duplicate samples shown for each test condition.

In the naturally aerated conditions, corrosion activity would be expected regardless of inoculation levels due to pH and chemical constituency of the inoculation medium. Indeed corrosion currents were high for all samples in the open environments. As described earlier, it was observed that some level of SRB activity occurred in the inoculated cases. Sulfide levels were generally high after inoculation events. The SRB would be expected to contribute to corrosion activity especially since apparent potential ennoblement measured after inoculation events would suggest enhanced anodic polarization. Corrosion currents were high (>1 $\mu A/cm^2$) but were consistently lower than the control non-inoculated cases. A corrosion product accumulated on the inoculated samples as observed by blackening of the steel surface that reddened after removal from solution. It was posed that this layer allowed for reduced exposure of the steel surface thus possibly reducing the exposed surface in electrochemical polarization tests. In comparison, a red corrosion product developed on the non-inoculated sample in solution that continued to accumulate. Corrosion currents were overall lower in crevice environments than open environments for similar reasons described earlier.

5.2.1.2.c Potentiodynamic Polarization

The potentiodynamic polarization scans for the CTRL samples (after the prolonged exposure in solution in the main component of electrochemical testing described in the previous sections) are shown in Figure 5.9. Scans were initiated at the open circuit potential near ~-700mV_{SCE} for all cases, cathodically polarized to -1 V_{SCE} and reversed to identify anodic behavior. Larger anodic currents were observed for the de-aerated and naturally aerated solutions inoculated with SRB than the control non-inoculated solutions for both open and crevice conditions. Even though sulfide levels were generally low by this time for the naturally aerated inoculated solutions and were higher (up to 2.33mg/L) for the de-aerated inoculated solutions, the anodic currents were similar between those two conditions. This would indicate that the rate of anodic reactions at the polarized potentials reflect more the corrosion environments developed by the biotic conditions set by the SRB rather than the biotic reactions themselves. The anodic polarization of the steel interface therefore is not directly influenced by the reactions involved in the SRB metabolism. Environmental conditions such as production of sulfides and aggravating conditions under biofilm would support larger anodic currents. Although iron sulfide precipitates from SRB reactions iron corrosion product deposits were surmised to reduce the effective surface area, the anodic polarization scans did not indicate large physical effects on the polarization behavior (such as when lower currents can develop with the presence of the hard crevice). The forward scan of the cathodic branch of the polarization curve generally showed Tafel-like behavior for the reduction reaction. There was not differentiation of the apparent current exchange density for the different aeration conditions (including within crevices) which would indicate that oxygen reduction may not be the sole reduction reaction. On that line of thought, larger current exchange densities for the reduction reaction was observed for the inoculated cases. It was uncertain if the sulfate reduction reaction could be readily observed by electrochemical test methods as it was thought that reactions would primarily account for steel surface reactions and not necessarily electro-biochemical reactions. However, the larger cathodic currents in the inoculated cases may be related to

reduction reactions as part of cathodic depolarization (such $H^+ + e^- \rightarrow H$) by the SRB hydrogenase enzyme to reduce sulfate to sulfide.

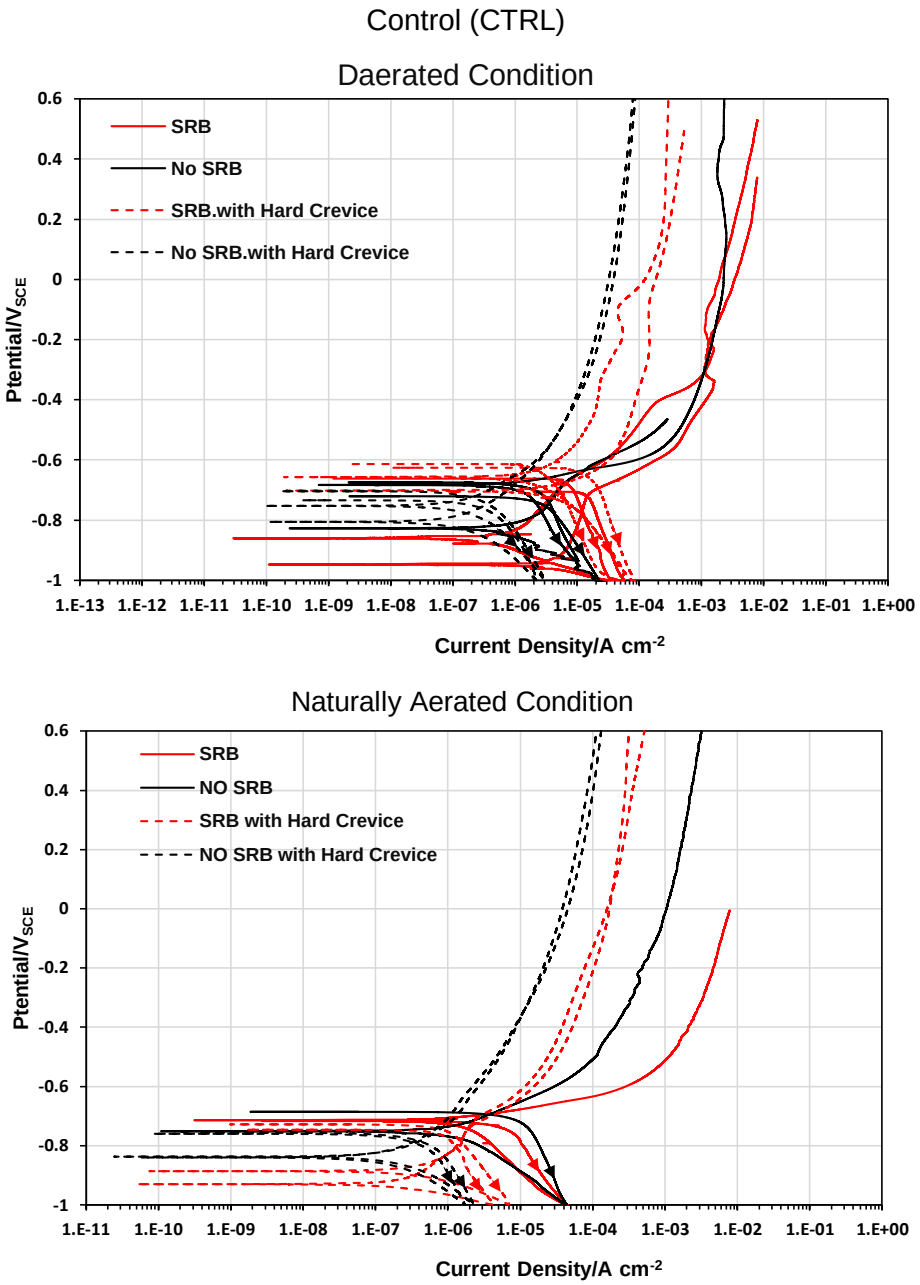

Figure 5.9. Potentiodynamic Polarization Scans for Test Setup A CTRL Samples.

5.2.1.3. Visual Assessment

A summary of the results from test setup A is summarized and followed by description of the physical appearance of the samples after testing.

5.2.1.3.a CTRL Conditions

High levels of iron sulfide precipitates and SRB populations developed on the surfaces of CTRL samples exposed in de-aerated inoculated cases suggesting enhanced SRB levels on the steel surface. Control non-inoculated cases did not develop this layer. Corrosion rates were higher for the inoculated cases than the control cases implicating MIC. Crevice environments were shown to support SRB growth and MIC. In naturally aerated conditions, development of iron sulfide precipitates was generally less (typically occurring after inoculation events) and lower planktonic SRB populations were measured indicating that high SRB growth was not sustained in time during testing. Control cases did not develop SRB. Corrosion rates for steel in the inoculated solutions were lower than for the non-inoculated cases. The crevice environment may support SRB growth but was not shown to substantially promote development MIC. Figure 5.10 shows the surfaces of the test samples after removal from solution. For the de-aerated conditions, the inoculated samples retained a thick layer of slime that formed due to the precipitation of iron sulfide. Under this film, a localized region of the steel surfaces showed surface oxidation. This corrosion eye was also observed at the center opening of the crevice samples. Surface rusting was observed for the non-inoculated case. For the naturally aerated test condition, the inoculated samples showed development of an orange surface oxide on the steel surface (at the crevice opening for crevice samples). At least for the open sample, this surface film was originally black in color prior to removal from solution. Localized surface oxidation was observed under the surface film. Or the non-inoculated case, corrosion developed on the steel surface accompanied by accumulation of iron corrosion products.

5.2.1.3.b SULF Conditions

SULF1 inoculated de-aerated samples and all SULF2 samples (both inoculated and non-inoculated cases showed development of small surface pit like features. The pitting features were attributed to corrosion in the sulfate solutions. All samples exhibited significant corrosion (Figure 5.11).

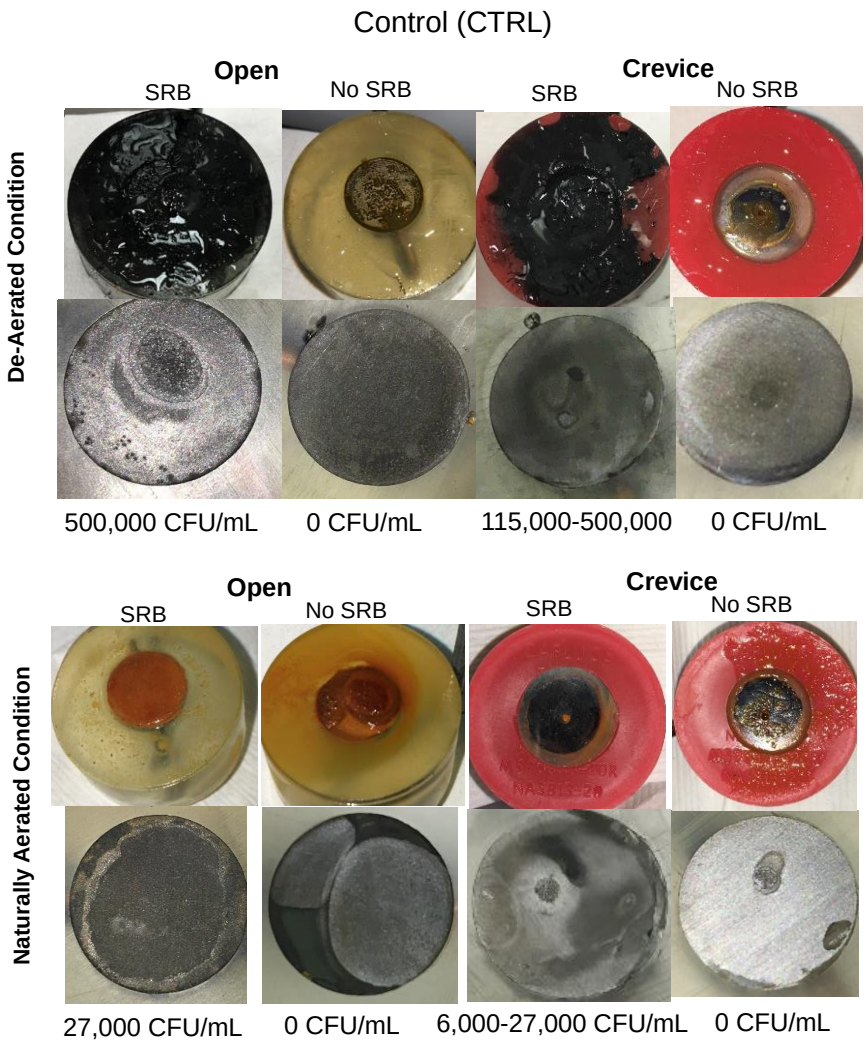

Figure 5.10. Photos of Test Setup A CTRL Electrodes after Testing.

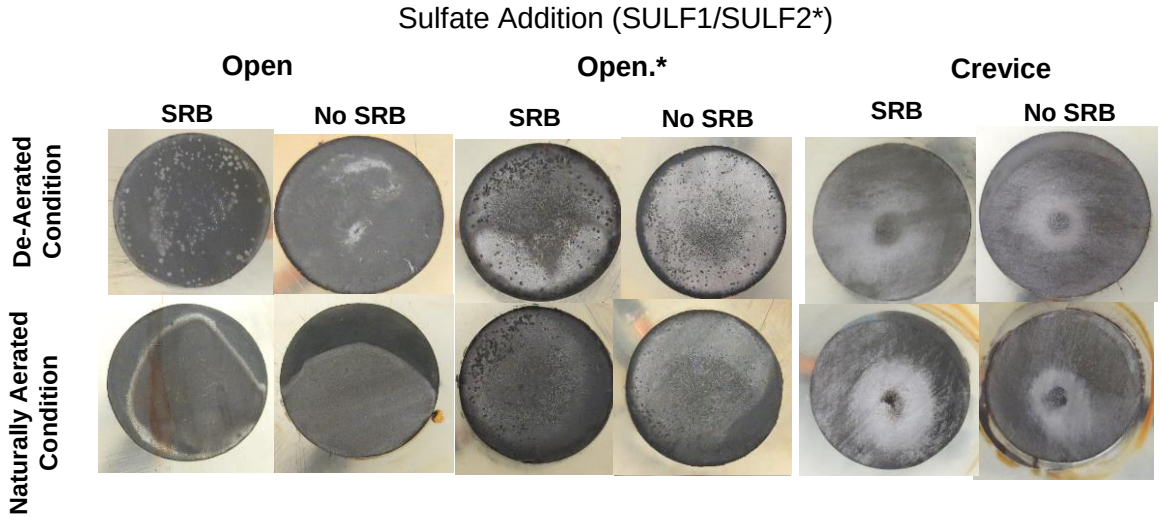

Figure 5.11. Photos of Test Setup A SULF1/2 Electrodes after Testing.

5.2.1.4 Summary of Results

Table 5.9. Summary of Findings for CTRL Samples in Open/Non-crevice Conditions.

Parameters	De-aerated Condition							
	Inoculation				No Inoculation			
	Sample 1		Sample 2		Sample 1		Sample 2	
	Day 2	Day 16	Day 2	Day 16	Day 2	Day 16	Day 2	Day 16
OCP (mV_{SCE})	-816	-643	-743	-660	-727	-737	-770	-716
Icorr (uA/cm^2)	0.65	0.95	1.11	1.53	1.41	0.48	0.53	0.33
COD (mg/L)	160	777	133	578	43	1132	14	695
SULFIDE (mg/L)	NA	2.26	NA	1.8	NA	0	NA	0
Parameters	Naturally Aerated Condition							
	Inoculation				No Inoculation			
	Sample 1		Sample 2		Sample 1		Sample 2	
	Day 2	Day 16	Day 2	Day 16	Day 2	Day 16	Day 2	Day 16
OCP (mV_{SCE})	NA	NA	-731	-679	-796	-753	-652	-741
Icorr (uA/cm^2)	NA	NA	1.78	1.83	1.54	6.96	1.49	5.54
COD (mg/L)	NA	NA	122	301	26	6	31	30
SULFIDE (mg/L)	NA	NA	0	0	NA	0	NA	0

Table 5.10. Summary of Findings for CTRL Samples with Hard Crevice.

Parameters	De-aerated Condition							
	Inoculation				No Inoculation			
	Sample 1		Samples 2		Sample 1		Samples 2	
	Day 2	Day 16	Day 2	Day 16	Day 2	Day 16	Day 2	Day 16
OCP (mV_{SCE})	-812	-552	-847	-690	-805	-674	-781	-710
Icorr (uA/cm^2)	0.31	0.12	0.38	0.14	1.01	0.22	0.63	0.19
COD (mg/L)	112	1046	151	751	15	334	7	133
SULFIDE (mg/L)	NA	1.48	NA	1.27	NA	0	NA	0
Parameters	Naturally Aerated Condition							
	Inoculation				No Inoculation			
	Sample 1		Samples 2		Sample 1		Samples 2	
	Day 2	Day 16	Day 2	Day 16	Day 2	Day 16	Day 2	Day 16
OCP (mV_{SCE})	-767	-695	-841	-633	-823	-653	-796	-758
Icorr (uA/cm^2)	0.32	0.14	0.36	0.11	0.72	0.63	1.27	0.59
COD (mg/L)	146	205	147	166	17	70	9	46
SULFIDE (mg/L)	NA	0.4	NA	0.159	NA	0	NA	0

Table 5.11. Summary of Findings for SULF2 Samples in Open/Non-crevice Conditions.

Parameters	De-aerated Condition							
	Inoculation				No Inoculation			
	Sample 1		Sample 2		Sample 1		Sample 2	
	Day 2	Day 22	Day 2	Day 22	Day 2	Day 22	Day 2	Day 22
OCP (mV_{SCE})	-743	-716	-752	-725	-733	-707	-737	-703
Icorr (uA/cm^2)	1.84	1.70	1.45	2.78	0.44	0.20	0.40	0.18
COD (mg/L)	1304	705	1500	1110	1462	1118	832	573
SULFIDE (mg/L)	0.424	1.59	0.424	1.76	0	0	0	0
Parameters	Naturally Aerated Condition							
	Inoculation				No Inoculation			
	Sample 1		Sample 2		Sample 1		Sample 2	
	Day 2	Day 22	Day 2	Day 22	Day 2	Day 22	Day 2	Day 22
OCP (mV_{SCE})	-746	-724	-747	-718	-726	-739	-721	-677
Icorr (uA/cm^2)	1.39	0.56	2.15	0.59	0.61	3.18	0.60	0.43
COD (mg/L)	1500	732	875	221	213	98	150	150
SULFIDE (mg/L)	0.424	0	0.424	0	0	0	0	0

Table 5.12. Summary of Findings for SULF1 Samples in Open/Non-crevice Conditions.

Parameters	De-aerated Condition							
	Inoculation				No Inoculation			
	Sample 1		Sample 2		Sample 1		Sample 2	
	Day 2	Day 22	Day 2	Day 22	Day 2	Day 22	Day 2	Day 22
OCP (mV_{SCE})	-731	-739	-741	-736	-741	-741	-749	-735
Icorr (uA/cm^2)	0.42	1.25	0.51	1.44	0.54	3.88	0.41	2.6
COD (mg/L)	160	162	141	194	106	24	103	44
SULFIDE (mg/L)	0	1.06	0	1.696	0	0	0	0
Parameters	Naturally Aerated Condition							
	Inoculation				No Inoculation			
	Sample 1		Sample 2		Sample 1		Sample 2	
	Day 2	Day 22	Day 2	Day 22	Day 2	Day 22	Day 2	Day 22
OCP (mV_{SCE})	-736	-739	-749	-709	-703	-735	-700	-738
Icorr (uA/cm^2)	2.18	0.88	2.48	1.34	0.92	7.10	0.74	6.76
COD (mg/L)	146	166	156	163	95	39	96	37
SULFIDE (mg/L)	0	0.424	0.424	1.484	0	0	0	0

Table 5.13. Summary of Findings for SULF1 Samples with Hard Crevice.

Parameters	De-aerated Condition							
	Inoculation				No Inoculation			
	Sample 1		Samples 2		Sample 1		Samples 2	
	Day 2	Day 22	Day 2	Day 22	Day 2	Day 22	Day 2	Day 22
OCP (mV_{SCE})	-763	-727	-776	-730	-773	-761	-787	-766
Icorr (uA/cm^2)	1.01	0.188	0.75	0.12	0.93	0.54	0.91	0.56
COD (mg/L)	250	132	208	156	124	71	133	69
SULFIDE (mg/L)	0.424	0.636	0.848	0.84	0	0	0	0
Parameters	Naturally Aerated Condition							
	Inoculation				No Inoculation			
	Sample 1		Samples 2		Sample 1		Samples 2	
	Day 2	Day 22	Day 2	Day 22	Day 2	Day 22	Day 2	Day 22
OCP (mV_{SCE})	-768	-740	-771	-735	-764	-762	-775	-764
Icorr (uA/cm^2)	0.75	0.16	0.80	0.19	1.24	0.70	1.06	0.64
COD (mg/L)	192	109	196	115	128	78	157	96
SULFIDE (mg/L)	2.12	1.06	1.908	1.06	0	0	0	0

5.2.2. Test Setup B

5.2.2.1. Microbiological Activity

5.2.2.1.a Sulfide Production

Similar to test setup A, sulfide measurements were made on select days after inoculation. In general, all inoculated samples for all test conditions showed blackening of the solution indicating iron sulfide precipitation from sulfide production from SRB, but the de-aerated solutions showed greater extent of sulfide precipitates (Figure 5.12). Visual indication of iron sulfide precipitation was not evident in the non-inoculated samples. Of note, there was a significant increase in turbidity for both inoculated and non-inoculated naturally aerated solutions.

Figure 5.12. Example of Solution Blackening Due to Iron Sulfide Precipitation.

CTRL B.The effect of additional nutrients (20 or 40 mL of the modified Postgate B solution) on SRB development was assessed in CTRL B20 and B40 test samples (Figure 5.13). In the de-aerated solutions, a large spike in sulfide concentration was observed at day 7 for both nutrient levels indicating high sulfide production with similar growth times. For the crevice condition, the higher nutrient levels showed prolonged lengths of sulfide production indicating positive effect of higher nutrient levels. In the naturally aerated solutions, low sulfide levels were measured after the initial inoculation for all test cases except for late sulfide production after 7 days for the open (non-crevice) solution with 40mL of additional nutrients.

CTRL A. The CTRL A tests were replicates of the CTRL B20 samples previously described. Similar results in sulfide development were observed but notably magnitudes were lower. This was attributed to the fact that CTRL B samples were inoculated with broth directly incubated from source river water. Regardless, a similar spike in sulfide production in both de-aerated open and crevice conditions indicated SRB activity. Like the CTRL B samples, less sulfide production was generally observed in the naturally aerated solutions (Figure 5.14). Here sulfide production in the soft crevice condition was observed. The addition of sulfates in SULF A de-aerated solutions showed an increase in sulfide production indicating positive effect of sulfate levels in SRB activity and relatively similar results in the naturally aerated solutions emphasizing the relatively adverse effects of high oxygen levels on SRB development and positive effects of crevices to support SRB in localized occluded spaces. Rougher surfaces (60 GRIT A) showed positive effect to encourage SRB growth.

(CTRL-B)

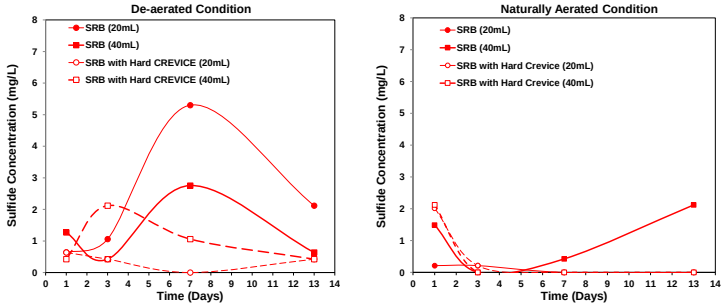

Figure 5.13. Sulfide Production Level for Setup B CTRL B Samples.

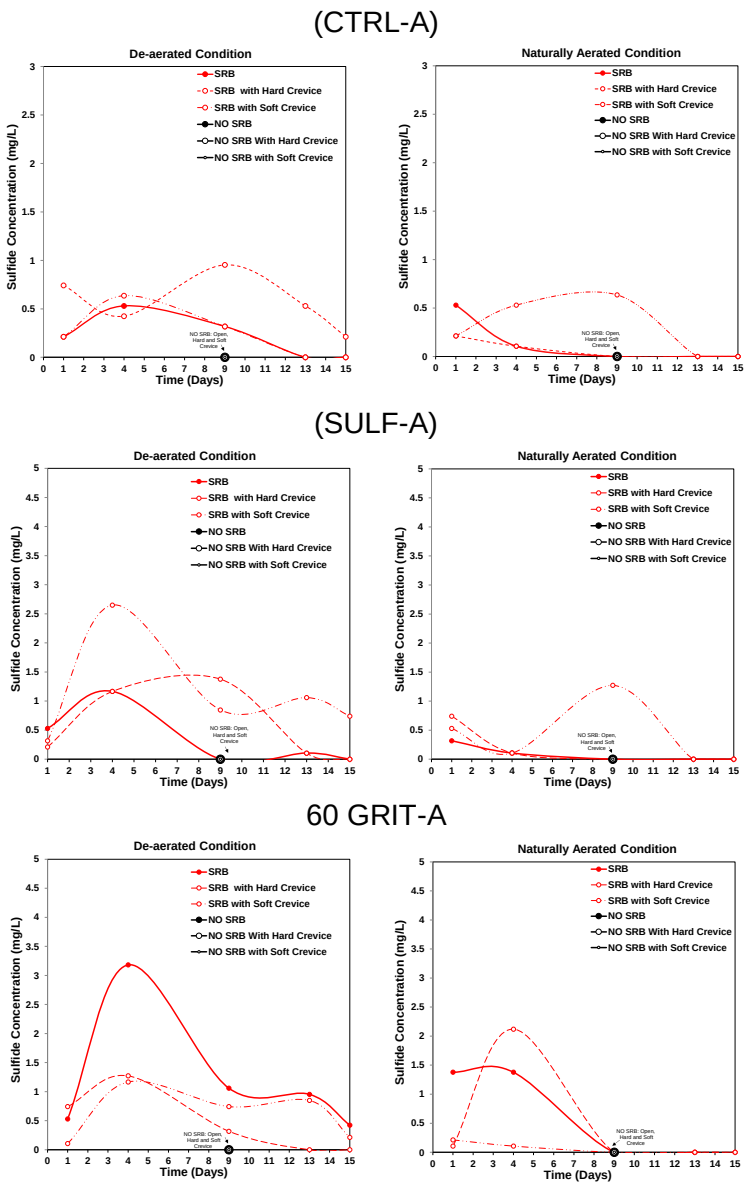

Figure 5.14. Sulfide Production Level for Setup B CTRL A Samples.

5.2.2.1.b Chemical Oxygen Demand

As discussed earlier for test setup A, proclivity of SRB activity in the test solution may be assessed by Chemical Oxygen Demand (COD). For each test condition in test setup B, an aliquot (2mL) of test solution was extracted and measured by colorimetric COD method at three times during the 15-day test. Test data for both COD and sulfide levels from test setup B were correlated as shown in figure 5.15. As expected, sulfide levels were higher in test solutions with higher COD. In general, sulfide levels larger than 0.1 mg/L were present when COD exceeded an lower minimum bound of 250 mg/L or a higher minimum bound of 400 mg/L.

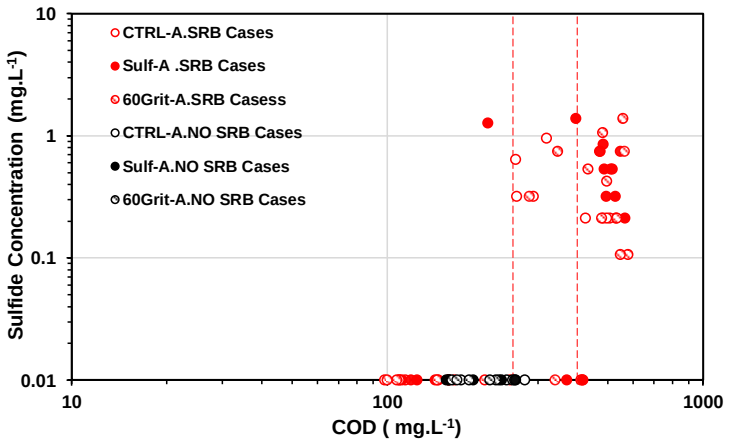

Figure 5.15. COD and Sulfide-correlated Data.
Vertical lines represent lower and higher minimum bound for COD.

In the naturally aerated solutions, high COD levels in the inoculated solutions dropped in time for all test conditions (Figure 5.16). This was consistent with early SRB activity where sulfide generation was detected and towards the end of the test where low sulfide levels indicated low SRB activity. COD levels for non-inoculated samples at the start of the tests were as expected lower than the inoculated samples. The effect of crevice environments, sulfates, and surface roughness was not well differentiated here.

For the de-aerated solutions, COD levels were elevated throughout the test for the inoculated samples, consistent with prolonged sulfide production (Figure 5.16). In midtest (around day 9), COD values showed a dip. This was generally consistent with the drop in sulfide levels after an initial spike where sulfides precipitated thus reducing electron donor concentration. Later spikes in sulfide levels would correspondingly account for the higher COD levels at the end of the test. For non-inoculated solutions, COD levels dropped to levels below where SRB was expected to be active (based on the sulfide testing). The prolonged periods of high COD were indicative gave indication of enhanced conditions to support SRB with the effect of crevice environments, sulfates, and surface roughness. COD for CTRL B tests showed similar trends as replicate tests in CTRL A tests but COD values were higher due to the higher activity with greater initial nutrient levels (Figure 5.17).

(CTRL-A)

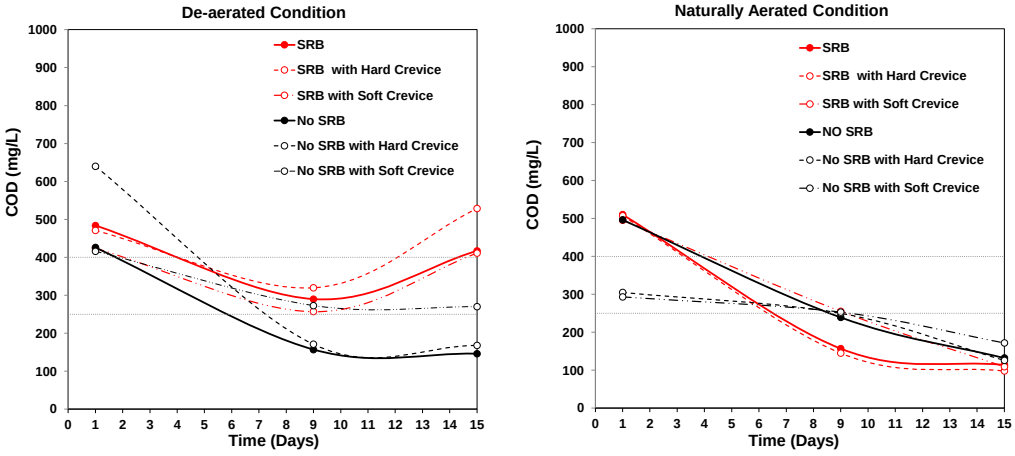

(SULF-A)

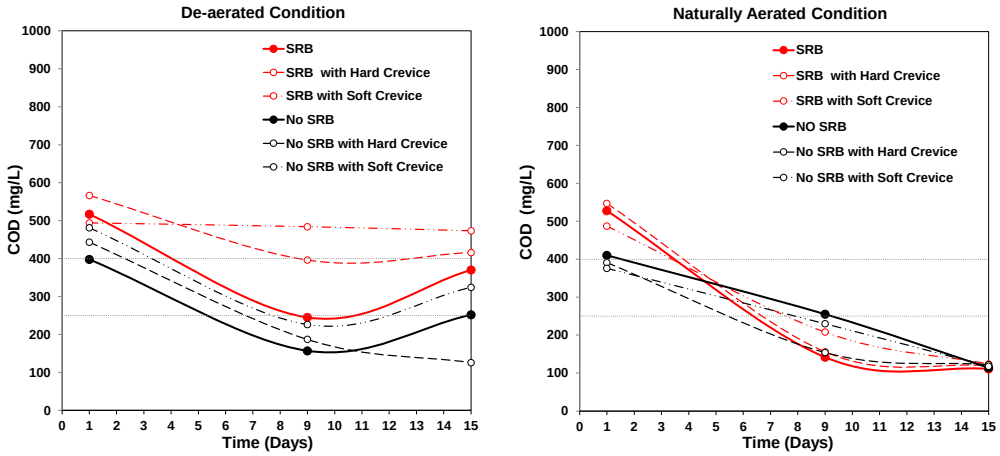

60 GRIT-A

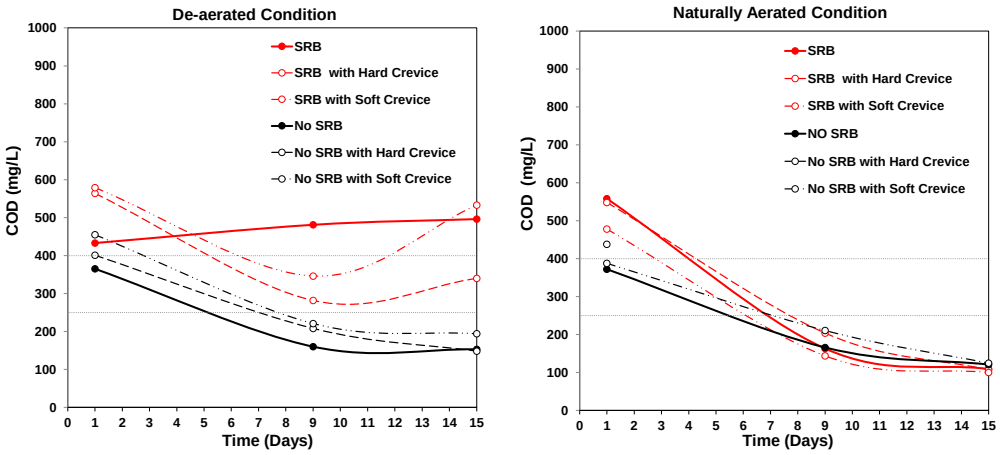

Figure 5.16. COD for Setup B CTRL A Samples.

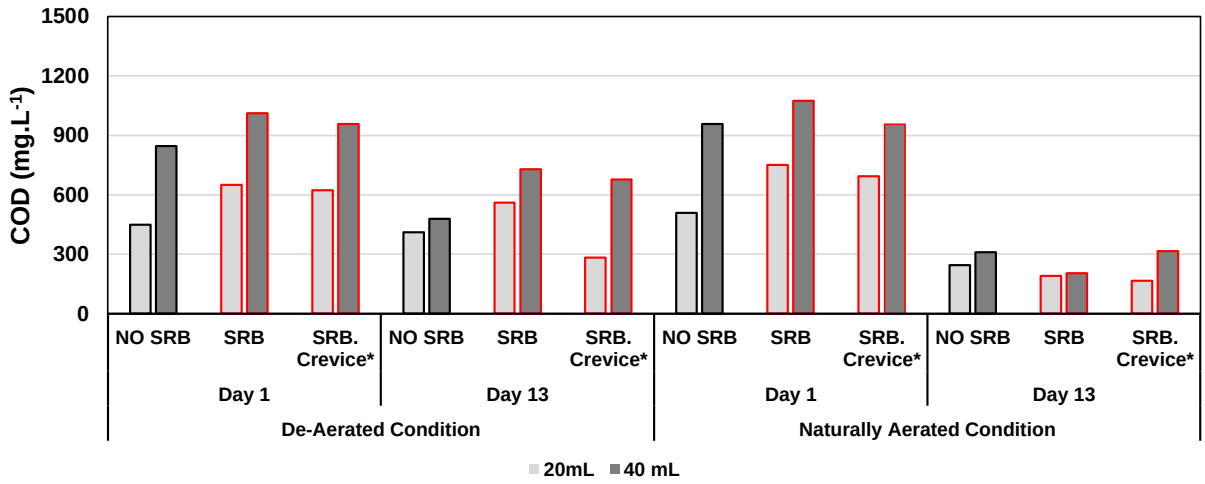

Figure 5.17. COD for Setup B CTRL B Samples.

5.2.2.1.c Microbiological Analysis

Surface swabs from the steel surface of samples in the CTRL-A, SULF-A, 60GRT-A, CTRL-B test conditions were analyzed using the Biotechnology Solutions sessile test kits to identify SRB populations (Table 5.14). In the de-aerated solutions for all inoculated samples, the SRB count per mL was high regardless of test conditions of sulfate additions, surface roughness, open, hard, or soft crevice. This is reflective of the ability of anaerobic environments to support SRB development. In non-inoculated, SRB levels were zero or low for similar test environments and conditions in the de-aerated solutions. Similar observations were made for the naturally aerated conditions however, SRB populations were lower than magnitude when compared to the de-aerated inoculated conditions. Like the de-aerated conditions, low or zero SRB levels were observed in the non-inoculated cases.

Table 5.14. Reported Bacteria per mL in Test Setup.

Test Condition	De-aerated condition					
	SRB	SRB with Hard Crevice	SRB with Soft Crevice	No SRB	No SRB with Hard Crevice	SRB with Soft Crevice
Control (CTRL-A)	$\geq 10^8$	$\geq 10^8$	10^7	0	10^3	0
Sulfate Ion Addition (SULF-A)	$\geq 10^8$	10^7	10^7	10^3	0	0
Rougher Surface (60GRT-A)	$\geq 10^8$	$\geq 10^8$	10^6	10^2	0	0

Test Condition	Naturally Aerated condition					
	SRB	SRB with Hard Crevice	SRB with Soft Crevice	No SRB	No SRB with Hard Crevice	SRB with Soft Crevice
Control (CTRL-A)	10^6	10^6	10^6	10	10	0
Sulfate Ion Addition (SULF-A)	10^6	10^6	10^6	0	10^4	0
Rougher Surface (60GRT-A)	10^6	10^6	10^6	10^3	10^2	0

Test Condition	De-aerated condition			Naturally Aerated condition		
	No SRB	SRB	SRB with Hard Crevice	No SRB	SRB	SRB with Hard Crevice
Control (CTRL-B20)	NA	$\geq 10^6$	$\geq 10^6$	NA	10^4	$\geq 10^6$
Control (CTRL-B40)	NA	10^5	10^3	NA	$\geq 10^6$	10^5

5.2.2.2. Corrosion Development

5.2.2.2.a Open-Circuit Potential

Uniform corrosion with high corrosion rates can be expected in natural water systems depending on oxygen levels, but localized corrosion can also occur. Crevice environments can cause localized corrosion with possible accumulation of aggressive chemical species and acidification. Furthermore, MIC due to SRB can further aggravate corrosion. SRB can cause potential ennoblement (cathodic depolarization) due to biotic activities as part of the reduction of sulfate to sulfide. Corrosion potentials can be reflective of these corrosion conditions.

As described in the results section for test setup A, oxygen reduction can be expected to be an important reduction reaction in open (non-crevice) conditions. In neutral pH solutions, steel can develop a layer of oxides where oxygen diffusion limitations can come into play. Furthermore, the de-aerated solutions here were bubbled with high purity nitrogen and oxygen levels were expected to be lower. Correspondingly, the open circuit potentials were electronegative. Potentials typical for steel in neutral pH solutions are in the order of ~-700m$V_{SCE.}$ More negative potentials were expected in de-aerated conditions. SRB activity was expected to show potential ennoblement.

CTRL-B. The initial OCP for CTRL B samples in de-aerated and naturally aerated solutions was <-650mV_{SCE} (Figure 5.18). In the de-aerated inoculated solution, the potential for CTRL-B20 and –B40 samples showed significant potential ennoblement after day 4. To a lesser extent, potential ennoblement was observed for the inoculated naturally aerated B20 sample. All other samples maintained potentials relative to their potential after day 1 to the end of the test (day 11). It was apparent that nutrient levels for both level of supplement were adequate to support SRB.

CTRL-A. In the de-aerated and naturally aerated inoculated condition, the open and soft crevice samples showed more positive potentials (~-650mV_{SCE}), although as sudden drop in potential was observed for the naturally aerated open (non-crevice) sample (Figure 5.19). Other de-aerated samples had OCP <-650m$V_{SCE.}$

SULF-A. Similarly, positive potentials were measure for the de-aerated inoculated open and soft crevice environments. Only the soft-crevice inoculated sample in the naturally aerated condition showed similar noble potentials (Figure 5.19).All other samples had OCP <-650mV_{SCE}.

60GRT-A. Coincidently, similar noble potentials were measured for the inoculated open and soft crevice samples in bot de-aerated and naturally aerated solutions. However, a sharp drop in potential was measured for the sample naturally aerated inoculated solution with open environment Figure 5.19). All other samples had OCP <-650mV_{SCE}.

Unlike the inoculated samples with open and soft crevice, more negative potentials were measured for all cases with hard crevices regardless of inoculation. Possible limitation of hydrogen gas formation within tight crevices and oxygen depletion may cause limitation on reduction reaction. It was postulated that lower availability of ads hydrogen and less sulfate availability would reduce SRB activity. As such the test results showed possibility reduced SRB activity in tight crevices.

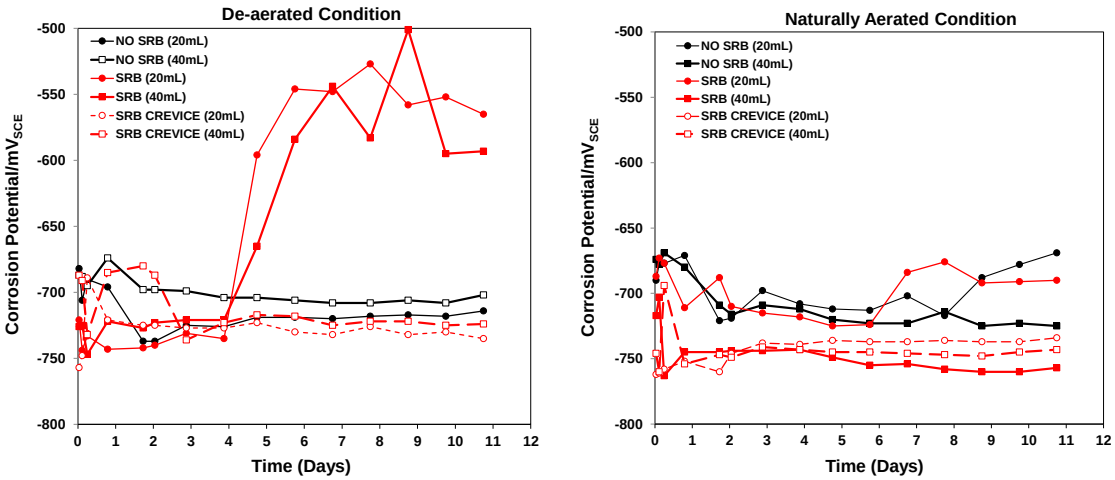

Figure 5.18. OCP for Test Setup B CTRL B Samples.

Control (CTRL-A)

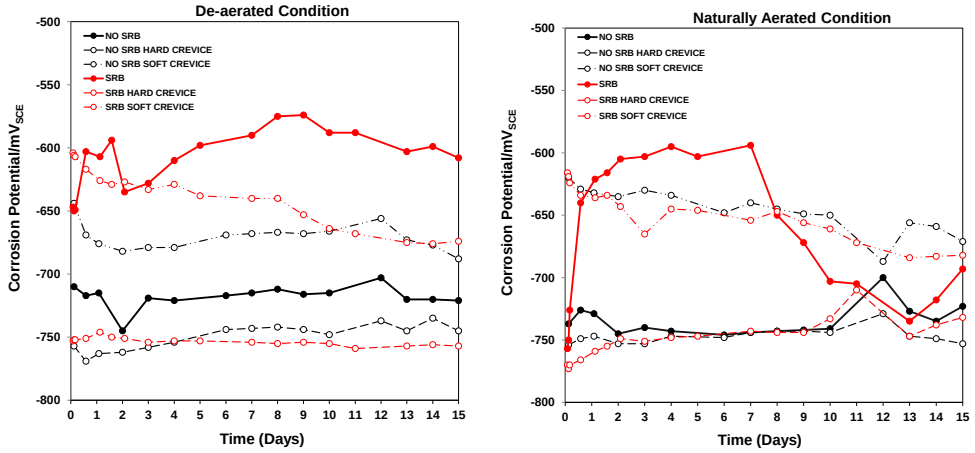

Sulfate Addition (SULF-A)

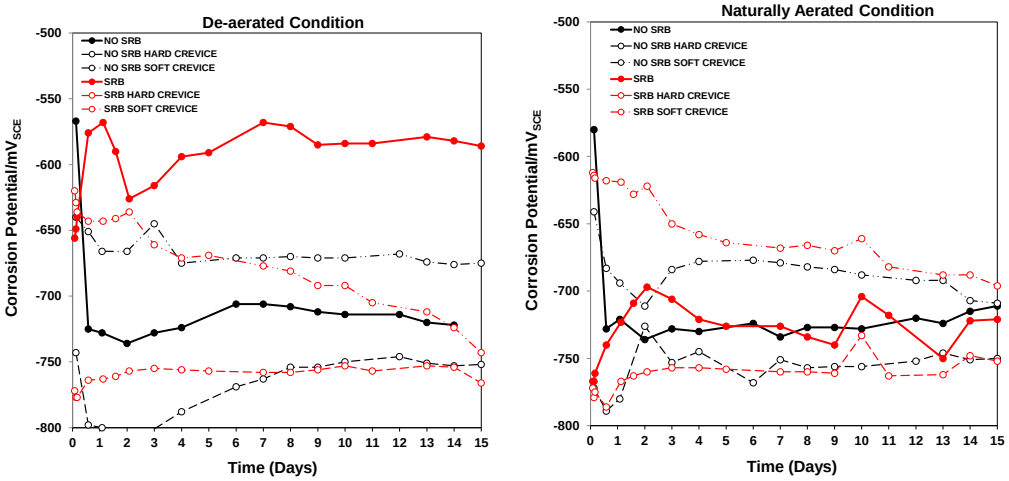

Surface Roughness (60GRT-A)

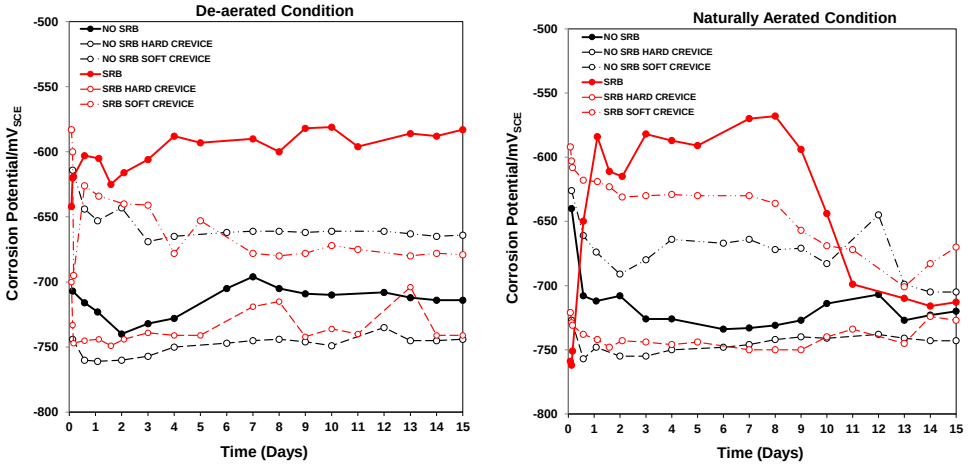

Figure 5.19. OCP for Test Setup B CTRL A, SULF-A, 60GRT-A Samples.

5.2.2.2.b Linear Polarization Resistance

As discussed previously, corrosion rates of steel in neutral pH solution was expected to be moderated by the oxygen reduction reaction and oxygen availability would be important. With MIC due to SRB, hydrogen cathodic reactions would be more important. Indeed, observations in measured electronegative OCP values gave indications of low oxygen levels in de-aerated solutions and instances in crevice environments. Fluctuations in potentials gave indication of SRB activity in inoculated solutions. Figure 5.20 and 5.21 shows the results of LPR measurements for each of the test condition in test setup B.

Correspondingly, there were variations in corrosion current densities in the range of $0.1<i_{corr}<1uA/cm^2$ for the inoculated cases. For the expected corrosion mechanisms due to SRB, the corrosion currents were expected to increase with the occurrences of potential ennoblement. In the OCP testing, there was indication of potential ennoblement for the inoculated solutions in both de-aerated and naturally aerated solution, but the corresponding corrosion currents showed inverse trend (notably in the naturally aerated cases). Where the potentials fluctuated to more positive potentials (presumably due to cathodic depolarization), the corrosion currents dropped.

From the viewpoint of corrosion kinetics, this behavior is due to a change in the anodic current- exchange current. This can be partially explained by account of the development of iron sulfide and biofilm on the steel surface where the effective surface area would be lower and net reaction involving iron oxidation would subsequently be lower. In the occluded spaces, this would not necessarily mean corrosion mitigation but rather a small anodic cell can develop and cause localized corrosion. Other complications may include the consumption of sulfate ions where the anodic current exchange density would decrease. In the small test volumes in test setup B, sulfate reduction by SRB would cause depletion of the available sulfate ions. However, this was not well reflected in the test cases with sulfate ion additions. Like in the CTRL case, a general trend of more positive potentials with time for the open and soft crevice (in both naturally aerated and de-aerated solutions) within the first week resulted in a corresponding decrease in current density in that time period. Samples with the soft crevice showed similar behavior. However, even though samples with hard crevices showed similar early decrease in potential, they had correspondingly lower current densities. In this case, the SRB population within the crevice would not have good interaction with planktonic SRB in the bulk solution. Therefore, the drop in potential (associated with reduced SRB activity at the steel surface) would consistently coincide with lower currents.

The rebound in corrosion currents in some cases after the redevelop of the more negative corrosion potentials after the first week of testing would likely reflect higher oxygen levels available at the steel surface after diminished SRB activity. This would be consistent with the observation of the inverse potential to current relationship being predominant in the naturally aerated solutions where the COD and sulfide levels dropped off significantly.

For the non-inoculated conditions, similar corrosion currents to the inoculated cases were measured even though potential ennoblement was not observed. As expected, corrosion rates were higher in the naturally aerated cases than de-aerated cases.

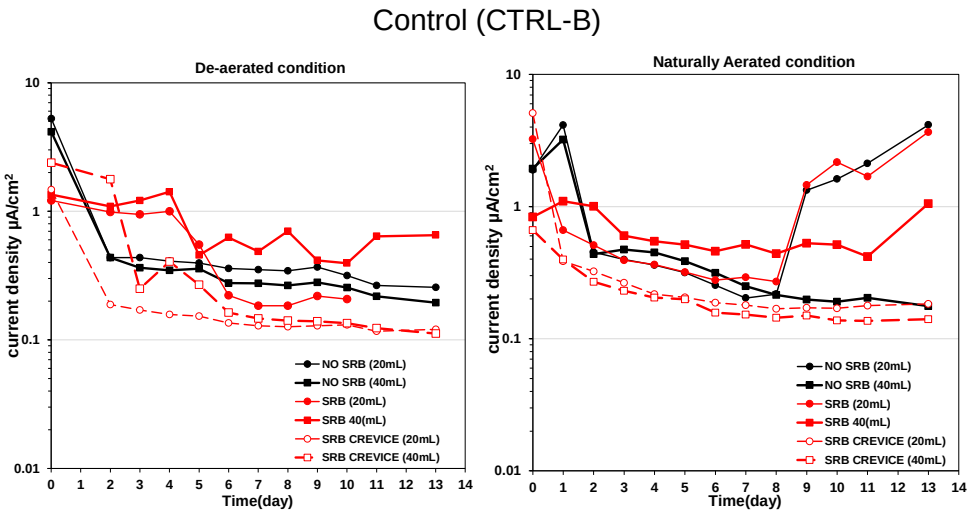

Figure 5.20. Corrosion Current Density for Test Setup B CTRL-B Samples.

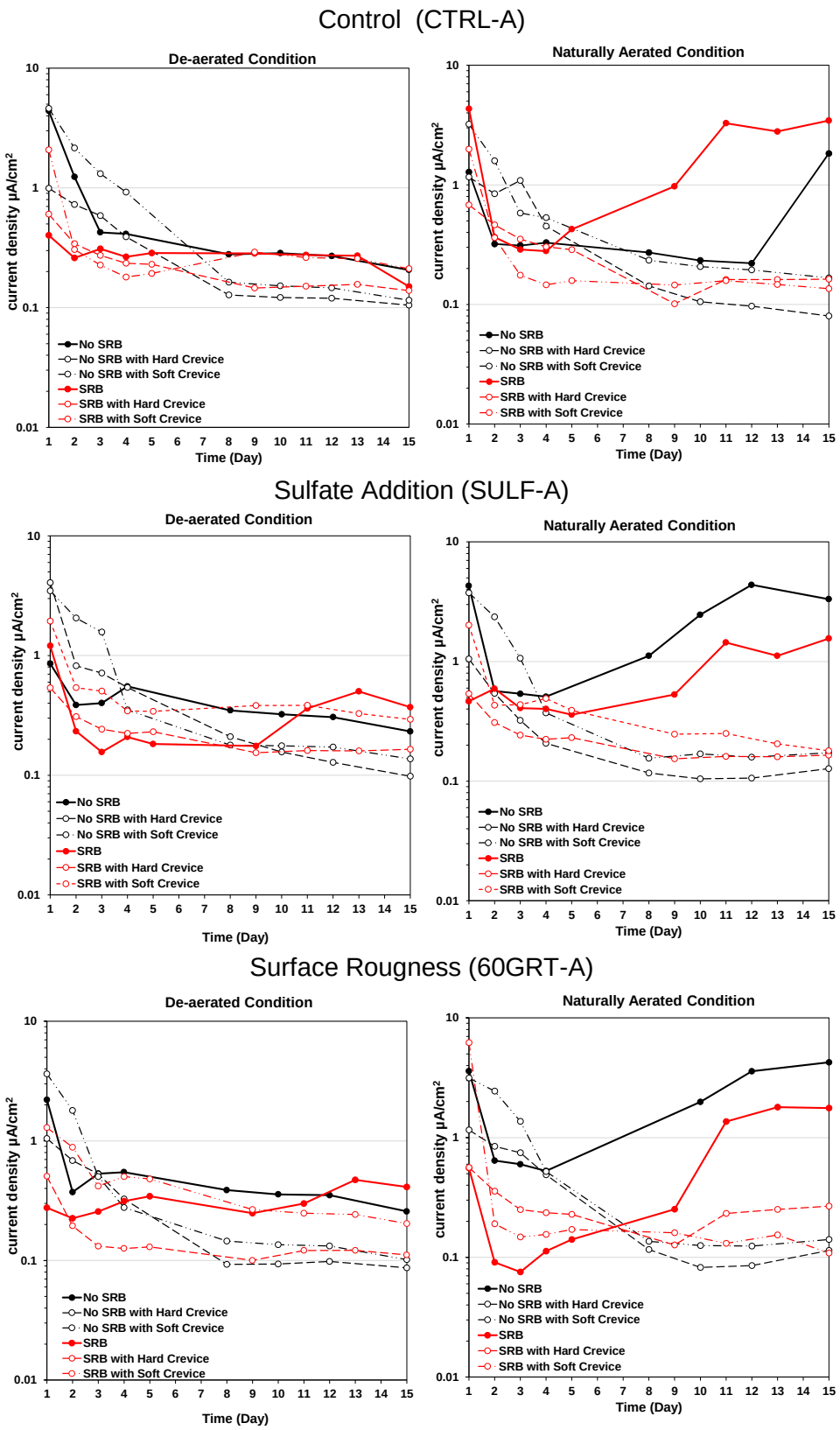

Figure 5.21. Corrosion Current Density for Test Setup B CTRL-A, SULF-A, and 60GRT-A Samples.

5.2.2.2.c Potentiodynamic Polarization

The potentiodynamic polarization scans for CTRL-B samples are shown in Figure 5.22 were made after OCP and LPR testing for up to 14 days. Scans were made starting at -1V_{SCE} and polarized anodically up to 0.6V_{SCE} and returned back to -1V_{SCE}.

For both de-aerated and naturally aerated solutions, somewhat larger anodic currents were measured for the inoculated open (non-crevice) conditions than the non-inoculated open conditions although not as distinct as was observed for test set-up A samples. Like samples in test setup A, the effect of aeration on anodic currents was not distinct and the currents were overall lower in crevice environments due to non-uniform polarization of the steel surface within the crevice. The influence of additional Postgate B nutrients did not appear to have a significant difference on the anodic behavior of the system.

Since the polarization curve was initiated at -1V_{SCE}, the initial currents reflected surface conditions in non-steady state condition. This polarization could then affect reduction reactions related to the SRB activity. For example, enhanced oxygen reduction could increase production of OH^- and increase local pH levels. Enhanced hydrogen reduction would produce hydrogen in excess of the level of rate of adsorbed hydrogen consumption and produce hydrogen that may disturb biofilm. As was observed in test setup A potentiodynamic polarization tests, after the forward sweep from the OCP, the cathodic curve had a reverse hysteresis showing a more negative OCP in the return scan. The starting condition of the potentiodynamic polarization tests in test setup B may be similar to the condition of the reverse scan in test setup A. Indeed, the apparent Tafel slopes of the forward curves here were similar to the return curves in test setup A. In consideration of this, the cathodic behavior may not reflect the influence of SRB.

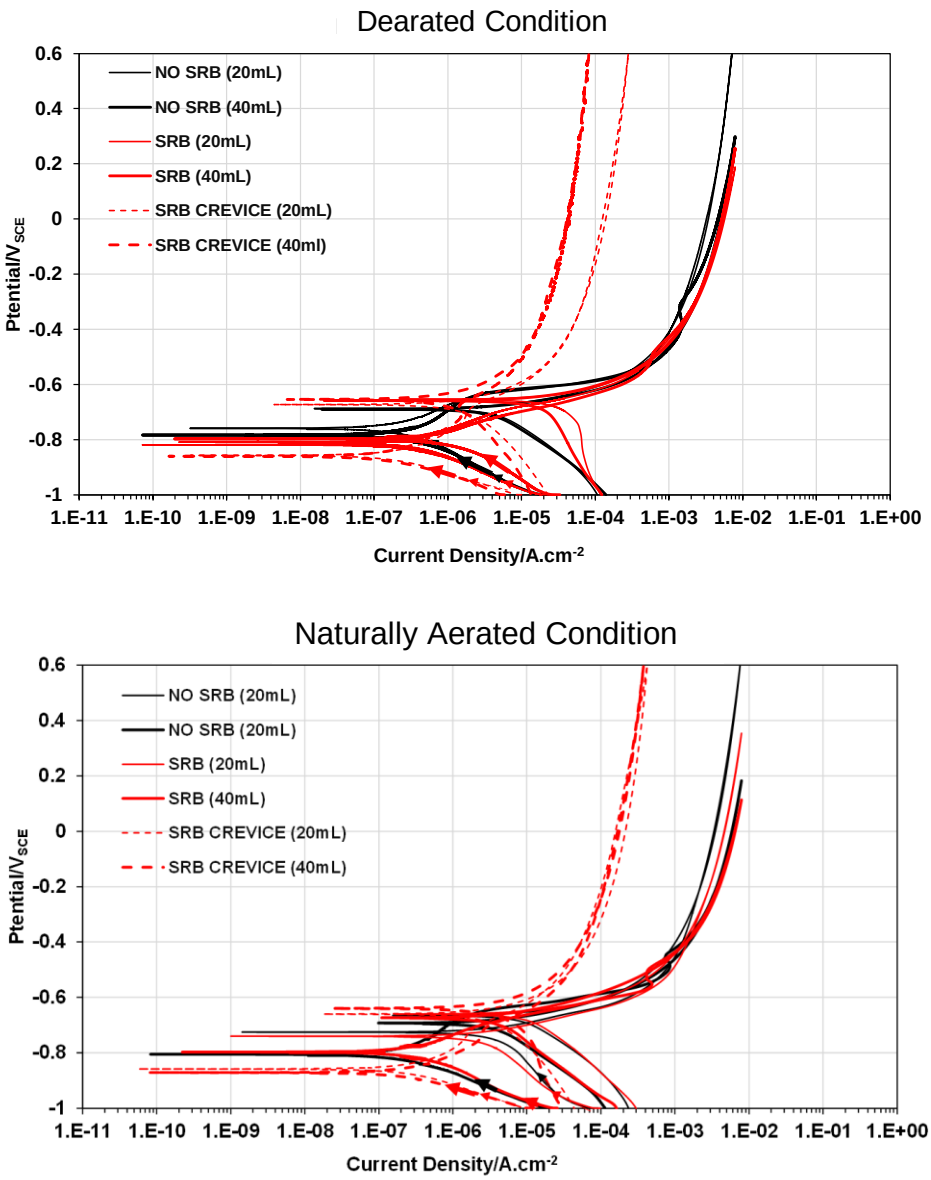

Figure 5.22. Potentiodynamic Polarization Scans for Test Setup B CTRL B Samples.

5.3.2.3 Visual Investigation

Figures 5.23-5.25 shows the visual condition of Test Setup B samples immediately after removal from solution, after cleaning and rinsing. Before cleaning, the inoculated samples had deposits of iron sulfide and likely biofilm. The non-inoculated showed surface rusting. All hard crevice samples showed indication of underfilm discoloration of the steel indicating onset of crevice corrosion. After cleaning, the steel surface showed some level of steel corrosion. Small corrosion pits were evident in the de-aerated inoculated samples especially in the SULF-A samples. Local corrosion was apparent at the opening of the hard crevice and throughout the

steel surface in the porous crevice for all samples. However, for both crevice states, the corrosion was more visually acute in the de-aerated inoculated conditions.

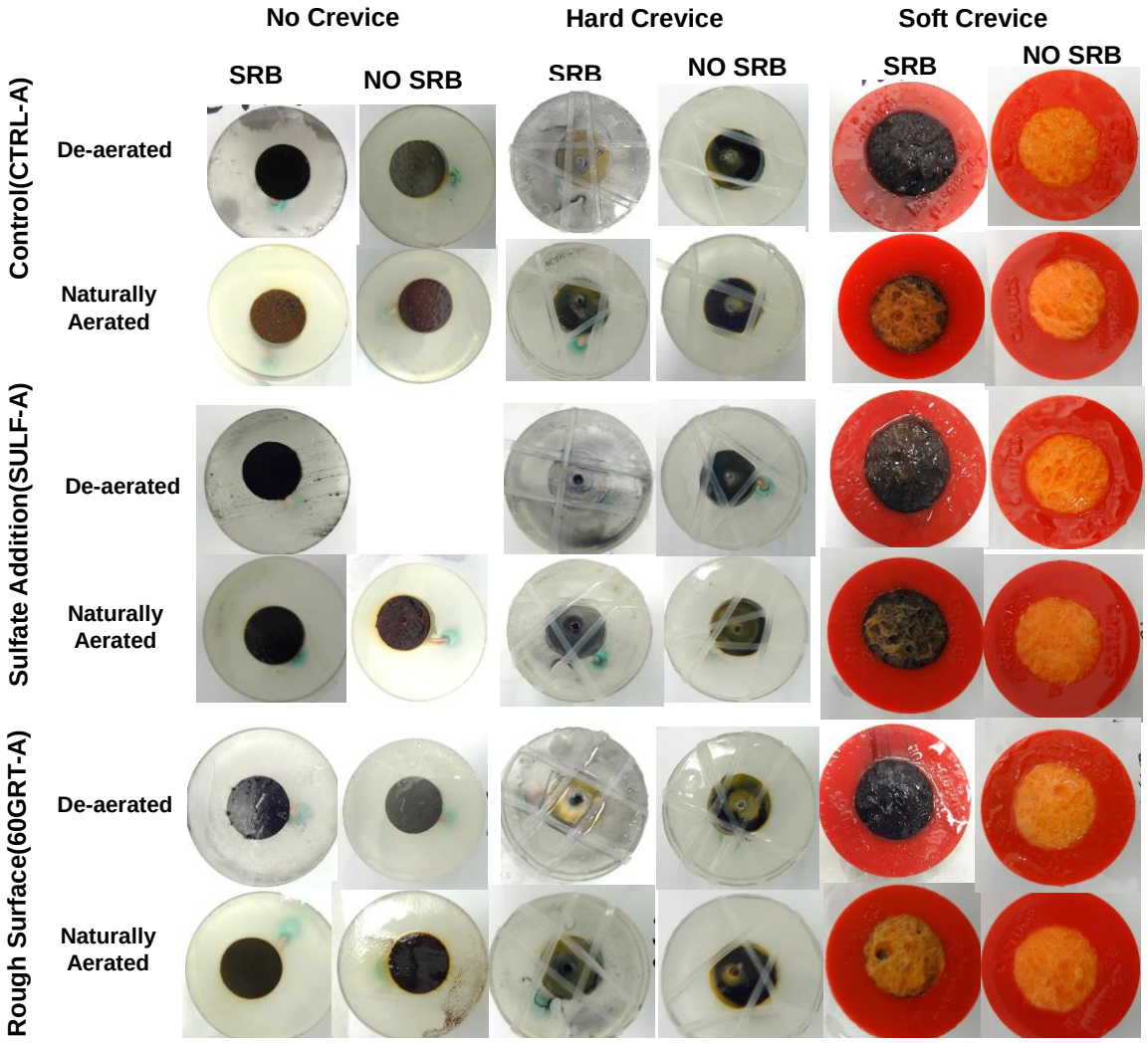

Figure 5.23. Test Setup B CTRL-A, SULF-A, and 60GRT-A Samples Before Sample Cleaning.

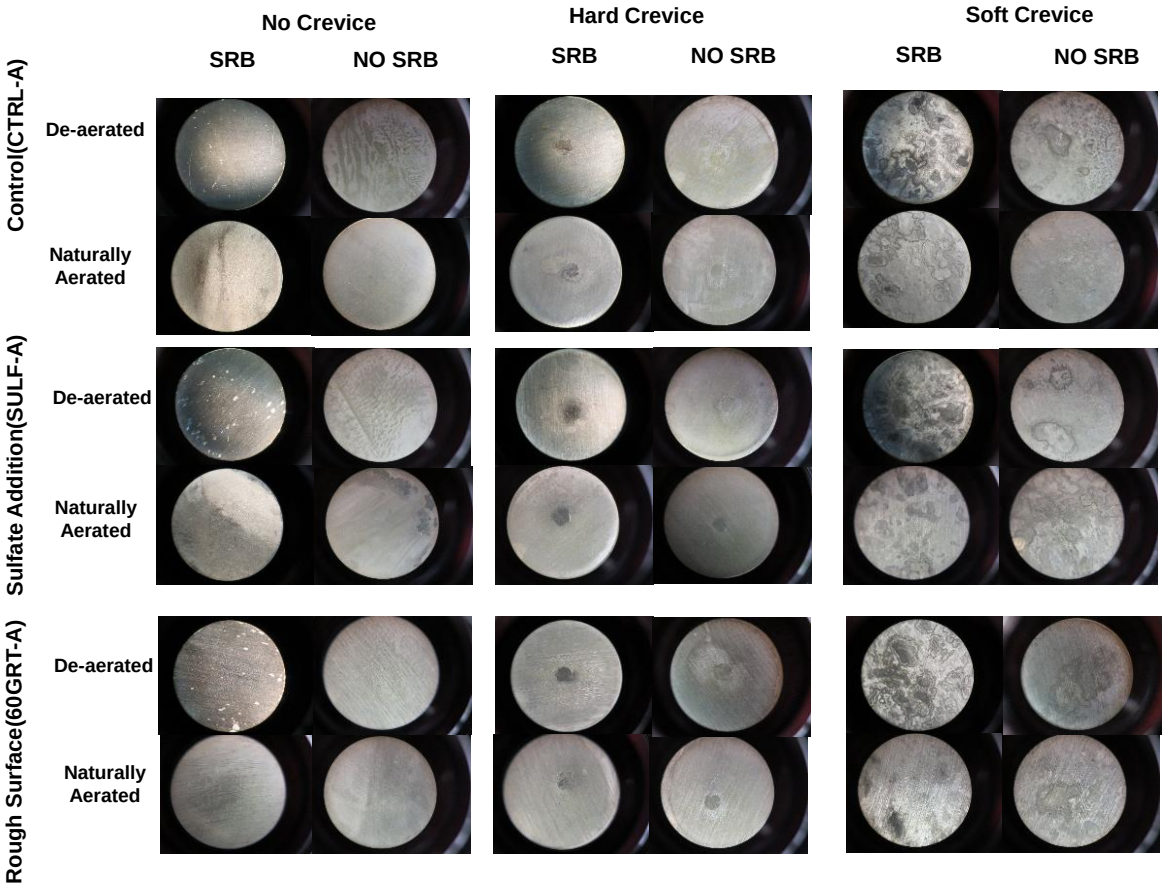

Figure 5.24. Test Setup B CTRL-A, SULF-A, and 60GRT-A Samples After Cleaning.

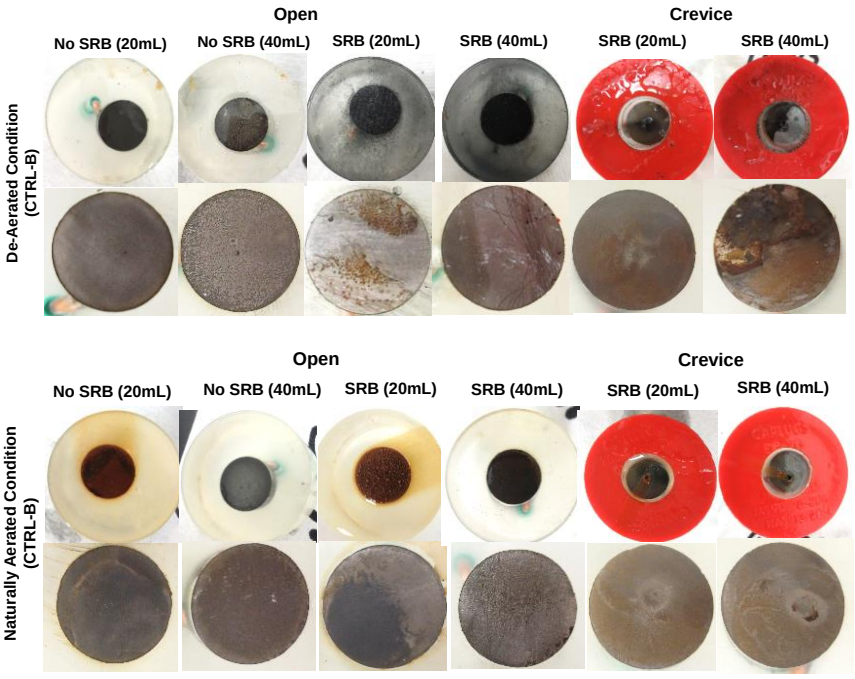

Figure 5.25. Test Setup B CTRL B Samples.

6. COATINGS TO MITIGATE MACRO- AND MICRO-FOULING

6.1. Methodology

The testing includes both outdoor field exposure and laboratory testing for antifouling and polyurea coated samples.

6.1.1. Outdoor Field Exposure Testing

Coated steel coupons were installed at three Florida bridge site locations with different environmental and water chemistry conditions for natural exposure condition (Table A and 6.1). Site I was located at Matanzas river, and site II and III were located in the Alafia river (downstream and upstream, respectively). The test site I Matanzas River site was where bridge steel piles exhibited corrosion associated with MIC as well as heavy marine fouling.[8] The steel coupons were prepared (5"x3"x1/8" with composition of 0.02%C, 0.16 % Mn, 0.006% S and 0.03% Si) and installed on a test frame made up of two polypropylene sheets (serving as test racks) vertically attached to aluminum supports secured to a bridge pier (Figure 6.1).

Sample placement was measured relative to the marine growth line, identified as distance below the marine growth line (BMG). The position of the test racks of each test site relative to the water surface varied due to the variation in the geometry of the test site bridge substructure where the test racks were installed as well as due to variation in tidal levels. Generally, the test sites had some samples exposed in atmospheric conditions but subjected to spray and tidal action as well as samples permanently submerged in water. Table 6.1 shows the depth locations of test sample and test condition at each test site. At site I, barnacles were predominant in the tidal region. Hydroids and marine flora amassed below low tide levels. At sites II and III, barnacles were the predominant macrofoulers down to the depth of the test frame. The barnacles were more prolific at site II.

A commercially available polyurea and a water-based copper-free antifouling coating were used for the field tests. Two layers of polyurea were applied to the steel coupon resulting in generally uniform but high dry film thickness. After the polyurea coating was applied to the steel coupons, three surface roughness conditions were prepared. The as-cured surface roughness, 60 grit, and 400 grit roughness were tested to identify possible effect of surface roughness on attachment of marine organisms (bacteria, marine flora and fauna). The antifouling coating consisted of a metal primer, two coats of a tie coat and one coat of the anti-fouling coating following manufacturer's recommendations. Only the as-cured thickness of the antifouling coating was tested. The average front and back coating thickness of the samples after surface preparation are shown in Table 6.2. Visual photo-documentation of coated steel coupon surface conditions and analysis of the developed surface bacteria population was conducted in the lab after sample retrieval. The surface fouling was left intact for the photo-documentation, but marine growth was removed from a small portion (~1 in^2) of the coupons where swabs were collected for the microbiological analyses. Microbiological tests were conducted with Biological Activity Reaction Test (BART) kits to estimate the population of the

four common MIC related bacteria (SRB, IRB, SLYM and APB) on the steel coupon surface below the layers of marine growth.

The retrieved test samples were immersed in sealed containers containing river water for transport back to the laboratory. In the laboratory, individual coupons were immersed in collected river water only exposing the top 1.5 inch of the coupons out of solution for electrical connections. The immersed surface area was ~52 in^2.

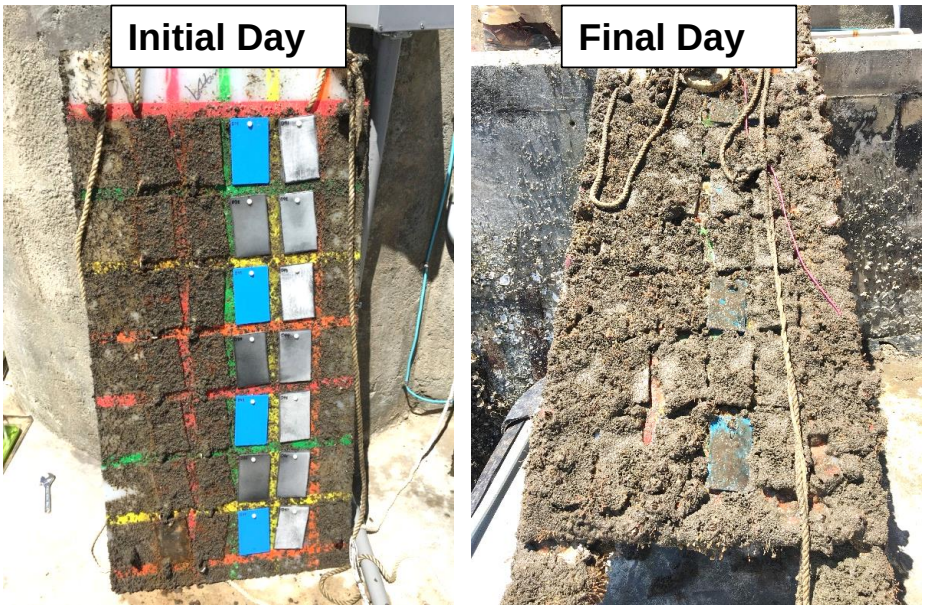

Figure 6.1. Example of Marine Growth on the Test Rack Setup in Site I.

Table 6.1. Field Test Sites.

Test Sites	Samples Installation Date	Samples Retrieval Date	Time of Exposure (Days)
Matanzas R. (Site I)	08/14/2017	01/31/2018*, 04/25/2018*	170, 254
Alafia R. (Downstream) (Site II)	11/12/2017	07/18/2018	248
Alafia R. (Upstream) (Site III)	01/30/2018	07/17/2018	168

Table 6.2. Experimental Test Conditions.

Test Site	Coating Material	Coating Surface Roughness		No. of Test Coupons	Distance Below Marine Growth (ft)	Coating Thickness Front/Back (mils)
I	Polyurea Coating	As-Cured	Set 1*	3	~3-5	39/18, 35/18, 25/27
			Set 2	3	~5-8	54/16 ,33/18,24/17
		400 Grit	Set 1*	3	~3-5	25/19, 36/20, 29/17
			Set 2	3	~5-8	40/18,34/17,26/17
		60 Grit	Set 1*	4	~2-5	38/18, 37/17, 3/21,27/24
			Set 2	4	~5-8	37/21,38/19,41/27,44/16
	Water Based Copper-Free Antifouling Coating	As-Cured	Set 1*	4	~2-5	6/7, 7/9, 6/6, 8/8
			Set 2	4	~5-8	6/7,5/4,7/8,7/5
II	Polyurea Coating	As-Cured		3	~0.5-5	36/-,37/-,28/-
		400 Grit		4	~0.5-5	-
		60 Grit		2	~0.5-5	-
	Water Based Copper-Free Antifouling Coating	As-Cured		7	~-0.5**-5.5	6/-,7/-,7/-,6/-,8/-,6/-,4/-
III	Polyurea Coating	As-Cured		6	~1-5.5	40/-,34/-,33/-,29/-,40/-,35/-
		400 Grit		2	~1-5.5	36/-,49/-
		60 Grit		2	~1-5.5	28/-,36/-
	Water Based Copper-Free Antifouling Coating	As-Cured		8	~0.5-6	12/-, 13/-, 5/-,7/-, 9/-,6/-,6/-,6/-

* Sample Retrieval at 170 Days, ** Minus sign denotes distance above the marine growth line.

. Figure 6.2 presents pictures of the test setup used in the laboratory. Corrosion evaluation consisted of measurements of the open circuit potential (OCP), linear polarization resistance (LPR), and electrochemical impedance spectroscopy (EIS). A saturated calomel electrode (SCE) was used as the reference electrode for all tests. An activated titanium mesh was used as the counter electrode. The scanned potentials for the LPR testing were made from the open-circuit potential and cathodically polarized 25 mV at a scan rate of 0.05 mV/s. The corrosion current was calculated from the polarization resistance, Rp, following the equation icorr=B/(Rp) where B was assumed to be 26 mV and A was the nominal surface area of steel coupon immersed in the solution. EIS testing was conducted at the OCP condition with 10 mV AC perturbation voltage from frequencies 1MHz > f >1Hz.

Figure 6.2. Example of Laboratory Electrochemical Test Setup.

6.1.2. Laboratory Testing

Six steel plates each for the polyurea and a water-based copper-free antifouling coating were also used for the laboratory. Each steel accommodated two test cells by placement of two separate cylindrical acrylic test vessels on the steel plate surface as shown in Figure 6.3. Experimental parameters for laboratory test setup shown in Figure 6.4. Testing was made for up to 25 days. Coating defects were made by drilling a 1/16-inch diameter hole in the middle of exposed coating surface. Electrical connection to the steel plate working electrode was made with a bolt stud mechanically tapped into the steel plate. An activated titanium mesh and a saturated calomel (SCE) electrodes were used as reference electrodes. An activated titanium mesh was used as a counter electrode.

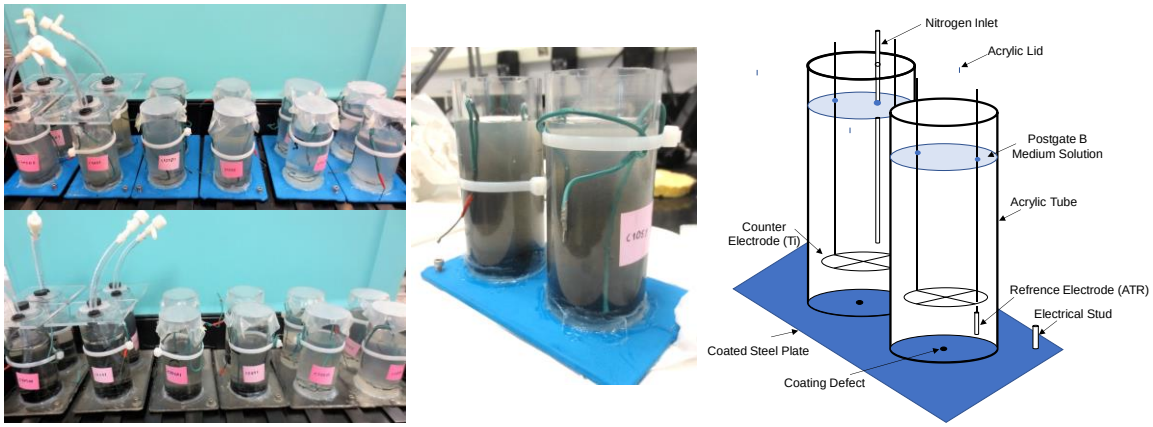

Figure 6.3. Laboratory Test Setup .

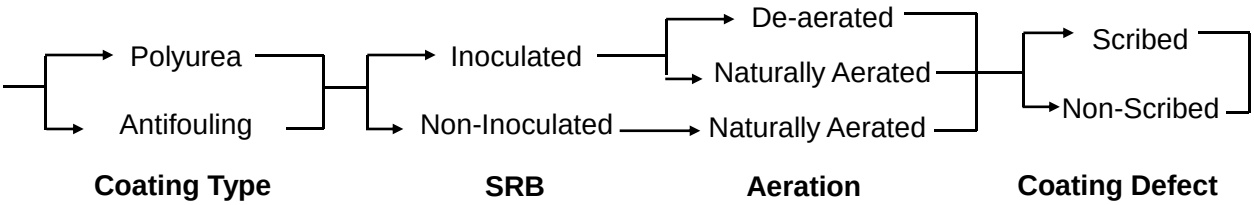

Figure 6.4. Laboratory Test Setup Conditions.

Test cells were filled with 80 mL deionized water and 10 mL of modified Postgate B medium solution (Table 6.3) (Postgate ,1984). The pH of all test solutions was ~6.5-8. For the inoculated test conditions, 10 mL of inoculated Postgate B broth containing SRB cultures that were previously isolated from water samples collected from the field where SRB levels were high, were used in serial dilutions following NACE standard TM0194-2002. For de-aerated test conditions, high purity nitrogen gas was bubbled through the solution for ten minutes on the first day. To prevent subsequent oxygen ingress, mineral oil (that formed a thin layer on the surface of the solution) was added. For naturally aerated-conditions, the head space above the test solution was open to the atmosphere.

Table 6.3. Composition of Modified Postgate B Medium.

Constituents	Composition (%)
Potassium Phosphate (KH_2PO_4)	0.05
Ammonium Chloride (NH_4Cl)	0.1
Sodium Sulfate (Na_2SO_4)	0.1
Sodium Chloride (NaCl)	2.5
Iron Sulfate ($FeSO_4.7H_2O$)	0.05
Sodium Lactate	0.5
Yeast extract	0.1

Assessment of microbial activity was made by chemical oxygen demand (COD) and sulfide production. COD of each samples was measured by a colorimetric COD method. A hydrogen sulfide color disc test kit was used for the sulfide estimation. Biotechnology Solutions sessile test kits were used for detection of sulfate reducing bacteria by serial dilution in Modified Postgate B (MPB) following NACE standard TM0194-2014.

Corrosion testing consisted of open circuit potential (OCP) and linear polarization resistance (LPR). Electrochemical impedance spectroscopy (EIS) was also periodically conducted. OCP was measured versus a saturated calomel electrode periodically. LPR testing was made from initial OCP to -25mV vs.OCP at a scan rate of 0.05mV/s. The corrosion current density was calculated from the polarization resistance, Rp, following the equation icorr=B/(RpxA) where B was assumed to be 26 mV and A was the nominal surface area of steel coupon immersed in the solution. EIS testing was made at the OCP condition with 10 mV AC perturbation voltage from frequencies 1MHz > f >1Hz. After ~25 days, photodocumentation for possible coating degradation and corrosion development was made.

6.2. Results and Discussion

This section covers the results from outdoor field exposure testing, laboratory testing on field samples and laboratory experiments.

6.2.1. Outdoor Field Exposure Testing Results

6.2.1.1. Visual Observation

Examination of the plain steel samples used (Figure 6.5), showed heavy accumulation of marine fauna for sites I, II, and III indicating that all three test sites are in aggressive environments in terms of barnacle growth. Barnacle growth varied in size and accumulation by immersion depth. The results of visual observations from the polyurea and anti-fouling coated samples and general comparison to fouling on steel samples are described below.

Figure 6.5. Barnacle Growth on Uncoated Plain Steel.

6.2.1.1.a Site I. Matanzas River

Polyurea Coating

For samples with as-received surface condition, a variety of marine flora and fauna developed on the surface of all samples 2-8 ft below marine growth (BMG) within a month of field exposure and the surface was covered with marine foulers by day 60. As shown in Figure 6.6, clustered formation of barnacles developed in the tidal region (0-5 ft. BMG) but soft marine masses populated with sedentary fauna developed at >4 ft. BMG. Due to the complexity of the field test setup, subsequent inspections of the steel coupons were not made concurrently. Set 1

samples were placed on test racks placed above Set 2 samples, so they were retrieved earlier on day 170 and set 2, with prolonged exposure, was retrieved on day 250.

By day 170, the level of soft and hard marine fouling increased for the set 1 samples placed at 0-5 ft BMG. By day 250, the level of soft and hard marine fouling on the set 2 samples likewise was also larger than those observed at day 60. However, there was differentiation of remnant barnacle plates sizes and population on the sample surface by depth. These observations were consistent with fouling on the plain steel samples. The difference in barnacle size and accumulation for both steel and polyurea coated samples were thought to be related to nutrient availability from the river flow and tidal levels.

For 60 grit and 400 grit roughened surface, similar levels of surface fouling were observed on the samples with roughened polyurea surfaces as the as-cured condition. Generally, marine fauna amassed on surfaces exposed >4 ft BMG, and barnacle development showed differentiation by depth.

Anti-Fouling Coating

Figure 6.7 presents the surface appearance of the water-based copper-free antifouling coating from test sets 1 and 2 in the initial condition, after field exposure, and after removal of marine growth for comparison. Also, early results after day 60 are provided as reference. As described elsewhere[42], by day 60, coating components (presumed to be topcoat) degraded, but the anti-fouling coating continued to suppress settlement of fouling organisms. By the time of sample retrieval for test set 1, there was visual indication of biomass developing on the coating surface, but no major fouling occurred. For the retrieved samples in test set 2, there was heavier growth of marine fauna and isolated barnacle growth. The observation of early coating degradation and surface marine fauna development would indicate that the anti-fouling characteristics of the coating became less effective. The disparity of barnacle growth between the time of retrieval of set 1 and 2 samples at day 170 and 250, respectively, was thought to be due to the further degradation of the anti-fouling coating and not the difference in depths between the two test sets. In any case, there was less barnacle growth on the anti-fouling coated steel samples than the comparative plain steel and polyurea coated steel samples.

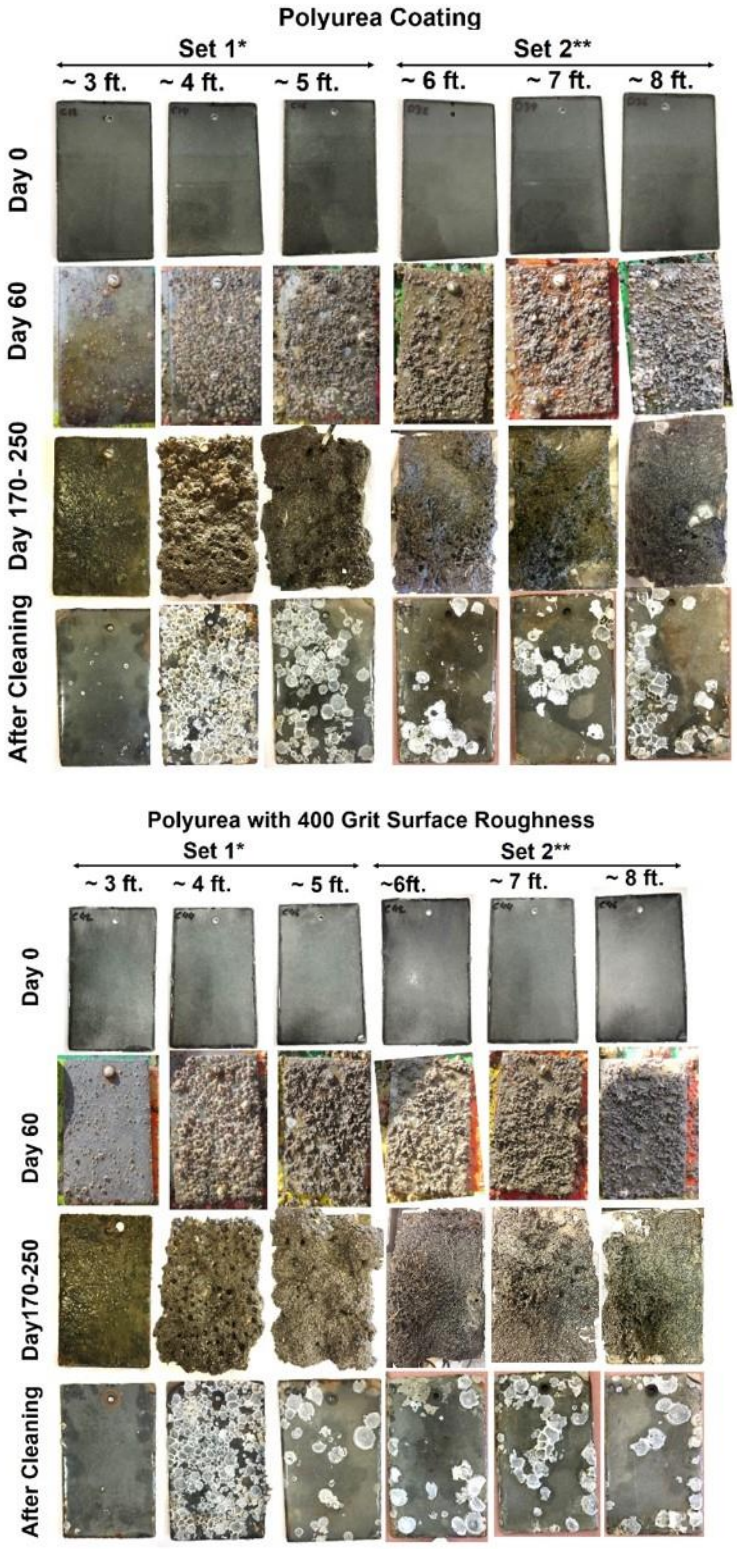

Figure 6.6. Surface Appearance of Field-exposed Polyurea-coated Coupons for Site I up to 170-250 Days. (* Retrieved after 170 days[42],** Retrieved after 250 days). (Continues).

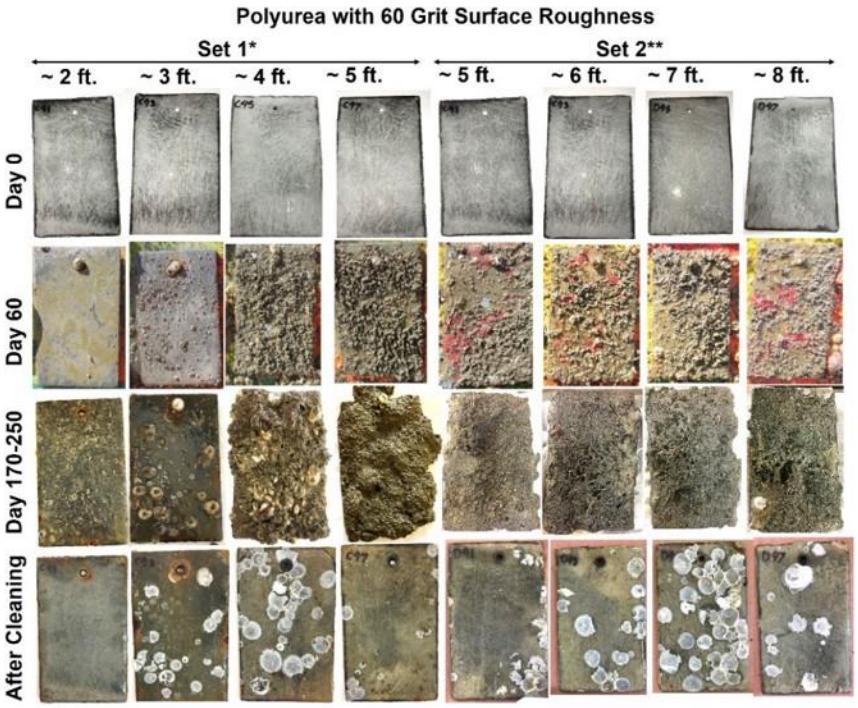

Figure 6.6. (Continued). Surface Appearance of Field-exposed Polyurea-coated Coupons for Site I up to 170-250 Days. (* Retrieved after 170 days[42], ** Retrieved after 250 days)

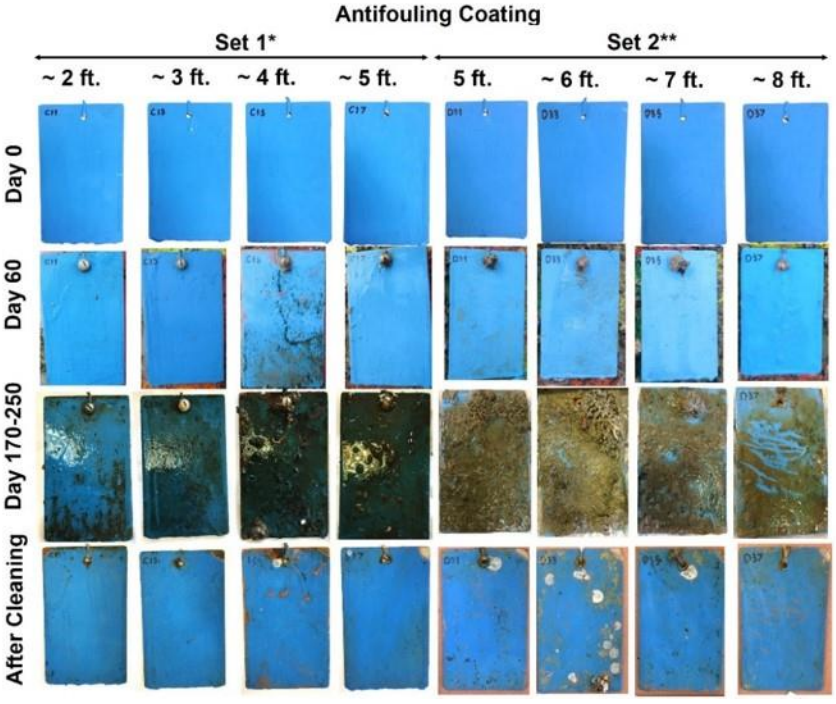

Figure 6.7. Surface Appearance of Field-exposed Antifouling-coated Coupons for Site I up to 170-250 Days. (* Retrieved after 170 days[42], ** Retrieved after 250 days).

6.2.1.1.b.Site II. Downstream Alafia River

Polyurea Coating

Figure 6.8 shows the surface appearance of coated steel coupons from Site II in the as-coated condition, after 244 days of exposure, and after hand cleaning. Clustered interlayers of bay barnacles formed at depth > 2ft BMG and had with larger basal plate diameter at larger depths, similar to that observed on plain steel samples from parallel testing (Task Deliverable 5). No differentiation in in fouling appearance was apparent for the various levels of roughness on the polyurea coating.

Anti-Fouling Coating

Figure 6.9 shows the surface appearance of steel coupons with the anti-fouling coating in the as-coated condition, after 244 days in marine exposure, and after hand cleaning. It was apparent that the marine fouling could develop on the coating. The level of barnacle formation was heavier at Site II than Site I even though barnacles greatly proliferate at both sites. Coating application on the steel plates for all sites were made from the same batch of steel plates and coating materials and coating application was done together. The difference in fouling may be related to fouling organism types. Whereas Site I generally could accommodate growth of tunicates, hydroids, acorn barnacles, sponges, mussels, and other marine fauna, Site II had predominantly bay barnacles. It was evident that the antifouling agents in the coating were not effective on the rate of proliferation of the barnacle specie in the saline environments at Site II.

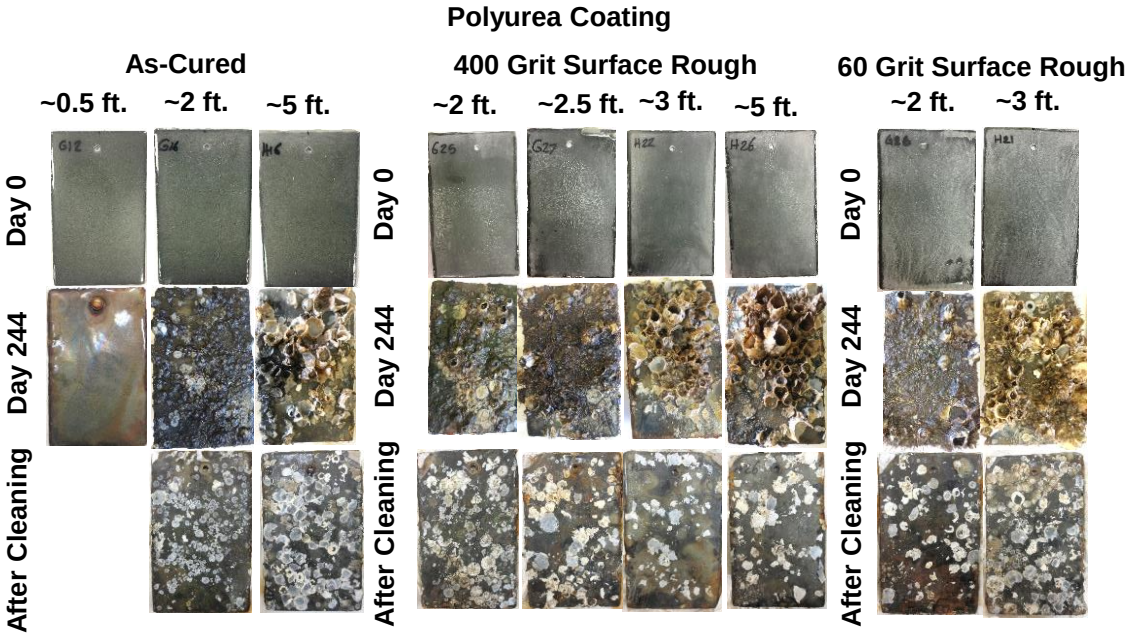

Figure 6.8. Surface Appearance of Field-exposed Polyurea-coated Coupons for Site II up to 244 days.

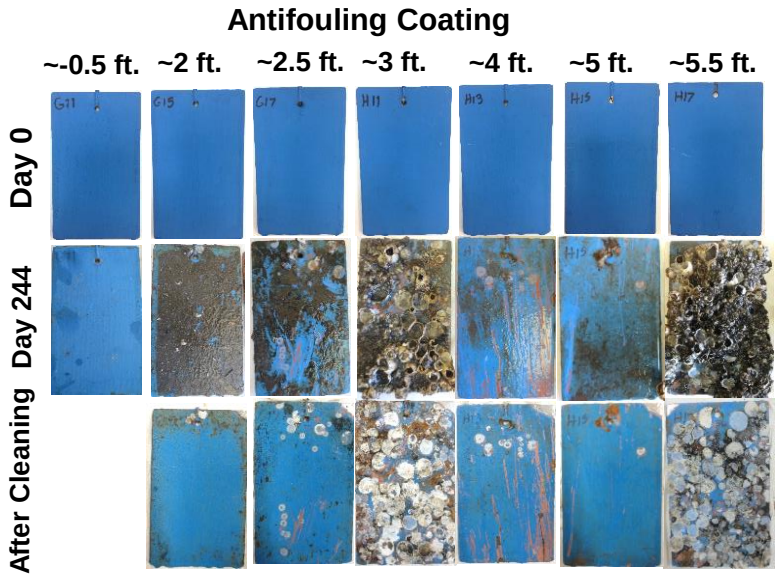

Figure 6.9. Surface Appearance of Field-exposed Antifouling-coated Coupons for Site II up to 244 Days.

6.2.1.1.c Site III. Upstream Alafia River

Polyurea Coating

Figure 6.10 shows the surface appearance of coated steel coupons in the as-coated condition, after 169 days of exposure, and after hand cleaning. Bay barnacles could develop on steel surfaces in upstream river locations where the salinity was lower than the downstream test site, even though the extent of barnacle growth was not as aggressive as in the latter. These trends were similar with the presence of the polyurea coating, indicating that the coating could not mitigate the settlement of barnacle larvae. The visual appearance showed somewhat lower level of barnacle settlement for the coatings with roughened surfaces, but this may be due to the generally lower levels of barnacle proliferation in the fresh water, at depths below 5 ft.

Anti-Fouling Coating

As mentioned above, the general activity of bay barnacles in upstream river locations was lower than downstream locations; but as described before, the barnacles can still accumulate to heavy levels. The application of the anti-fouling coating did appear to substantially reduce barnacle settlement as observed in Figure 6.11, where only a few spots with the initial growth of the barnacle shell was observed. In the upstream location, lower barnacle populations could be expected in the fresh water where less nutrients are available. This would provide lower fouling tendency where anti-fouling agent concentrations (such as Zn and Ti oxides) would remain at effective levels for longer service times. In such conditions, the anti-fouling coating may be effective for prolonged periods.

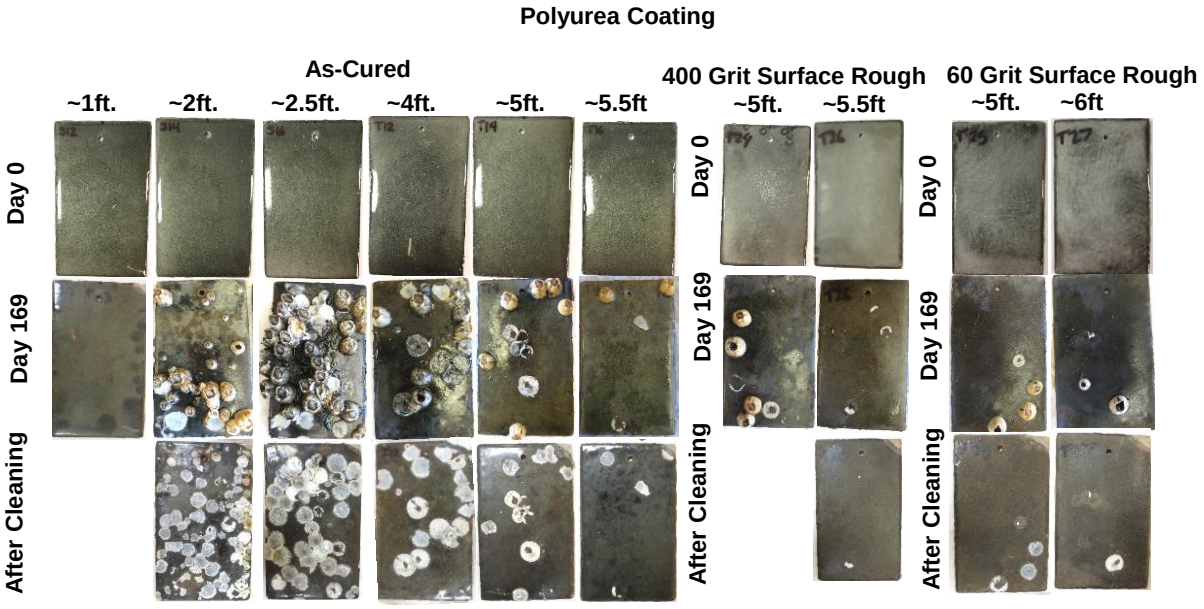

Figure 6.10. Surface Appearance of Field-exposed Polyurea-coated Coupons for Site III up to 169 Days.

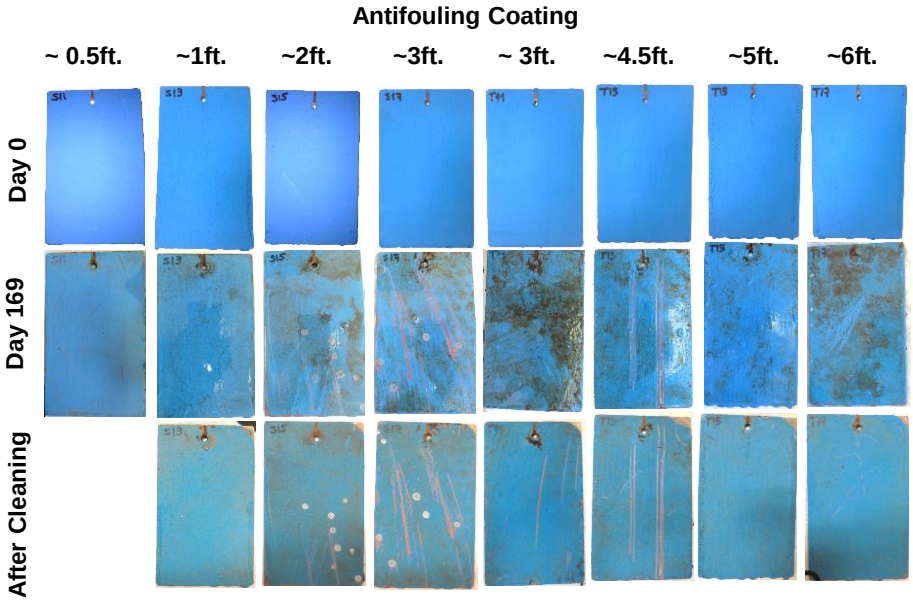

Figure 6.11. Surface Appearance of Field-exposed Polyurea-coated Coupons for Site III up to 169 Days.

6.2.1.2. Surface Fouling

Surface fouling by marine foulers naturally formed on the sample surfaces shortly after initial immersion at the test sites. Figure 6.12 shows a comparison of the developed marine fouling for all test samples. Barnacle size was thought to be related to depth, immersion time and nutrient availability. The presence and size of the remnant barnacle base plate on the coated steel samples after cleaning was considered to reflect the sustainability of barnacle development for the coated surface condition. Presence of barnacles indicate adequate surface conditions for larval site selection but not necessarily continued growth. Presence of larger diameter barnacles indicates conditions supportive of continued growth.

For Site I, as described earlier for plain steel samples, and as shown in Figure 6.12, barnacles with diameters less than 0.5 inch developed at ~3-4 ft BMG. Barnacle presence was sparse at depths 4-7 ft BMG. At depths greater than 6 ft BMG, only isolated populations of barnacles grew but their sizes were larger than 0.5 inch in diameter. The polyurea coated steel samples likewise had clustered barnacle growth less than 0.5 inch at depths 3-4 ft BMG. At 4-7 ft BMG, there was visual indication of greater barnacle development on the polyurea coated samples. At Site II, the layered barnacle clusters could develop on the polyurea and antifouling coating similar to that observed on the plain steel samples for depths >2 ft BMG. At Site III, it was apparent that relatively large barnacles can develop in the fresh water even with the presence of the polyurea coating. The coating surface >2 ft BMG had less coverage of attached barnacles in comparison to bare steel surfaces, but the environment allowed those settled barnacles to continue to grow. The steel coupons with the antifouling coating generally had few small barnacles.

Barnacle development was not well differentiated on the polyurea with roughened coating surfaces. The observations of barnacle growth at all test depths would evidently indicate that barnacle larva can settle on select sites on the polyurea coating regardless of its mechanical surface properties; barnacle larva settlement and barnacle growth occurred on all polyurea samples with as-cured surface finish and surfaces roughened to 400 and 60 grit (Figure 6.12). In comparison to plain steel samples, polyurea coating did not provide effective mitigation for fouling.

The antifouling coating had barnacle growth with sizes as much as ~0.5 inch in diameter. The early degradation of the topcoat and presumable depletion of biocide agents allowed for the onset of fouling organisms to grow (albeit at significantly lower population levels than the plain steel and polyurea coated steel samples). The onset of fouling within 250 days at site I, 241 days at site II, and 169 days at site III would indicate that coating maintenance would be required throughout the bridge service life.

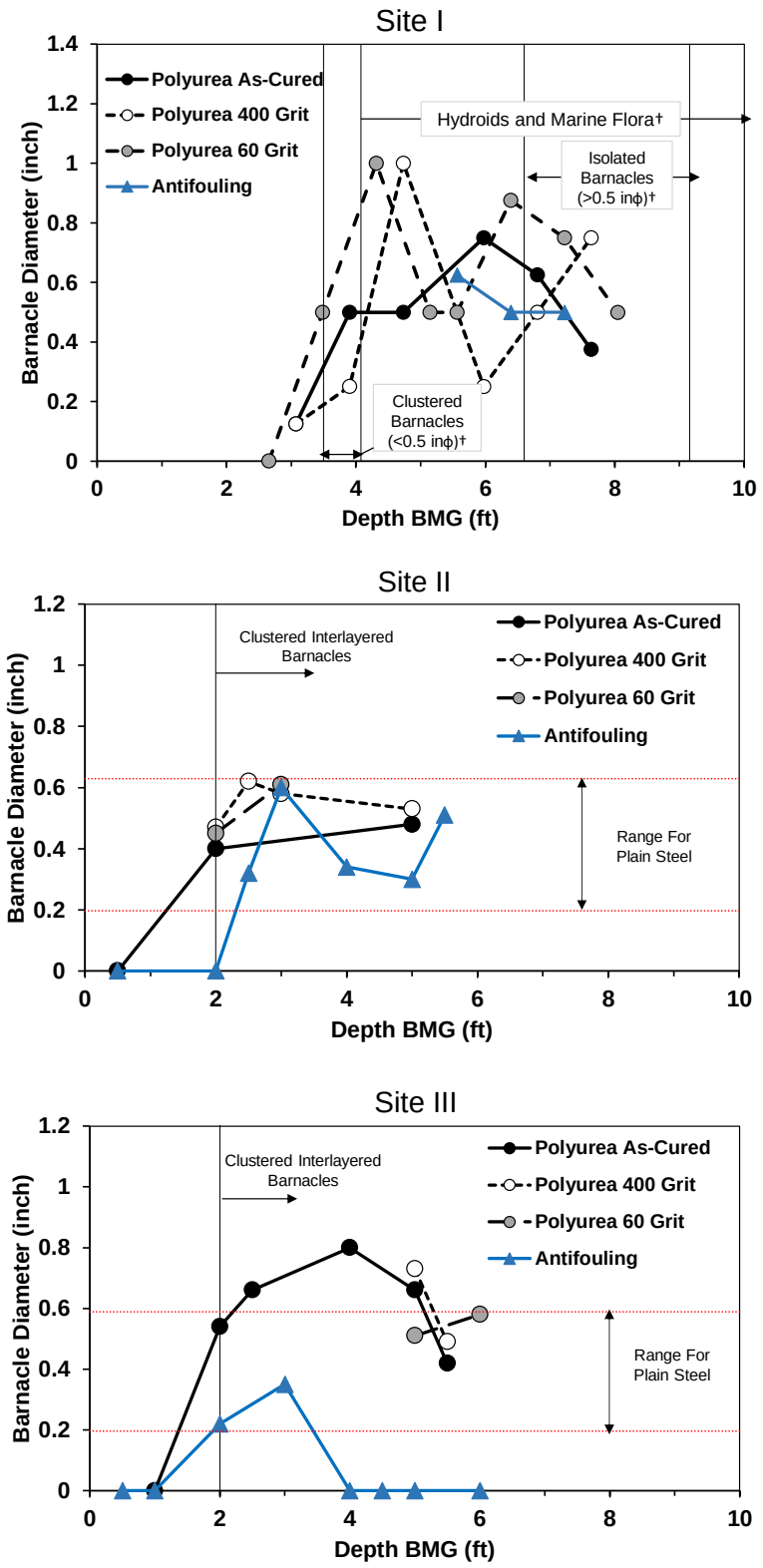

Figure 6.12. Maximum Barnacle Plate Diameter on the Coated Steel Coupons. (†Marine fouling on plain steel).

6.2.1.3. Surface Microbiological Activity

The results of BART tests on the coated steel samples from all three sites are shown in Figure 6.13. The largest measured population of SRB, IRB, APB, and SFB under marine growth layers are shown. The SRB population measured on the polyurea coated test plates showed variability but the testing indicated that large SRB populations at levels indicative of aggressive environments can develop at site I and II. Lower levels (non-aggressive) was observed at site III. For the antifouling coating, SRB populations were categorized as non-aggressive to moderately aggressive at all three test sites. At site III, the lower SRB populations that were measured regardless of coating application, can in part reflect the lower density of marine foulers there in comparison to the more nutrient rich waters at sites I and II. At all three test sites, IRB, APB and SFB maintained high populations for both the polyurea-coated and the antifouling-coated steel (generally categorized as aggressive). Generally, for surfaces without the effect of biocides such as plain steel and polyurea coated steel, presence of large surface bacteria populations coincided with the settlement of fouling organisms and subsequent heavy surface fouling. It was also observed that the anti-fouling coating had differential effects on various bacteria species (incidentally, negligible population of SRB).

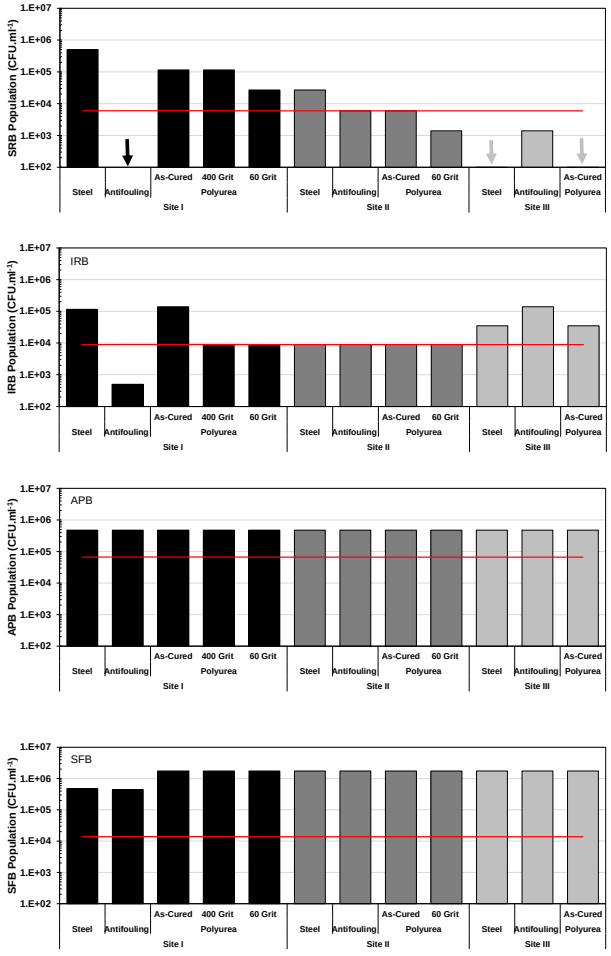

Figure 6.13. Surface Bacteria Population (CFU.mL-1) after Outdoor Exposure at Three Sites.

6.2.2. Field Sample Laboratory Testing

6.2.2.1 OCP

The combined results of OCP for the polyurea- and antifouling-coated samples for the three test sites are shown in Figure 6.14 and 6.15. In general, the corrosion potential at all three sites were in the range of -700 <E < -600 mV_{SCE}. There were some samples at site III with more noble potentials, but those values were associated with samples that were in the tidal region where a thick oxide developed. Complementary control as-received polyurea and anti-fouling coating samples that were conditioned in river water for 30 days showed more noble potentials and was likely reflective of the barrier characteristics of the coating. Even though environmental conditions of the field collected test solution (e.g., aeration levels) are likely to be different, the measured potentials of the field extracted coated samples showed electronegative potentials within the range of potentials for plain steel samples measured in the field. This may reflect sufficient coating degradation on the field exposed samples where the electrochemical reactions at the steel surface may become important.

6.2.2.2 LPR

Generally high corrosion currents were measured for the polyurea coated steel samples, in the order of 100 µA in sites I and II and 10 µA in site III (Figure 6.16 and 6.17). Although high, these values were lower than that of comparative plain steel samples. Nevertheless, the results (consistent with the measured OCP) indicated that there was significant degradation of the polyurea coating. This was likely due to degradation of the polyurea coating where the multiple and thick applied layers of polyurea may in part account for non-representative and non-ideal conditions that can lead to premature coating failure.

The corrosion currents for these coated samples throughout the test exposure (up to 250 days) were much smaller than the plain steel samples and lower than that of the polyurea coated samples, indicating beneficial effect of the coating. As indicated above, the level of fouling was small at site III and sometimes significant at sites I and II. The corrosion currents coincidently were significantly smaller at site II (and much reduced in comparison to control plain steel samples) which gave indication that marine foulers can have effect on coating degradation. Indeed, at site III, the corrosion current was somewhat higher where some minor fouling did occur. At sites I and II, the largest corrosion currents were measured for those samples where barnacles were present. It was posed that the topcoat of the antifouling coating system can degrade with time especially in environments that heavily promote proliferation of marine fouling organisms. The degradation and reduced concentration of antifouling agents would then allow settlement of the biofoulers.

6.2.2.3 EIS

To verify coating degradation, EIS measurements were made for the coated samples. The results from EIS in Nyquist plots (Figure 6.18 and 6.19) generally showed double loops, which can be associated not only with dielectric characteristics of the coating but also metal/solution interfacial behavior. As a first approach to assess coating quality, the total impedance magnitudes taken at 1 Hz were compared (Figure 6.20 and 6.21). The reference control as-cured coating samples had high impedance values (1 to 3 orders of magnitude larger than the exposed samples). Total Z at 1Hz were low (<500 ohm) for polyurea and anti-fouling coatings indicated coating degradation and poor barrier coating characteristics but were significantly lower for the polyurea-coated samples. There, the polyurea samples had values as low as ~10 ohms, consistent with the high corrosion currents. The antifouling coating had low total impedance consistent with the relatively high corrosion current and observations of physical topcoat degradation and development of surface fouling.

Site III samples showed high frequency larger loops in the Nyquist representation of impedance. On first principles, the impedance could be in part idealized as a coating pore resistance for a degraded coating. The impedance at all three sites for both coatings exhibit this characteristic, further implicating coating degradation. The lower conductivity of the river water at site III than sites I and II would then in part result in higher pore resistance and exhibit the larger high frequency loop. For the antifouling coating, differentiation in electrical characteristics of the coating resulting from biofouling may be identified. Indeed, at shown in Figure 20, locations in sites II and III where significant biofouling developed, the high frequency impedance loop was smaller than comparative exposed and control samples without development of biofouling. Further work here may be of interest as a means to identify extent of biofouling degradation.

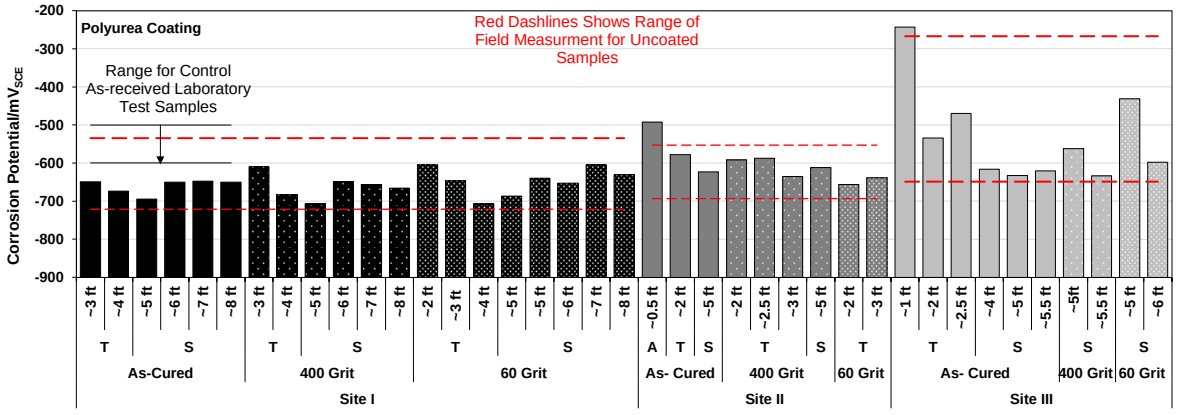

Figure 6.14. Corrosion Potential of Field-exposed Polyurea-coated Steel Coupons at Three Sites.

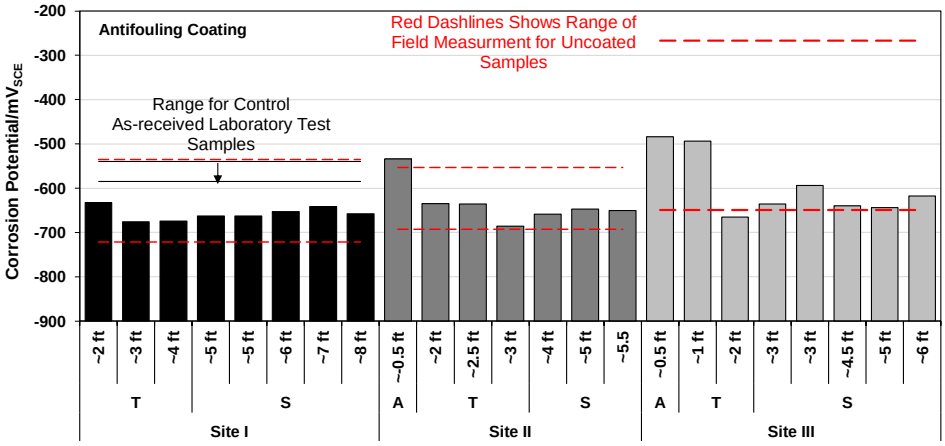

Figure 6.15. Corrosion Potential of Field-exposed Antifouling-coated Steel Coupons at Three Sites.

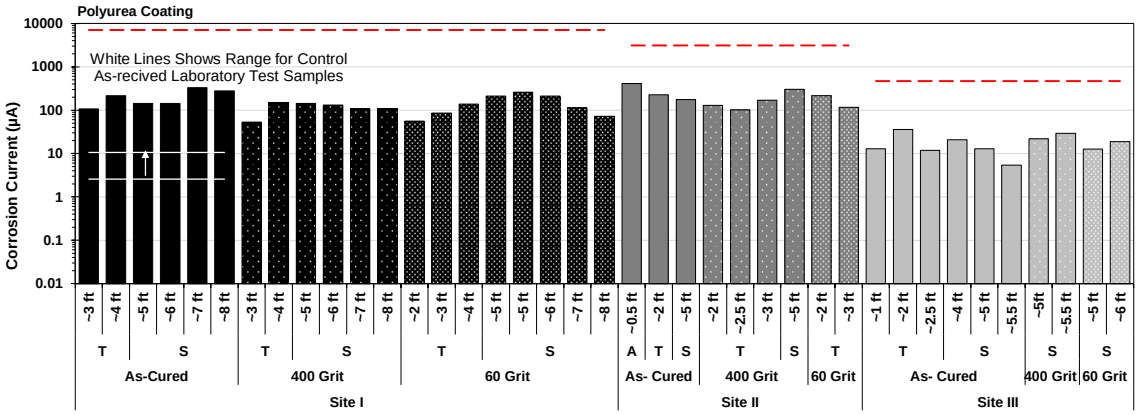

Figure 6.16. Corrosion Current Density of Polyurea-coated Steel Coupons at Three Sites. (Red line shows the measured current for plain steel coupons).

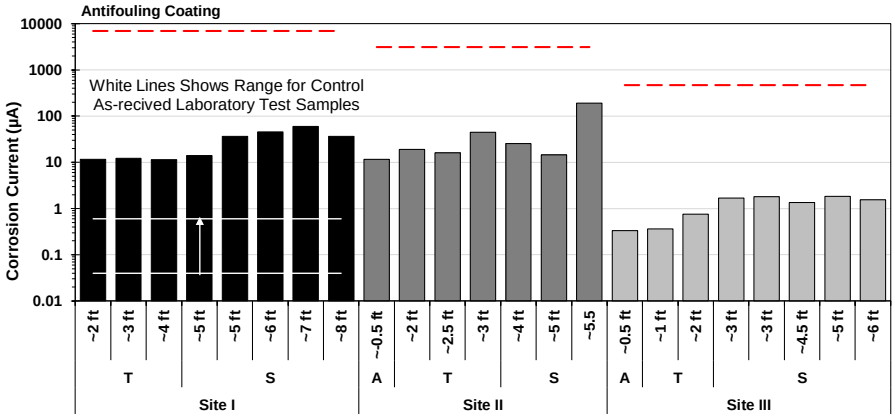

Figure 6.17. Corrosion Current Density of Antifouling-coated Steel Coupons at Three Sites. (Red line shows the measured current for plain steel coupons, * Shows the barnacle development on the samples).

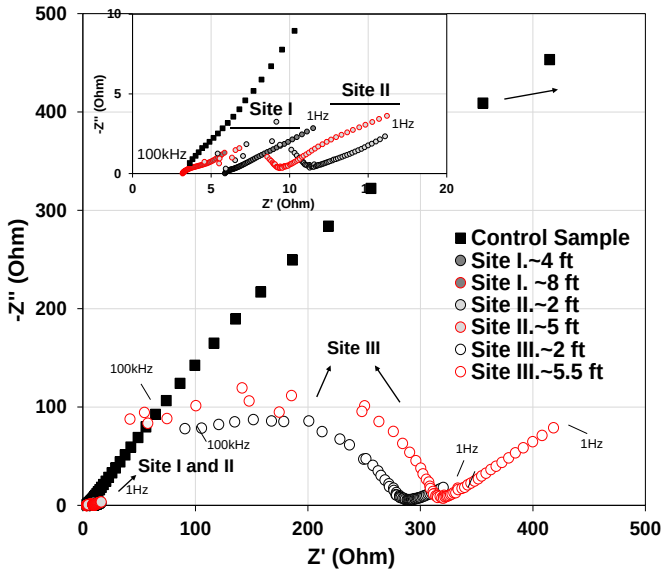

Figure 6.18. Electrochemical Impedance Spectroscopy Nyquist Diagrams for Polyurea-coated Coupons for Three Sites.

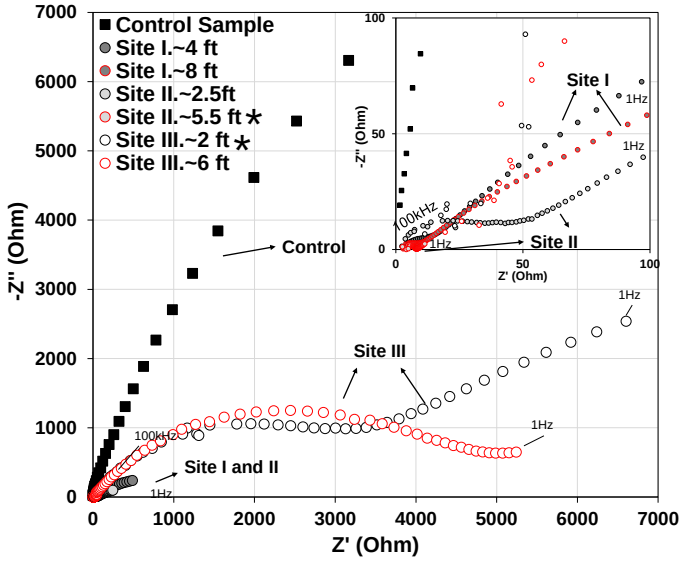

Figure 6.19. Electrochemical Impedance Spectroscopy Nyquist Diagrams for Antifouling-coated Coupons for Three Sites.

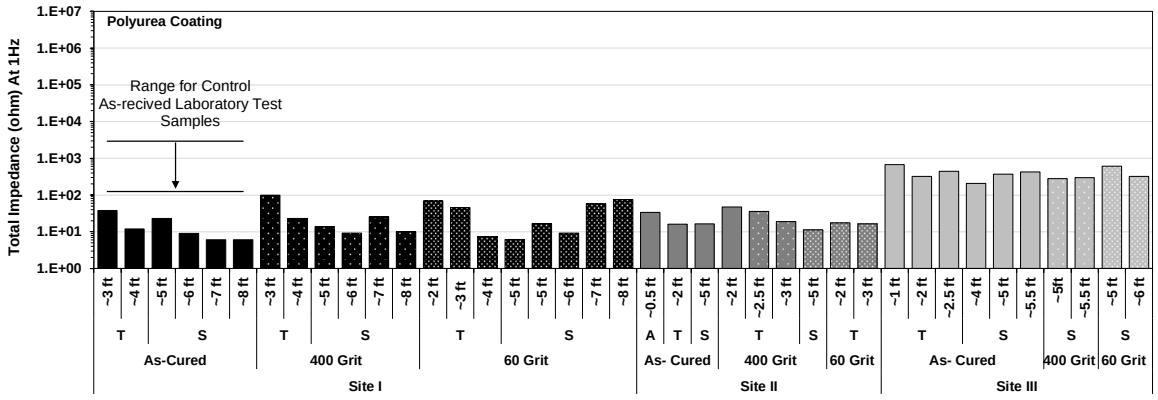

Figure 6.20. Total Impedance at 1Hz for Polyurea-coated Steel Coupons at Three Sites.

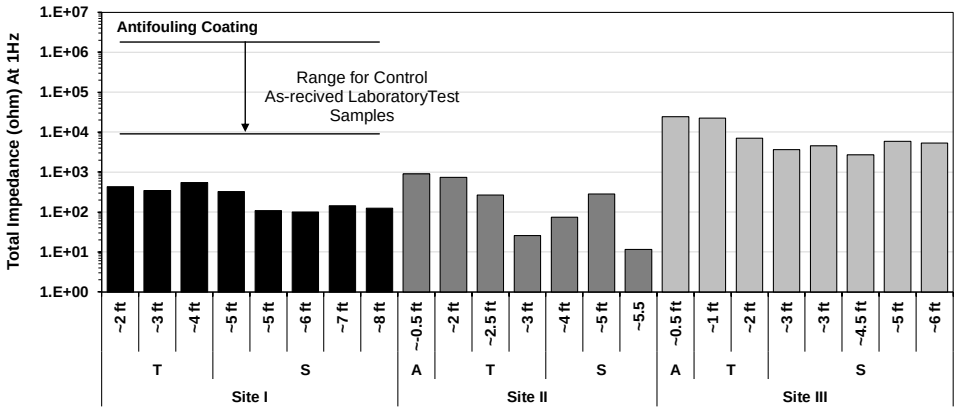

Figure 6.21. Total Impedance at 1Hz for Antifouling-coated Steel Coupons at Three Sites.

6.2.3. Laboratory Testing Results

Laboratory testing was made to identify SRB development on the surfaces of polyurea and antifouling coatings and possibly any coating degradation that may occur with the proliferation of SRB. It was evident that observations of polyurea coating degradation in the field exposure was in part related to moisture penetration after significant loss of coating adhesion. The laboratory testing of the material was made whereby only the surface of the coating was exposed to solution where the exposure would not promote coating disbondment. It was expected that any degradation of the coating and growth of SRB on the surface of the polyurea would be identified.

6.2.3.1. Microbiological Activity

Figure 6.22 shows the chemical oxygen demand results for both coatings with and without defect. The initial COD results for all inoculated samples for both coatings had high level of COD and were consistent for the Postgate B solutions used to promote SRB metabolic activity. COD at the end of testing were lower indicating less favorable environments for SRB activity. Low COD was measured throughout the test period for the non-inoculated solutions. No differentiation in COD was observed with the presence of the coating defect.

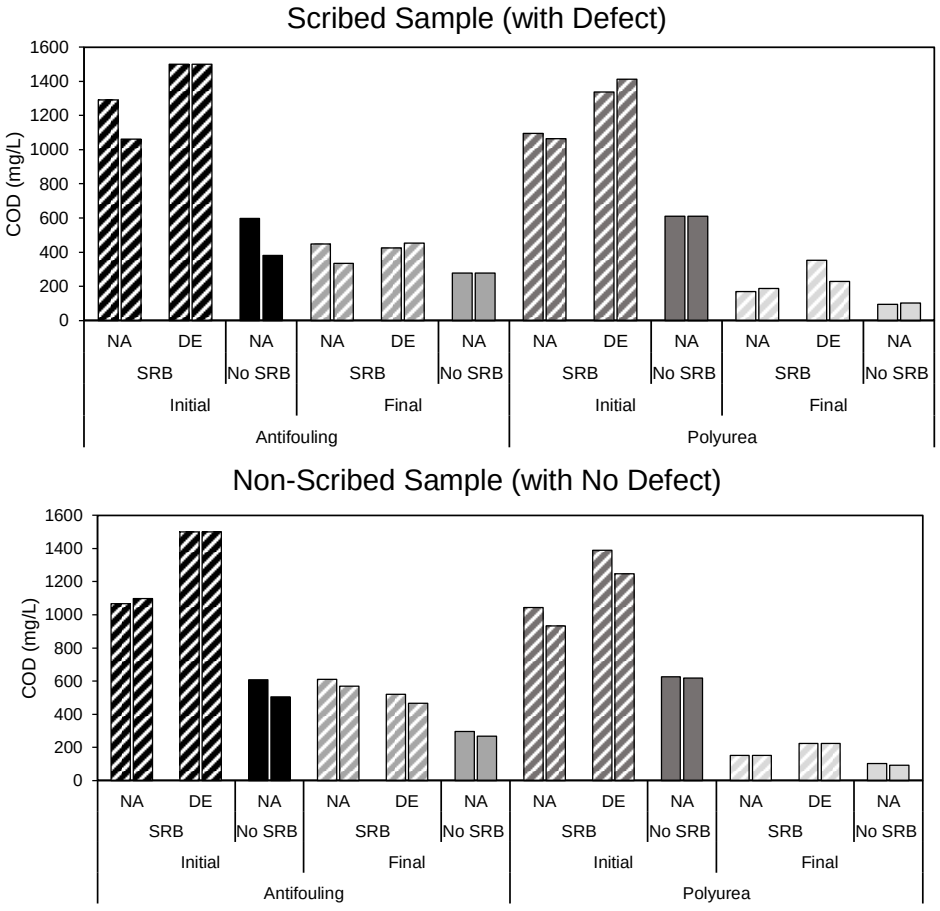

Figure 6.22. Chemical Oxygen Demand for Laboratory Coated Samples.

Sulfide production as the major metabolic activity of SRB was measured during the laboratory testing (~25 Days). As show in Figure 6.23, higher sulfide concentration was measured for all inoculated samples with the polyurea coating in comparison to the antifouling coating and the SRB remained active for longer period of time in the former. As the results shows, polyurea coating failed to prevent any metabolic activity of SRB, whereas there was indication that the antifouling agents in the antifouling coating may influence SRB growth.

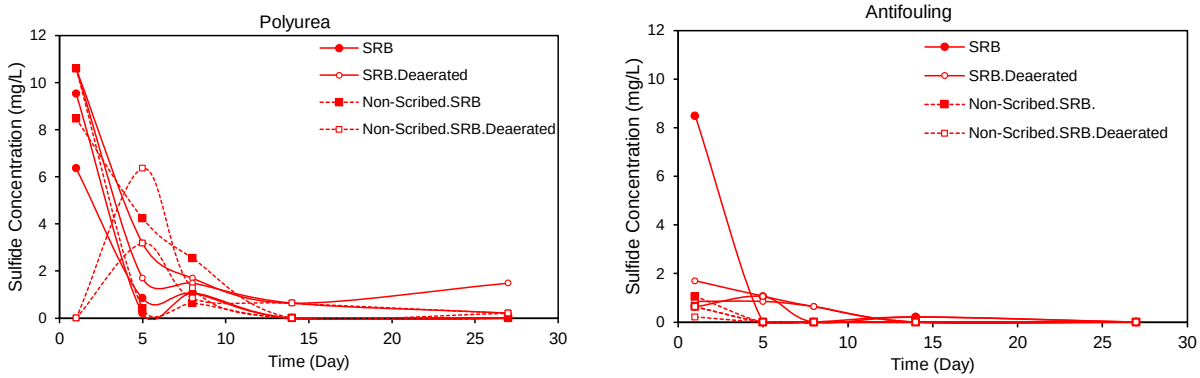

Figure 6.23. Sulfide Concentration for Laboratory Coated Samples.

The test cells were decommissioned after 25 days of testing and all test coupons were swabbed for the microbiological analysis. Total SRB population is shown in Table 6.4. In agreement with sulfide concentration results, SRB developed on the surface of the polyurea-coated samples.

The SRB population was as high as 10^6 for scribed samples in de-aerated condition. In contrast, the surface of the coupon with the antifouling coating generally showed zero population of SRB, except one sample in naturally aerated condition where the SRB population was 10^4 per ml. That same sample also showed higher sulfide concentration as initial measurement. (Figure 24)

Table 6.4. Reported Bacteria per mL for Laboratory Coated Samples.

Coating	De-Aerated Condition		Naturally Aerated Conditions			
	Scribed with SRB	None Scribed with SRB	Scribed with SRB	None Scribed with SRB	Scribed with No SRB	None Scribed with No SRB
Antifouling	$0\text{-}10^1$	0	$0\text{-}10^4$	0	0	0
Polyurea	10^6	10^4	$10^2\text{-}10^4$	$10^2\text{-}10^3$	0	0

6.2.3.2. Electrochemical Testing

Electrochemical testing including open circuit potential (OCP), linear polarization resistance (LPR) and electrochemical impedance (EIS) measurements were made during the test exposure.

Polyurea-coated steel samples without surface defects showed noble potentials indicative of good barrier coating characteristics. LPR testing of these samples yielded poor results likewise indicative of large coating electrical resistance. For samples with the intentional coating defects, the developed OCP was characteristic of steel interface in aqueous solution, but there was distinct differentiation between the inoculated and non-inoculated cases (Figure 6.24). Non-inoculated samples had OCP ~-800 mV_{SCE} indicative of active corrosion conditions.[59] The inoculated samples however showed a positive shift (~100 mV) of OCP from -700 mV_{SCE} to -600 mV_{SCE} within 5 days. The potential ennoblement coincided with the early high SRB activity where large sulfide concentrations were measured. The corrosion current density for the coated samples with exposed steel defects placed in non-inoculated solution showed relatively lower corrosion currents than the comparative samples placed in inoculated solutions. The higher corrosion activity and potential ennoblement would be indicative of MIC relating to SRB.

Steel with the antifouling coating without coating defects generally showed noble potentials upon exposure to solution, representative of little interaction of the steel interface with the bulk solution as may be expected for polymeric coatings. With longer exposure times, the potentials dropped to electronegative potentials in the order of -400 to -500 mV_{SCE} that could relate to wetting of the coating possibly associated with coating degradation (Figure 6.25). Concurrently, LPR decreased with time.The test coupons with intentional defects with non-inoculated solution generally developed OCP of ~-700 mV_{SCE} representative of electrochemical interaction of the steel interface with the solution. Of duplicate test samples, one sample in inoculated solution showed similar results and one sample showed characteristics of potential ennoblement. The latter sample coincidently also showed higher SRB activity (high sulfide concentration and SRB population) during the test exposure. Correspondingly, the corrosion current density for the samples in non-inoculated solutions was lower than for the sample in inoculated solution where SRB activity was evident.

It was posed that MIC due to SRB can occur only with the presence of coating defects exposing steel. For the antifouling coatings, local concentrations of antifouling agents may be reduced near the steel interface. For both polyurea and antifouling coatings, subsequent formation of SRB biofilm on the steel defect would be in the vicinity of electron donors from the steel and available nutrients from the solution. If localized MIC were to continue, coating defects such as disbondment may occur. In the field site testing, disbondment was significant. It was initially attributed to poor coating adhesion and localized corrosion under fouling organsms, but MIC may contribute to this form of coating degradation as well.

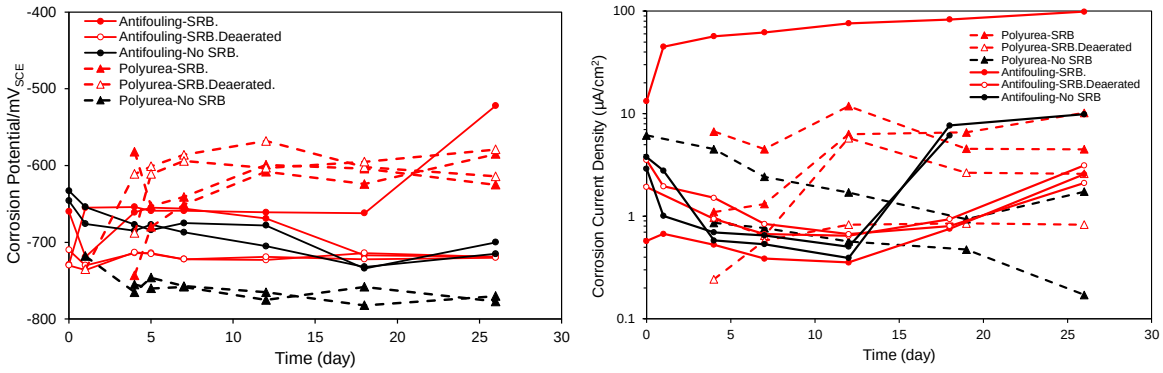

Figure 6.24. Corrosion Potential and Corrosion Current density for laboratory Coated Samples (with Defect).

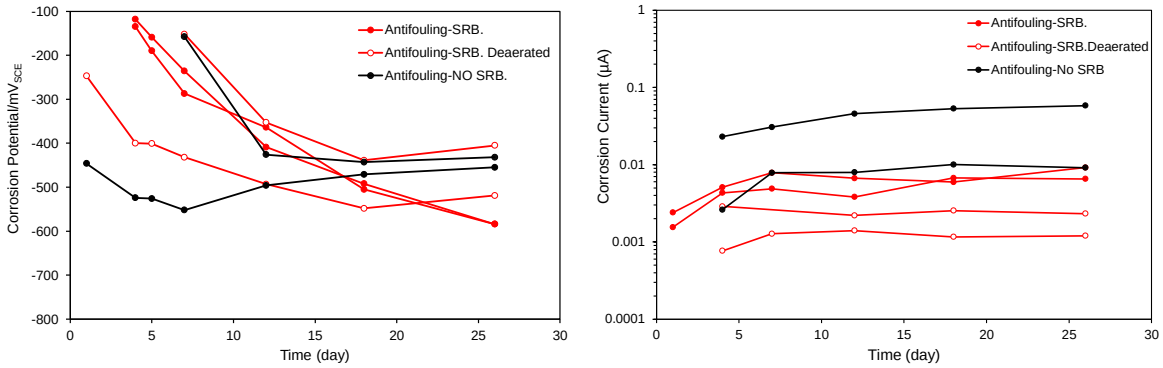

Figure 6.25. Corrosion Potential for Laboratory Antifouling-coated Samples (with No Defect).

In order to verify the coating degradation in presence of SRB inoculum, impedance measurements were made on the samples. The results from EIS testing in Nyquist plots (Figure 6.26-6.30) generally showed one or two loops characteristic of coated steel with varying levels of coating defects. As first approach, the total impedance at 1 Hz was compared to identify general coating characteristics. As shown in Figure 6.26 and Figure 6.30, the polyurea coated sample with no exposed steel showed large impedances characteristic of a pure capacitor (exceeding 1 Tohm) throughout the testing regardless of SRB activity. This impedance characteristic is indicative of excellent barrier characteristics and no indication of coating degradation during the time of testing. The samples with coating defects showed two impedance loops indicative of interaction of the steel substrate with the bulk solution (Figure 6.27). The resistance of the first impedance loop for the inoculated samples were consistently smaller than the non-inoculated cases which may give possible indication of enhanced degradation that may occur with ongoing MIC at the steel defect. As expected, the total impedance was lower than the defect-free coating sample. Consistent with LPR test results, the samples with inoculated solution where SRB developed showed lower total impedance due to the greater corrosion activity there.

As shown in Figure 6.28 and Figure 6.30, the samples coated with the antifouling coating with no exposed steel showed initially large impedance (~1 Gohm) that dropped after a

few days (~1Mohm). The drop in total impedance would reflect wetting of the coating as described earlier but otherwise good barrier coating characteristics were retained.

The total impedance for the samples with coating defects was distinctly lower than the defect-free samples regardless of inoculation due to the exposure of steel at the defect site (Figure 6.29). The overall total impedance was nevertheless generally high (in the order of $1x10^4$ to $1x10^5$ ohm). All samples with defects placed in inoculated solution showed some extent of current dispersion as exemplified by non-ideal impedance loops in the Nyquist graphs. Due to the high corrosion activity for one of these samples where SRB activity was high, the total impedance was very low (~100 ohm). The other samples with the coating defect placed in inoculated solutions where lower level of SRB activity was identified showed similar dispersion in the high frequency loop but in some cases, evolved into three impedance loops by the end of the exposure. The cause of the dispersion and the intermediate impedance loop could not be elucidated but was thought to be associated with non-uniform current distribution at the defect site, possibly relating to the antifouling agents in the topcoat. Indeed, as described later, significant degradation of the topcoat was shown to be possible in part associated with SRB activity.

The resistances associated with the coating itself (size of the high frequency impedance loop) were somewhat smaller for cases in inoculated solutions but this would likely be attributed to the slightly more conductive test inoculated test solution.

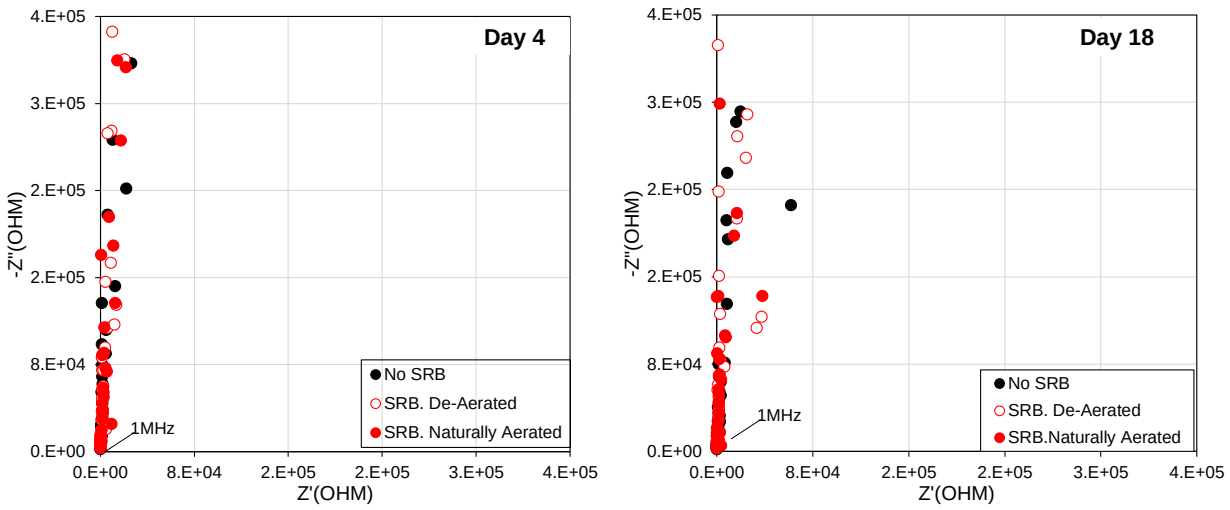

Figure 6.26. Electrochemical Impedance Spectroscopy Nyquist Diagrams for Polyurea Coated Laboratory Samples (With No Defect).

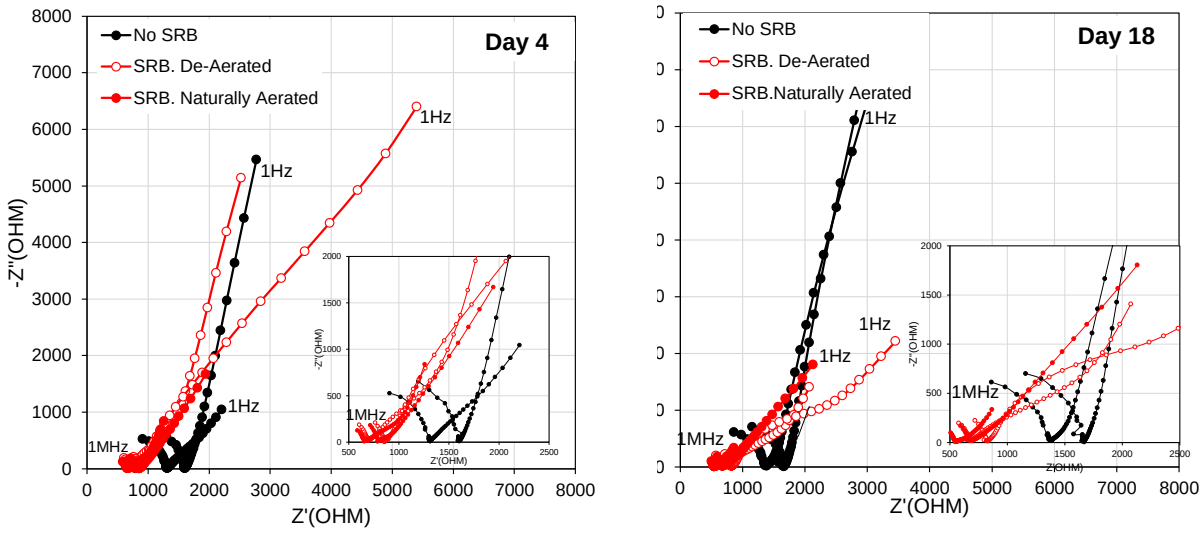

Figure 6.27. Electrochemical Impedance Spectroscopy Nyquist Diagrams for Polyurea Coated Laboratory Samples (With Defect).

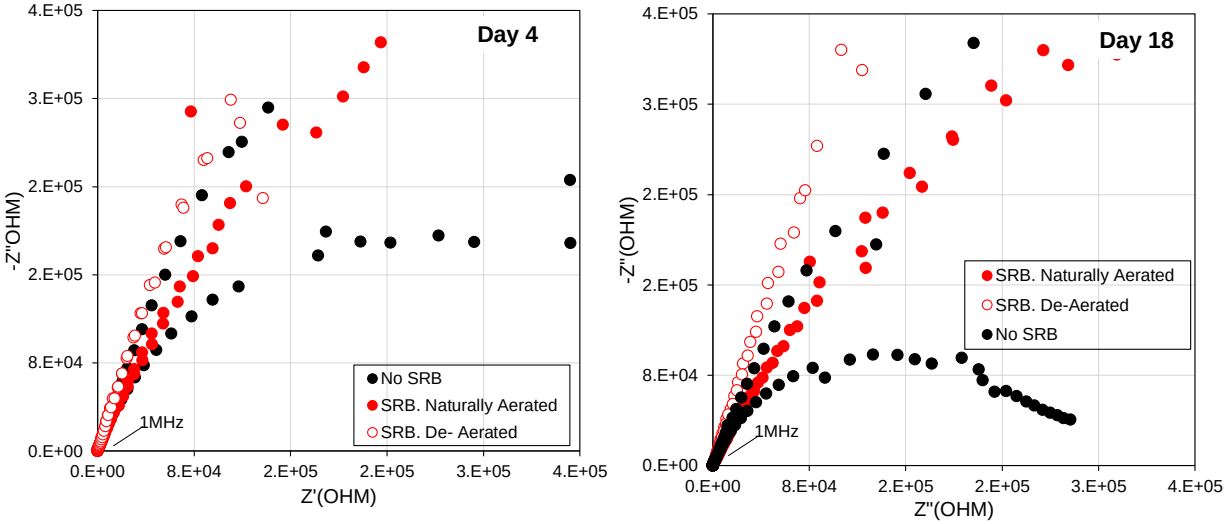

Figure 6.28. Electrochemical Impedance Spectroscopy Nyquist Diagrams for Antifouling Coated Laboratory Samples (With No Defect).

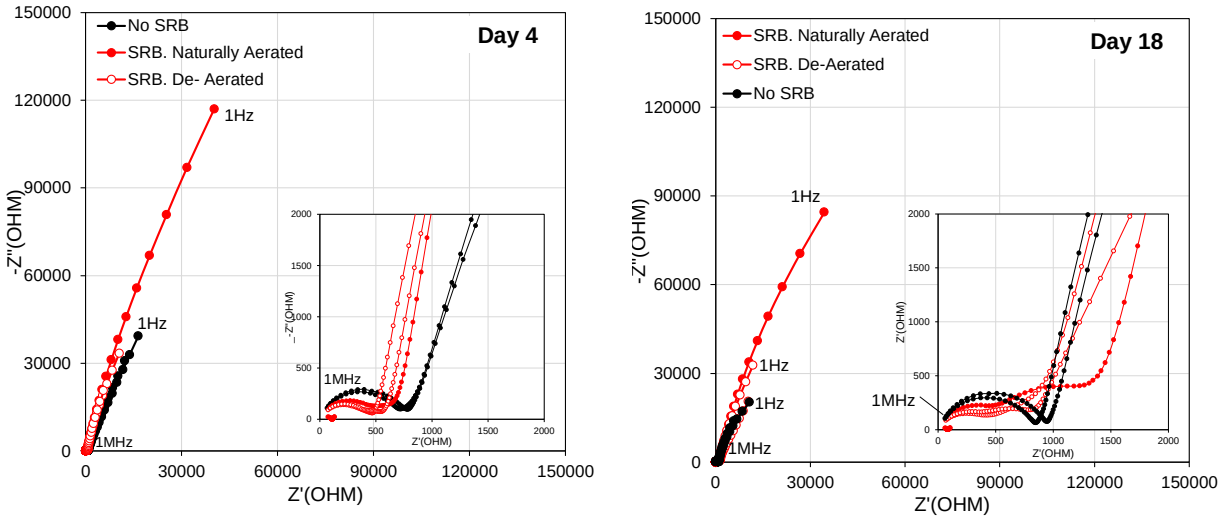

Figure 6.29. Electrochemical Impedance Spectroscopy Nyquist Diagrams for Antifouling Coated Laboratory Samples (With Defect).

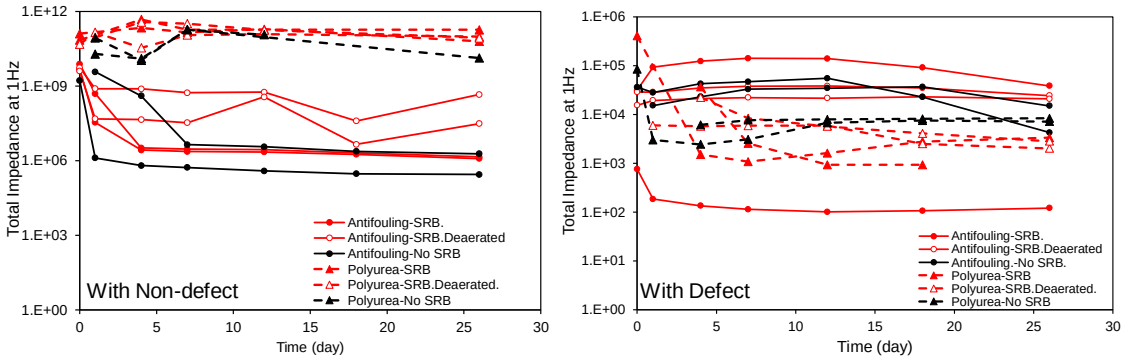

Figure 6.30. Total Impedance at 1Hz and 1MHz for Laboratory Coated Samples (with Defect and No Defect).

6.2.3.3. Visual Observation

Figure 6.31 shows the surface appearance of the test samples immediately after testing.There was no strong visual indicators that there was degradation of the bulk polyurea coating during the test exposure. For the defect-free samples, the coating retained its smooth surface texture even under a layer of deposited precipitates including iron sulfide for the samples with inoculated solutions. For the samples with the coating defect, the surface finish was likewise not affected and there was not strong visual indication that the coating had any form of blistering or disbondment from the exposed steel defect site. Even though not strongly manifested in the lab testing, corrosion at the steel defect site could allow subsequent coating degradation including anodic blistering and disbondment.

The steel coupons coated with the antifouling coating placed in non-inoculated solutions did not exhibit strong visual indicators of coating degradation regardless of the presence of the coating defect. The surface retained color and no differentiation in surface texture was apparent. In contrast, samples exposed to inoculated solutions where SRB activity was high showed

distinct discoloration and some flaking of the topcoat. This visual observation would be consistent with the earlier indicators that the concentration of antifouling agents within the topcoat may be reduced and would subsequently allow for the higher levels of SRB development and steel corrosion. The concentration of antifouling agents on the surface of the topcoat may not be effective for long-term mitigation in aggressive environments where there is strong planktonic SRB concentrations. It was evident that degradation of the topcoat and loss of antifouling performance would allow enhanced SRB surface development.

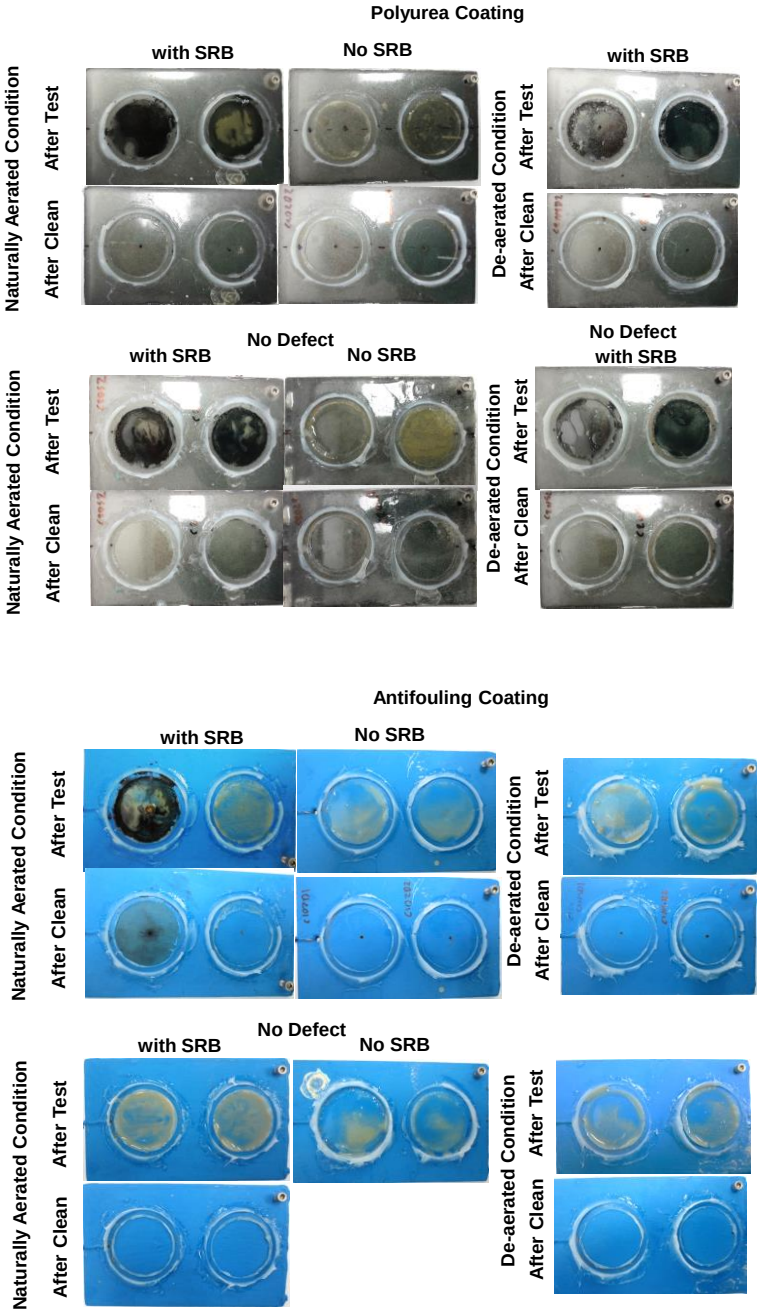

Figure 6.31. Laboratory Samples after Testing and before Sample Cleaning.

7. CATHODIC PROTECTION TO MITIGATE MIC WITH PRESENCE OF FOULING

7.1. Methodology

The field site testing sought to identify applicability of bulk zinc anodes to provide sufficient polarization to mitigate MIC in presence of macrofoulers in natural exposure conditions. Field sample lab testing sought to identify how macrofoulers affect electrochemical corrosion characteristics as well as bacteria proliferation. Laboratory cathodic polarization tests sought to elucidate the effect of physical attributes of fouling (with and without the presence of SRB) on CP current distribution. Anodic polarization tests were made in part to identify corrosion behavior of nonprotected regions of crevice environments where local anodes may develop (such as under crevices due to biofouling for example) as well as the effect with the proliferation of SRB.

7.1.1. Field Site Testing

Steel coupons, 3x5x~1/8 inch, (composition of 0.02%C, 0.16 % Mn, 0.006% S and 0.03% Si) were installed on test racks made up of a polypropylene sheet attached to an aluminum frame secured to a bridge pier. The steel coupons were attached to the board, each with a single nylon bolt. The front steel coupon surface was freely exposed, but the back surface was partially separated from the polypropylene sheet by a nylon washer around the connection bolt. The test frames were placed in two Florida natural waters (Table A and 7.1) that support proliferation of bacteria often associated with MIC as well as heavy marine fouling of bridge substructure elements.

At Site I (Matanzas River), hydroids and marine flora amassed with sporadic growth of barnacles at test depths. At Site II (Alafia River), barnacles were the predominant macrofoulers at test depths. Figure 7.1 shows representative marine growth. All test samples were fully immersed, and Table 7.2 lists the exposure depth for each test sample.

At both test sites, a set of steel coupons (Group A) were electrically coupled to a commercial bulk zinc anode (composition of 0.1-0.5% Al, 0.02-0.07% Cd, 0.005% Fe, 0.006% Pb, 0.005% Cu, and balance Zn) with 18-gauge marine-grade shielded copper wires for ~200-250 days. A second zinc anode was installed to monitor the free zinc anode potential. The electrical connections were encapsulated with epoxy to prevent moisture intrusion. The copper wires were terminated at a control box with an electrical switch to accommodate current measurements between the steel samples and the zinc anode. For Site I, the steel coupons were corroded at the open-circuit potential (OCP) condition prior to coupling of the steel samples to the zinc anode. There, the zinc anode was installed and coupled to the steel coupons 88 days after initial sample installation. In Site II, the zinc anode was installed together with the steel coupons but due to a possible bad electrical contact to the initial zinc anode, reconnection to an auxiliary zinc anode was made at day 80. A complementary set of steel coupons (Group B) were maintained at OCP throughout the exposure test period.

Figure 7.1. Typical Outdoor Exposure Test Rack.

Table 7.1. Field Test Sites.

Test Sites	Samples Installation Date	CP Start Date	Samples Retrieval Date	Duration of CP (Days)	Duration of Exposure (Days)
I. Matanzas R.	07/18/2017	10/16/2017	04/25/2018	191	279
II. Alafia R.	11/12/2017	11/12/2017 01/30/2018*	07/18/2018	245 (169*)	245

* Connection to auxiliary zinc anode.

Table 7.2. Experimental Test Condition.

Test Sites	Steel Condition	No. of Coupons	Distance BMG (ft)
I. Matanzas R.	Cathodic Protection (Group A)	14	~5 to 8
	Control (Group B)	7	~5 to 8
II.Alafia R.	Cathodic Protection* (Group A)	14	~ 3 to 6
	Control (Group B)	7	~ 3 to 6

* Coupling to zinc anode upon steel immersion.

For Site I, the initial free corrosion potential of the uncoupled steel coupons and zinc anodes as well as the subsequent mixed potential after coupling of the coupons and zinc anodes were measured for Group A samples. The free corrosion potentials were measured for the OCP samples in Group B. Similar potential measurements were made for samples in Site II except that there were no uncoupled samples for Group A samples. A copper/copper-sulfate reference electrode (CSE) was used.

For all coupled samples in Group A for both sites, the electrical current between three configurations of coupled steel coupons and zinc anodes were made with an ammeter immediately after decoupling of the electrodes (that were normally in the coupled on-condition) via the electrical switch (Figure 7.2). For the first test configuration, the global CP current from the zinc anode to the coupled array of test coupon was measured. For the second test configuration, the local CP current from the steel-anode system to a single isolated test coupon was measured. For the third test configuration, the local CP current from the anode to a single isolated test coupon was measured. The test racks were decommissioned after ~279 days for Site I and~245 days for Site II.

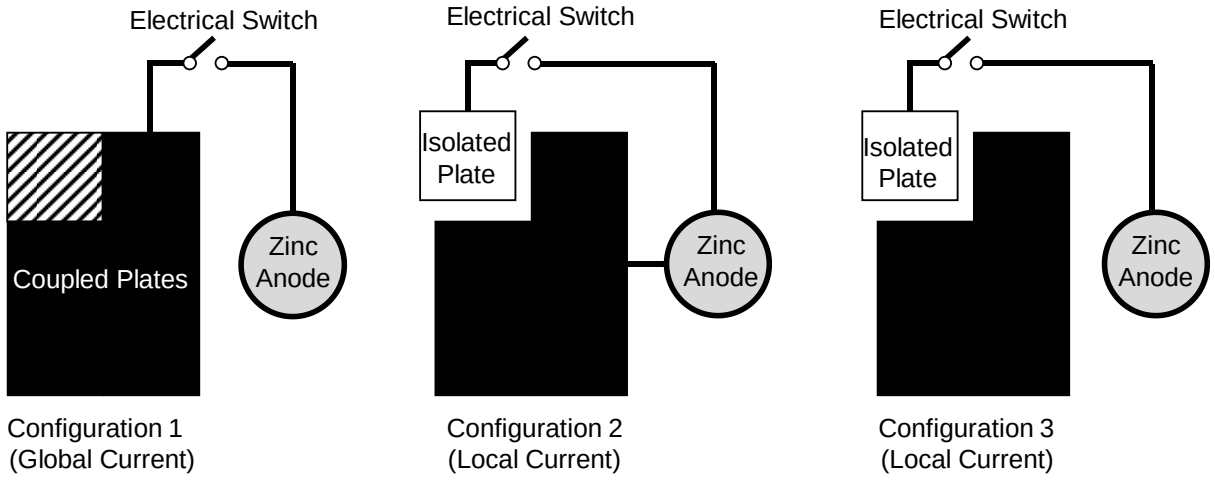

Figure 7.2. Different Test Configurations of Coupled Steel Coupons and Zinc Anodes.

All retrieved samples were hand cleaned to remove surface fouling and photo documentation of surface corrosion was made under magnification with a stereo microscope. Remnant traces of barnacle attachment as well as steel corrosion including maximum corrosion pit diameter and pit depths were documented. Select samples from various immersion depths were further cleaned following ASTM G1-03 but immersed in cleaning solution for up to 2 hours.[23] The difference in mass before and after outdoor exposure was used to calculate the apparent corrosion rate.

7.1.2. Field Sample Lab Testing

The test samples were removed from the test rack and stored in sealed containers containing river water for transport back to the laboratory. In the laboratory, individual coupons were immersed in collected river water only immersing 3.5 inch of the coupon in solution. The immersed surface area was ~52 in^2. Additional electrochemical tests were made in the laboratory (Figure 7.3). Corrosion testing consisted of measurements of the open circuit potential (OCP), linear polarization resistance (LPR), and electrochemical impedance spectroscopy (EIS). A saturated calomel electrode (SCE) was used as a reference electrode for all tests. An activated titanium mesh was used as the counter electrode. The scanned potentials for the LPR testing was made from the open-circuit potential and cathodically polarized 25 mV at a scan rate of 0.1 mV/s. The corrosion current density was calculated from the polarization

resistance, Rp, following the equation i_{corr}=B/(RpxA) where B was assumed to be 26 mV and A was the nominal surface area of steel coupon immersed in the solution.

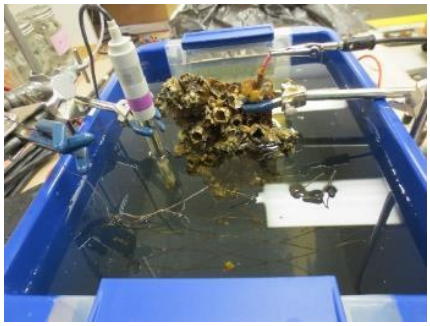

Figure 7.3. Example of Laboratory Electrochemical Test Setup.

Verification tests to identify marine fouling and surface bacterial growth were made at the end of the ~9- month test exposure. Tests included visual photo-documentation of steel coupon surface conditions and analysis of developed surface bacteria population. Small sections of marine growth (~1 in^2) were removed where swabs of the steel substrate were collected for the microbiological analysis. Biological Activity Reaction Test (BART) kits were used to assess the population and the activity of four common MIC related bacteria (SRB, IRB, SLYM and APB).

7.1.3. Laboratory Cathodic and Anodic Polarization Testing

Cathodic potentiostatic polarization tests (at -850 and -950 mV_{SCE}) were for up to 7 days. Supplemental testing at -500 mV_{SCE} was also made as comparative testing with anodic polarization. Experimental parameters for the test setup are shown in Table 7.3. For the working electrode, a copper electrical wire was soldered to an auxiliary steel screw attached to the steel sample. The exposed electrode surface was wet-ground to uniform P2000 grit (10µ) finish. Crevice environments were also introduced. Testing included both representations of physical hard and porous crevice conditions characteristic of hard-shell barnacles and soft marine flora and fauna. Hard crevices with a controlled height (3 mils), radial depth (7/32 inch) and opening (1/16-inch diameter) was made by using plastic film of known thickness. The plastic shims were affixed on the surface of the mounted samples as shown in Figure 7.4. Soft crevice conditions were replicated by placing a porous sponge on the working electrode surface. Activated titanium mesh and saturated calomel (SCE) electrodes were used as reference electrodes. Another activated titanium mesh was used as counter electrodes. All test cells and equipment were cleaned with ethanol. Test cells were filled with 300 mL deionized water and 20mL of modified Postgate B medium solution (Postgate,1984). A picture of test cells for test setup is shown in Figure 7.5.

Table 7.3. Test Setup Conditions.

De-Aerated or Naturally Aerated Conditions
SRB
with Hard Crevice
SRB with Porous Crevice
No SRB
with Hard Crevice
with Porous Crevice

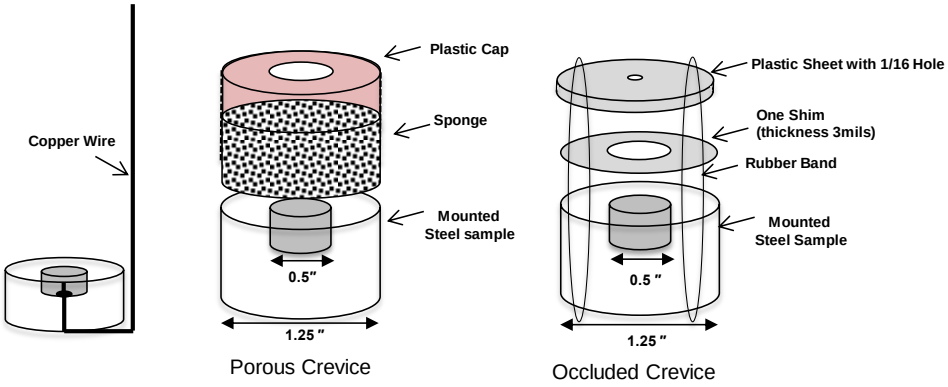

Figure 7.4. Schematic of Working Electrode in Test Setup B.

The pH of all test solutions was ~6.5-8. For de-aerated test conditions, high purity nitrogen gas was bubbled in the solution for ten minutes on the first and third day. To prevent subsequent oxygen ingress, a thin layer of mineral oil was added to the solution surface for these samples. Test cells for all test conditions to assess SRB presence (Table 4) were inoculated with10 ml of the inoculated broths.

Assessment of microbial activity was made by chemical oxygen demand (COD) and sulfide production. COD of each samples was measured by a colorimetric COD method at the first and final day. A hydrogen sulfide color disc test kit was used for the sulfide estimation. After ~7 days, the steel working electrode was removed from the test solution. Coverings were removed from crevice samples. Biotechnology Solutions sessile test kits were used for detection of sulfate reducing bacteria by serial dilution in Modified Postgate B (MPB) following NACE standard TM0194-2014. Sterile cotton swabs were used to gently scrape the sessile sample area (1 cm^2 area) and the slime (solid) was placed into a sterile Phosphate Buffer Solution (PBS). Serial dilution of the 1 ml PBS ranged from 4-8 times. All samples were rinsed with ethanol and dried. Photodocumentation for corrosion development and remnant physical effects of microbial activity was made.

Figure 7.5. Test Setup B Test Cells.

7.2. Results and Discussion

7.2.1. Field Site Testing

Bulk zinc anodes were coupled to arrays of steel coupons at Site I and II to identify the extent to which cathodic galvanic polarization provided by the zinc anodes can mitigate corrosion in sites that can support marine fouling and MIC.

7.2.1.1. Electrical Potential Measurements

Table 7.4 lists the measured electrical potentials for the test system at Site I and II. The open circuit potential of the uncoupled bulk zinc anodes was electronegative (<-1,000 mV_{CSE}) indicating sustained zinc corrosion activity throughout the ~200-day exposure in the brackish waters at both test sites. Figure 7.6 shows the measured potentials for the steel coupons. The test samples prior to coupling to the zinc anode showed OCP ~-690 to -720 mV_{CSE} for Site I and and ~-650 to ~-670 mV_{CSE} for Site II. The depths of the submerged test samples (Table 7.4) at Site I were somewhat deeper and marine growth at the two sites were quite different. Different oxygen levels at the steel interface could account for the variations in potentials, but the somewhat more negative potentials at Site I may indicate larger anodic current exchange density and thus greater corrosion activity there. As reference, the Group B control steel coupons showed OCP ~-610 to -800 mV_{CSE} for Site I and ~-630 to -770 for Site II during its ~300 days of immersion. Potentials measured after coupling of the bulk anode (on day 107 at Site I) indicated cathodic polarization of the steel array. At Site I, the on-potential was ~-1,000 mV_{CSE} throughout the exposure, indicating up to ~300 mV cathodic polarization of the steel array.

At Site II, the measured on-potential was not distinctly different from the initially measured steel OCP even though the zinc anode itself was ~-1000 mV_{CSE}. However, instant-off measurements on day 77 showed distinct shift to more noble potentials indicating that some effect of the cathodic polarization was present. Nevertheless, due to apparent electrical connection problems of the steel array to the initial zinc anode, coupling of the steel array was

then switched to an auxiliary bulk zinc anode. After that, the system potential was measured to be ~-1,000 mV_{CSE}. As expected, due to the more electronegative corrosion potential of the steel array at Site I, the coupled on-potential was likewise more electronegative. Per test site, no differentiation in corrosion potentials was observed by marine depth.

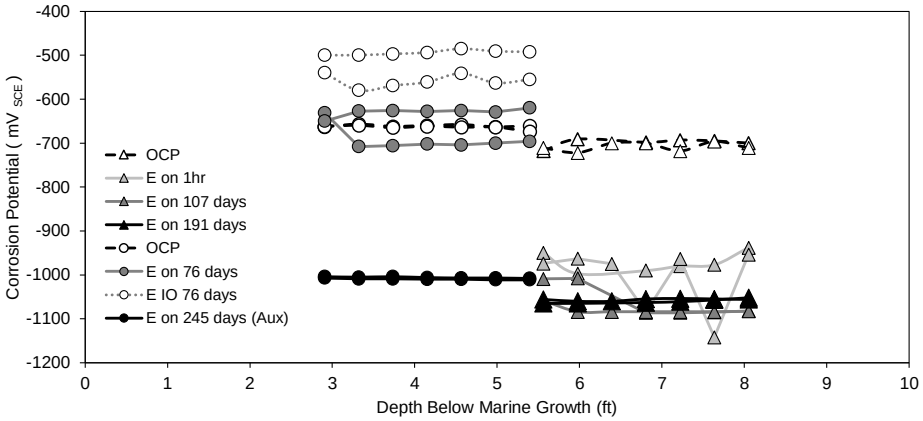

Figure 7.6. Potential Measurement for Field Exposed Samples (Group B).

Table 7.4. Electrochemical Potential (mV_{CSE})

	Site I			Site II		
	Exposure Time /Days *Total (Coupled)*		Potential /mV_{CSE}	Exposure Time /Days *Total (Coupled)*		Potential /mV_{CSE}
E_{Zinc}	107	(0)	-1148, -1037*Aux*	0	(0)	-1104, -1090*Aux*
	290	(191)	-1135, -1370*Aux*	245	(245)	-1018, -1074*Aux*[2]
E_{OCP}	107	(0)	-691 to -722	0	(0)	-657 to -674
E_{OCP}[1]	*0*	*(-)*	*-754 to -774*	-		-
	107	*(-)*	*-694 to -798*	*0*	*(-)*	*-637 to -710*
	195	*(-)*	*-684 to -712*	*77*	*(-)*	*-727 to -772*
	290	*(-)*	*-612 to -723*	*245*	*(-)*	*-688 to -725*
E_{ON}	107	(0)	-928 to -1142	0	(0)	-
	195	(107)	-1008 to -1086	77	(77)[2]	-620 to -708[3]
	290	(191)	-1052 to -1065	245	(245)	-1004 to -1011
E_{IO}	290 (191)	1 sec	-1022	245 (245)	1 sec	-832 to -1036
E_{OFF}	290 (191)	10 min	-990	245 (245)	4 hrs	-704 to -887

1. Control sample shown as reference (Group B), 2. Initial and Aux. electrodes switched at Day 77. 3. E_{ON} potentials prior to switching zinc anode.

7.2.1.2. CP Current Measurements

The current provided by the anode to the steel coupons was measured in three configurations to identify differentiation in anodic behavior of individual steel coupons in the array as well as the global current between the zinc anode and the entire steel array. It was thought that localized corrosion cells, that could develop at discrete locations in the steel array, can have an effect on the efficacy of the zinc anode. Test configuration 1 related to the current afforded by the zinc anode to the entire steel array. Test configuration 2 related to the extent to which CP is afforded at local steel sites with respect to the mixed potential of the entire steel array. Test configuration 3 related to the extent to which CP is afforded to individual steel sites by the zinc anode.

Figure 7.7 shows the afforded CP current at Site I and II at the various sample submerged depths. As described earlier, the system on-potential was ~-1,000 mV_{CSE} indicating generally good polarization by the zinc anode. Correspondingly, CP currents to the steel array exceeded 10 mA (current density >30mA/m^2) (Chess et al.,2003). As expected for the polarization (provided by the zinc anode to the coupled steel array), local CP currents at individual steel plates were smaller than the global current provided to the entire array.

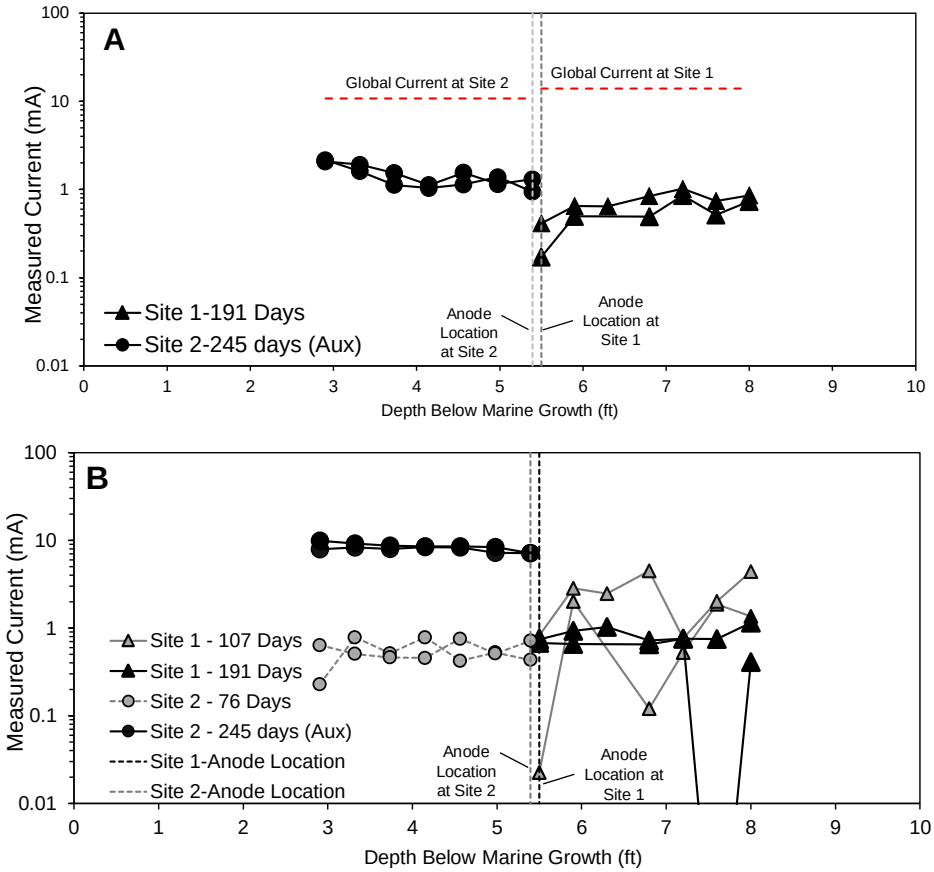

Figure 7.7. CP Current Measurement for Field Exposed Samples. A) Configuration 2, B) Configuration 3.

As shown in Figure 7.7A, some localized steel regions (as highlighted by test configuration 2 at Site I which had CP currents as low as ~0.1 mA) may have less relative polarization possibly due to the initial steel corrosion activity or other surface changes. As shown in Figure 7.7B, local currents between the zinc anode and individual isolated steel plates were not well differentiated within each test site indicating that the testing could not capture differences in local steel corrosion behavior or current demand due to surface modifications. For both test configuration 2 and 3, no major differentiation in current was observed by sample submersion depth within each test site, and the data series did not suggest significant effect due to solution resistance by distance (up to 3 ft) from the zinc anode. Also, any differentiation in marine growth within the vicinity of the individual test site depths did not significantly affect CP current but may be a contributing factor for the differences observed between the two test sites.

Figure 7.8 relays the same data points but arranged by test configuration for Site I and II. For the given test geometry, the total global current to the steel array was 14 and 11 mA for Site I and II, respectively. Local current was 0.1 to 1 mA for Site I and 1-10 mA for Site II for test configurations 2 and 3. For comparison, current density was calculated by steel area (13 and 14 plates for test configuration 1 at Site I and II, respectively; and 1 plate for the local test configurations 2 and 3 for Site I and II). Global current density was ~5 and 3 uA/cm^2 for Site I and II, respectively. For Site I, the local corrosion current density was ~1-6 uA/cm^2 for test configurations 2 and 3 but were generally larger for the latter. Similar trends were observed at Site II, but there was greater differentiation in the local current for samples between test configuration 2 and 3. At Site II, current density was ~5-10 and ~30-50 uA/cm^2 for test configuration 2 and 3, respectively.

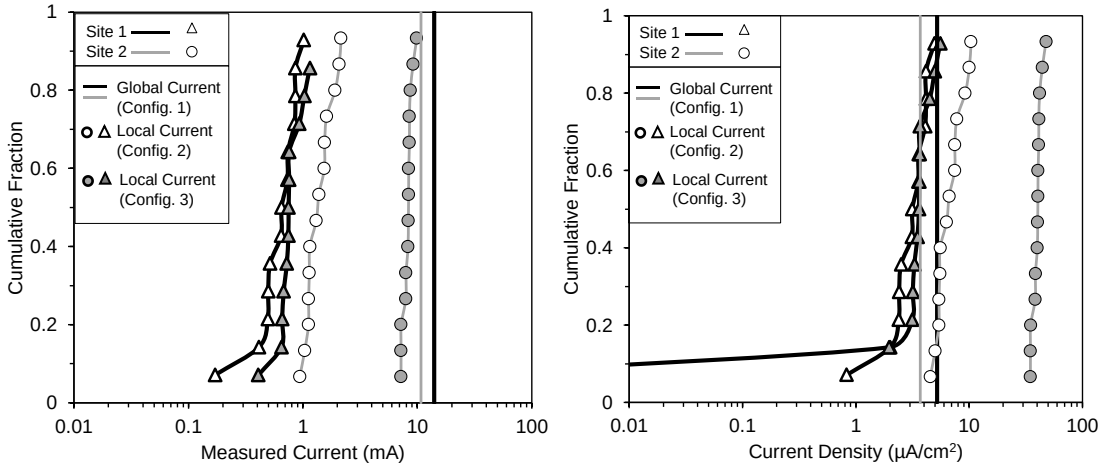

Figure 7.8. CP Current Distribution for Field Exposed Samples by Three Configurations.

In test configuration 3, the steel array was decoupled, and current was isolated between individual samples and the anode. The decoupling of extended reactive surfaces from the large steel array provided the system potential to become more electronegative due to the reduced overall rate of cathodic reaction for the test configuration compared to configuration 2. Due to the larger developed cathodic polarization from OCP in the test configuration, larger cathodic current could be provided by the zinc anode in configuration 3. Current measurements between isolated steel coupons and the steel array coupled to the zinc anode in configuration 2

conversely were lower due to the more noble system potentials. However, the effect may not be largely manifested if cathodic current limitations exist (as may be expected at -1,000 mV_{CSE}) and would in part explain the differences in the data sets from Site I and II. Site I would then seem to have conditions where bulk solution oxygen would not be readily accessible to the steel substrate possibly relating to the marine fouling type.

The cathodic area effect would seem to satisfy the trends in the current afforded by the anode at Site I and II for the various test configurations. Compilation of data from both sites showed that smaller currents were afforded by the zinc anode at Site I compared to Site II. This would indicate that there were smaller cathode surfaces in the former. This would be consistent with the more noble steel OCP and on-potentials at Site II.

7.2.1.3. Corrosion Mass Loss

The corrosion rates were calculated from the field sample mass loss data (Table 7.5). At Site I, coupling of the steel array to the zinc anode was made at day 107. At Site II, coupling to the initial zinc anode was made at day 0 but switched to the auxiliary anode at day 77. Final mass measurements were made at the end of the field exposure at day 291 and 245 for Site I and II, respectively. Due to the initial free corrosion at Site I for the first 107 days and the corrosion due to partial CP coupling at Site II for the first 77 days, the apparent corrosion rates for the different test intervals were calculated including an upper and lower bound for Site II. It was assumed that the free corrosion rates of the steel samples prior to coupling to the zinc anode was equal to the rates determined by the mass loss of control steel coupons at concomitant submerged depths. The steel mass loss that occurred during the time of zinc coupling was calculated by calibrating the final mass loss by its associated free corrosion rate prior to electrode coupling.

For Site II, the upper and lower bound were calculated by assuming either the entire 245 days had CP or that the first 77 days had free corrosion and CP was only provided in the last ~170 days. It is noted that the assumption of free corrosion rate would not reflect any partial corrosion mitigation afforded by the partial CP connection, but it was likely that corrosion mitigation there may not be significant as the supposed on-potential was the same as the initial steel OCP (-600 mV_{CSE}), when coupled to the initial zinc anode. The assumption that CP was provided for the entire 245 days would then provide an overestimation of corrosion rate values. The actual rate values would lie in between the upper and lower bounds but likely better estimated by the lower bound.

Table 7.5. Apparent Corrosion Rate (MDD) for Field Exposed Samples.

	Site I	Site II
Free Corrosion	46-56 Avg:54	17-27 Avg:21
CP	4-19 Avg:12	6-13 Avg:9* *13-15 Avg:14***

* Lower bound assuming free corrosion for the first 77 days and CP for ~170 days. ** Upper bound assuming effective CP for entire 245 days exposure.

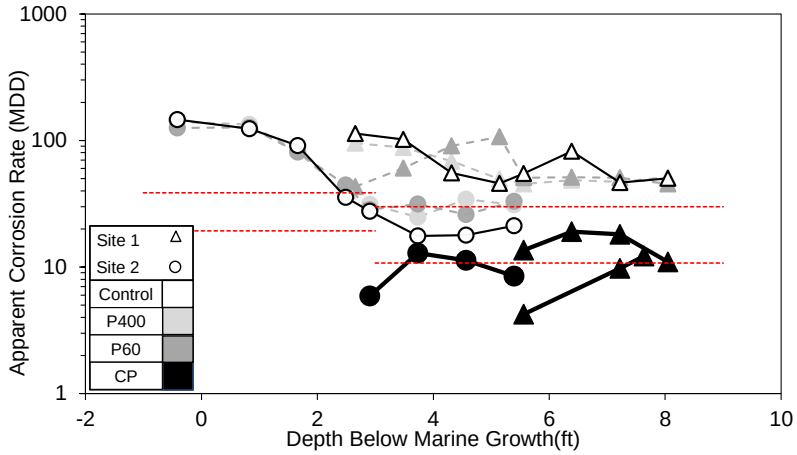

Figure7.9. Apparent Corrosion Rate for Field exposed Samples by Depth. (Lower bound apparent CP corrosion rates shown for Site 2) (Red Dash line are representative of average corrosion at intertidal and immersion zone[33]).

Figure 7.9 shows the apparent corrosion rates for steel samples at OCP and coupled to the zinc anode at Site I and II. It was evident by comparison of the apparent corrosion rate to reported average and maximum corrosion rates that the submerged region of Site I was quite aggressive where the apparent corrosion rate was as much as 2 times greater than maximum values reported for marine environments (Tomlinson,2014). Nevertheless, coupling of the steel to the zinc anodes did allow for reduced apparent corrosion rates. From the CP current data, it was observed that generally lower currents were measured at Site I than Site II, and it was proposed that the cathode area effect could account for the observations in the current data.

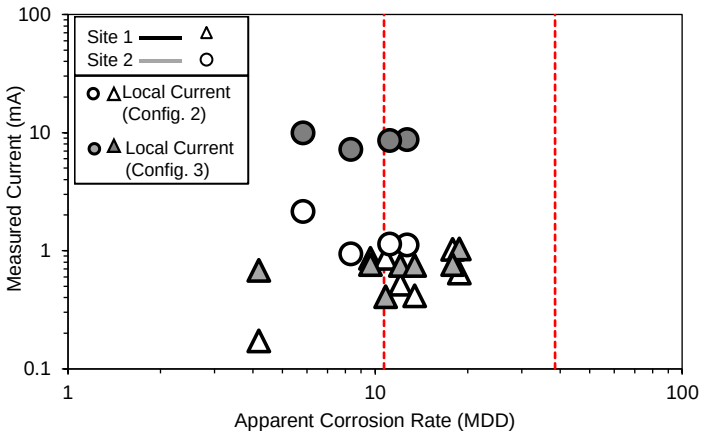

Figure 7.10. Apparent Corrosion Rate Corresponding to CP Current Measurement for Field exposed Samples. (Only lower bound apparent corrosion rates shown for Site 2).

Figure 7.10 compares the CP current data to the apparent corrosion rates. The lower CP currents at Site I generally corresponded to larger apparent corrosion rates, further supporting that there were portions of the steel surface that did not receive sufficient cathodic polarization thus allowing for differential corrosion cells to develop. Reciprocally, Site II had higher CP currents and lower overall apparent corrosion currents. As will be discussed in the following sections, the type and coverage of marine fouling at Site I would allow less efficient steel surface polarization in comparison to Site II.

Figure 7.11 shows a compilation of apparent corrosion rates calculated in terms of mass loss as described earlier and in terms of apparent sample thickness. The final apparent sample thickness was determined as the average of 6 measurements using a micrometer with 0.001-inch precision. Samples with irregular cross section loss (with heavy corrosion or with sinuous surface texture) or localized corrosion would not be well quantified. However, comparison to the corrosion rate by mass loss may aid to parse the extent of localized corrosion for the control and CP systems in test sites 1 and 2. Details on surface corrosion conditions are described later.

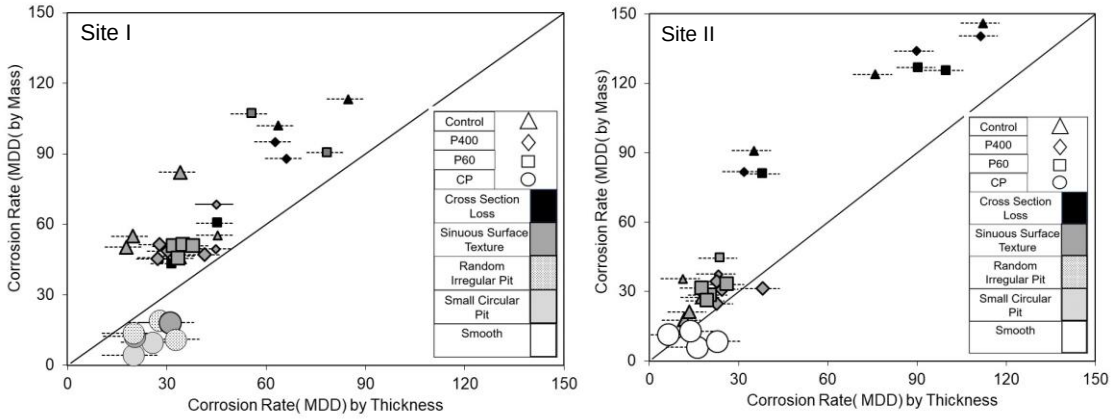

Figure 7.11. Compilation of Corrosion Rate by Mass and Thickness.

The apparent corrosion rates calculated by plate thickness would not identify localized corrosion. The apparent corrosion rates calculated by mass loss did identify samples with gross localized corrosion such as samples with irregular sinuous cross-section loss. Pitting was not identified by either apparent corrosion rates. Overall, it was evident that the free corrosion at both test sites will cause significant heavy localized corrosion as evident by the greater apparent corrosion rates calculated by mass loss when compared to apparent corrosion rates calculated by sample thickness. The application of CP at both sites did substantially reduce the overall rate of steel corrosion. Application of cathodic polarization at Site II did appear to mitigate development of localized corrosion where no pitting was observed on the steel plates coupled to the zinc anodes and comparatively heavier localized steel loss was observed on the control samples. It was uncertain if coupling of the zinc anodes to the steel array at Site I had similar effect as free corrosion was allowed for the first 88 days there, but as will be described later, localized corrosion (irregular surface corrosion) was reduced in magnitude when coupled to the zinc anode in comparison to the free-corrosion test samples. However, significant isolated pits still formed in the former.

Following the general discussion above, the greater apparent corrosion rates and lower CP currents at Site I indicated that there remained localized regions on the steel array where CP may not be effective, possibly indicating the detrimental effects of marine fouling or MIC under biofilm. It was proposed that localized corrosion can continue to form when marine fouling create localized corrosion cells and where MIC can develop in regions unprotected by CP.

7.2.1.4. Surface Fouling

Heavy fouling occurred during the time of exposure at both sites. Figure 7.12 and 7.13 shows the general visual appearance on the steel coupons at the end of the field exposure, before and after hand cleaning. The general fouling organisms at Site I included hydroids, bryozoans, acorn barnacle and oysters and at Site II were predominantly bay barnacles. During the test exposure period, fouling organisms at Site I consisted mostly of soft marine masses (hydroids) at 4-8ft BMG along with isolated acorn barnacle (diameters > 10 mm diameter). At Site II clustered and interlayered populations of barnacles (diameters from 5 to 16 mm) were observed from 2-5.5 ft. BMG. No major differentiation in marine fouling was observed between the free-corrosion (Group B) and the CP (Group A) samples.

The steel substrate of Group A and B samples from Site I and II was exposed after surface abrasion and chemical cleaning. Figure 7.11 parses the steel substrate condition by the apparent corrosion rates for representative test samples. In the figure, the samples were categorized according to the most severe level of surface corrosion. The different surface corrosion categories in order of severity were smooth, small circular pits, irregular pits, sinuous surface texture, and heavy cross-section loss. However, samples often had multiple steel surface corrosion modalities. In particular, samples with sinuous surface texture typically coincided with pit development. As described before, severe corrosion developed on the freely corroded test samples at both Site I and II. The submerged samples typically developed localized corrosion in the category of sinuous surface texture and lower. This type of localized

corrosion is highlighted in Figure 7.14. The irregularity of the sinuous surface texture and pitting was posed to be related to surface irregularities due to the marine fouling and possibly MIC. Figure 7.14 also identifies a location where differential mass loss occurred under the base of a barnacle. With the application of CP, it was apparent that the cathodic polarization at Site II was related to the mitigation of localized corrosion development. In Figure 7.14, the samples with CP application had generally smooth surface textures indicating that the measured mass loss was better represented by general corrosion in contrast to the control samples where irregular steel surface corrosion was apparent. At Site I, the irregular steel surface corrosion was apparent on both control and CP samples, but it could not be deciphered if that localized corrosion occurred prior to coupling to the zinc anode. The application of CP on those samples however, did prevent growth of the local corrosion sites as mainly pitting was observed.

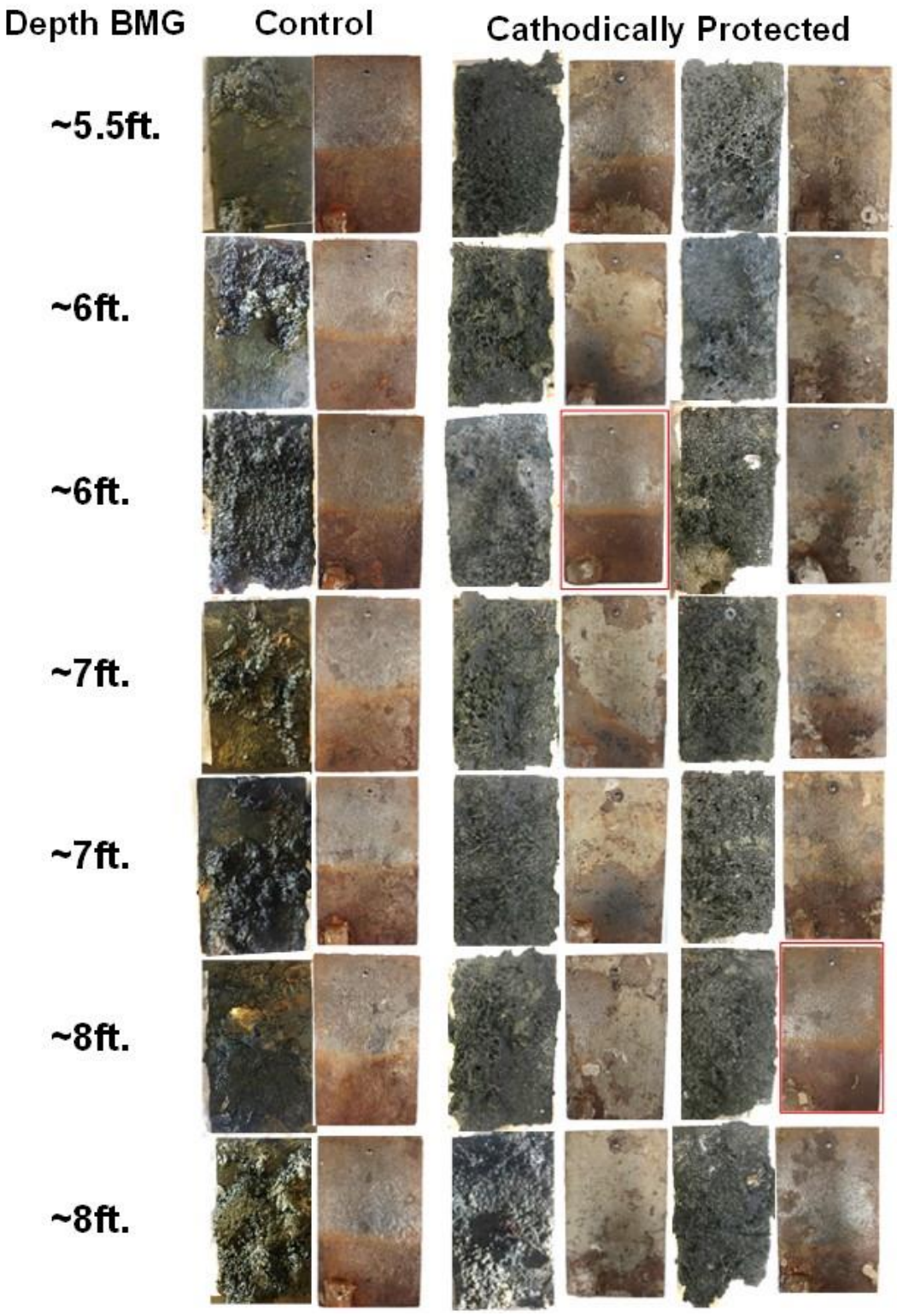

Figure 7.12. Test Coupons Exposed at Site I.

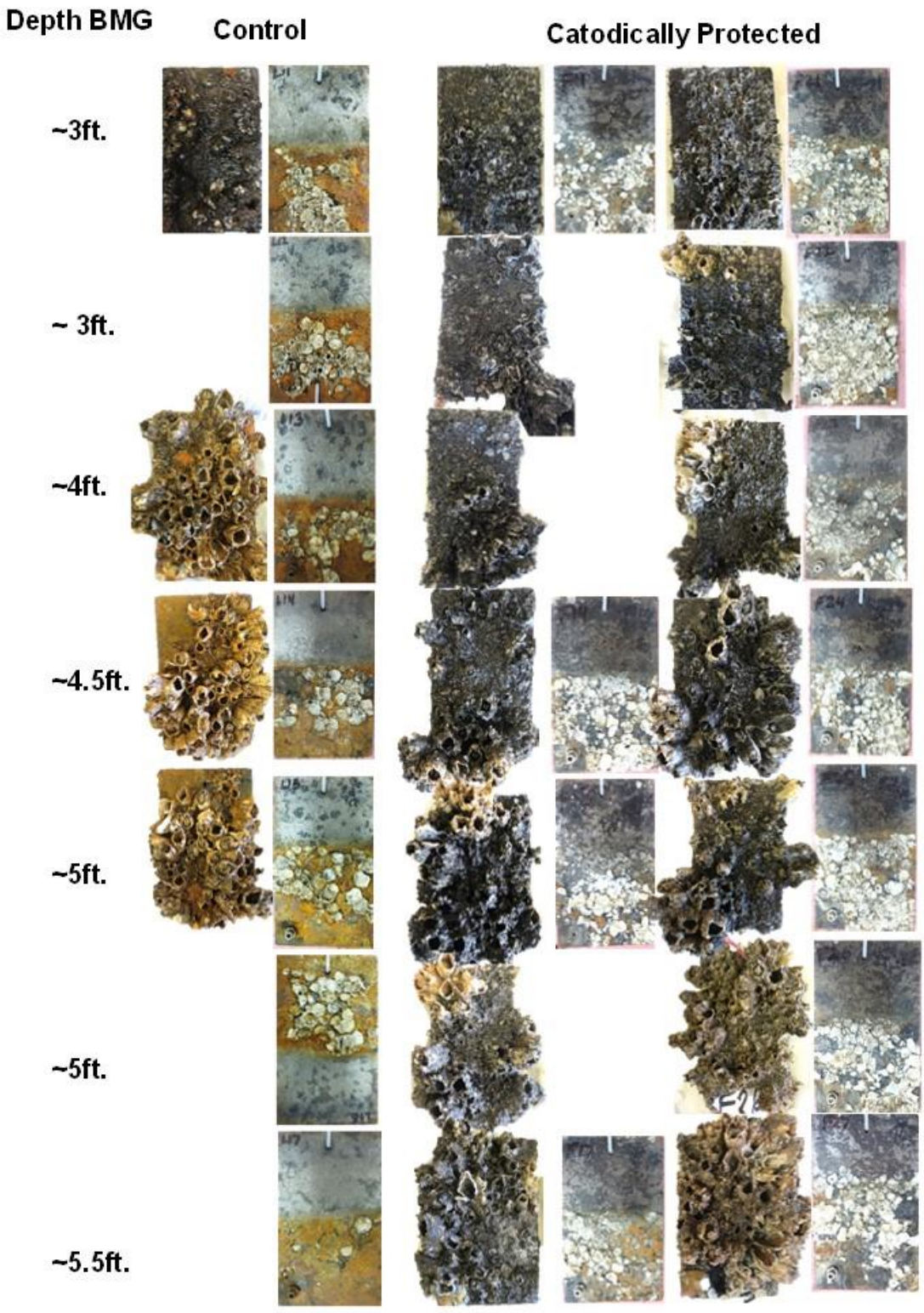

Figure 7.13. Test Coupons Exposed at Site II.

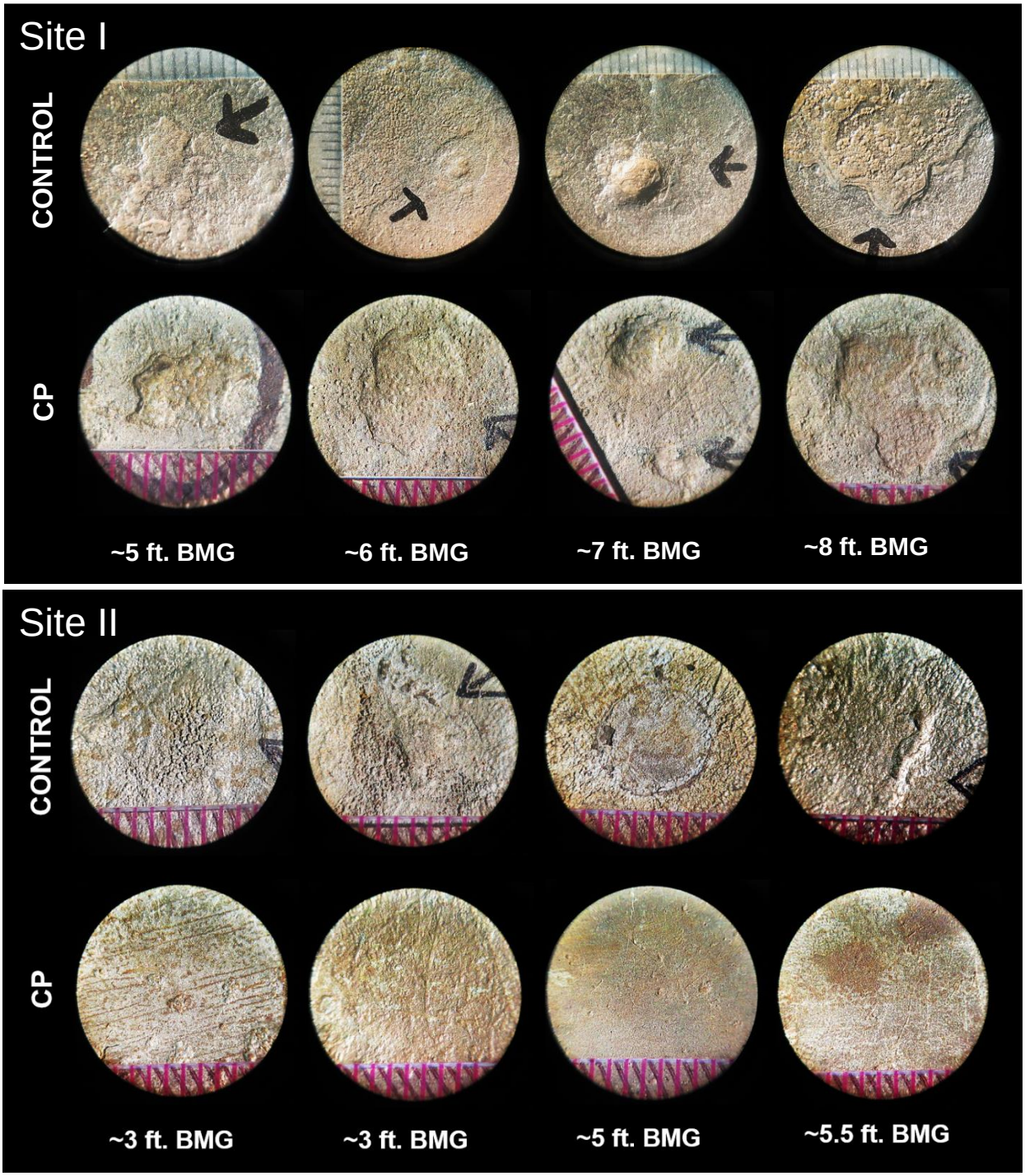

Figure 7.14. Magnified View of Surfaces of Field Exposed Samples, Arrows highlight notable features such as pitting, surface corrosion, remnant barnacle location. Rule at 1 mm intervals.

7.2.2. Field Sample Lab Testing

7.2.2.1.OCP and LPR

Field test coupons were removed from the outdoor test site and stored in river water for additional testing in the laboratory. The OCP and corrosion rates measured in the laboratory would not necessarily be representative of in-situ field conditions as oxygen levels and other steel surface parameters could be different. Nevertheless, the lab testing would ideally identify differing surface characteristics that developed in the field including the effects of fouling and film development.

Figure 7.15 shows the measured potentials plotted by placement of the steel coupons at various submersion depths along with the corresponding in-situ field measurements. The results for the control samples maintained in the OCP condition were previously discussed in Chapter 4 but are again discussed in context of the CP testing. In the laboratory testing, oxygen may abound in the open shallow test solutions, especially since the test samples had to be decommissioned from the field test rack, transported, and re-instrumented for testing in the lab. Nevertheless, lab-measured potentials of the freely corroding samples were not dissimilar to in-situ field measurements indicating that the effects of changes in the steel electrode were minimal.

The lab and field in-situ measured potentials showed more negative values for the freely-corroded samples originally placed at depths with permanent submersion (>5 ft BMG for Site I and >3 ft BMG for site II). This can be in part reflective of greater coverage of the substrate by biofouling. For example, marine flora amassed at depths greater than 5 ft BMG at Site I and interlayers of clustered barnacles formed at depths greater than 3 ft BMG for Site II. The presence of the marine fouling could possibly reduce surface area for oxygen reduction or possibly create local anodes below the occluded regions. These regions could develop local differential aeration cells and support MIC. The OCP was more electronegative for the samples that were coupled to the zinc anode during the field exposure, likely reflecting the development of calcareous deposits, especially on samples from Site I where thicker deposits were apparent (Figure 7.12).

Lab LPR measurements for samples at permanent submersion depths showed greater instantaneous corrosion rates at Site I than Site II (Figure 7.16). This trend was similar to that identified from the average corrosion rates calculated from mass loss measurements. However, even though similar trends in corrosion aggressivity of submerged water conditions in the field test sites were identifiable, the instantaneous rates determined in the lab testing were consistently greater than the largest average corrosion rates calculated by mass loss, reflecting test errors (such as oxygen levels) in the test setup. Furthermore, the instantaneous corrosion rates for samples collected from tidal regions (measured in a static lab test solution) did not capture the aggressive conditions (such as cyclic wetting) at the field site. A simplified analysis approach for the EIS test data (assuming that the total impedance magnitude at 1 Hz would

capture trends of the interface activity) showed supporting trends for the measured instantaneous corrosion rates (Figure 7.17).

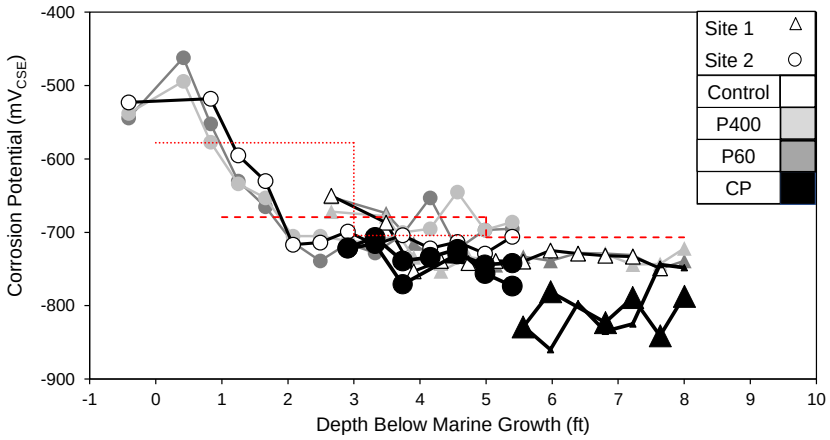

Figure 7.15. Laboratory Measurement of Corrosion Potential for Field Exposed Samples.

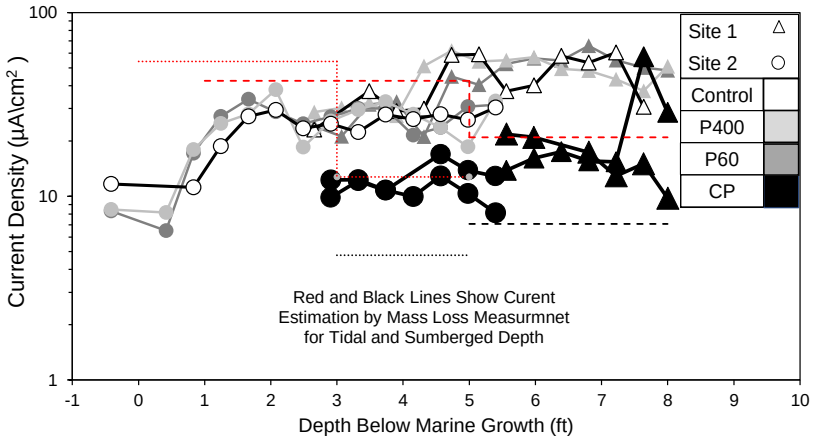

Figure 7.16. Laboratory measurement of Corrosion Current Density for Field Exposed Samples.

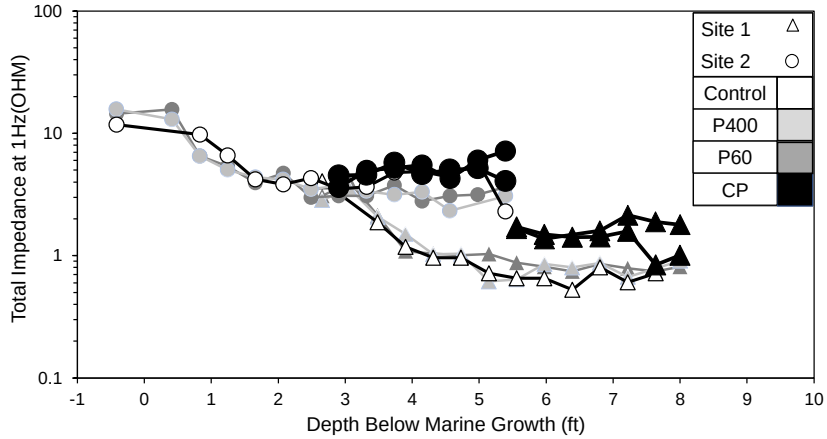

Figure 7.17. Laboratory Measurement of Total Impedance at 1Hz for Field Exposed Samples.

7.2.2.2. Microbiological Analysis

Table 7.6 shows the population of the four types of bacteria for both group A and B at Sites I and II, that are commonly associated with MIC. Both Sites I and II had high populations of the tested bacteria. It was apparent that proliferation of the bacteria was not inhibited in the presence of the cathodic polarization at ~-1000mV$_{CSE}$. Higher pH (developed in occluded regions by the enhanced oxygen reduction rates) that could diminish bacteria activity did not seem to be a factor in the testing. Conversely, the cathodic polarization that could help sustain anoxic regions may support SRB beneath marine fouling occluded spaces such as the dense coverage barnacles and soft marine masses. The measured bacteria count indicated that aggressive conditions to maintain high levels of SRB, IRB, APB, and SFB were maintained. These conditions could then support MIC of the steel.

Table 7.6. Bacteria Content (CFU mL^{-1}) for Field Exposed Samples.

Bacteria	Site I		Site II		
	Control	CP	Control	CP	Zinc Anode
Sulfate Reducing Bacteria (SRB)	6,000 (A)	1,400 (M)	27,000 (A)	27,000 (A)	325 (M)
Iron-Reducing Bacteria (IRB)	35,000 (A)	2,200 (M)	9,000 (A)	35,000 (A)	25 (M)
Acid Producing Bacteria (APB)	82,000 (A)	475,000 (A)	475,000 (A)	475,000 (A)	82,000 (A)
Slime-Forming Bacteria (SFB)	1,750,000 (A)	1,750,000 (A)	1,750,000 (A)	1,750,000 (A)	440,000 (A)

Aggressivity. (NA) Not Aggressive, (M) Moderately Aggressive, (A) Aggressive. General guidelines for BART test for corrosion

7.2.3. Laboratory Polarization Testing

7.2.3.1. Cathodic Polarization Behavior in Crevice Geometries

The laboratory cathodic polarization tests were made at either -850 or -950 mV$_{SCE}$ to provide differentiation of cathodic behavior of steel in crevice conditions with and without the presence of SRB. In the control tests without SRB inoculation, the extent of shielding of the steel surface due to the crevice geometry was examined. As shown in Figure 7.18, the measured cathodic currents at both cathodic polarization levels was significantly lower for samples with crevices and was lower for the hard crevice than the porous crevice due to better electrolytic exchange in the latter through the pore spaces of the sponge. This observation would suggest that biofouling organisms may reduce the effectiveness of cathodic protection systems by inhibiting the level of cathodic current in occluded regions. Generally, similar trends in current were observed in tests with the SRB inoculation with the exception of the test case for

steel with porous crevices in de-aerated inoculated solutions. It would appear that the porous medium in these conditions would not have large electrical resistances associated with non-uniform current distribution in crevice environments. However, cathodic reduction reactions associated with SRB within the open pore spaces may be significant. Indeed, as described later, SRB was shown to proliferate in both open and crevice environments.

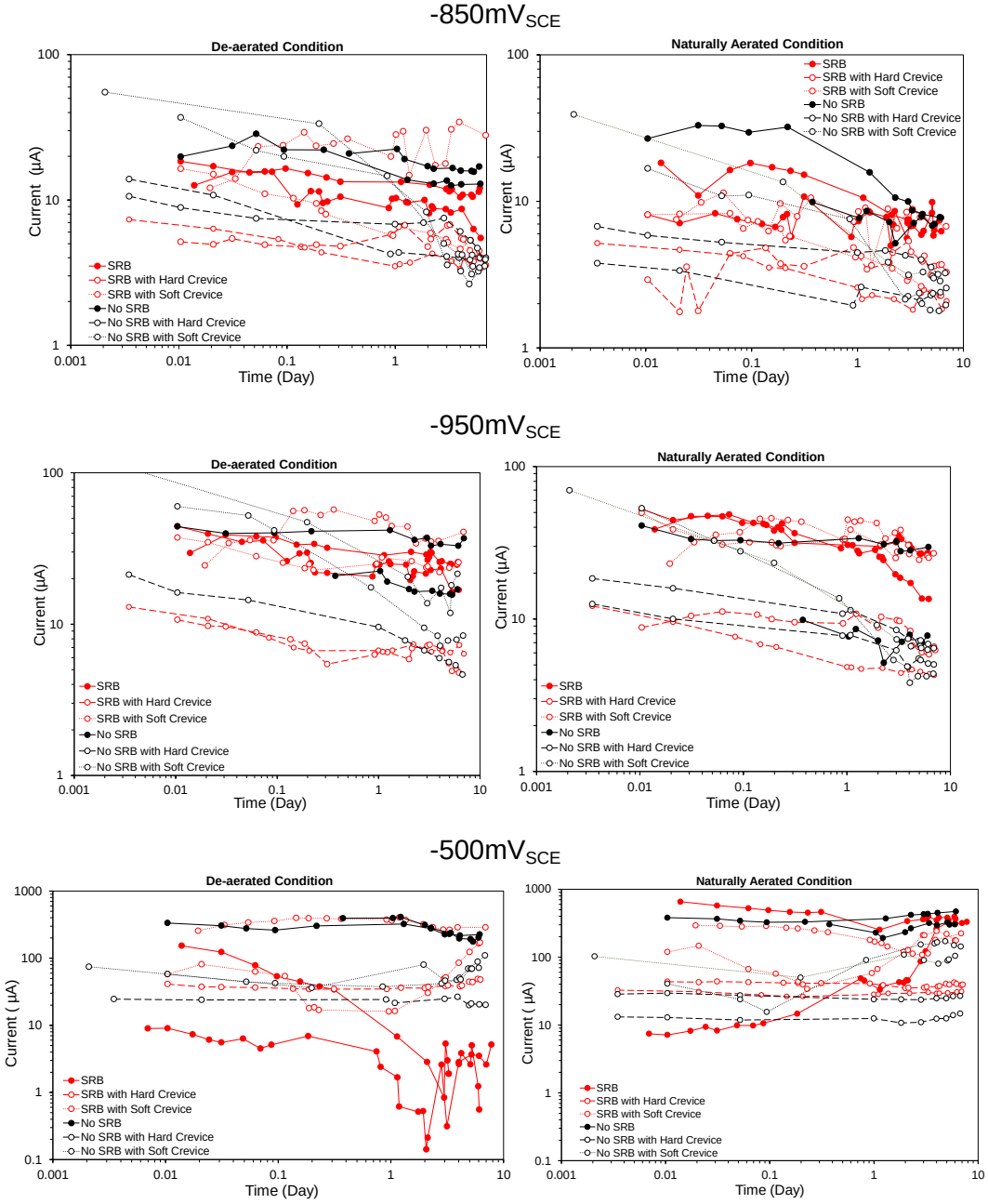

Figure 7.18. Current Measurement for Laboratory Samples at Polarization level of -850 mV$_{SCE}$, -950 mV$_{SCE}$, -500 mV$_{SCE}$.

Figure 7.19 shows the cumulative charge associated with the measured cathodic reactions. The cumulative cathodic charge for the -850 and -950 mV_{SCE} potentiostatic polarization tests relate an increase in the inoculated and non-inoculated solutions. The hard crevice conditions consistently had lower cathodic reactions regardless of inoculation. The porous crevice conditions had greater cathodic reactions in inoculated solutions. For the open, the magnitude of the cumulative cathodic charge was not dissimilar in the inoculated and non-inoculated solutions. The total net cathodic reaction in the presence of the cathodic polarization could include oxygen reduction and hydrogen formation by activation polarization and the sulfate reduction associated with SRB. In the non-inoculated solutions, the reduction reactions would include oxygen reduction and hydrogen reduction. The results would indicate that crevice environments that prevent interaction with bulk solutions can reduce the level of cathodic reactions, but there is indication (as in the porous crevice condition) that cathodic reactions related to SRB also can be important. In the following section, identification of SRB activity was made so that the effect of its presence on cathodic reaction rates may be elucidated. It was posed that in the presence of cathodic polarization, sulfate reduction by SRB can be identified by measure of current.

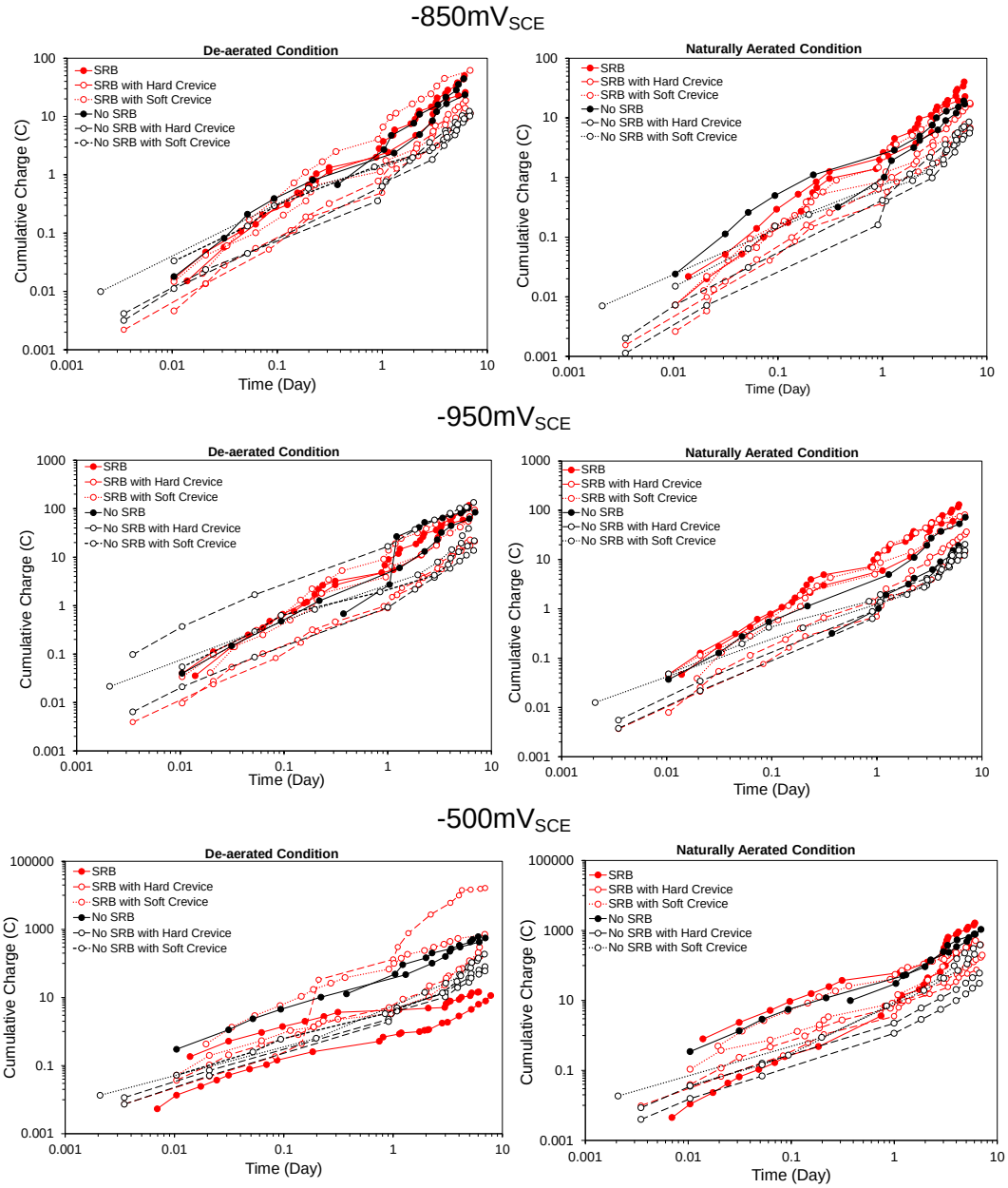

Figure 7.19. Cumulative Charge Measurement for Laboratory Samples at Polarization level of -850 mV$_{SCE}$,-950 mV$_{SCE}$, -500 mV$_{SCE}$.

Chemical and microbiological analysis was made for the solutions of the cathodic polarization test samples to identify levels of SRB activity (Figure 7.20). COD measurements of the test solutions at the onset of the test showed high COD levels indicating environments that can support SRB growth. The COD levels typically dropped overall by the end of the testing, but final COD levels were consistently higher in the inoculated solution than the control non-inoculated solutions indicating that the environments in the former had conditions better supportive of SRB growth as well as indication of increase in organic content that could develop with SRB growth. The low final COD levels in the non-inoculated solutions conversely would then be indicative of low SRB activity. The COD levels were higher for the open surface

conditions in the de-aerated solutions than the naturally aerated solutions indicating benign low oxygen environments to sustain SRB growth in the former. However, similar COD levels were measured for the de-aerated and naturally aerated inoculated solutions for the samples with crevice environments and any preferential SRB development in the occluded spaces were not captured.

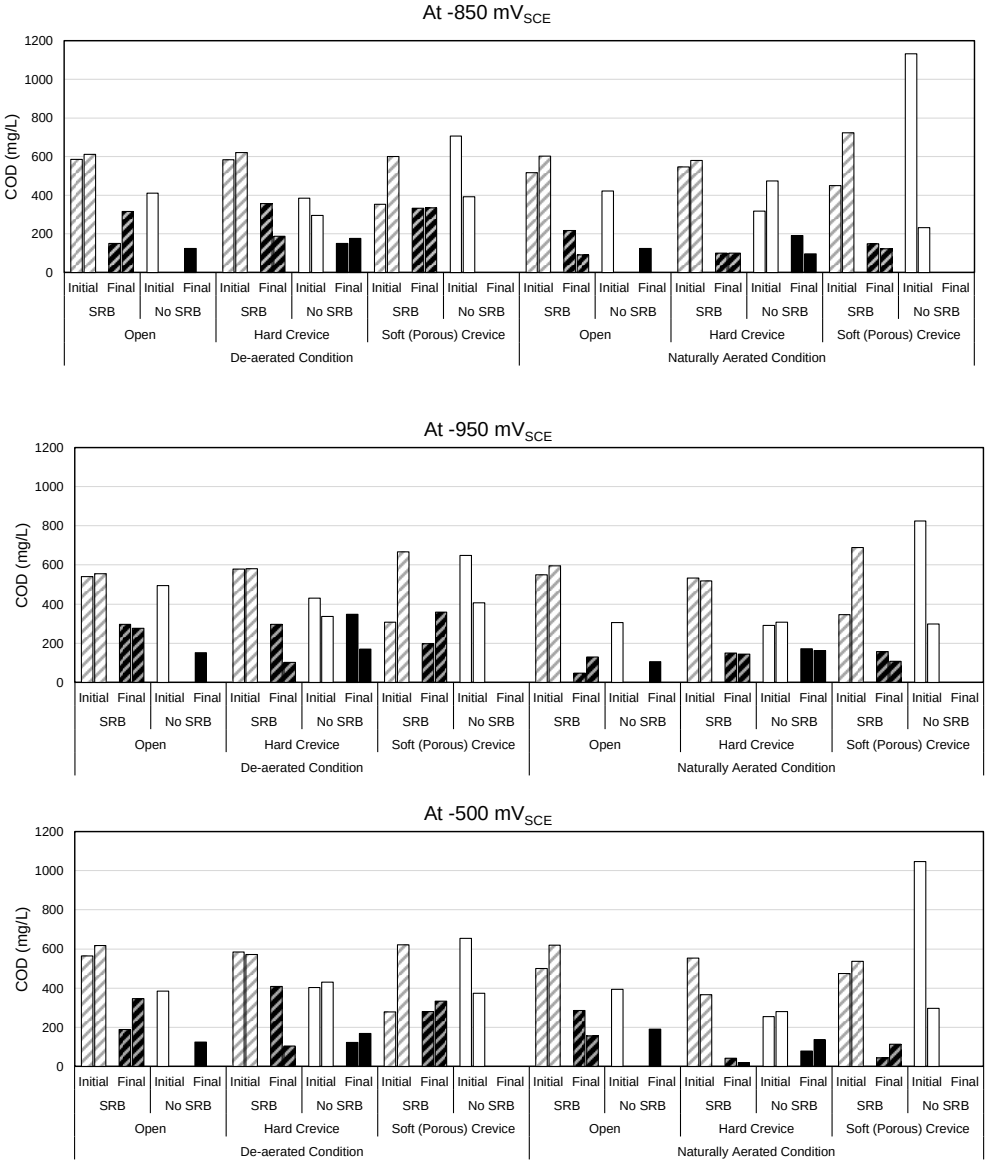

Figure 7.20. Chemical Oxygen Demand for Laboratory Test Samples at Polarization level of -850 mV$_{SCE}$, -950 mV$_{SCE}$, -500 mV$_{SCE}$.

The total SRB population measured by serial dilution indeed showed high SRB levels in all inoculated solutions but were overall lower with the applied cathodic potentials than comparative control tests at the open circuit conditions (Table 7.7). This may suggest the positive effects of cathodic polarization to reduce SRB as suggested by some. The crevice environments were shown to be able to promote SRB growth possibly relating to providing anaerobic environments and shelter within the occluded space, but consistent explanation of the

mechanism is lacking in the literature. It has been posed that the cathodic polarization can create local chemical change near the surface of the steel that affect the attachment or growth of SRB. Larger reduction rates such as oxygen reduction or hydrogen formation could then reduce SRB proliferation. However, the crevice geometries apparently can have effect on the level of polarization of the steel within occluded spaces. Low cathodic currents here could be indicative of less effective cathodic protection due to non-uniform polarization under the crevice or even blocking of the steel surface from sufficient cathodic current. In this case, SRB may be protected in crevice spaces even with strong cathodic polarization. However, in the lab tests, steel under porous crevices with SRB showed high cathodic currents possibly reflecting better electrical properties (low resistance) through the sponge that allowed relatively high cathodic currents but did not produce a change in environment that could reduce SRB growth.

Table 7.7. Reported Bacteria per mL for Laboratory Test Samples.

Aeration	Polarization mV_{SCE}	SRB Inoculation			Control No SRB Inoculation		
		Open	Hard Crevice	Porous Crevice	Open	Hard Crevice	Porous Crevice
De-aerated	-950	10^2-10^6	10^3-10^8	0-10^6	10^4	0-10^2	0
	-850	10^1-10^3	10^1-10^8	0-10^8	10^1	0-10^2	0
	OCP (-600 to -750)*	≥10^8	≥10^8	10^7	0	10^3	0
	-500**	10^2-10^4	10^1-10^6	0-10^3	0	0-10^2	0
Naturally Aerated	-950	10^2-10^4	10^3-10^6	0-10^6	0	0-10^2	0
	-850	10^2-10^4	10^3-10^8	0-10^6	0	10^2-10^3	0
	OCP (-600 to -750)*	≥10^8	10^7	10^7	10^3	0	0
	-500**	10^3-10^8	10^2-10^4	0	10	0-10^4	0

* From comparative testing described in chapter 4. **Comparative anodic polarization tests.

Sulfide concentrations in the form of hydrogen sulfide and metal sulfide from extracted aliquots of solution was measured with a color disc test kit during the course of the lab tests. Figure 7.21 shows the sulfide concentrations for the various test configurations including polarization levels, aeration levels and crevice geometries. The test results showed that sulfide production occurred at various levels throughout the duration of the test regardless of the level of cathodic polarization. Also, sulfide production was measured in extracted solution associated with the porous and hard crevice geometries. The various forms of hydrogen sulfide detected by the test kit derived from sulfide, S^{2-}, produced by the sulfate reduction reaction as part of SRB metabolic activities are part of associated charge transfer reactions.

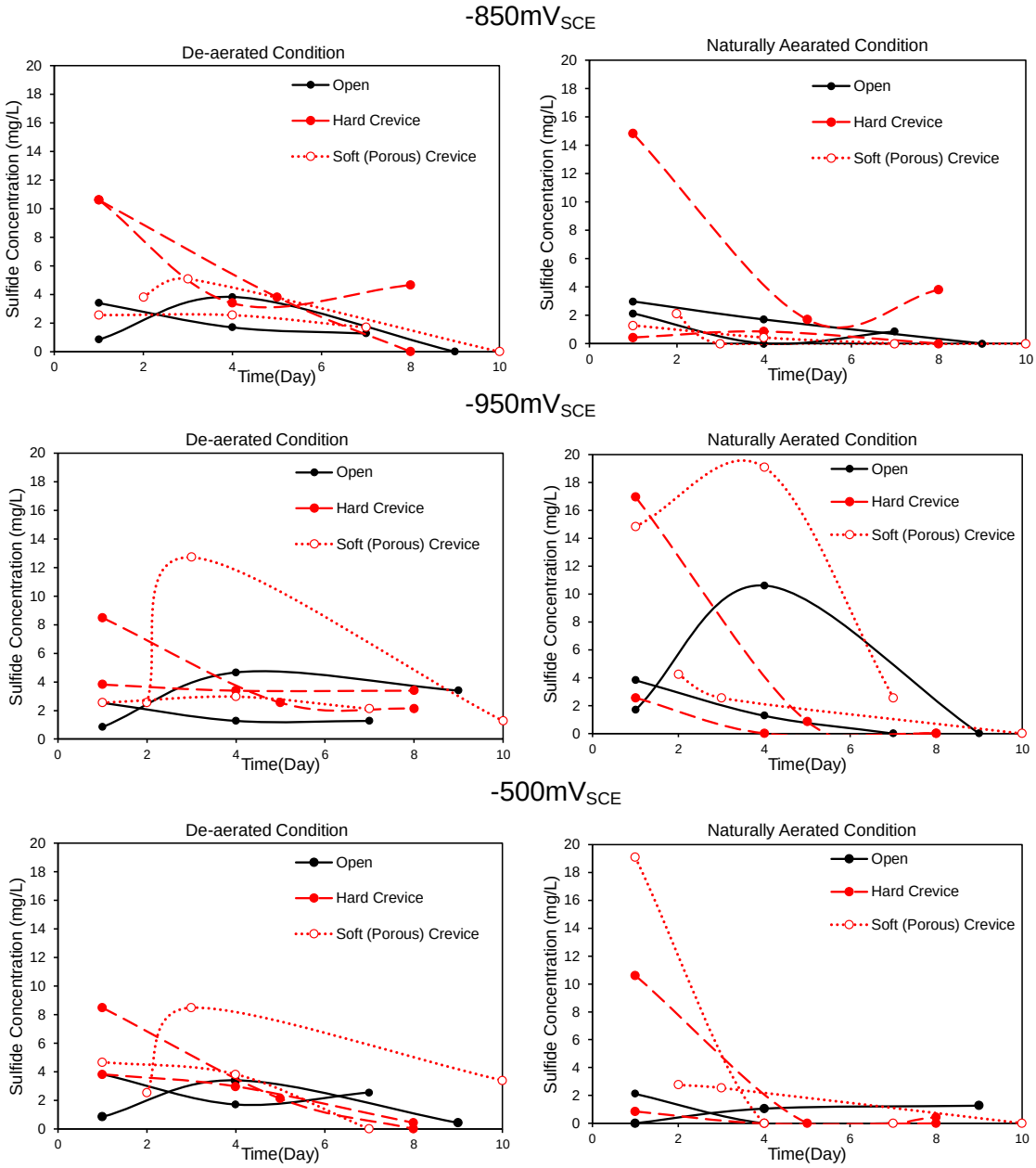

Figure 7.21. Sulfide Production Level for Laboratory Inoculated Test Samples at Polarization level of -850mV$_{SCE}$, -950 mV$_{SCE}$, -500 mV$_{SCE}$.

The sulfide levels measured at discrete times during the exposure was then used to calculate an apparent rate of sulfide production within the fixed solution volume (Figure 7.22). The apparent rate of sulfide production was assumed to be constant for the time intervals between sulfide measurements as was thought to be primarily related to SRB presence. It was apparent that in the test condition with cathodic polarization that the level of sulfide production decreased with time indicating decrease in SRB activity. However, it was also apparent that SRB continued to grow to some extent as sulfide production continued in many cases throughout the test exposure. Also, in congruity with the high total bacteria population in the

crevices, the apparent sulfide production rate for the samples with crevices was higher and appeared to be prolonged relative to the open geometry. The effects of oxygen and iron levels and ionic strengths were assumed to not be significant in the oxidation of sulfide (Millero,1986). With the assumed rates of sulfide production, the cumulative molar content of sulfide was calculated. Based on the stoichiometry of the sulfate reduction reaction ($SO_4^{2-} + 8H = 4H_2O + S^{2-}$) and associated reaction with surface absorbed hydrogen ($H^+ + e^- = H$) by the hydrogenase enzyme in SRB, a charge associated to the sulfate reduction reaction derived from the sulfide levels may be ascribed by Faradaic conversion.

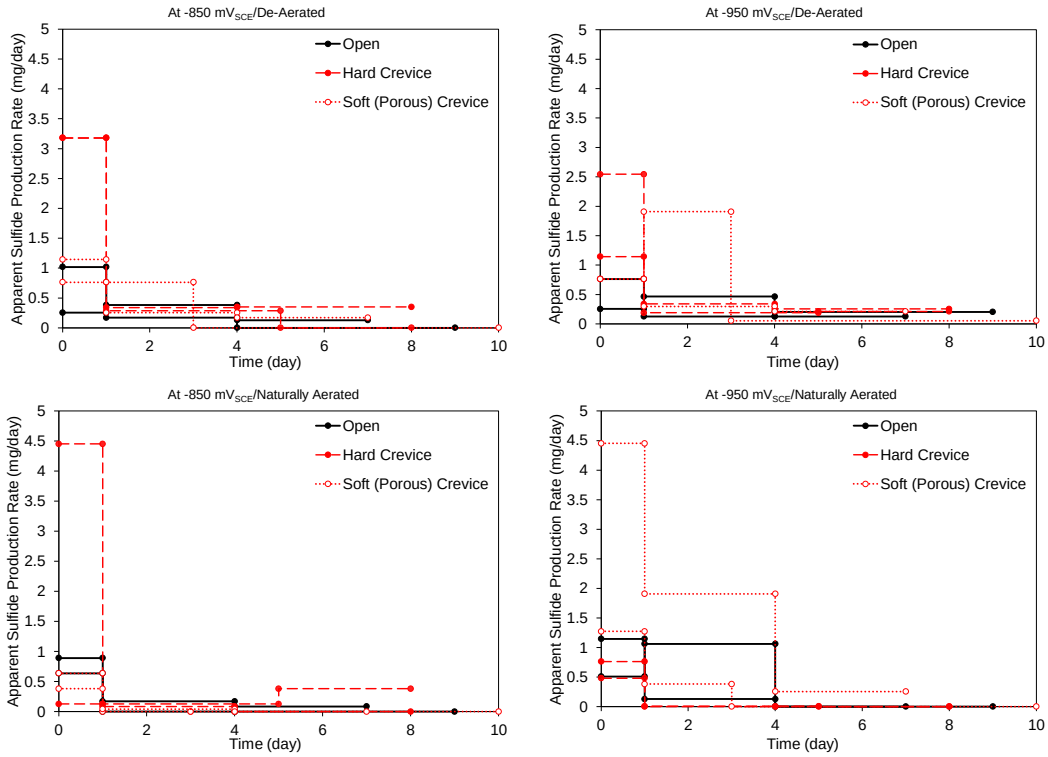

Figure 7.22. Apparent Sulfide Production Rate for Laboratory Inoculated Test Samples During Testing.

A comparison of cumulative charge associated with the sulfide production and the net cathodic reaction rates is shown in Figure 7.23. For the open surface and porous crevice geometries, a positive trend relating the net cathodic charge to charge relating to sulfate reduction was generally observed. Larger cumulative charge relating to sulfate reduction corresponded to the greater levels of cathodic polarization. This observation would indicate that sulfate reduction reactions due to SRB are a significant part of the electrochemical process for steel with cathodic polarization as part of CP. Also it was evident that activation polarization from oxygen and hydrogen reduction alone does not necessarily account for the larger currents associated with cathodic polarization with the presence of SRB. Large cathodic currents would typically indicate cathodic polarization of the steel to reduce the anodic corrosion currents. In contrast, in presence of SRB, greater sulfate reduction would be associated with charge transfer where the electron donor would normally come from the steel at open-circuit conditions. The larger cathodic rates for the steel in the cathodically polarized condition in presence of SRB

however would not necessarily mean enhanced general steel corrosion if the electron donor is ascribed to the CP source. However, heterogeneities at the steel surface due to a multitude of reasons including biofilm and marine fouling may create local steel anodic sites.

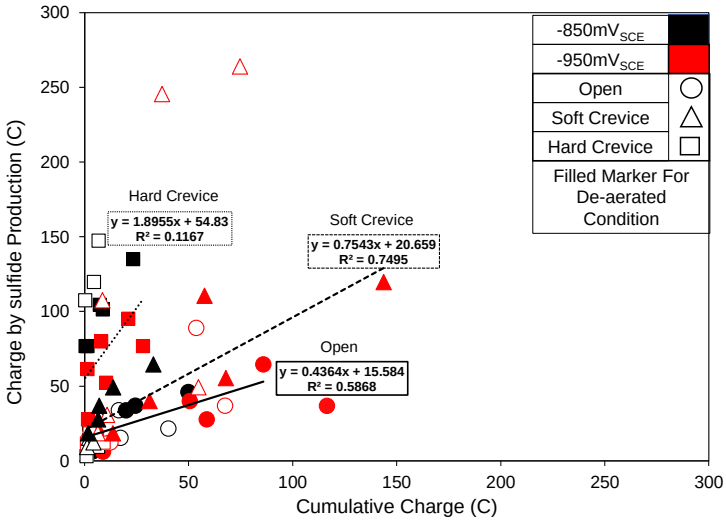

Figure 7.23. Cumulative Charge Associated with Sulfide Production and Net Cathodic Reaction Rates.

The observation of lower measured cathodic current relative to the charge associated with sulfide production for the hard crevice conditions indicate that occluded spaces may have non-uniform polarization and linear resistances along the length of the crevice that would reduce cathodic reactions overall. Presence of biofilm may contribute to this effect as well. Non-uniform cathodic polarization for CP systems would allow localized corrosion to occur. The porous crevice geometry used in the laboratory did not strongly exhibit this behavior reflecting the good ionic connectivity through the pores. Nevertheless, some portions of the steel in contact with the sponge may exhibit similar non-uniform cathodic polarization as well.

Figure 7.24 shows the visual surface appearance of the test samples immediately upon removal from the test solution. The test samples placed in inoculated solutions all showed thick accumulation of iron sulfide precipitates consistent with the chemical and microbiological analysis discussed previously. The surface of the steel samples with hard crevice geometries showed indication of corrosion coincident with the sulfide precipitation within the crevice regardless of the level of cathodic polarization. The steel samples with hard crevices in non-inoculated solutions also developed corrosion in the cathodic polarization test condition, but the corrosion there was exemplified by development of a red-orange corrosion product.

After removal of the crevice coverings and surface cleaning, it was evident that non-uniform corrosion could develop in crevice environments regardless of inoculation (figure 7.25). In particular, irregular surface oxidation relating to the porousness of the soft crevice was observed, and concentric surface oxidation developed radially outward from the hard crevice center opening. However, the localized corrosion appeared to be enhanced in inoculated

solutions. These observations were consistent with earlier discussion on non-uniform cathodic polarization under the hard and porous crevice.

Surface heterogeneities due to the biofilm may also contribute to localized crevice environments (even for samples with open surface geometries) which can accommodate non-uniform corrosion. As shown in Figure 7.25, the cathodically polarized steel samples with open geometries in inoculated solution had irregular and localized surface tarnishing compared to the smooth surfaces observed of the steel samples in non-inoculated solutions.

The trends in measured cathodic current and apparent sulfide production rate shown in Figure 23 were consistent with the observed surface corrosion characteristics for samples subjected to SRB. For the open surface geometry, sulfate reduction reactions and local cells under sulfide precipitates and biofilm create irregular and local tarnishing even though overall large cathodic reduction reactions including oxygen and hydrogen reduction can develop with the polarization provided by CP. For the porous crevice environments, the large cathodic currents and corresponding high level of sulfate reduction corresponded to the enhanced SRB development. Under the porous crevice, localized surface heterogeneities developed where the cathodic ennoblement mechanism related to MIC would allow anodic charge transfer processes of the steel, resulting in the sinuous irregular surface corrosion as observed in the Figure. Similar mechanisms would occur under the hard crevice, especially as non-uniform protection of the steel within the crevice could be exacerbated by high electrical resistances under the hard crevice. This would be consistent with the observed concentric geometry of the surface corrosion. Severe corrosion was not observed for the 7-10 day test exposure, but in consideration of SRB development, localized crevice environment, and non-uniform cathodic polarization, continued localized corrosion may be expected.

7.2.3.2. Anodic Corrosion Characteristics

The laboratory anodic potentiostatic polarization tests were made at -500 mV_{SCE}. The open-circuit potential in these environments were in the range -600 to -700 mV_{SCE} and thus the polarization would be expected to enhance anodic steel oxidation. The anodic polarization tests were made in part to identify corrosion behavior of crevice environments where local anodes may develop (such as under crevices due to biofouling for example) as well as the effect with the proliferation of SRB.

Chemical and microbiological testing (including COD, sulfide, and total bacteria population) indicated that SRB can still be prolific even in presence of conditions that form with anodic steel polarization (Figure 7.20 and 7.21, Table 7.7). Similar surface corrosion characteristics for steel with porous and hard crevice geometries as described for the cathodic polarization tests were observed in the anodic polarization tests (Figure 7.24 and 7.25). But, whereas the steel with open surface geometry were protected by the cathodic polarization in non-inoculated solutions, steel corrosion developed as expected in presence of the anodic polarization.

The development of irregular surface corrosion of the steel under the sulfide precipitates when subjected to cathodic polarization was also observed in presence of anodic polarization. However, the extent of the localized corrosion was greater in the latter. Anodic currents were expectedly high for all test conditions (Figure 7.18); however, the anodic currents that developed in the case for steel with open surface geometries in de-aerated inoculated solutions dropped with time of testing. This was thought to be related to a secondary effect of the thick level of iron sulfide precipitates that formed on the surface where the total area of the steel interface subjected to the anodic polarization would be smaller. However, under film corrosion can continue and significant localized steel consumption may be high despite of reduced overall anodic currents.

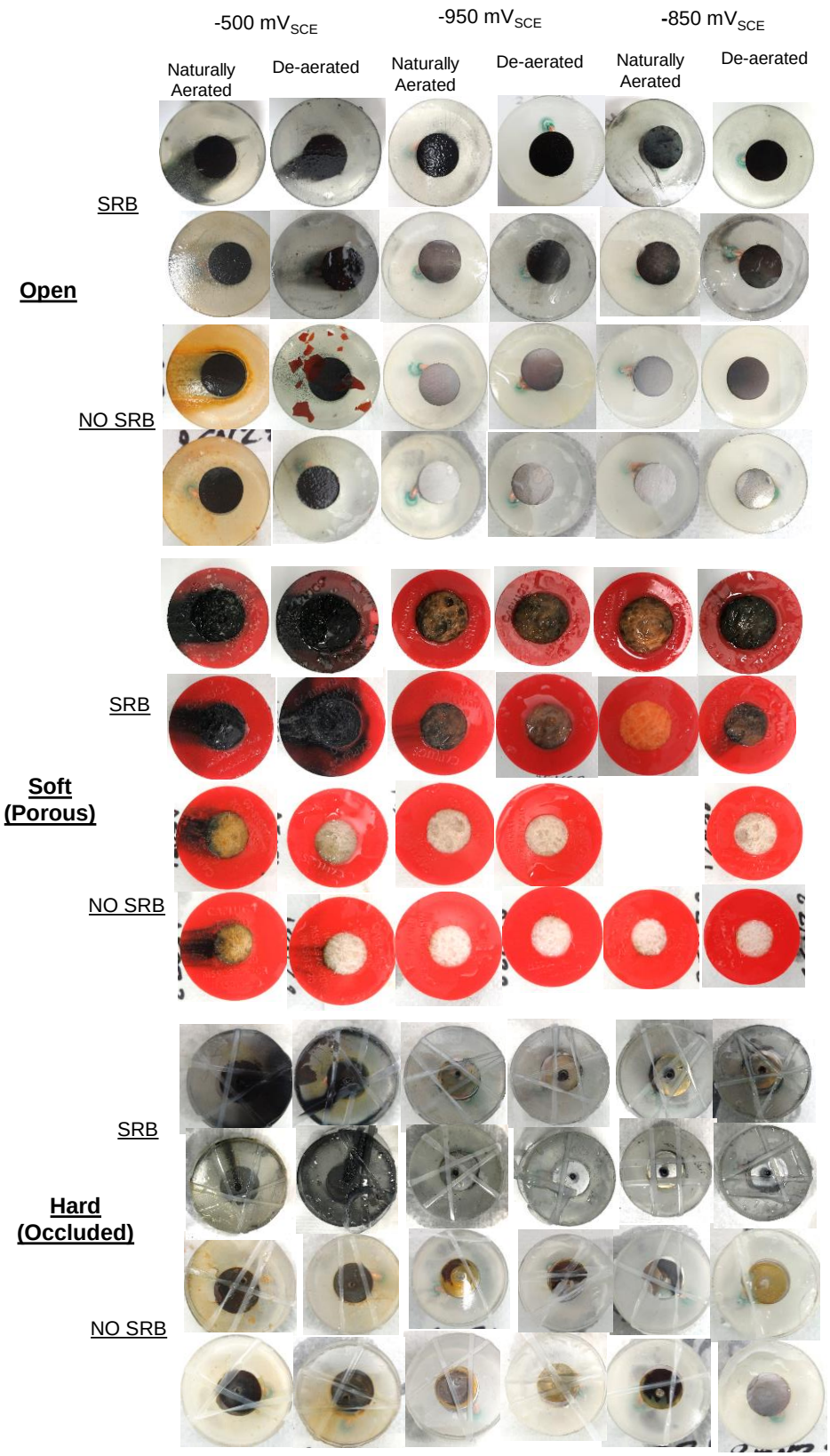

Figure 7.24. Laboratory Samples after Testing and Before Sample Cleaning.

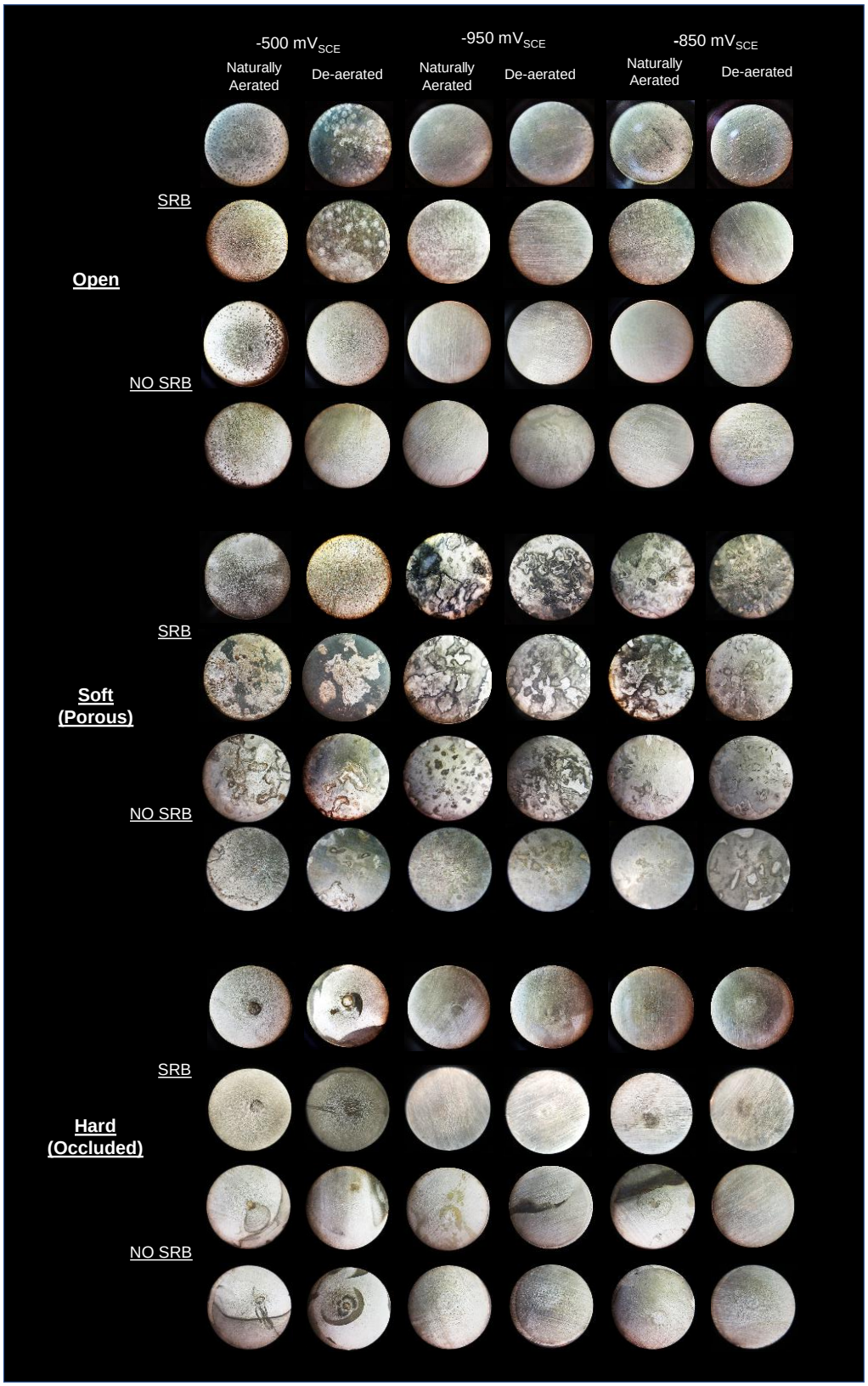

Figure 7.25. Laboratory Samples after Testing and After Sample Cleaning.

8. MICROBIALLY INFLUENCED DEGRADATION OF CONCRETE

8.1. Methodology

The testing included field exposure and laboratory experiments for uncoated plain and polyurea coated concrete specimens. Concrete cylinders of 3" diameter and ~7 ¾'' height were prepared with Portland cement, aggregate and water, with a water/cement ratio ~0.43. After casting, the concrete cylinders were immersed in lime water for around a year. After that time, concrete cylinders were cut in small discs of ~1'' thickness that were used for laboratory and field tests.

8.1.1. Laboratory Test Setup

Cyclic immersion tests were carried out in the laboratory condition. The intention was to expose concrete samples to simulated environments with the presence of sulfate reducing bacteria (SRB).

8.1.1.1 Test Setup

Figure 8.1 shows the experimental setup used. A Plexiglas cylinder of 3.14 in internal diameter was fixed with silicon to one face of the concrete samples. In that space (filled with test solution), an activated titanium wire (placed ~1 cm above the concrete surface) was used as a reference electrode. An activated titanium mesh was used as a counter electrode. On the other face (bottom) a wet sponge and an external steel plate (used as a temporary working electrode) were placed to facilitate testing of the concrete sample.

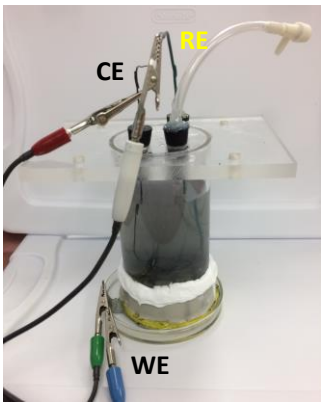

Figure 8.1. Test cell Setup for Immersion Test.
WE: working electrode, CE: counter electrode and RE: reference electrode.

SRB cultures were isolated from water samples collected from the case study site (SR-312 bridge, St. Augustine, Florida). For this purpose, the water samples were collected from 10 ft. depth and cultured within 24 hrs. One mL of river water was used for the initial culture in the modified Postgate B broth, and the bacteria was grown in the incubator at 30 °C. After an

incubation period of 3-5 days, bacteria growth was detected by the production of hydrogen sulfide and the subsequent blackening as a result of iron sulfide (FeS) precipitation.

Subsequent inoculations used serial dilutions from the initial source where one mL of the inoculated broth was initially injected into growth media (modified Postgate B) and placed in the incubator at 30^{o}C. From the growth media, test cells were inoculated with 5 mL of isolated species in 10 mL of modified Postgate B medium, used as a nutrient source to support bacteria activity.

The isolated organism inoculated in media was used in testing 3-4 days after incubation. The inoculation was done at day 1 (beginning of cycle 1) and the same at the beginning of each week (cycle) until the last cycle.

The SRB inoculated solution was ponded on the concrete samples. The solution contained up to 200 mL of deionized water and up to 10 mL of modified Postgate B. The growth media (modified Postgate B) was chosen based on NACE standard TM0194-2002. Modified Postgate B medium is an effective media for the isolation and growth of SRB cultures (Postgate, 1984). The pH of all solutions was~6.5-8. This pH range has been confirmed to be suitable for sustaining the growth of SRB.

8.1.1.2. Plain Concrete

The plain concrete surfaces were ground (72, 20 and 10 μm diamond discs) and polished (1 μm polishing cloth) to facilitate the observation of possible damage on the tested surfaces. The external surface of the concrete samples (excluding top and bottom circular areas) were covered with Sikadur epoxy to avoid water evaporation through the specimen edges during immersion test.

For the plain concrete specimens, both the SRB inoculum and the modified Postgate B solution were added to the deionized water at the beginning of every week (start of a new cycle). For the first three cycles the solution was not renewed with fresh deionized water and only SRB and the Postgate B were added. For subsequent cycles, the test solution was changed weekly.

During the test, the concrete samples were exposed to different conditions such as: bacteria inoculation, aeration, and surface condition (artificial crevice or not). Table 8.1 summarizes the 10 test conditions considered for the immersion test. Each case was identified by a combination of letters (related to the condition tested), followed by a number determining the replicate. For non-aerated (anoxic) test conditions, the solution was de-aerated by introducing high purity nitrogen gas for 5 minutes for two days. Also, two types of crevices (identified as B) were used, soft (S) and hard (H), simulating real sponges or barnacles, respectively, observed in the underwater pile bridges during site visits inspections. The soft crevice was made with an artificial sponge (~0.55 in thickness) that was placed in close contact to the concrete surface. The hard crevice was made with an acetate sheet of ~ 0.0031 in

thickness with a hole of ~1/16 in located in the center to facilitate the solution access to the surface. The hard crevice was placed in contact to the concrete surface for the time of the test. The non-inoculated cases did not contain the inoculated SRB broth (6 samples) and only deionized water and modified Postgate B was introduced. Every test condition with crevice (hard or soft) has a control case. Also, there are other two control samples (identified as C1 and C2) that represents the base case (no crevice, no bacteria inoculation, no Postgate B). For this condition concrete samples were only exposed to deionized water.

Table 8.1. Test Conditions for Plain Concrete Samples for Laboratory Testing.

Bacteria Inoculation	Aeration	Crevice and Type	Identification
SRB (S)	Aerated (O)	Hard Crevice (BH)	BHOS1, BHOS2
		Soft Crevice (BS)	BSOS1, BSOS2
		No crevice (control)	COS1, COS2
	Non-aerated (N)	Hard Crevice (BH)	BHNS1, BHNS2
		Soft Crevice (BS)	BSNS1, BSNS2
		No crevice (control)	CNS1, CNS2
No SRB (Z)	Aerated (O)	Hard Crevice (BH)	BHOZ1, BHOZ2
		Soft Crevice (BS)	BSOZ1, BSOZ2
		No crevice (control)	COZ1, COZ2
No SRB (Z)	Aerated (O)	No crevice (control case) [A]	C1, C2

A: Control experiment with deionized water as a test solution.

8.1.1.3. Polyurea-Coated Concrete

Polyurea was applied on the entire surface area of the coated concrete specimens and the polyurea surfaces were examined as-coated after the exposure period. For the coated concrete specimens, after one week, 5 mL of SRB bacteria was inoculated into the solution and also the Postgate B. Also, two control samples were tested in 150 mL deionized water, representing the base case without bacteria inoculation. Table 8.2 shows the sample identification for the lab coated concrete specimens.

Table 8.2. Test Conditions for Coated Concrete Samples for Laboratory Testing.

Samples Condition	Samples ID
Control (No SRB)	1 and 2
With SRB	3 and 4

8.1.2. Field Test Setup

The selection of the sites was done considering the presence of bacteria, availability of nutrients and other water chemistry parameters (temperature, pH) that may support bacteria

activity and consequently concrete degradation due to MID. Table A shows the characteristics of Florida environments selected, including water chemistry, bacteria activity and general parameters. One location (site 1) is the SR-312 bridge over Matanzas river (St. Augustine, FL) and the other two are the US-41 (site 2) and the US-301 (site 3) bridges over Alafia river (Tampa, FL.).

Underwater visual inspection of steel piles of SR-312 bridge during FDOT inspections and subsequent site visits confirmed the presence of heavy marine growth and macrofoulers attached to piles. The marine growth was mainly barnacles and sponges, more predominant in the tidal region. The other locations, US-41 and US-301 were also inspected and underwater video images reaffirmed the presence of macrofoulers attached to the submerged portions of concrete piles. A set of concrete samples were prepared for field testing. Table 8.3 shows samples identification and experimental test condition for each location.

Table 8.3. Field Sample Experimental Test Condition.

	Concrete Specimen. Plain, (Polyurea)		
Location	**ID**	**No. of samples**	**Distance BMG (ft.)**
Site I SR-312	C21, (C31)	1, (1)	~ 2
	C22, (C32)	1, (1)	~ 3
	C23, (C33)	1, (1)	~ 4
	C24, C25, (C34, C35)	2, (2)	~ 5
	C26, (C36)	1, (1)	~ 6
	C27, (C37)	1, (1)	~ 7
	C28, (C38)	1, (1)	~ 8
Site II US-41	E11, (E21)	1, (1)	~ -0.5
	E12, (E22)	1, (1)	~ 0.5
	E13, E14, (E23, E24)	2, (2)	~ 1
	E15, E16, (E25, E26)	2, (2)	~ 2
	E17, (E27)	1, (1)	~ 2.5
	E18, (E28)	1, (1)	~ 3
Site III US-301	Q11	1, (0)	~ 0.5
	Q12, Q13	2, (0)	~ 1
	Q14, Q15, (Q24, Q25)	2, (2)	~ 2
	Q16, (Q26)	1, (1)	~ 2.5
	Q17, (Q27)	1, (1)	~ 3

ID: Identification, BMG: Below marine growth

Concrete samples were installed on a partly submerged test rack constructed from a polypropylene sheet attached to an aluminum frame which was secured to a bridge pier (Figure 8.2). The test rack was positioned at a certain depth below (SR-312 site: ~ 2 ft. and US-301 site: ~ 0.5 ft.) or above (US-41 site: 0.5 ft.) the marine growth line where the samples were at the water line or above during typical low tide levels.

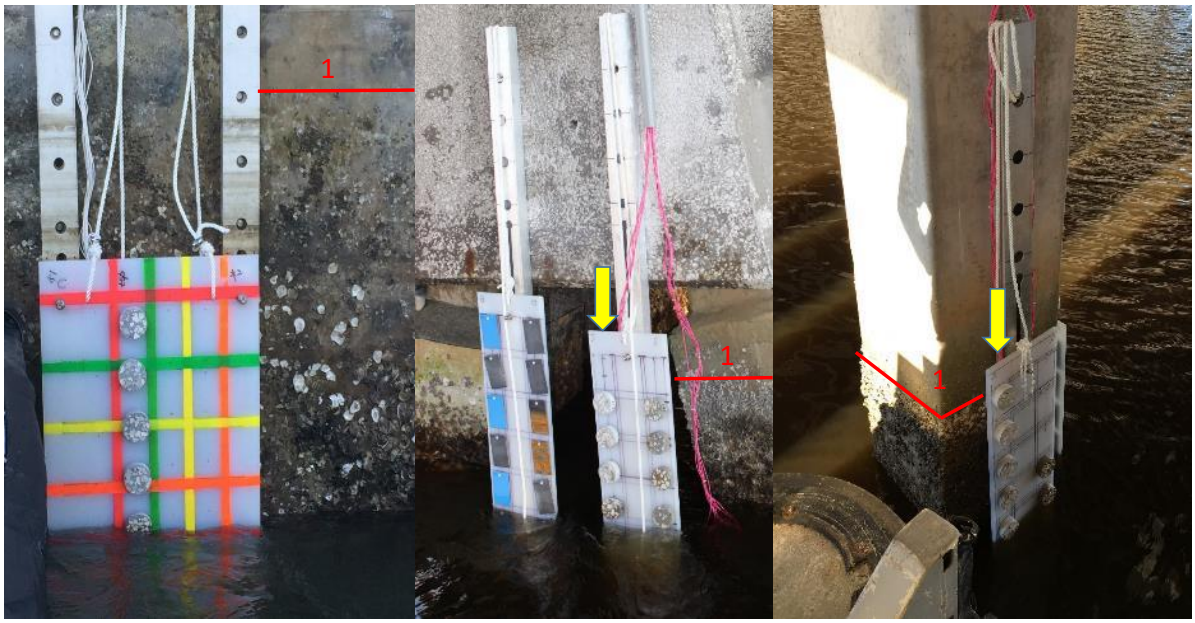

Figure 8.2. Concrete Sample Setup at Field Conditions.
Yellow arrows indicate where the concrete samples were located and the red straight lines indicate the marine growth level.

8.1.3. Experimental Measurements

8.1.3.1. Laboratory Samples

A three-electrode arrangement was used for EIS measurements, consisting of a titanium wire (reference electrode), a titanium mesh (counter electrode) and a steel sheet (working electrode). Impedance measurements were carried out with time at the open circuit potential (OCP) condition with 10 mV potential perturbation in a frequency range from 1MHz to 1Hz.

COD and sulfide content were measured the day after bacteria inoculation. Both determinations were repeated every cycle and at the end of the test. The sulfide content allows quantifying the activity of SRB bacteria due to the formation of iron sulfide (black color). The COD may also give an indirect indication of the SRB activity, since COD refers to the oxygen demand necessary to oxidize the organic matter in the media and SRB may reduce sulfate into sulfide ions through the oxidation of organic matter. A colorimetric method was used for determining COD and a hydrogen sulfide color disc test kit was used for the sulfide estimation.

The SRB sessile test was done at the end of the experiment following the biotechnology solutions (BTS) sessile test kit instructions. Once the experiment was finished, the test solution inside the cell was collected and the still wet concrete surface was swabbed with a sterile cotton stick to collect the sessile bacteria samples for the SRB test.

Conductivity and pH measurements of the test solution were recorded with time. Also, the pH of the samples surface was measured at the end of the immersion test with an indicator paper, after removing the electrolyte of the cell. For those samples with artificial crevices, the surface pH was measured once the crevice was removed to be able to reach the surface. Also, in-situ bulk resistivity measurements of the concrete samples were carried out with time by the two point and the four point method (Figure 8.3).

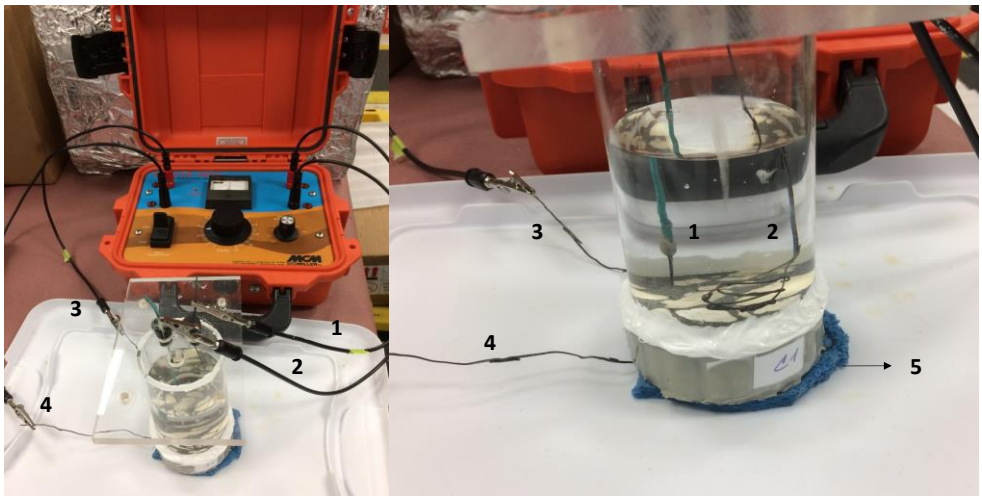

Figure 8.3. In-situ Resistivity Measurements Setup.
1: Titanium rod reference electrode, 2: titanium mesh counter electrode, 3, 4: titanium mesh as counter and reference electrodes and 5: wet sponge.

Visual photo-documentation of the test solution with time was done to confirm the formation of iron sulfide due to the SRB presence, easily detected due to its black color. Hence, the darkness of the samples with time provide valuable information about the bacteria activity. Also, images with a Spencer stereo microscope were taken before and after testing with the intention to detect possible concrete deterioration.

8.1.3.2. Field Samples

Photo-documentation of the field samples was carried out in order to capture possible changes of specimen surface condition with time.

The biological activity reaction test (BART) was conducted with time after field installation. BART kits were used to monitor the population and the activity of the four common MIC/MID related bacteria (SRB, IRB, SLYM and APB) on the concrete sample surface below the layers of marine growth. The test racks were temporarily removed from the bridge pier to

allow closer onsite inspection. The surface fouling was left intact for the photo-documentation but marine growth was removed on small portions (~1 in^2) of the samples where swabs were collected for the microbiological analyses. The test racks were reset on the bridge pier after sample analysis but were decommissioned at the end of field test. The test samples were then immersed in sealed containers containing river water for transport back to the laboratory.

The same EIS setup used for laboratory samples was used for field samples too, with the exception that two Plexiglas plates, one at the bottom and one at the top, fixed the sample with 4 screws, as can be seen in Figure 8.4. Also, samples were immersed in the collected water for each location.

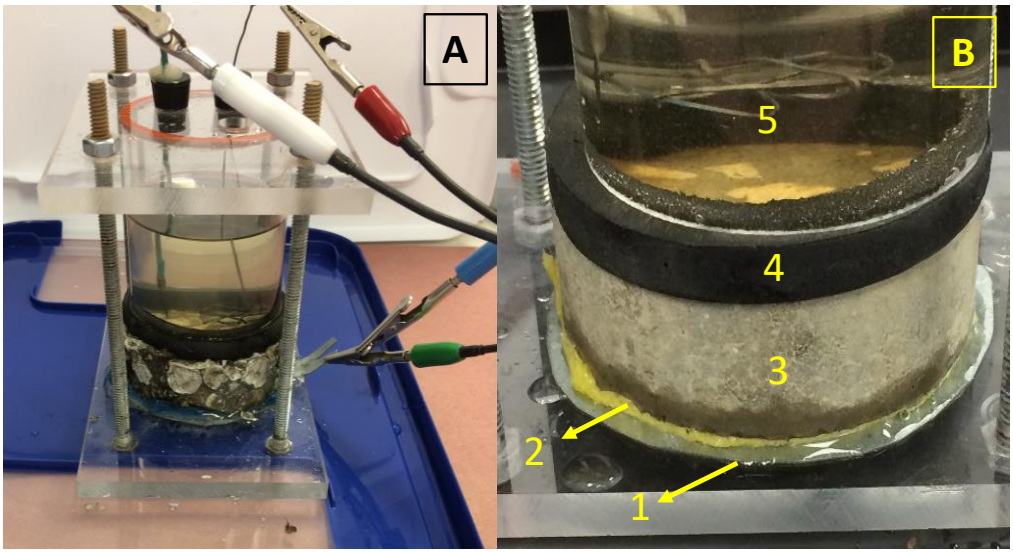

Figure 8.4. EIS Setup for Field Samples. A: Frontal view and B: Zoom of picture 1: steel plate, 2: wet sponge, 3: concrete sample, 4: rubber gasket and 5: plexyglass cylinder.

The objective was to study the dielectric properties of the concrete and the polyurea coating. Hence, impedance measurements were performed from 1MHz to 1Hz, at the open circuit potential (OCP) condition with 10 mV perturbation. Bulk resistivity measurements of the plain concrete specimens, before and after the test were carried out. The same test setup used for lab samples was also employed here.

8.2. Laboratory Samples Results for Plain Concrete Cylinders

8.2.1. Concrete Visual Inspection Results

Figure 8.5 shows the surface appearance of the concrete samples before and after the immersion test taken with the stereo microscope. In general, presence of white particles on the tested concrete surfaces can be seen. Deposition of the white particles was not observed on two test cases: the hard crevice cases (non-inoculated (BHOZ1,2) and inoculated (BHOS1,2) cases) with aeration.

Concrete degradation was also observed for some tested cases (inoculated and non-inoculated with bacteria), characterized by a rougher surface with certain cement paste lost. This was more evident for control cases (COS1, COS2, CNS1, and CNS2).

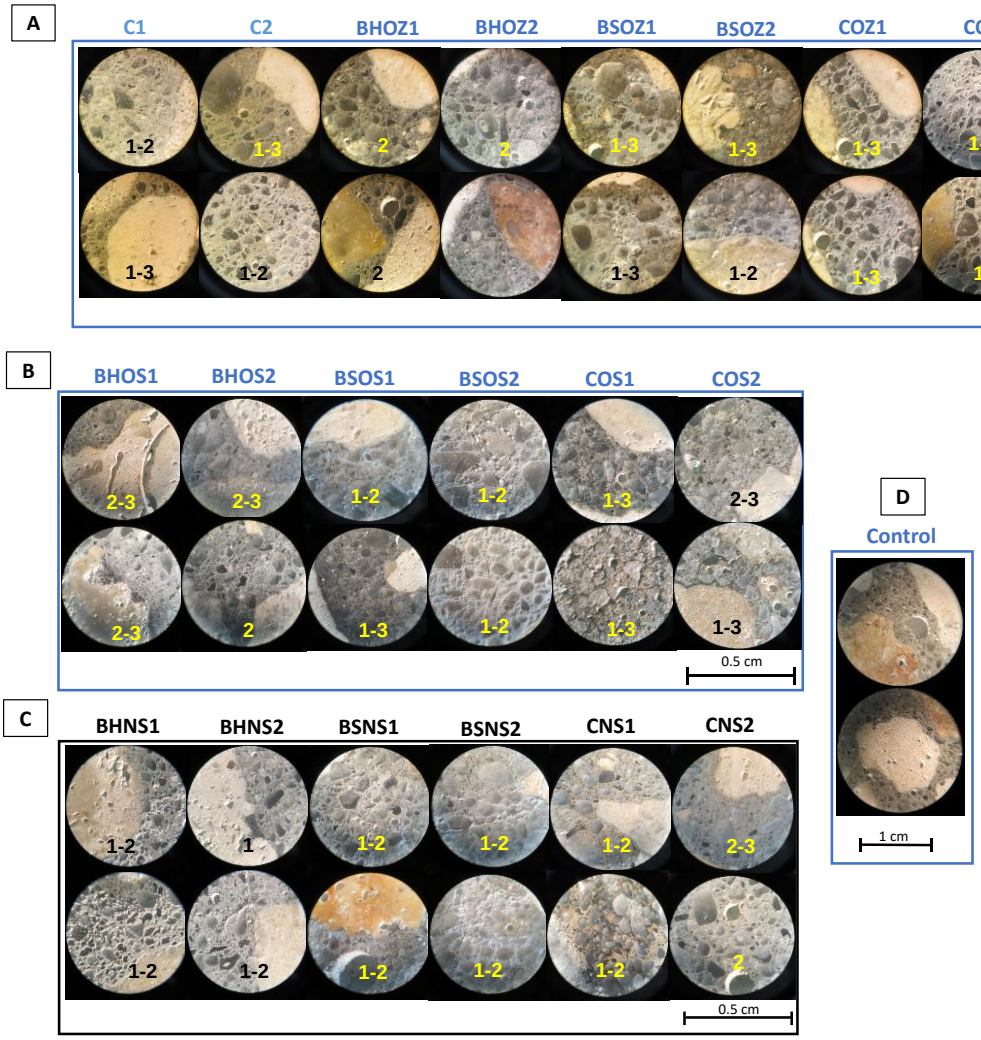

Figure 8.5. Concrete Samples Surface Appearance After Immersion Test.
A: Non-inoculated/Aerated cases, B: Inoculated/Aerated cases, C: Inoculated/Non-Aerated cases and D: control sample/aerated case. 1: White powder, 2: Rough surface, 3: color change in boundary regions (between cement paste and aggregates)

8.2.2. Iron Sulfide

As referred in the experimental section, the SRB bacteria activity was monitored with time by observation of solution darkening related to the formation of iron sulfide.

Figures 8.6 and 8.7 depict solution coloration with time for all the tested cases, inoculated and non-inoculated. The non-inoculated/aerated cases presented in Figure 8.6 (A and B) show clear non-turbid test solution. However, those sample cases where the bacteria was inoculated

depict a black color due to the presence of SRB promoting the formation of iron sulfide (Figure 8.7).

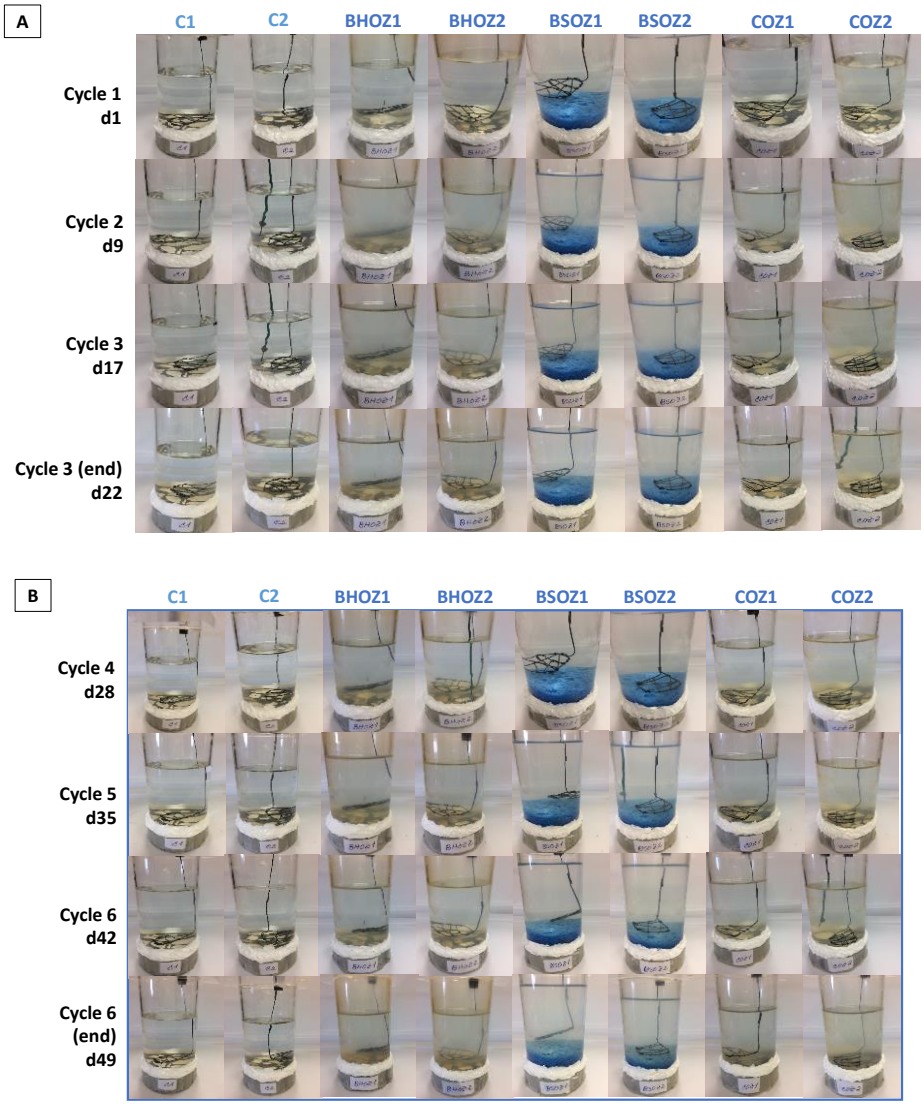

Figure 8.6. Color Change of the Test Solution for the Non-inoculated Cases with Time. A: Cycles 1-3 and B: Cycles 4-6.

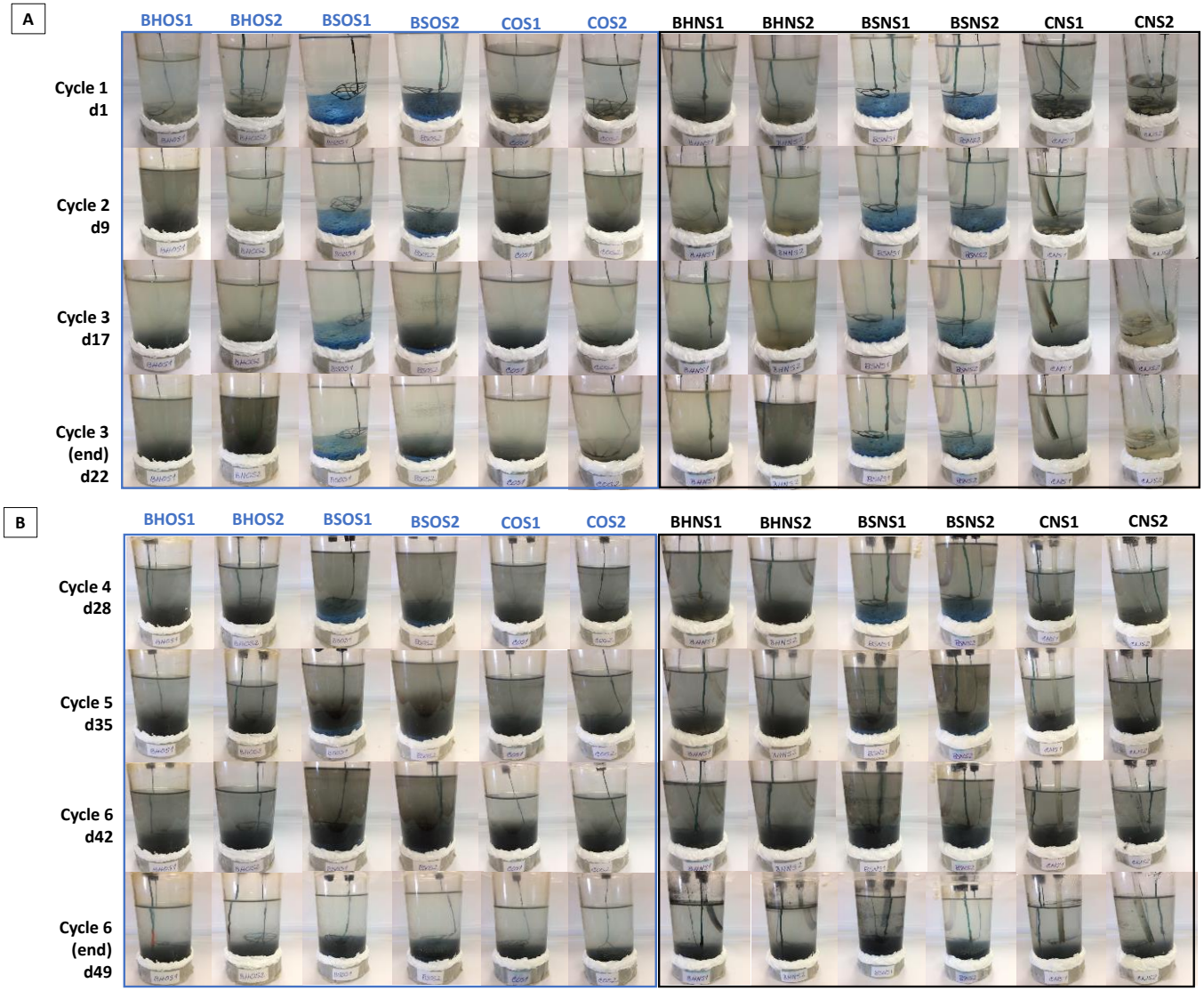

Figure 8.7. Color Change of the Test Solution for the Inoculated Cases with Time.
A: Cycles 1-3 and B: Cycles 4-6.

In general, the solution blackening was stronger after cycle 4 to the end of the experiment. This could be related to two factors: the freshness of the electrolyte and the extent of serial dilutions of the inoculated bacteria source. As mentioned in the experimental section, the electrolyte was not renewed with fresh deionized water during the first three cycles. Only bacteria and modified Postgate B were added at the beginning of every week. During cycles 4-6, the test solution was renewed weekly. So, it seems that the freshness of the test solution may have a beneficial effect in the bacteria activity. The other factor could be that the bacteria used during the first three cycles was from a longer series of serial dilutions. For subsequent cycles, a new series of serial dilutions were made from a renewed stock of river water (obtained between cycles 3 and 4).

According to the blackness of the samples, it can be seen that in general, aerated and non-aerated control cases (COS, CNS), and aerated and non-aerated hard crevice cases (BHO and BHN) were more active than the rest.

8.2.3. Bacteria Activity Results

Figure 8.8 and Table 8.4 show the SRB test results for bacteria count performed at the end of the immersion test.

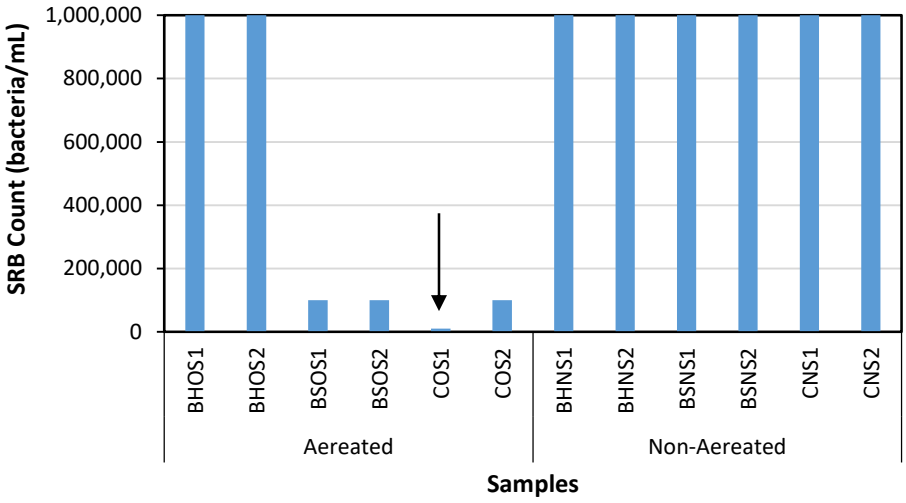

Figure 8.8. SRB Test Results for Enumeration Sessile Bacteria.
Arrow indicates small SRB count.

Table 8.4. SRB Test Results for Bacteria Enumeration.

Case	Samples	Positive Vials/Tested Vials	SRB Count (bacteria/mL)
Aerated	BHOS1	6/6	1,000,000
	BHOS2	6/6	1,000,000
	BSOS1	5/6	100,000
	BSOS2	5/6	100,000
	COS1	4/6	10,000
	COS2	5/6	100,000
Non-Aerated	BHNS1	6/6	1,000,000
	BHNS2	6/6	1,000,000
	BSNS1	6/6	1,000,000
	BSNS2	6/6	1,000,000
	CNS1	6/6	1,000,000
	CNS2	6/6	1,000,000

Presence of SRB bacteria was detected in all of the inoculated cases under study at the end of the test. The highest SRB counts (1,000,000 bacteria/mL) were obtained for the inoculated/non-aerated cases (BHNS1-2, BSNS1-2, and CNS1-2) and also for the inoculated /aerated cases with hard crevice (BHOS1-2). Lower SRB counts were observed for the inoculated/aerated cases with soft crevice (BSOS1-2) and the control case (COS1-2), with 100,000 bacteria/mL and 10,000 bacteria/mL, respectively.

As stated previously in the experimental section, COD is the demand of oxygen necessary to oxidize the organic matter present in the media and SRB bacteria may reduce sulfate ions to sulfide ions through the oxidation of organic matter (heterotrophic reduction, see reaction 2). Hence, SRB activity can be associated with the oxidation of organic compounds (such as in waste water systems) and changes in COD with time could ideally provide some indication on media conditions due to SRB population changes.

Figure 8.9 shows the COD trend with time for the inoculated and non-inoculated cases under study. After SRB inoculation, a drop in COD may indicate the oxidation of vestigial organic compounds as a food source for SRB. Deviation from this drop may indicate reduced SRB activity associated with biological sulfate reduction.

The highest COD values were for the inoculated cases (Figure8.9A), with values ranging from 200 to 800. Among them, the soft crevice cases (aerated and de-aerated) and the control cases (for the de-aerated condition) showed the highest magnitudes (Figure8.9A). On the other hand, the non-inoculated cases depicted COD values lower than 200, with the exception of some spikes (between 200 and 400) for the soft crevice (BSOZ1, 2) and control (C1, C2) cases. Low COD values were measured for the hard crevice cases. Environmental conditions due to the crevice may be important.

As a general trend, COD increased for the first three cycles, which could be related with the organic matter accumulation because the electrolyte was not refreshed with new deionized water during these three weeks (cycles 1-3). The COD increment does not necessarily mean that SRB bacteria activity is low, because there could be a build-up of organic matter. Also, sulfide production could lead to increase in COD.

At the beginning of cycle 4 there was a drop in COD values, regarding previous cycles, associated with the use of fresh electrolyte. Later, COD values showed a slight increment with time, with some exceptions (i.e. CNS1, 2). Again, the behavior observed doesn't give a clear indication of SRB activity other than that the increase in COD would give indication of conditions that would support SRB.

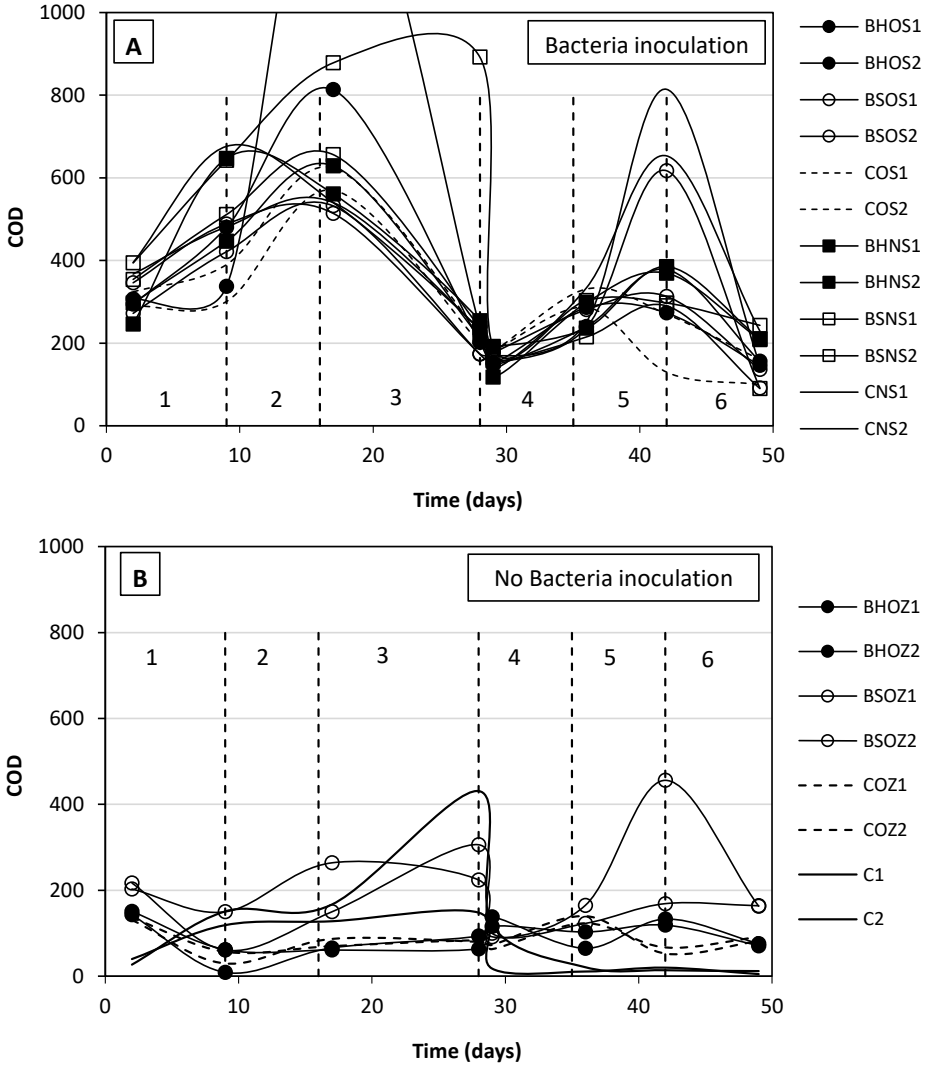

Figure 8.9. COD for Bacteria Inoculation (A) and No Bacteria Inoculation (B) Cases with Time. Dashed-line represents the end of each cycle. On the day of inoculation, COD was measured after the inoculation event.

The sulfide content gives information about the activity of SRB bacteria that produce hydrogen sulfide due to the reduction of sulfate. Figure 8.10 shows the level of sulfide production in the test solutions (only for the bacteria inoculated cases). In general, most of the measurements showed a sulfide content below 1 mg/L, except some peaks detected with values as high as 2 mg/L and 3 mg/L for the control aerated case (COS1,2) and the soft crevice non-aerated case (BSNS1,2), respectively. It is highlighted that the hard crevice cases (aerated and non-aerated) presented higher sulfide production than the rest of the tested cases.

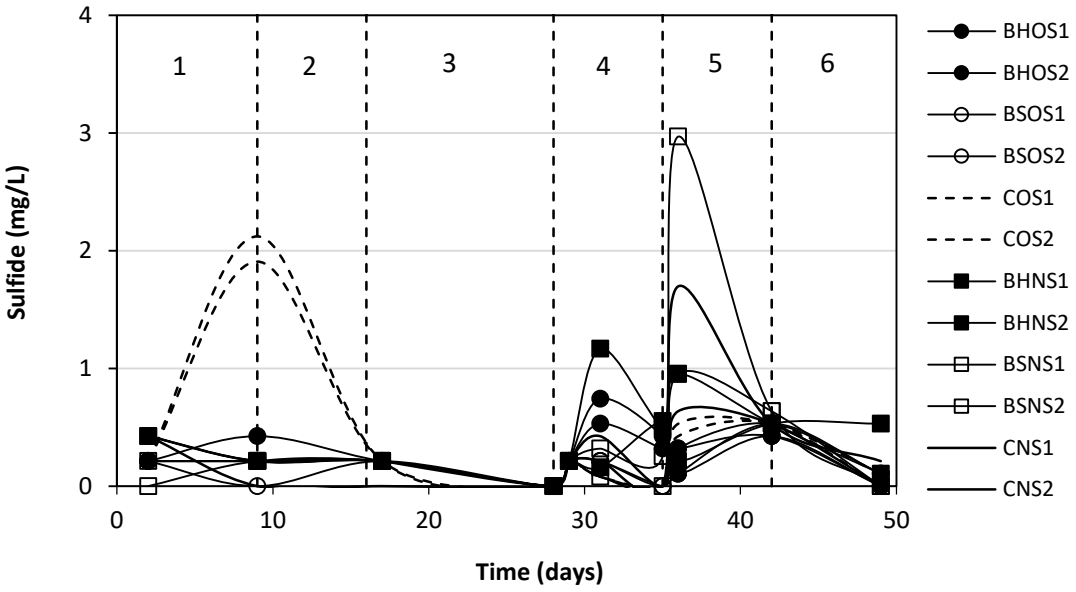

Figure 8.10. Sulfide Content with Time for the Bacteria Inoculated Cases. Dashed-line represents the end of each cycle.

8.2.4. Conductivity and pH Results

Conductivity and pH measurements of the electrolyte for all the tested cases are shown in Figures 8.11. The pH values fluctuated after inoculation events and ranged from 6 to 9 for all the tested cases (inoculated and non-inoculated with or without aeration). These pH values can support SRB growth and activity (Eštokov et al., 2012).

Table 8.5 below lists the surface pH of concrete samples exposed to different exposure conditions (aeration, bacteria inoculation, and crevice). The highest surface pH values (around 12) were obtained for concrete samples with hard crevice case, regardless of bacteria inoculation and aeration condition. The high pH value is related to the occluded crevice space on the sample surface (only a small hole in the center was present), limiting the electrolyte access to the surface and consequently preventing dilution with the bulk solution. Those samples with soft crevices (porous surface) and some of the control samples (for bacteria inoculation and aeration conditions) reached lower values from 8 to 10. The lowest surface pH values ~ 7 were observed for the control samples C1 and C2 (only exposed to deionized water

and aeration condition) and the control samples CNS1 and CNS2 (exposed to bacteria and no aeration condition).

Table 8.5. Surface pH Values for Concrete Samples at the End of Immersion Test.

Sample Case		**pH values**					
Bacteria Inoculation	*Aerated*	***BHOS1***	***BHOS2***	***BSOS1***	***BSOS2***	***COS1***	***COS2***
		12	12	9	9	8	8
	Non-aerated	***BHNS1***	***BHNS2***	***BSNS1***	***BSNS2***	***CNS1***	***CNS2***
		12	12	8	9	7	7
No Bacteria Inoculation	*Aerated*	***BHOZ1***	***BHOZ2***	***BSOZ1***	***BSOZ2***	***COZ1***	***COZ2***
		12	12	10	9	9	9
Control	*Aerated*	***C1***	***C2***	-	-	-	-
		7	7	-	-	-	-

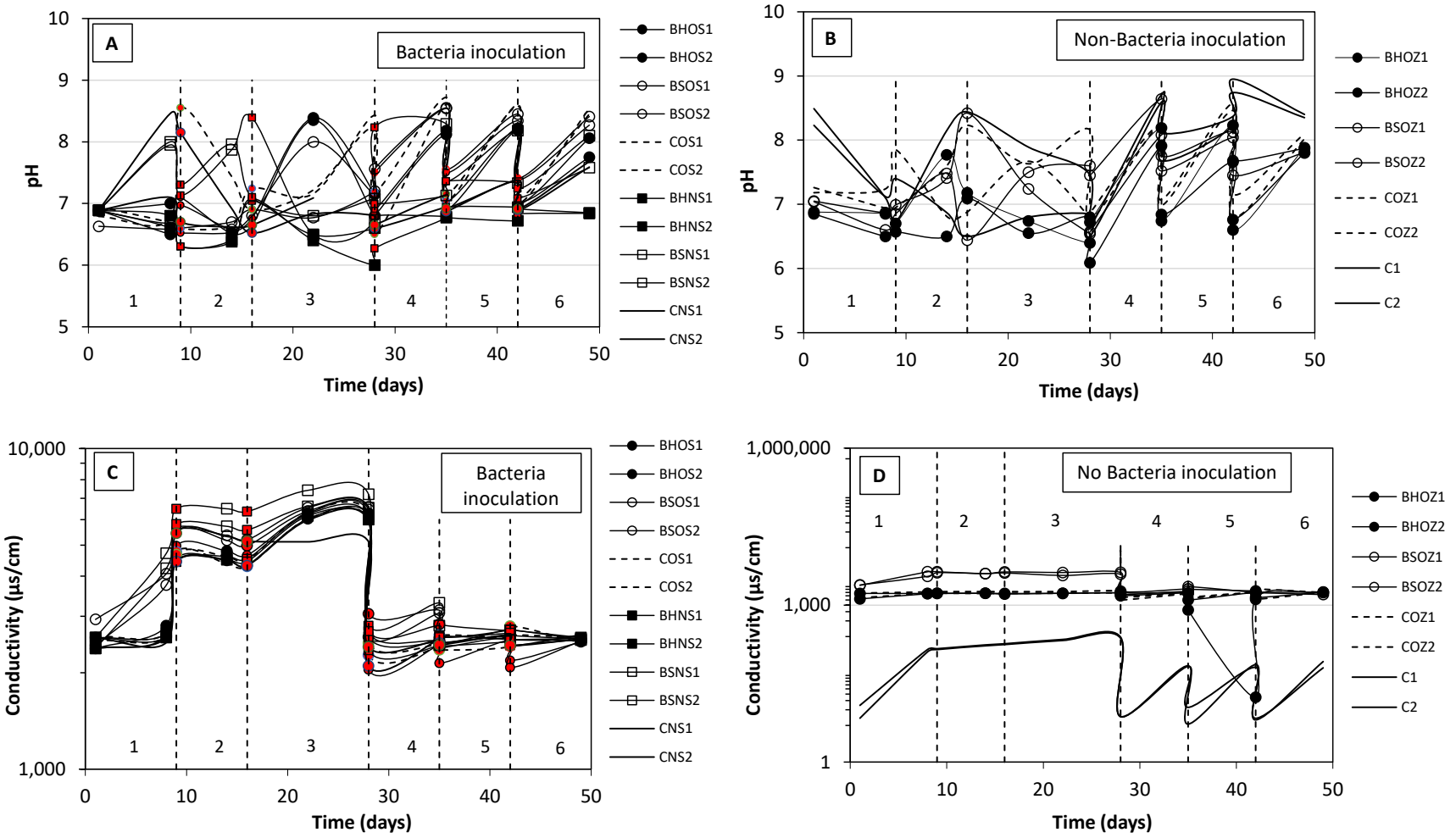

Figure 8.11. pH (A-B) and Conductivity (C-D) Values with Time for the Electrolyte Used During Immersion Test. Red symbols represent measurement made after inoculation and dashed line represents end of each cycle.

The conductivity of the inoculated cases (Figure 11) shows an increment during cycles 1-3 of the experiment, with values in the range of 2.10^3 to 7.10^3 µS/cm. Later, from cycles 4 to 6 the conductivity dropped to lower values from 2.10^3 to 3.10^3 µS/cm. The behavior observed could be related to the fact that during cycles 1-3 the test solutions were not renewed every week and only bacteria inoculation and modified Postgate B were added every week to the old solution. Hence, it's clear that the addition of nutrients (Postgate B) every week for the bacteria growing, which has ions in the composition (i.e. Na^+, K^+, Cl^-, etc.) to the media, supported the conductivity increment due to ions build up in the test solution. This effect was much less for cycles 4-6 where the test solution was weekly renewed with fresh deionized water, fresh bacteria and modified Postgate B.

The leaching of ionic species (OH^- and Ca^{2+}) from the cement will increase the pH of the external test solution (OH- ions effect). The expected leached calcium ions can react with the dissolved CO_2 from the atmosphere and precipitate calcium carbonate. Leaching will also affect the conductivity, as can be seen in the base case (C1, C2), where the samples were exposed to deionized water. An increment of conductivity during the first three cycles and then a drop at cycle 4 when the electrolyte was renewed was evident. This cycle of a conductivity increase followed by a drop after solution renewal continued to the end for cycles 5 and 6. For the other test cases, with Postgate B addition, the conductivity values were higher and therefore the leaching effect was not easily observable.

8.2.5. Resistivity Measurement Results

Concrete bulk resistivity is expected to be lower for concrete saturated with water. For the as-received condition, samples were immersed in limewater for around a year after initial casting and later removed and cut for testing. Prior to cutting, the sides of the samples were sealed with epoxy to minimize moisture loss. After cutting, the sample top axial surface was ground and polished. Sample preparation took ~1-2 weeks and the samples were only kept in ambient laboratory conditions prior to test cell assembly where some drying likely occurred. The samples were subsequently exposed to cyclic immersion test for 50 days where only the top axial surface of the concrete cylinder was directly exposed to the water.

Figure 8.12 shows the 2-point bulk resistivity measurements for concrete samples prior to test cell assembly as well as after cell deconstruction. The as-received resistivity measurements were made after lime water immersion, cutting, and grinding. The after-test resistivity measurements were made after some level of ambient drying after cell deconstruction. Due to the possible inconsistent level of moisture presence due to surface drying at the times of measurements, the before and after comparison of bulk resistivity cannot be easily parsed. The overall larger resistivity values observed after testing related to sample surface drying cannot be ruled out. The initial values (after prolonged immersion in lime water) showed a range between 0.5 and $2.5.10^5$ ohm-cm. After-test values were as high as 4.10^5 ohm-cm.

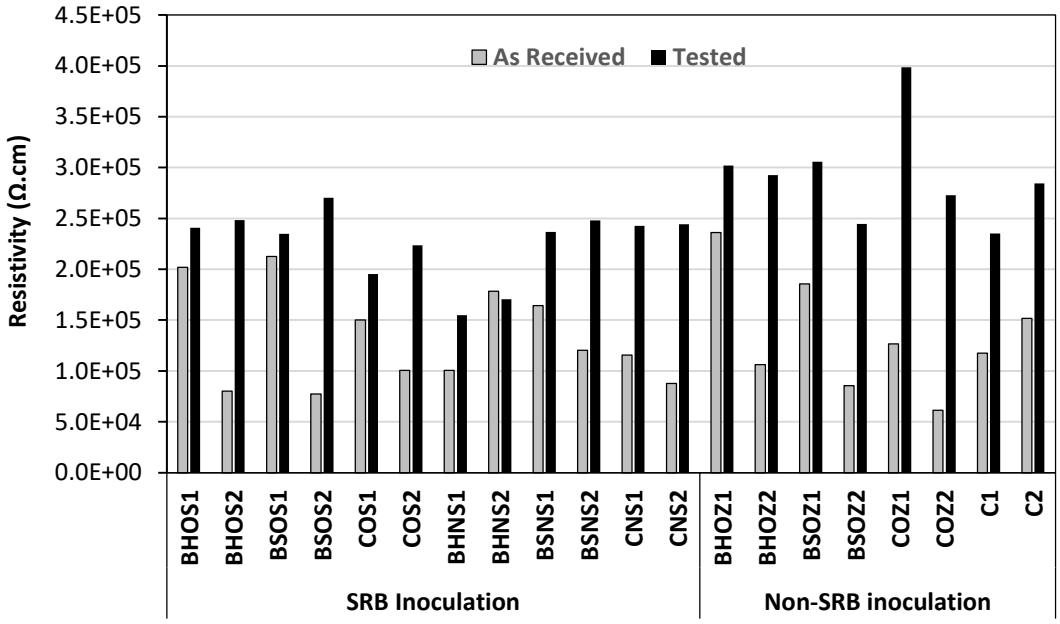

Figure 8.2. Bulk Resistivity for all The Tested Cases Before and After Immersion Test.

Figure 8.13 shows in-situ 3-point measurements made during the course of testing. With the exception of the samples with the presence of the hard crevice, the resistivity values were similar to the values obtained for the samples in the as-received condition. The similar resistivity values when compared from the as-received condition in Figure 8.12 to the near constant values with exposure time shown in Figure 8.13 would indicate that any concrete surface changes or degradation due to the test exposure (as shown earlier) could not be distinctly identified by bulk resistivity measurements. For those samples with hard crevices, regardless of the presence of bacteria in the media, the higher values may be due to the poor ionic path through the crevice between the test electrodes and the decrease in value within a few days indicating subsequent moisture ingress into the crevice. Figure 8.14 summarizes the results comparing values from the beginning and end of the test.

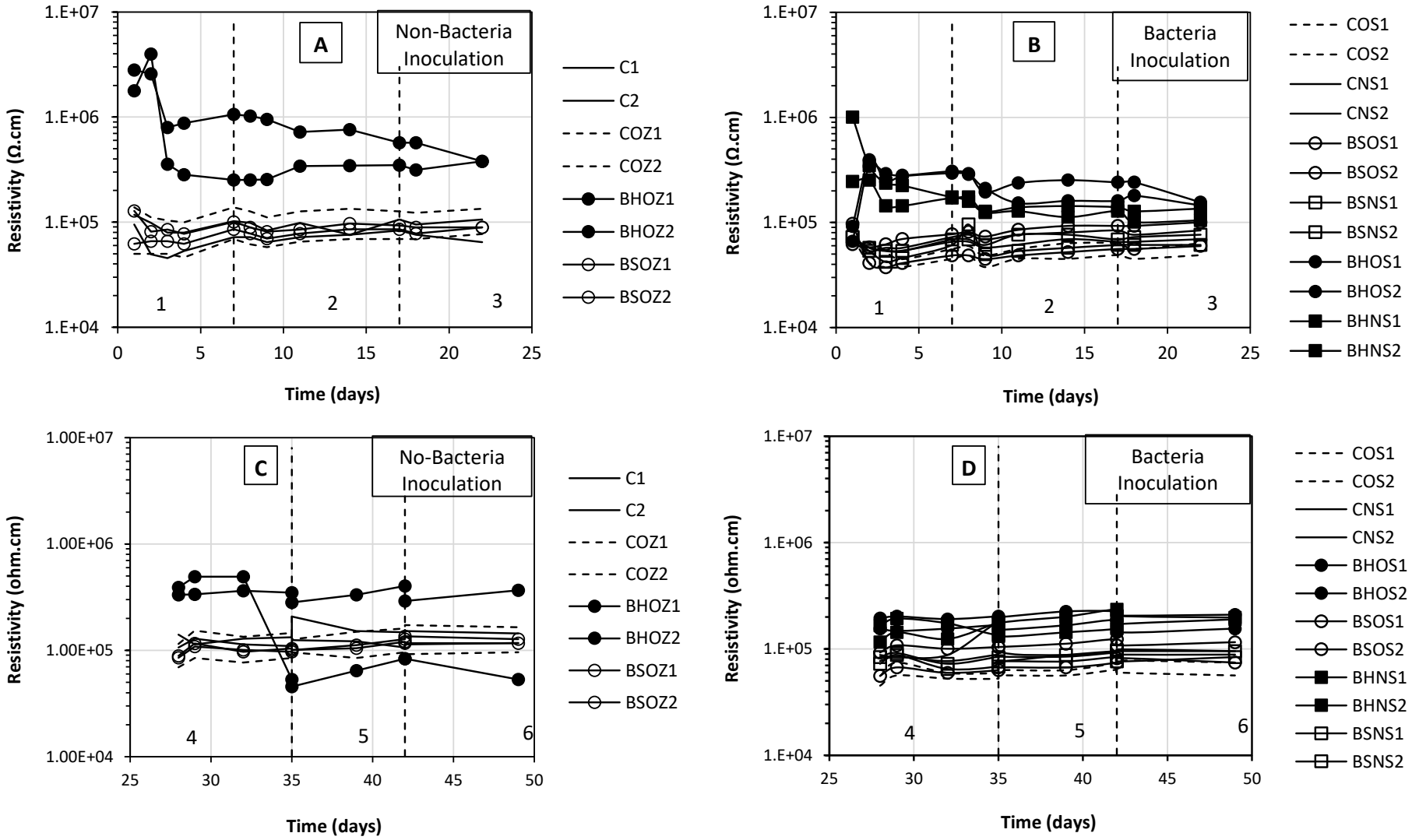

Figure 8.13. In-situ Resistivity Measurements During the Cyclic Experiment. A-B: Cycles 1-3 and C-D: Cycles 4-6. Dashed-line represents the end of each cycle.

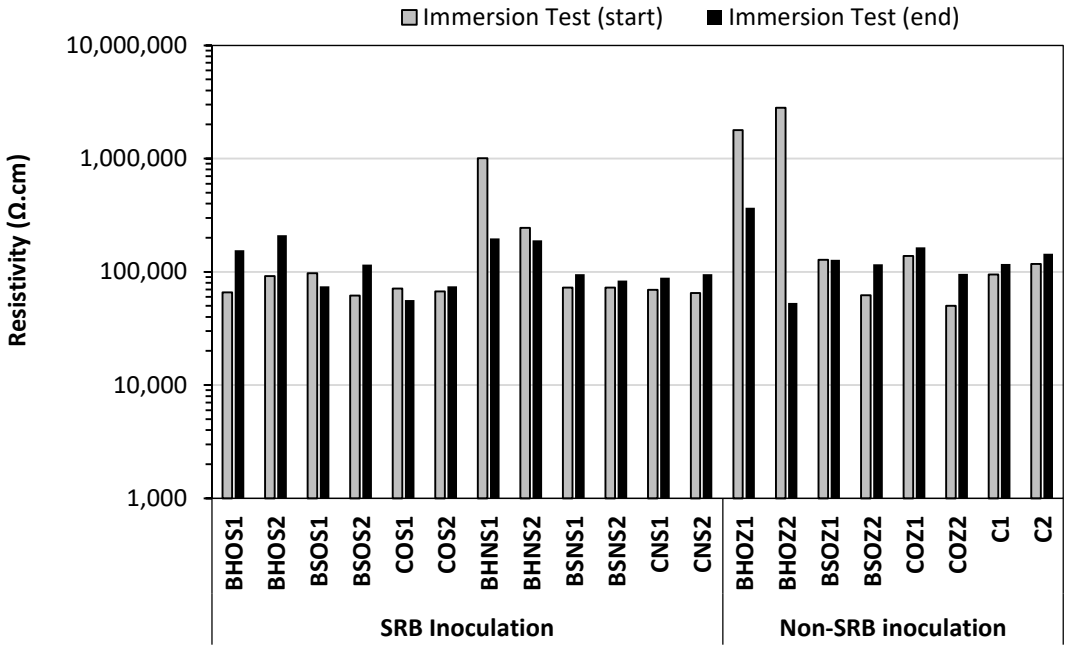

Figure 8.3. In-situ Resistivity Measurements of Laboratory Samples Exposed to a Simulated Environment with and without SRB.

8.2.6. Impedance Results

Figure 8.15 shows the comparative Bode plots for the control case sample at selected exposure times.

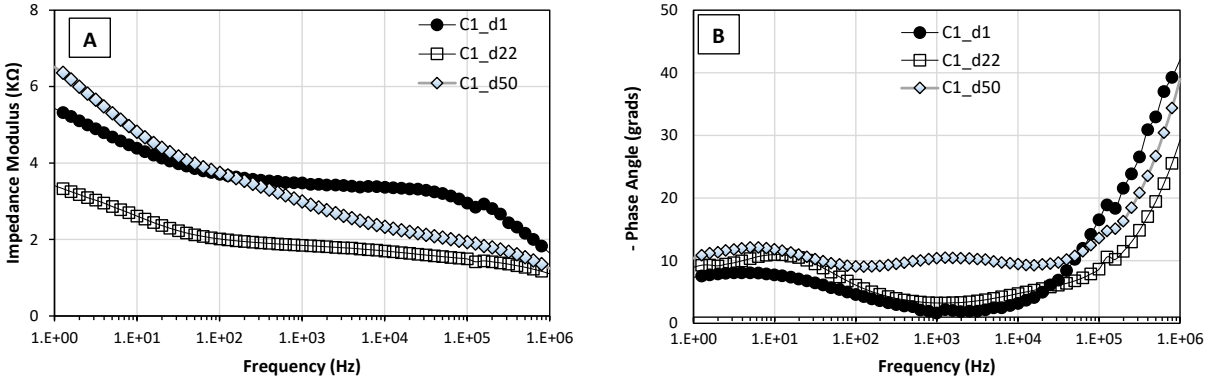

Figure 8.4. Comparative Bode Plots of C1 at Selected Immersion Times. A: Impedance modulus, B: Phase angle.

The impedance modulus at 1 Hz fluctuated during the 50 days immersion test (Figure 15A).These values may in part represent impedance associated with steel interfacial characteristics. At the higher frequencies (i.e., at the high frequency arrest observed ~10-100kHz), there was a general decrease in total impedance after initial testing at day 1. The Bode plots typically show multiple time constants and high frequency behavior was posed to be related to the concrete material and pore characteristics.

Figure 8.16 shows the comparative Bode plots for the inoculated/aerated cases. Most of the samples tested show impedance modulus lower than 5 kΩ from day 1 to the end of the test. A slight decrease of the impedance modulus (around 1 order) with time was evident. The sample containing hard crevice (BHOS1) showed the highest impedance modulus at the beginning of the test of around 20 kΩ that later decreased to around 5 kΩ at the end of the test. This value seems to be related to the presence of the hard crevice that delayed the entry of water and ions through the concrete pores.

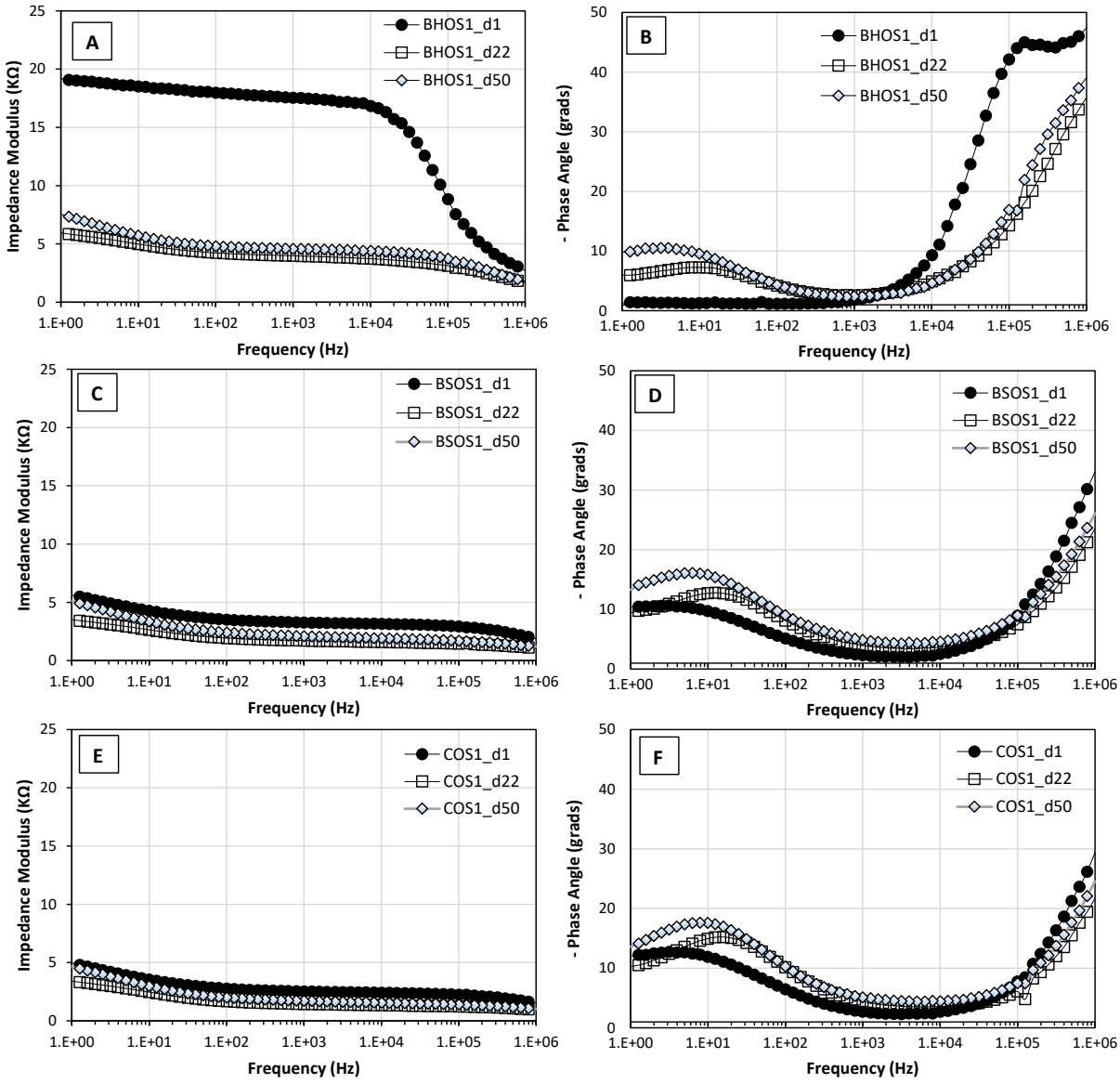

Figure 8.5. Comparative Bode Plots for Inoculated/aerated Cases After 50 Days Immersion Test. A-B: Hard crevice case, C-D: Soft crevice case and E-F: Control case.

Similar analysis was carried out for the inoculated cases in the absence of oxygen. Figure 8.17 depicts the behavior of impedance modulus and phase angles for these tested cases.

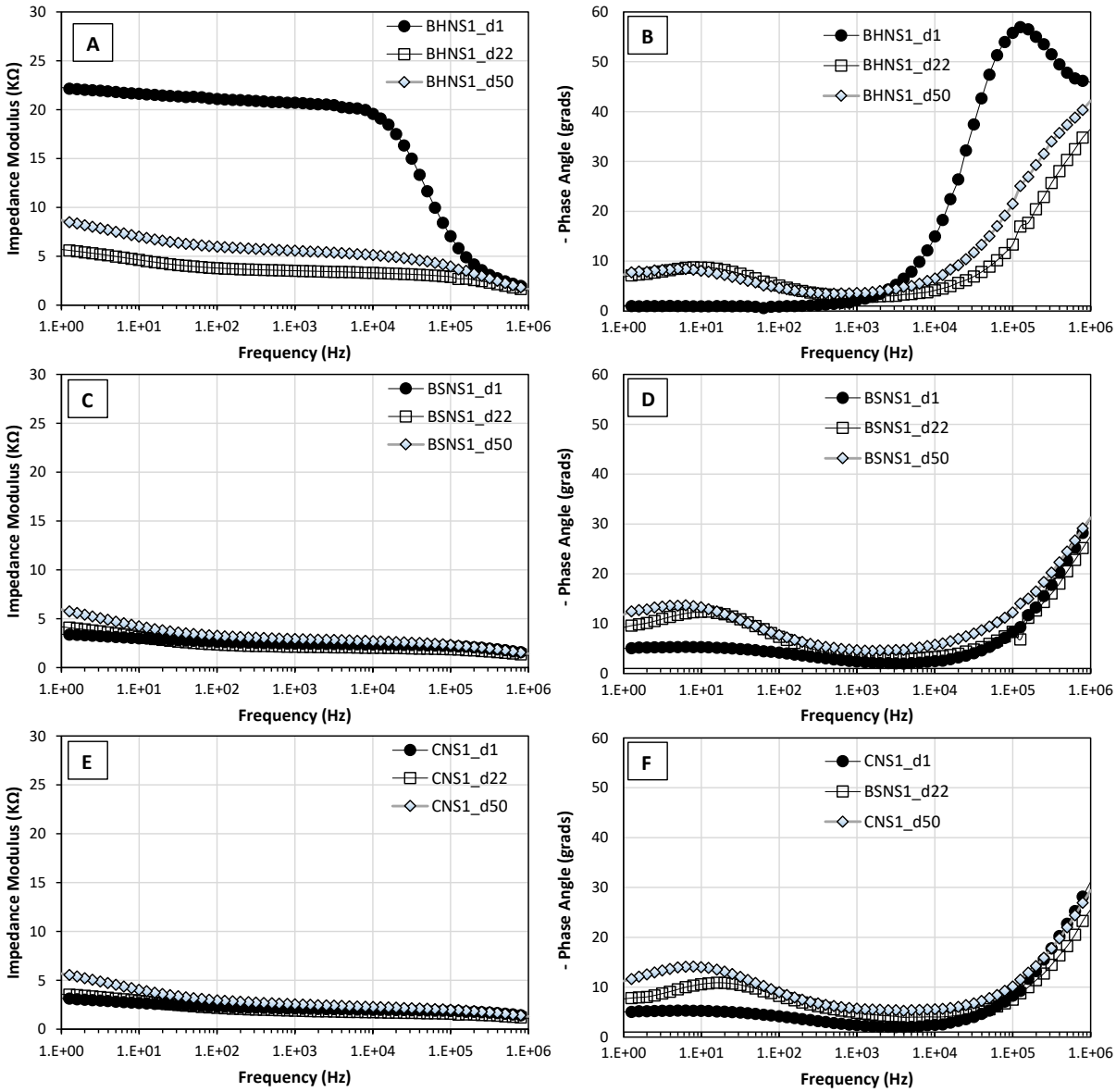

Figure 8.6. Comparative Bode Plots for Inoculated/non-aerated Cases After 50 Days Immersion Test. A-B: Hard crevice case, C-D: Soft crevice case and E-F: Control case.

In general, the impedance modulus at 1Hz was around 5 kΩ for the time of the experiment. A decrease in impedance with prolonged exposure was not observed, except for the samples with hard crevice (BHNS1) and a slight increase of the impedance modulus values was observed at the end of the test for all the tested cases. Again, the hard crevice case

samples shows the highest impedance modulus at the beginning of the test (~20 kΩ) that was related with the barrier effect of the hard crevice, mentioned before.

The last cases analyzed through the Bode plots are the non-inoculated/aerated cases. Figure 8.18 depicts the impedance modulus and the phase angles with time. In general, the impedance modulus was in the order of 5 to 10 kΩ. The highest impedance modulus values were reached for the hard crevice case (BHOZ1). As mentioned previously, the presence of the hard crevice layer on top of the surface seems to act like a barrier for water and ions diffusion.

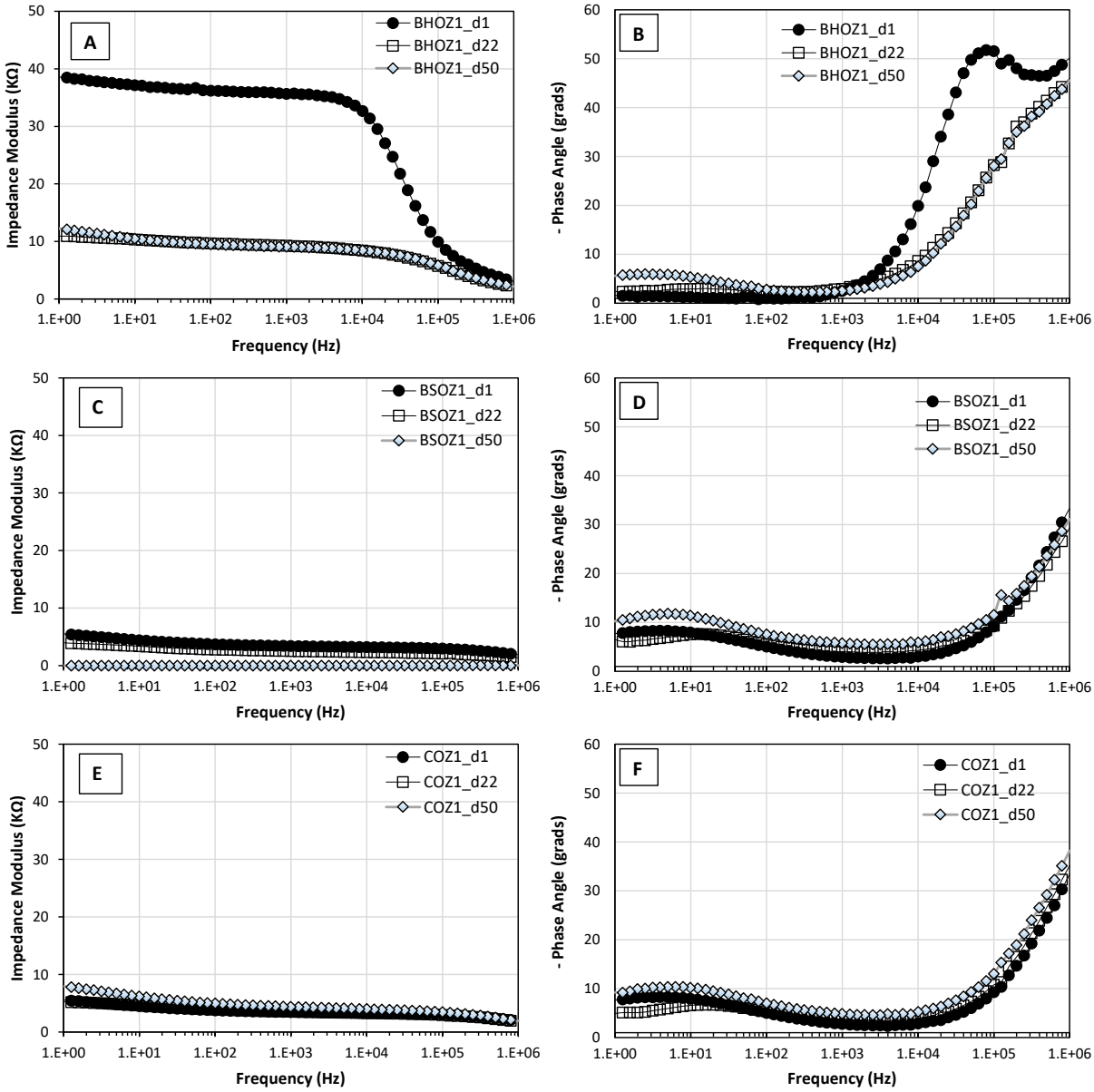

Figure 8.7. Comparative Bode Plots for Non-inoculated/aerated Cases After 50 Days Immersion Test. A-B: Hard crevice case, C-D: Soft crevice case and E-F: Control case.

Experimental impedance data were fitted by using a model with a constant phase element (CPE). The impedance (Z) of the CPE is presented in the Equation 8-1 below:

$$Z = \frac{1/Y_0}{jw^{\alpha}} \quad (8\text{-}1)$$

For systems representative of non-ideal capacitive behavior, the exponent α is less than one. Figure 8.19 depicts the equivalent electrical circuit analog used for experimental impedance data fitting.

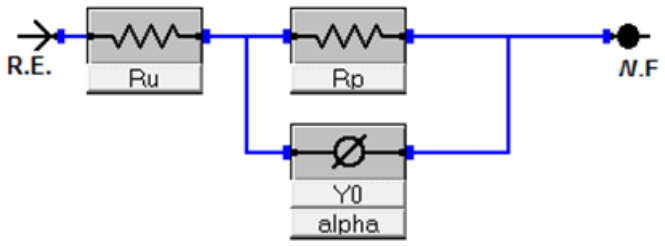

Figure 8.8. Electrical Equivalent Circuit Model Used for Fitting Experimental Data. Ru: Electrolyte resistance, Rp: porous resistance and Yo: non-ideal capacitance**.**

Selected replicates for each tested conditions were used for data fitting of the first time constant (concrete dielectric properties). Results of experimental data fitting, Yo and Rpo, are depicted in Figure 8.20.

As expected, for all the tested conditions there is an increase of the Yo with time, which could be indicative of water uptake into the concrete pores (Figure 8.20 A, C and E). Yo values were between 1.10^{-8} to 4.10^{-8} $S*s^a$, except for the sample case BSOS1, inoculated/aerated with the soft crevice, that reached the highest Yo values ~6.10^{-8} $S*s^a$. In general, samples with soft crevices, for any of the tested conditions (inoculated, non-inoculated, aerated and non-aerated) showed the highest Yo values and the lowest values were observed for the control case samples exposed to deionized water.

On the other hand, Rpo slightly decreased with time for all the tested cases. The highest Rpo values are reached for the hard crevice cases, specifically for the hard crevice BHOZ1 (Figure 20F) case (~10 kΩ). The rest of the cases showed lower Rpo in the order of ~5 kΩ. In general, the results obtained showed a similar behavior among all the tested cases (with and without bacteria inoculation).

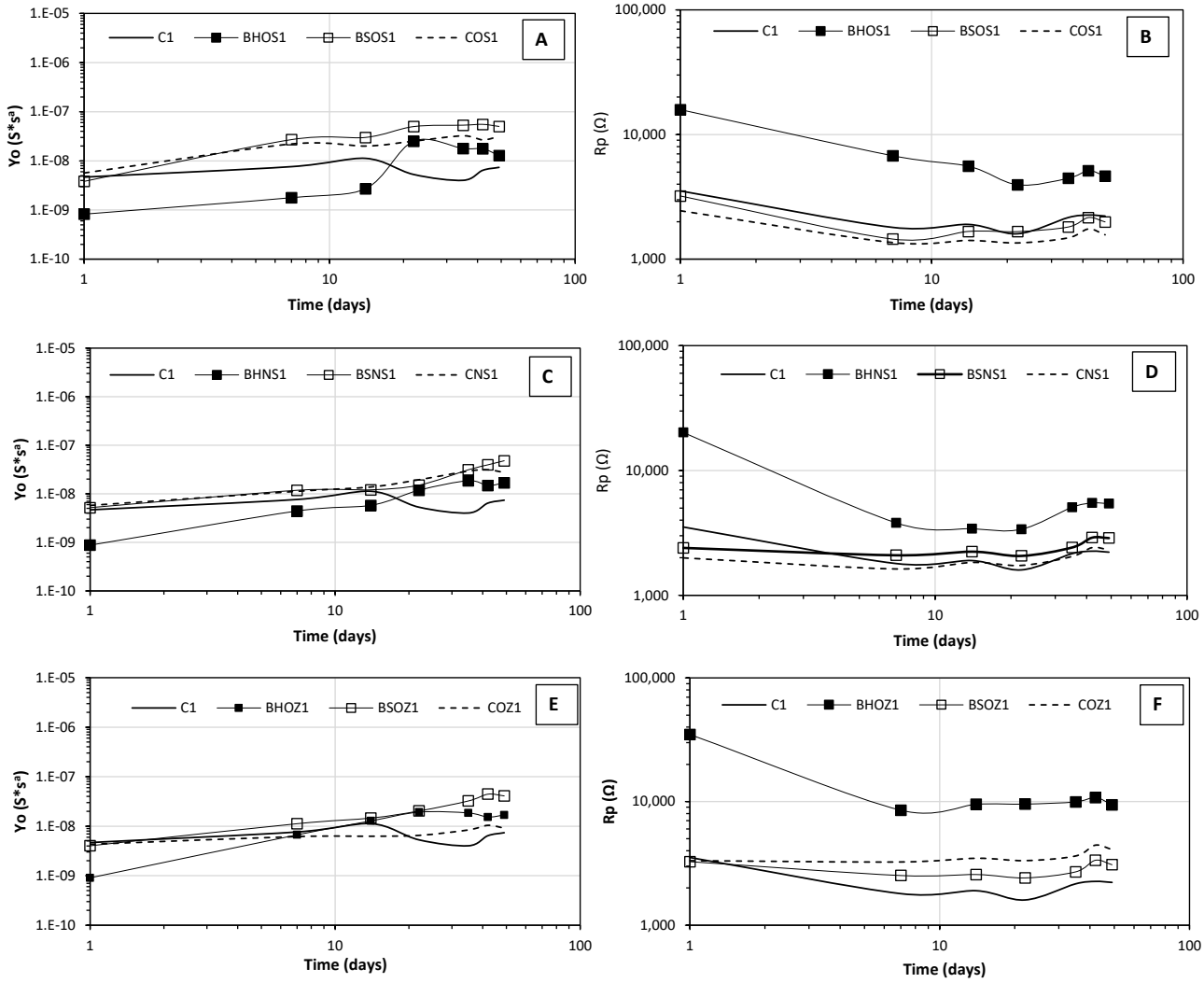

Figure 8.9. Experimental Fitted Data with Time for Different Sample Conditions. A, B: Inoculated/Aerated cases, C-D: Inoculated/Non-Aerated cases and E-F: Non-inoculated/Aerated cases.

Figure 8.21 shows the evolution of the in-situ bulk resistivity with the pore resistance (Rpo). All the tested cases depict a linear relation between the two variables. Concrete samples with high resistivity and high pore resistance will have good dielectric properties and consequently good resistance to deterioration. The data were fitted to a straight line equation (Y=mX) where “m” is the slope of the line. Considering the following equation:

$$\rho = R * K\frac{A}{L} \tag{8-2}$$

where ρ is the resistivity (ohm cm), R is the pore resistance (Rp), K is the porosity constant and A and L are the total area and thickness of the sample, respectively. The average thickness of the samples was 2.38 cm and the area was 45.58 cm^2. Table 8.6 shows the results of the fitted

equations for each tested case and the area calculated from the slope. The K value could be descriptively in the range of 0 to 1 (where the higher values indicate greater porosity).

Table 8.6. Data Fitting Results to a Straight Line Equation.

	Case	Equation	Slope	R2	K
Base Case (control)	C1	Y=95.119X - 94428	95.119	0.88	4.966
Inoculation /Aeration	BHOS1	Y=38.92X	38.92	0.68	2.032
	BSOS1	Y=35.971X	35.971	0.87	1.878
	COS1	Y=33.199X	33.199	0.644	1.733
Inoculation /Deaeration	BHNS1	Y=47.139X	47.139	0.98	2.461
	BSNS1	Y=38.141X	38.141	0.81	1.991
	CNS1	Y=32.975X	32.975	0.82	1.721
No-Inoculation /Aeration	BHOZ1	Y=45.411X	45.411	0.92	2.371
	BSOZ1	Y=39.205X	39.205	0.77	2.047
	COZ1	Y=39.216X	39.216	0.93	2.047

The calculated K values were generally as order of magnitude larger than expected. It was evident that the analog used for fitting impedance data is a simplification of the concrete system. Furthermore, the fitted data points were collected from bulk resistivity and EIS measurements made in time. Any deterioration formed during testing that could affect pore spaces would create error in the fitting of the data points that was assumed to describe constant pore spaces. Also, the degradation observed in lab samples occurred in a very thin layer of the samples but the resistivity and Rpo account for bulk material characteristics. Parsing of pore characteristics of the cement hydrate and course aggregate is also difficult. Application of EIS to monitor concrete degradation require further consideration.

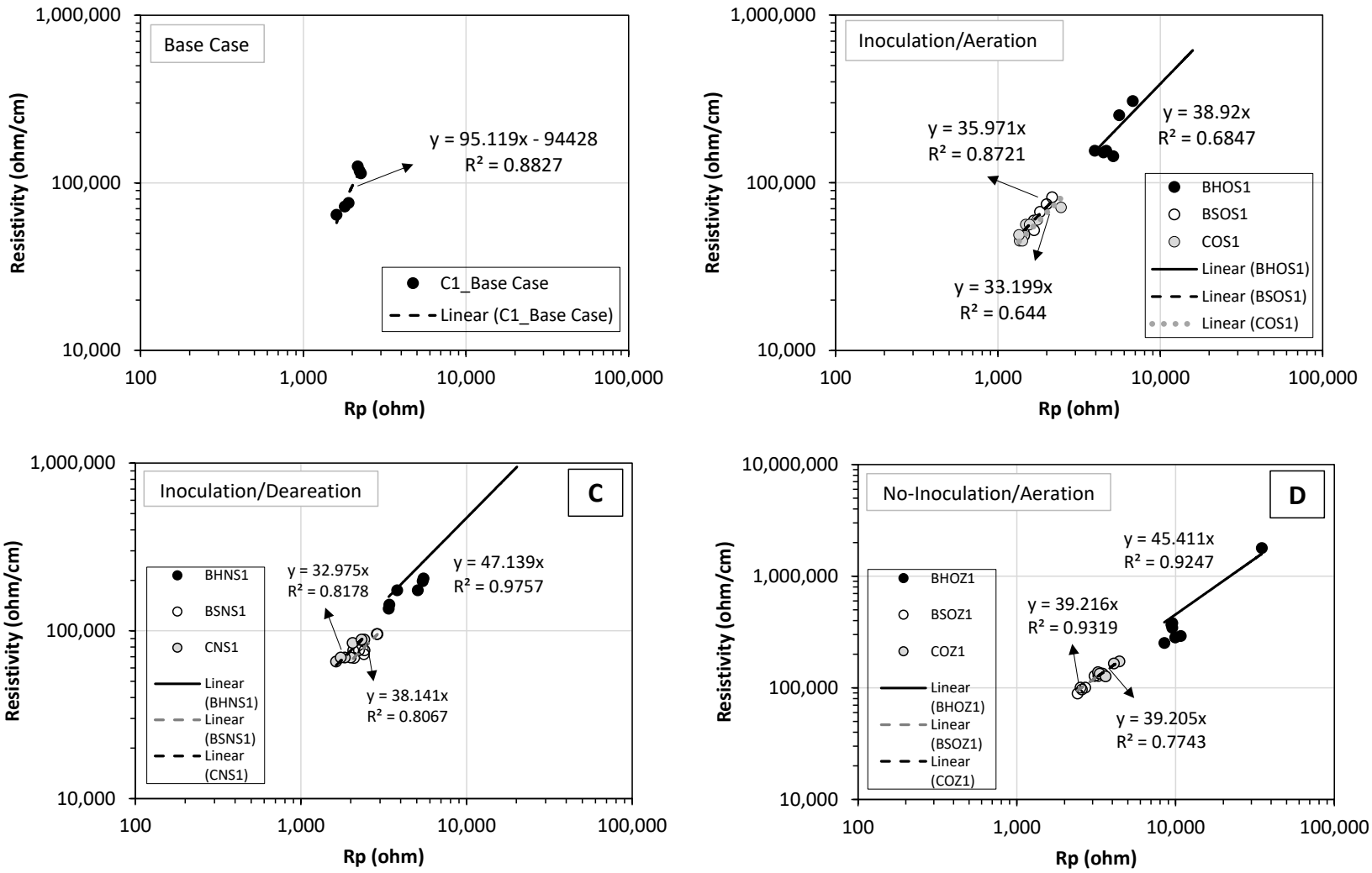

Figure 8.10. Resistivity vs Rp (fitted data) for Concrete Samples Exposed to Cyclic Immersion Test.

8.3. Field Samples Results for Plain Concrete Cylinders

8.3.1. Visual Inspection Results

8.3.1.1. SR-312 Location

Figure 8.22 depicts the surface conditions of the concrete samples exposed to outdoor exposure from day 0 to day 270, and after cleaning the surface (barnacles and marine growth removal). As expected, a variety of marine flora and fauna quickly developed on the surface even though frequent tide shifts often allowed atmospheric exposure and surface drying for several hours. After ~ 30 days exposure the sample surfaces exhibited a change in color. The apparent formation of biofilm and marine growth on the surfaces that was greater for samples between ~ 6 to ~ 8 ft BMG. Around two months later, ~ 90 days of exposure, the presence of barnacles on concrete surfaces was observed, whose size and population (density) increased with depth. At later exposure times (~ 180 days of exposure and to the end of test) the barnacle's size and population further increased with heavy marine flora at ~ 5 to ~ 8 ft depths. In general, barnacles developed at all depths in the tidal region but the lower depth locations supported greater size/population. The barnacles attached to the concrete surfaces can present hard crevice environment and the soft flora can present porous crevices as was simulated in lab conditions described earlier.

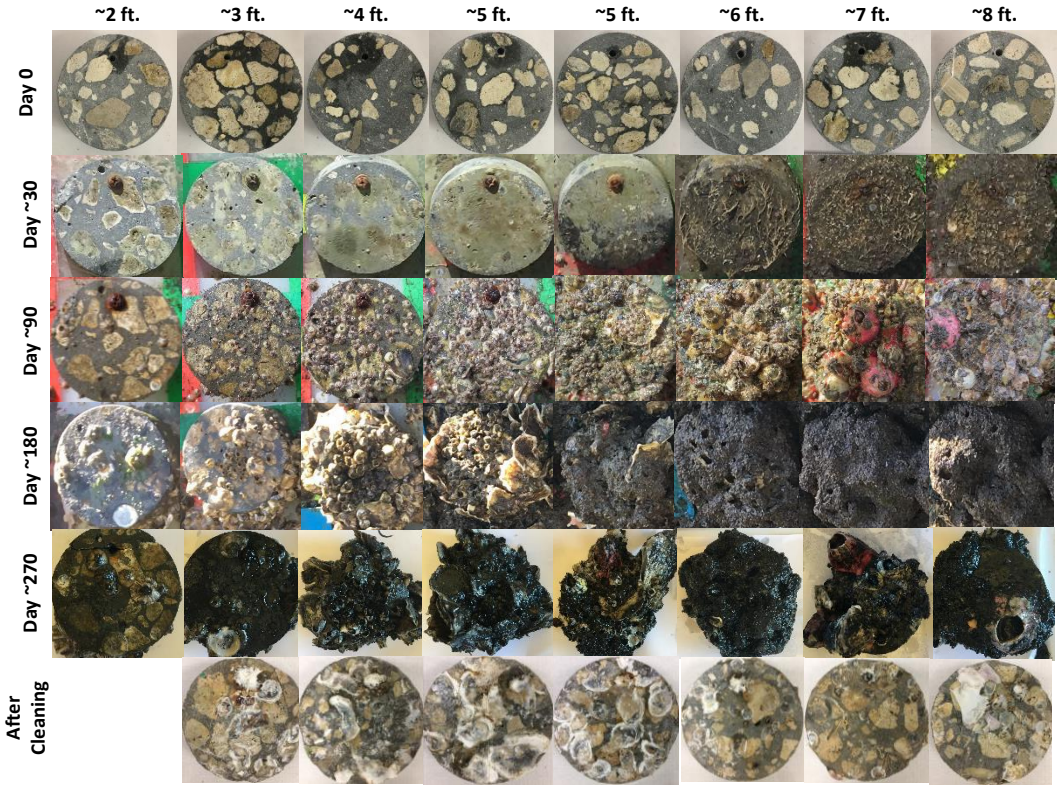

Figure 8.11. Images of Concrete Samples Exposed to SR-312 Outdoor Conditions.

8.3.1.2. US-41 and US-301 Locations

Figures 8.23 and 8.24 show the visual aspect of concrete samples exposed to outdoor exposure at the US-41 and US-301 bridges over Alafia River for ~ 240 and ~ 180 days, respectively. Barnacle formation was observed for the two sites from ~ 2 ft BMG depth and below. Those samples exposed above ~ 2 ft BMG didn't show barnacles formation on the surface. Also, the size and density of barnacles didn't show a greater increment with depth compared with samples exposed to SR-312 environment, which were much bigger in size and density with depth. Soft fouling due to flora attached to the samples was not as heavy as observed at the SR-312 site.

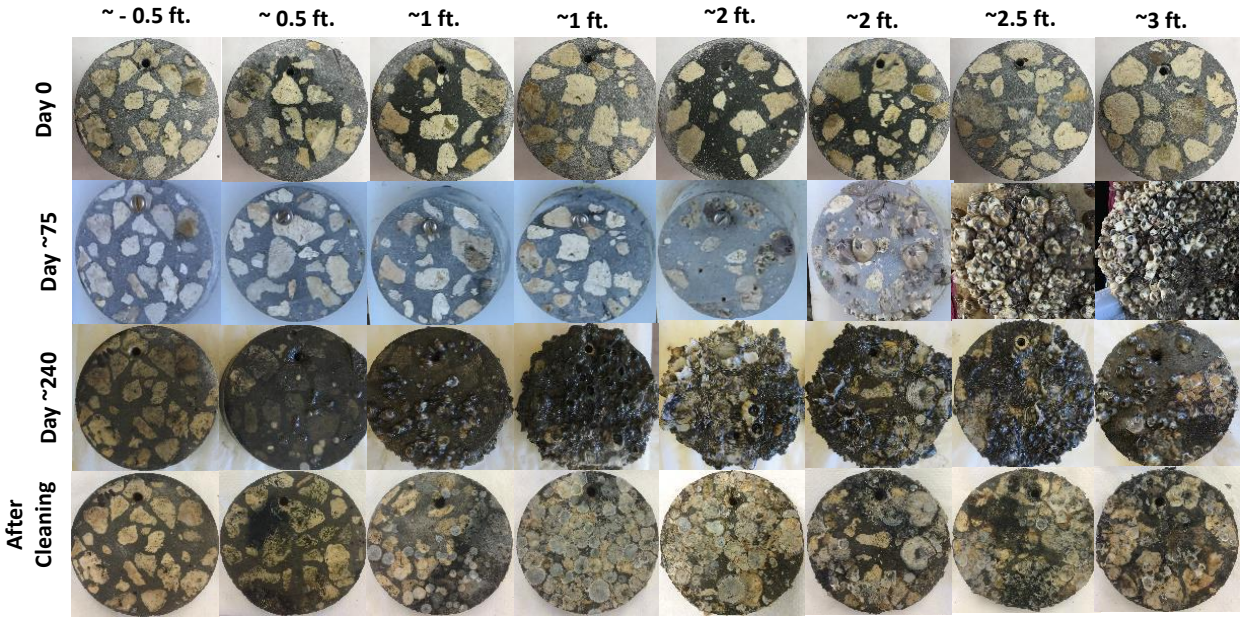

Figure 8.12. Images of Concrete Samples Exposed to US-41 Outdoor Conditions.

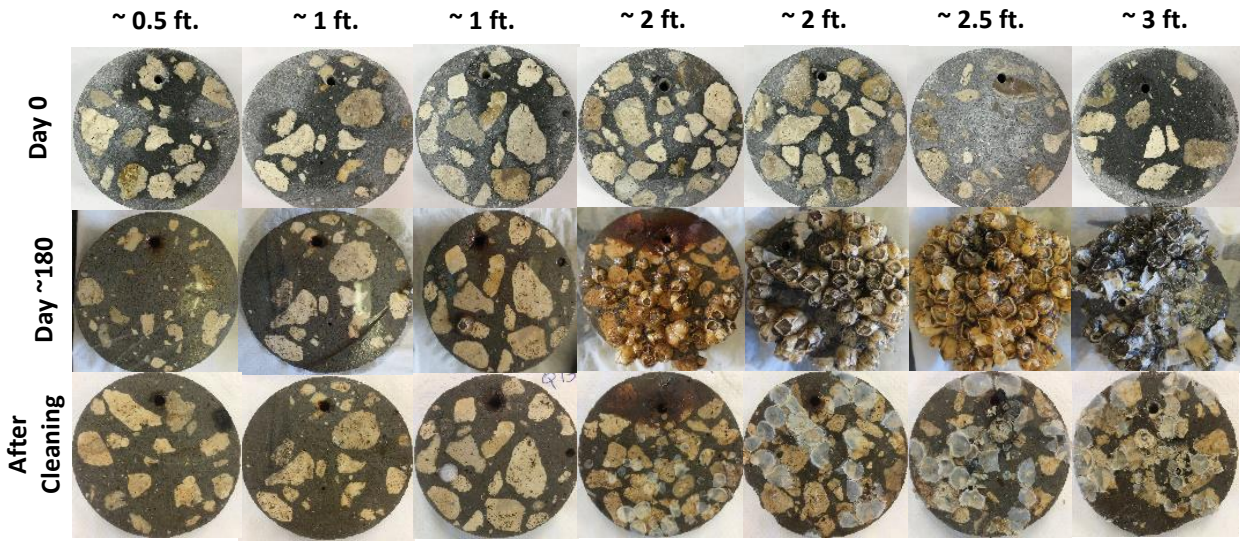

Figure 8.13. Images of Concrete Samples Exposed to US-301 Outdoor Conditions.

8.3.2. Surface Bacteria Activity Results

Table 8.7-8.9 summarize the surface bacteria activity (BART test) results for all the concrete samples tested (selected samples), at each outdoor exposure condition. The four bacteria SRB, IRB, APB and SFB were detected in all the tested samples. In most of the cases, the bacteria content were in the aggressive range. The results confirmed that the surface condition and outdoor environmental conditions supported the bacteria activity

Table 8.7. BART Test Results for Samples Exposed to SR-312 Outdoor Condition.

	October 2017/ ~ 90 days	**April 2018/ ~ 270 days**
Bacteria (CFU.mL-1)	**C27 (Concrete)**	**C27 (Concrete)**
Sulfate Reducing Bacteria (SRB)	27,000(A)	325 (M)
Iron-Reducing Bacteria (IRB)	35,000(A)	2,200 (M)
Acid Producing Bacteria (APB)	475,000(A)	14,000(A)
Slime-Forming Bacteria (SFB)	67,000(A)	440,000(A)

NA: Not Aggressive, M: Moderately Aggressive and A: Aggressive. General guidelines for BART test for corrosion (Droycon Bioconcepts Inc. http://www.dbi.ca/).

Table 8.8. BART Test Results for Samples Exposed to US-41 Outdoor Condition.

	January 2018 / ~ 75 days	**July 2018 / ~ 240 days**
Bacteria (CFU.mL-1)	**E18 (Concrete)**	**E 18 (Concrete)**
Sulfate Reducing Bacteria (SRB)	1,400 (A)	<1 (NA)
Iron-Reducing Bacteria (IRB)	150(M)	9,000(A)
Acid Producing Bacteria (APB)	82,000(A)	475,000(A)
Slime-Forming Bacteria (SFB)	1,750,000(A)	1,750,000(A)

NA: Not Aggressive, M: Moderately Aggressive and A: Aggressive. General guidelines for BART test for corrosion (Droycon Bioconcepts Inc. http://www.dbi.ca/).

Table 8.9. BART Test Results for Samples Exposed to US-301 Outdoor Condition.

	July 2018 / ~ 180 days
Bacteria (CFU.mL-1)	**Q17 (Concrete)**
Sulfate Reducing Bacteria (SRB)	2,200,000 (A)
Iron-Reducing Bacteria (IRB)	140,000(A)
Acid Producing Bacteria (APB)	475,000(A)
Slime-Forming Bacteria (SFB)	1,750,000(A)

NA: Not Aggressive, M: Moderately Aggressive and A: Aggressive. General guidelines for BART test for corrosion (Droycon Bioconcepts Inc. http://www.dbi.ca/).

8.3.3. Impedance and Resistivity Results

Figure 8.25 shows the bulk resistivity results of concrete samples exposed to outdoor exposure. As general trend, resistivity values of concrete samples decrease after testing for all the outdoor exposure sites. Final resistivity values were around 2.10^4 Ω.cm for all the tested concrete samples. There are different factors that could influence the results such as the water type and the samples wet condition. For example, samples tested at SR-312 and US-41 locations were exposed to brackish water. Brackish waters are characterized by having a certain content of ions such as chlorides that can affect concrete properties and consequently may deteriorate the material. Then, the entry of ions to the samples could promote the observed resistivity decrease (Figure 8.25 A and B). The increment observed for some samples (C22-C23) could be explained by the dryness of the samples due to tide variabilities and sample depth. For the case of samples exposed at US-301, the resistivity increment seems to be associated with the water type, fresh water. The fresh water could favor the leaching of concrete pore alkaline compounds favoring the resistivity increment detected. Also, it is very likely that most of the samples (not included the last three) of this site were most of the time exposed to the air, so the surface was almost dry favoring the resistivity increment.

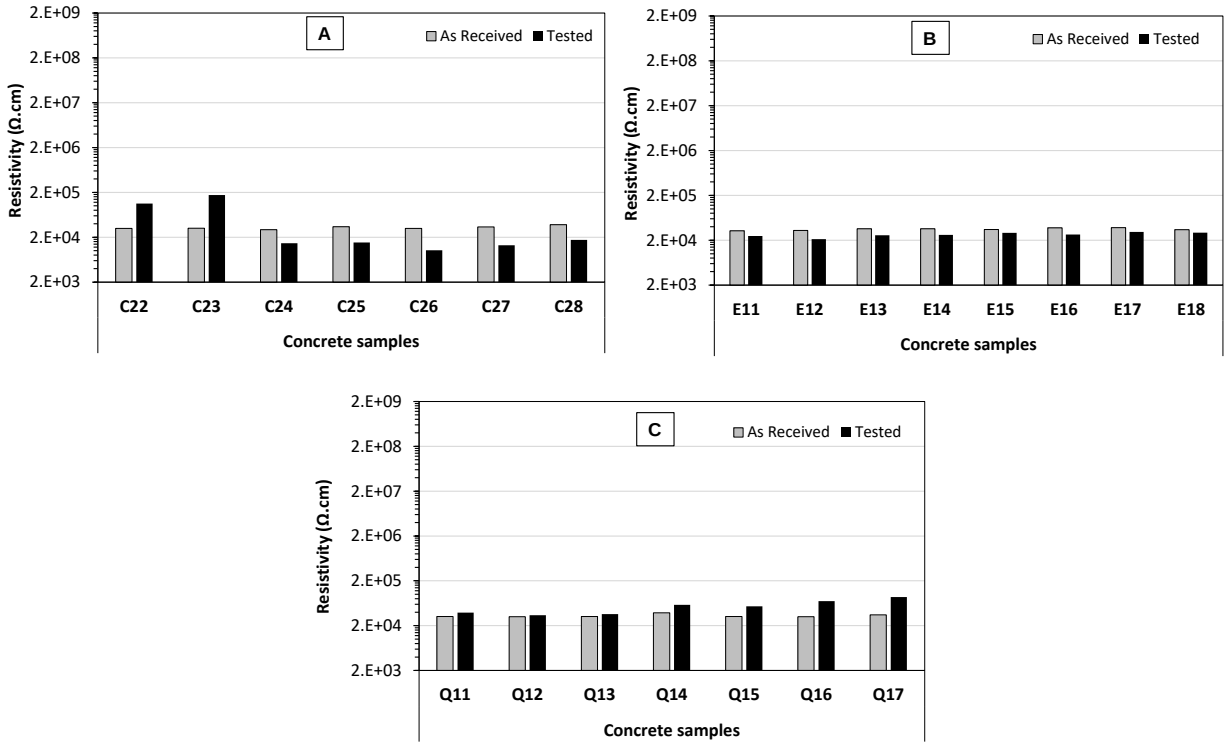

Figure 8.14. Bulk Resistivity Measurements for Concrete Samples at Different Florida Outdoor Environments. A: SR-312 site, B: US-41 site and C: US-301 site.

Figure 8.26 depict the fitted experimental data (Yo and Rp) of concrete samples at different outdoor exposure condition and water depth. The experimental EIS data was fitted to the CPE equivalent model mentioned before and only the first time constant was fitted to get the Yo and Rp values.

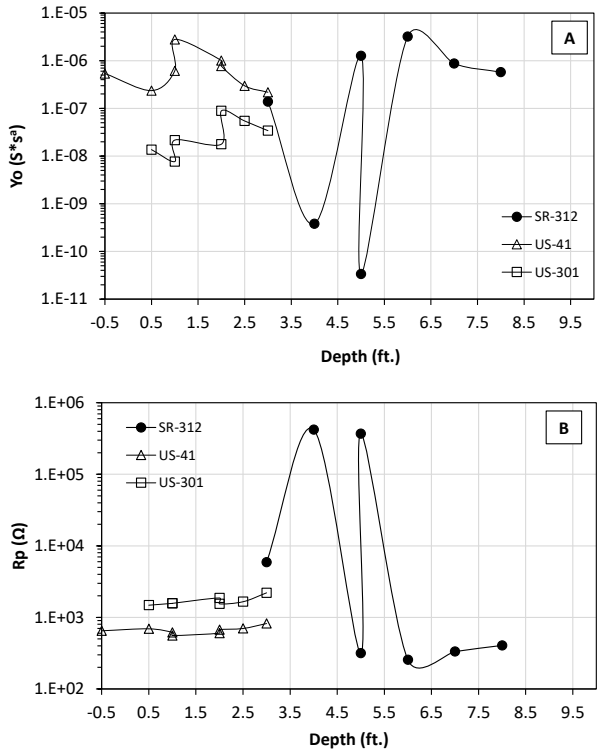

Figure 8.15. Experimental Fitted Data for the Concrete Samples at Different Depths and Different Outdoor Exposure (SR-312, US-41 and US-301). A: Yo and B: Rp.

In general, Yo values increased with water depth showing some fluctuations representing tidal behavior but generally greater moisture presence in concrete with prolonged immersion periods at higher depths. Rpo values showed relatively constant behavior for samples at US-41 and US-301 locations. Rather large variation in Rpo values were resolved for samples exposed at the SR-312 site. In relation to water depth, some of the samples had prolonged atmospheric exposure (i.e. mainly those samples between 0.5 to 2 ft. depth exposed to US-41 and US-301 locations). Also, the exposure site/depth could also determine samples surface condition, associated with the flora and fauna developed at each site and consequently on top of the surface. Hence, the variations already mentioned could influence in the differences observed in the results.

8.4. Laboratory Samples Results for Polyurea-coated Concrete Cylinders

8.4.1. Visual Inspection Results

Figure 8.27 shows the surface appearance of the coated concrete samples before and after the immersion test. Inoculated samples (3 and 4) shows an accumulation of black products on top of the tested surface due to the formation of iron sulfide (black color). In general, there was no strong visual indicators of coating degradation after two weeks experiment.

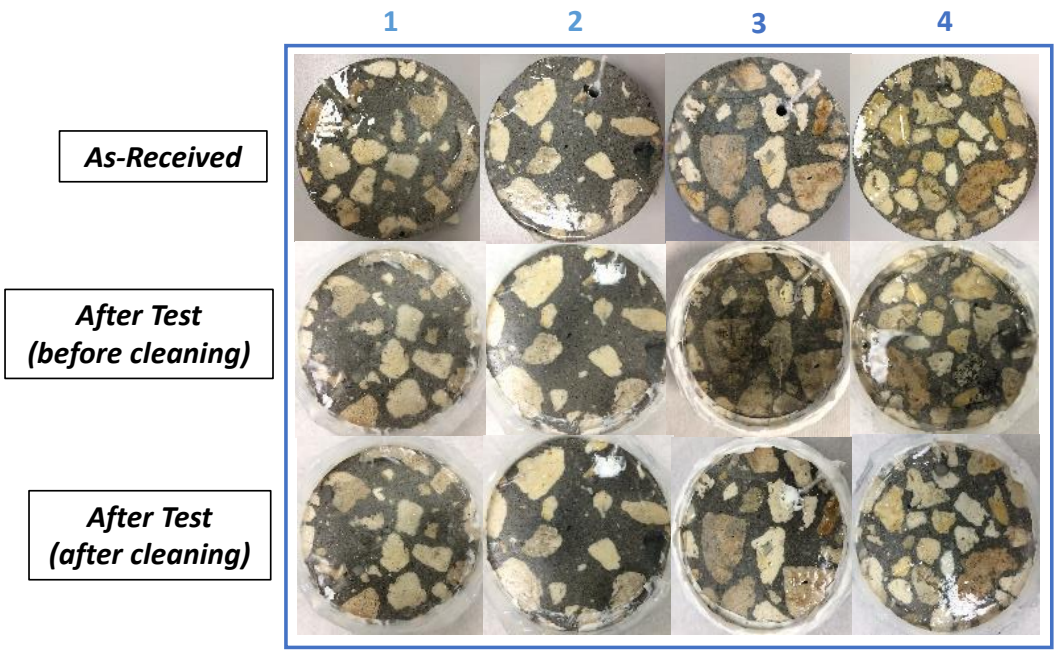

Figure 8.27. Polyurea-Coated Concrete Surface Appearance Before and After Immersion Test.

8.4.2. Visual Inspection of Bacteria Activity

Figures 8.28 shows test solution color for all specimens with time (inoculated and non-inoculated). The non-inoculated cases (control case 1 and 2) show a clear color (no turbidity) solution for all the testing time. However, samples that were inoculated with SRB bacteria depict solutions with high turbidity on the day of inoculation that subsequently reduces with with time. It can be seen that at day 8 the solution is mostly clear and then darkens after re-inoculation of the bacteria.

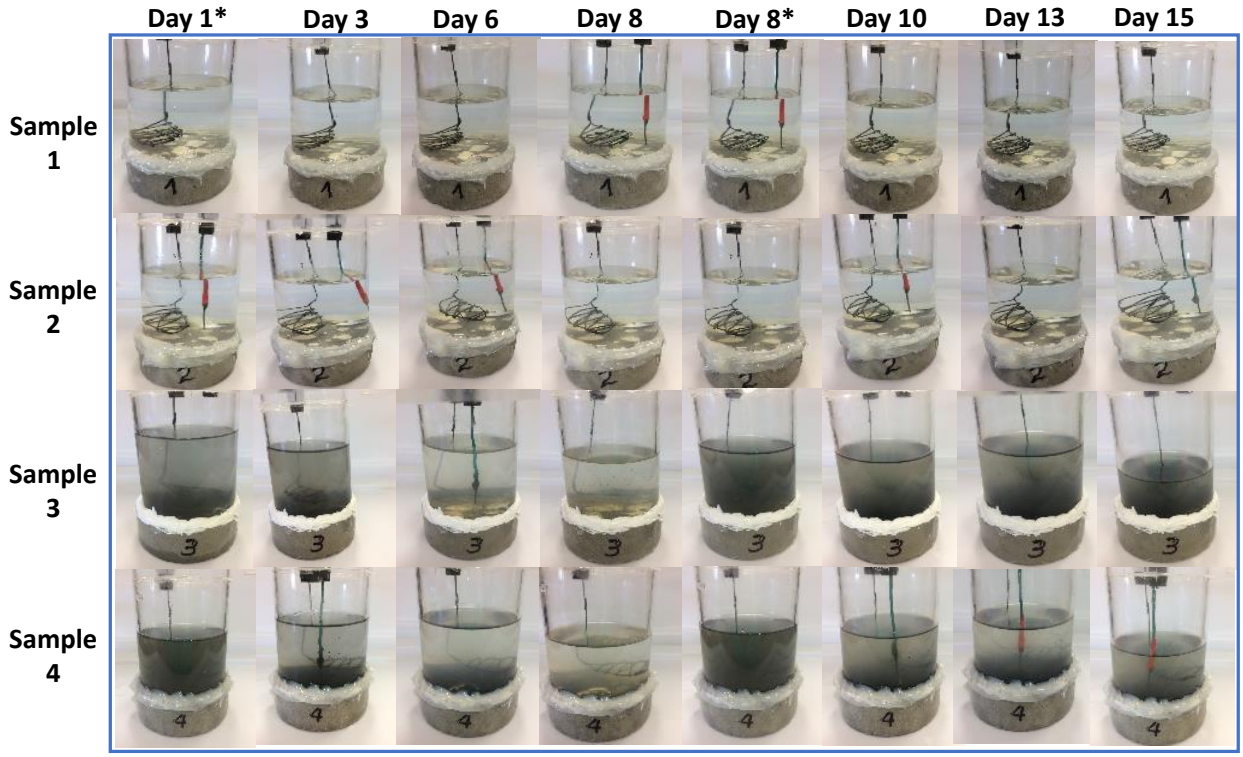

Figure 8.28. Color Change of the Test Solution for the Non-inoculated (Samples 1-2) and Inoculated (Samples 3-4) Cases with Time.

8.4.3. Bacteria Activity Results

Table 8.10 shows the SRB test results for bacteria count performed at the end of the immersion test. It is confirmed the presence of SRB bacteria in the two inoculated tested cases, with bacteria counts higher than 100,000 bacteria/mL.

Table 8.10. SRB Test Results for Bacteria Enumeration.

Case	Samples	Positive Vials/ Tested Vials	SRB Count (bacteria/mL)
Inoculated/Aerated	3	6/6	1,000,000
	4	6/6	100,000

The chemical oxygen demand (COD) is the demand of oxygen necessary to oxidize the organic matter present in the media and SRB bacteria may reduce sulfate ions to sulfide ions through the oxidation of organic matter (heterotrophic reduction, see reaction 2).

Figure 8.29 shows the COD with time for the inoculated and non-inoculated cases under study. COD shows an increment with time, followed by a decrease at the end of the experiment. The higher increment is for the inoculated cases (3 and 4) and in general, there is a peak at day

9 (for the inoculated and non-inoculated cases), which could be related with the accumulation of organic matter from the first week and the second one.

After SRB inoculation, a drop in COD may indicate the oxidation of vestigial organic compounds as a food source for SRB. Deviation from this drop may indicate reduced SRB activity associated with biological sulfate reduction. However, the COD increment does not necessarily mean that SRB bacteria activity is low, because there could be a build-up of organic matter. Also, sulfide production could lead to increase in COD. Again, the behavior observed doesn't give a clear indication of SRB activity other than that the increase in COD would give indication of conditions that would support SRB.

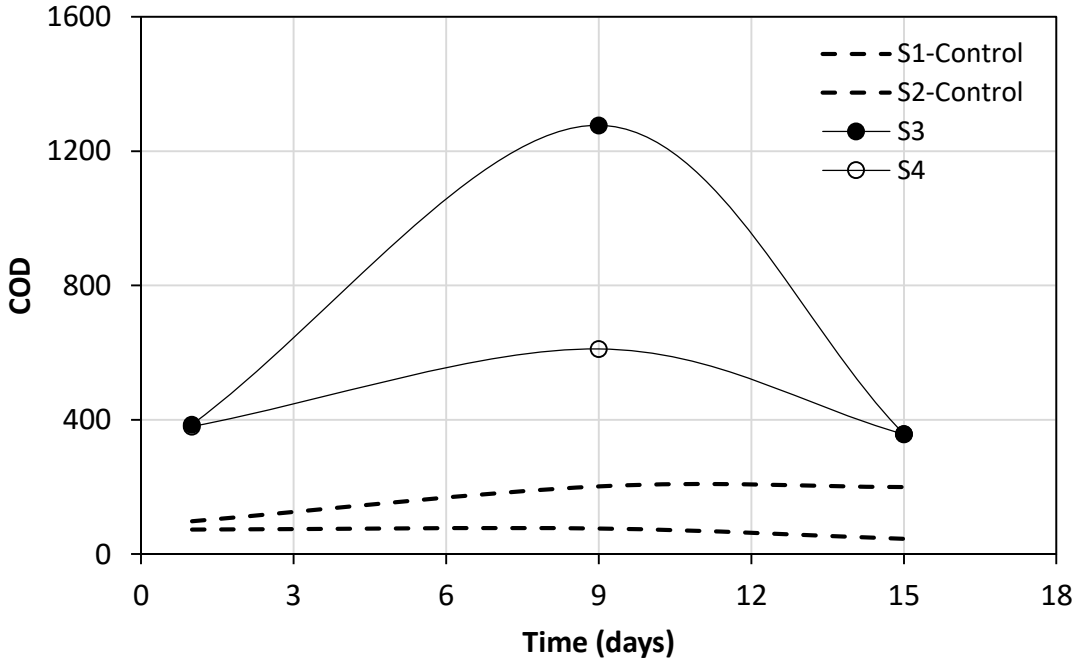

Figure 8.29. COD for Inoculated (S3, S4) and Non-Inoculated (S1, S2) Tested Cases with Time. COD was Measured after the Inoculation Event.

The sulfide content gives information about the SRB activity that produce hydrogen sulfide due to the reduction of sulfate. Figure 8.30 shows the level of sulfide production in the test solutions (inoculated cases). The sulfide measurements shows fluctuations with time, in general with values below 1 mg/L, except one peak of 2 mg/L at the end of the test (one replicate). It is highlighted the SRB activity during all the experiment.

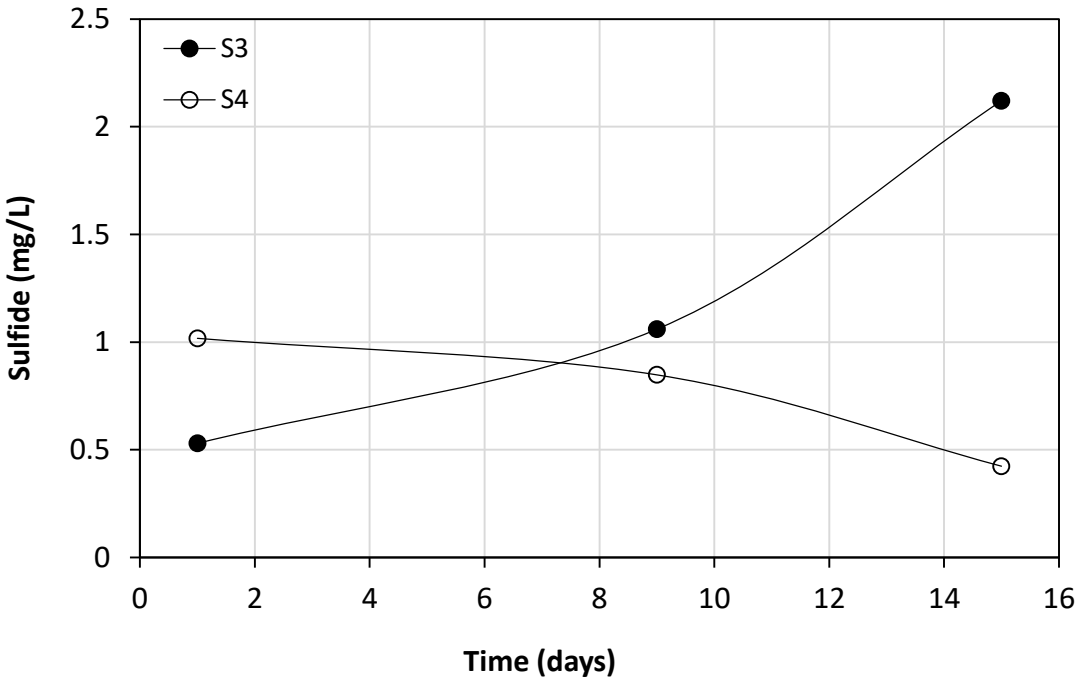

Figure 8.30. Sulfide Content with Time for the Bacteria Inoculated Cases.

8.4.4. Conductivity and pH Results

Figure 8.31 shows the pH and conductivity of the test solution for all the tested cases. The pH values generally increase after inoculation events and ranged from 7 to 8.5 for all the tested cases (inoculated and non-inoculated). These pH values can support SRB growth and activity (Eštokov et al., 2012). The non-inoculated cases shows lower values (7 – 7.5). The pH increments could be related with the polyurea coating.

The conductivity increases with time for the inoculated and non-inoculated cases, as observed in Figure 8B. Higher increment is observed for the inoculated cases. After the second inoculation (2nd red dots) the conductivity increment is greater. This behavior could be explained by the fact that the test solutions were not renewed after one week test, only bacteria inoculation and modified Postgate B were added to the old solution. Hence, it's clear that the addition of nutrients (Postgate B) every week for the bacteria growing, which has ions in the composition (i.e. Na^+, K^+, Cl^-, etc.) to the media, supported the conductivity increment due to ions build up in the test solution.

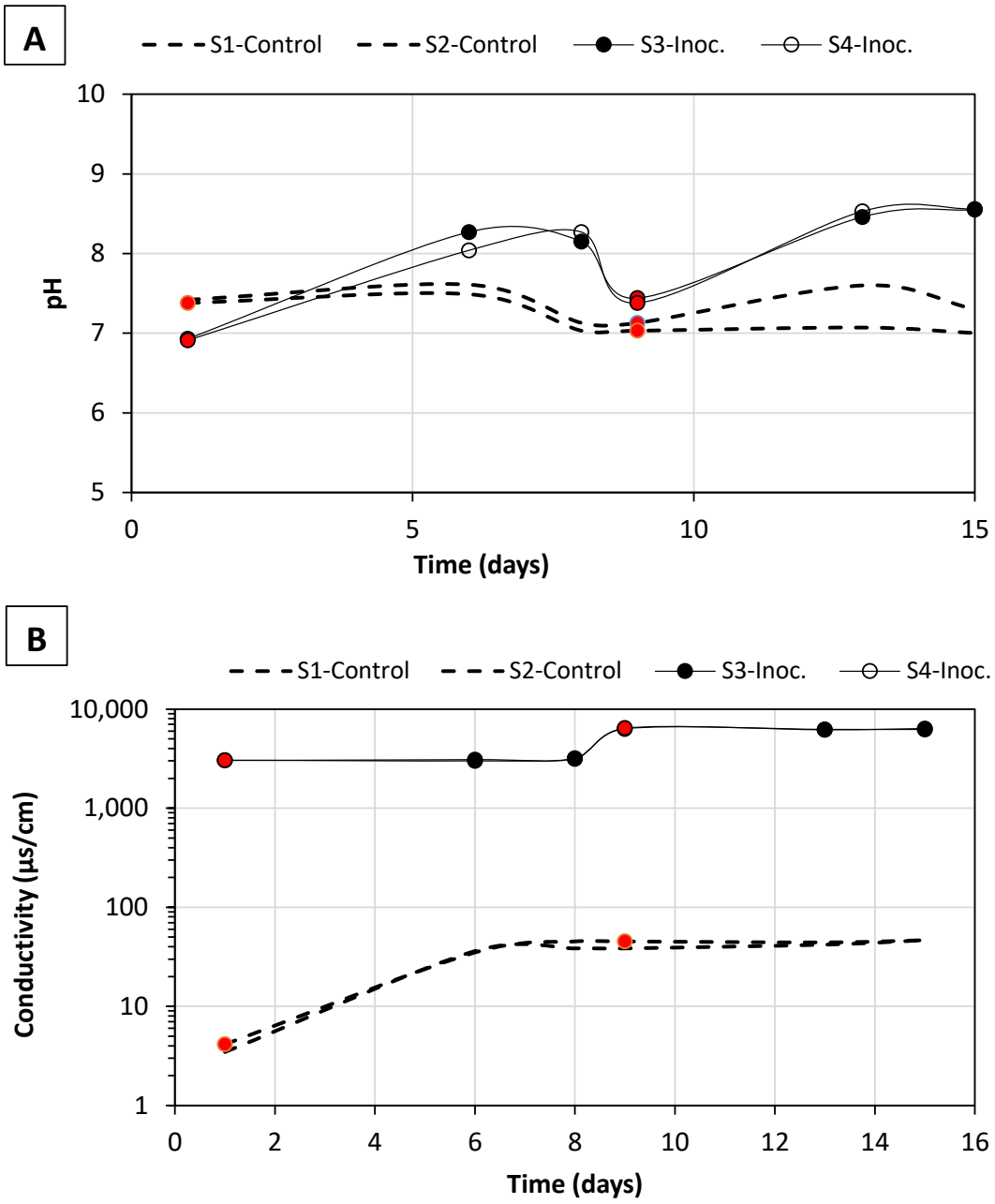

Figure 8.31. pH (A) and Conductivity (B) Values with Time for the Electrolyte Used During Immersion Test. Red symbols represent measurement made after inoculation.

8.4.5. Impedance Results

Figure 8.32 shows the Nyquist diagrams with time for the control case samples (S1) exposed to deionized water.

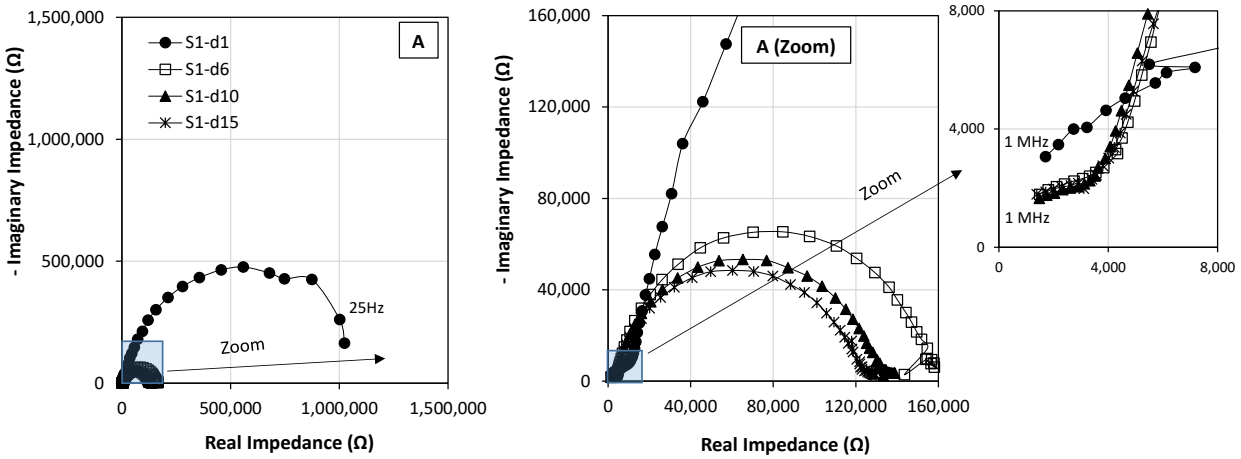

Figure 8.32. Nyquist Diagram of the Control Case at Selected Immersion Times.

The polyurea coating shows a high impedance value (1MΩ) at the beginning of the experiment and then a decrease to ~120 kΩ after two weeks immersion test (Figure 8.33). The impedance decrease could be related with the entry of water to the coating film trough the pores. Two loops are observed from the beginning to the end of the test, a small one, at very high frequency and a second one, at the high frequency too.

The inoculated cases (S3-S4) show similar behavior, with a decrease of the impedance from ~100 KΩ to ~40 KΩ after 15 days immersion test in the SRB media (Figure 10). Also, two loops are observed at the high frequency region, related with coating protective properties.

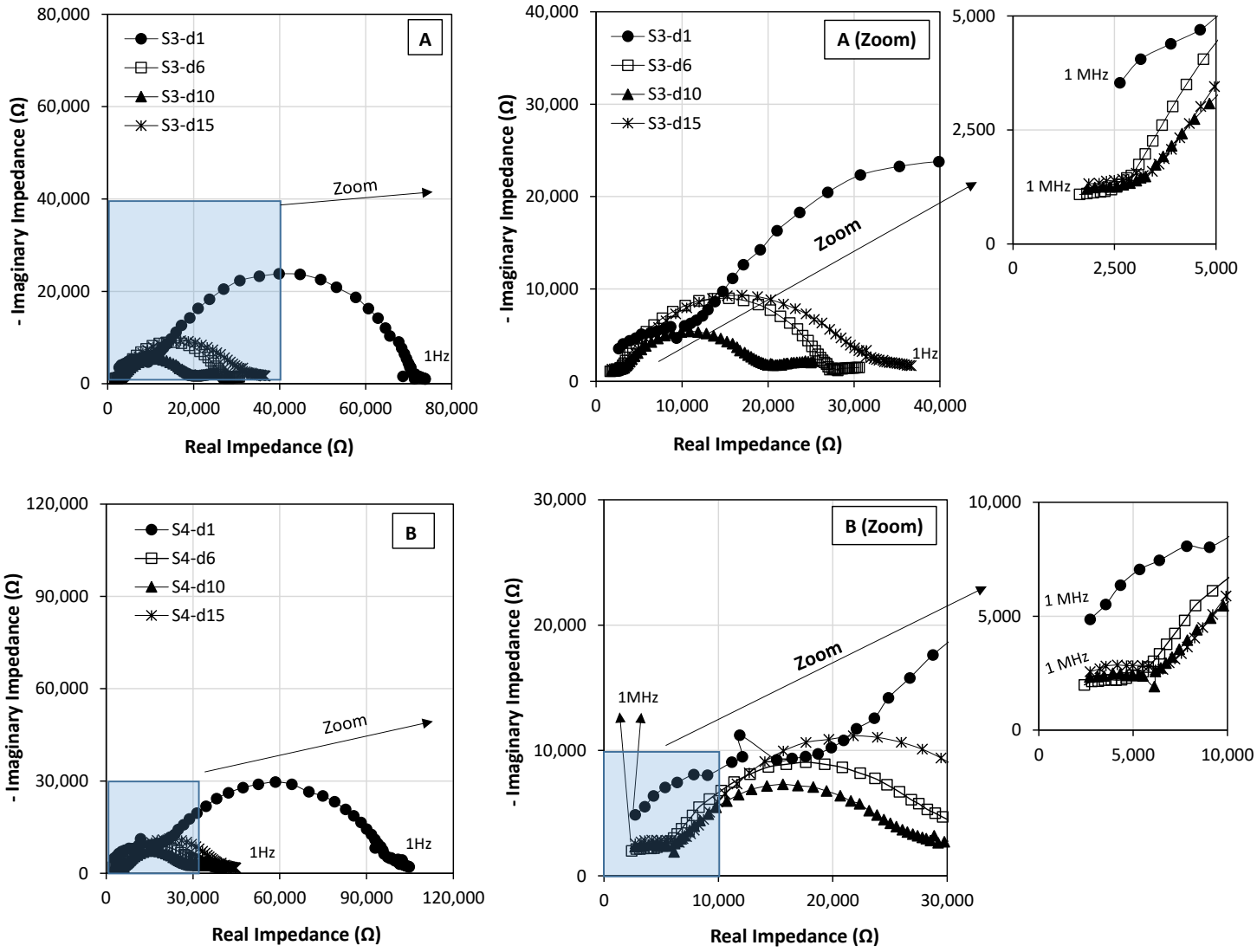

Figure 8.33. Nyquist Diagram for Inoculated/Non-inoculated Aerated Cases with Immersion Time.

8.5. Field Samples Results for Polyurea-coated Cylinders

8.5.1. Visual Inspection Results

8.5.1.1. SR-312 Location

Figure 8.34 depicts the surface appearances of the coated concrete samples exposed to outdoor exposure from day 0 to day 240, and after cleaning the surface (barnacles and marine growth removal). After the ~ 60 days exposure formation of barnacles on the surfaces were observed. The size and population (density) increase with depth and with immersion time. Then, at later exposure times (~150 days) black sediments/marine flora developed from ~ 5 to ~ 8 ft depth. In general, barnacles could develop at all depths in the tidal region but the lower depth locations supported greater size/population. As expected, a variety of marine flora and fauna quickly developed on the surface even though frequent tide shifts often allowed atmospheric exposure and surface drying for several hours. Results confirmed that the polyurea coating could not prevent the growing of marine flora and fauna on top of the surfaces.

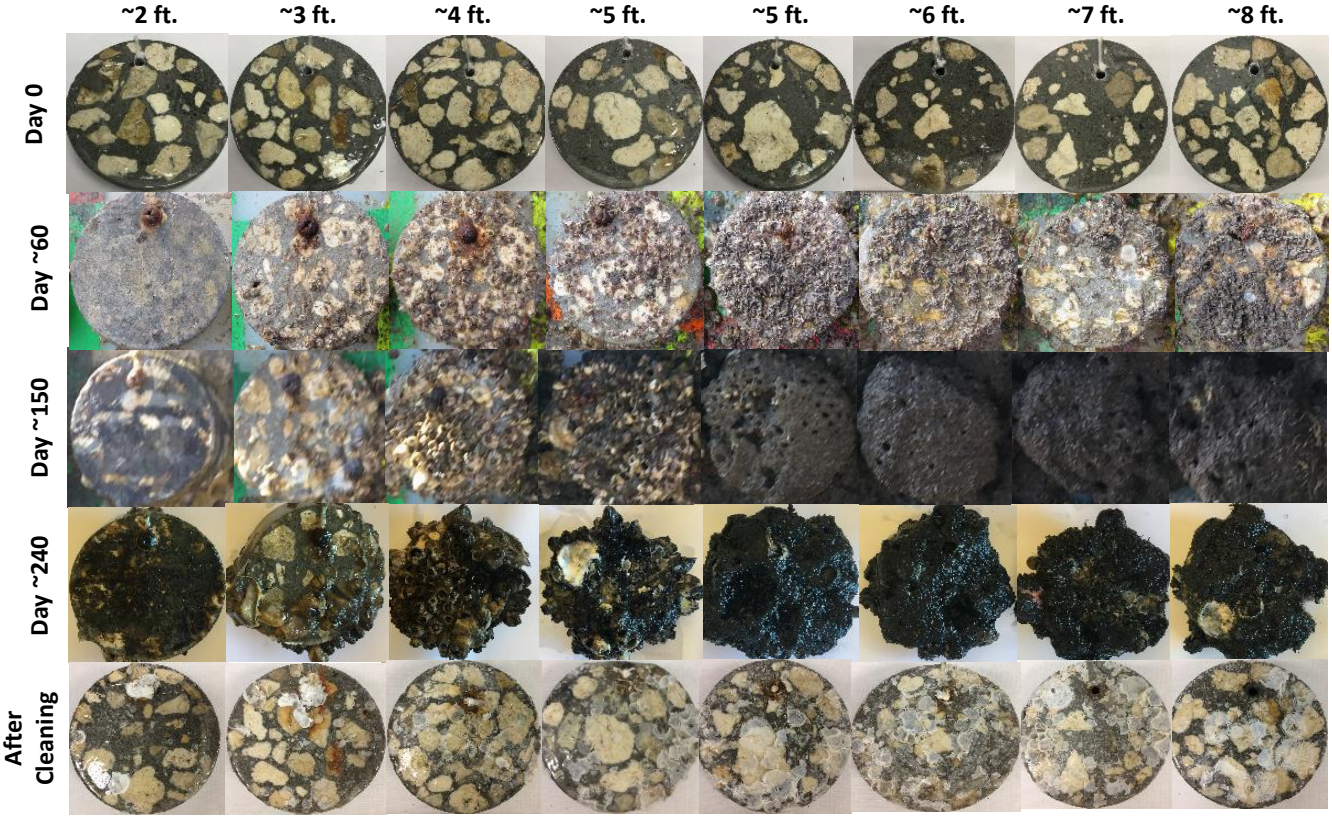

Figure 8.34. Images of Coated Concrete Samples Exposed to SR-312 Outdoor Conditions.

8.5.1.2. US-41 and US-301 Locations

Figures 8.35 and 8.36 show the visual aspect of the coated concrete samples exposed to outdoor exposure at the US-41 and US-301 bridges over Alafia river, Tampa for ~ 240 and ~ 180 days, respectively. It is observed barnacles formation for the two selected sites from ~ 1 ft BMG depth and below. Also, the size and density of barnacles doesn't show a greater increment with depth compared with samples exposed to SR-312 environment, which were much bigger in size and density with depth. It was not observed the presence of soft fouling and flora attached to the samples as observed in SR-312 site. As mentioned before, the polyurea coating could not prevent the growing of barnacles and flora on top of the coated surfaces.

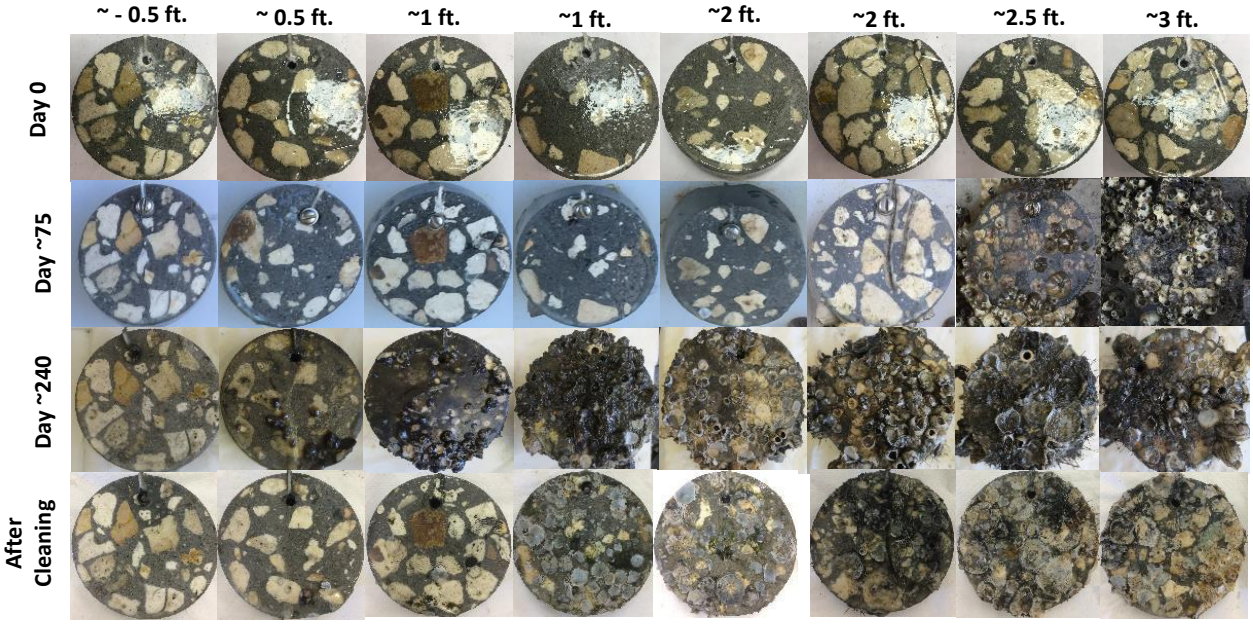

Figure 8.35. Images of Coated Concrete Samples Exposed to US-41 Outdoor Conditions.

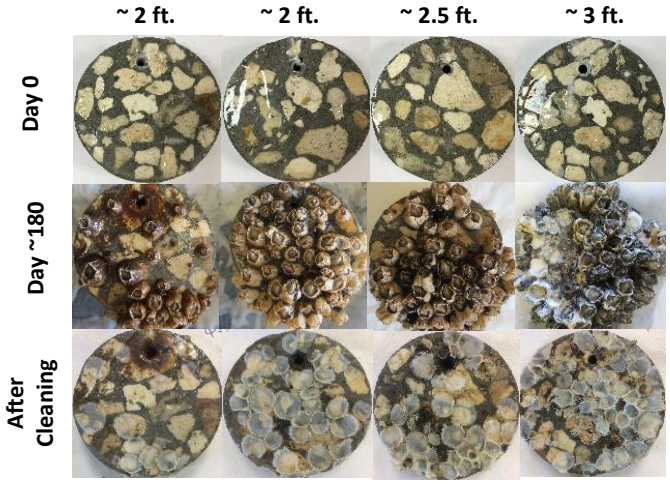

Figure 8.36. Images of Coated Concrete Samples Exposed to US-301 Outdoor Conditions.

8.5.2. Surface Bacteria Activity Results

Table 8.11-8.13 summarize the surface bacteria activity (BART test) results for all the coated concrete samples tested (selected samples), at each outdoor exposure condition. The four bacteria SRB, IRB, APB and SFB were detected in all the tested samples. In most of the cases, the bacteria content were in the aggressive range. The results confirmed that the surface condition and outdoor environmental conditions supported the bacteria activity

Table 8.11. BART Test Results for Samples Exposed to SR-312 Outdoor Condition.

	October 2017/ ~ 90 days	**April 2018/ ~ 270 days**
Bacteria (CFU.mL-1)	**C37 (Coated Concrete)**	**C37 (Coated Concrete)**
Sulfate Reducing Bacteria (SRB)	115,000(A)	<1(NA)
Iron-Reducing Bacteria (IRB)	35,000(A)	<1(NA)
Acid Producing Bacteria (APB)	475,000(A)	82000(A)
Slime-Forming Bacteria (SFB)	1,750,000(A)	13,000(M)

NA: Not Aggressive, M: Moderately Aggressive and A: Aggressive. General guidelines for BART test for corrosion (Droycon Bioconcepts Inc. http://www.dbi.ca/).

Table 8.12. BART Test Results for Samples Exposed to US-41 Outdoor Condition.

	January 2018 / ~ 75 days	**July 2018 / ~ 240 days**
Bacteria (CFU.mL-1)	**E28 (Coated Concrete)**	**E28 (coated concrete)**
Sulfate Reducing Bacteria (SRB)	75 (M)	6,000(A)
Iron-Reducing Bacteria (IRB)	2,200(M)	35,000(A)
Acid Producing Bacteria (APB)	82,000(A)	475,000(A)
Slime-Forming Bacteria (SFB)	1,750,000(A)	1,750,000(A)

NA: Not Aggressive, M: Moderately Aggressive and A: Aggressive. General guidelines for BART test for corrosion (Droycon Bioconcepts Inc. http://www.dbi.ca/).

Table 8.13. BART Test Results for Samples Exposed to US-301 Outdoor Condition.

	July 2018 / ~ 180 days
Bacteria (CFU.mL-1)	**Q27 (Coated Concrete)**
Sulfate Reducing Bacteria (SRB)	500,000(A)
Iron-Reducing Bacteria (IRB)	140,000(A)
Acid Producing Bacteria (APB)	475,000(A)
Slime-Forming Bacteria (SFB)	1,750,000(A)

NA: Not Aggressive, M: Moderately Aggressive and A: Aggressive. General guidelines for BART test for corrosion (Droycon Bioconcepts Inc. http://www.dbi.ca/).

9. CONCLUSIONS

9.1. Summary of Chapter 4 Results

Test setup C serves as control testing in natural conditions to validate lab observations. The three sites included a saline (SR-312), brackish (US-41), and fresh (US-301) natural waters with different nutrient levels. All three sites had heavy marine fouling of different marine organisms. The SR-312 site had hard fouling from barnacle encrustations representing hard crevice environments and soft fouling from marine flora representing porous crevices. The US-41 and US-301 sites had hard fouling from barnacle encrustation that can create hard crevices. High SRB populations were measured under the hard and soft fouling. Other bacteria such as IRB, APB, and SFB were also detected at all three sites. Under the fouling encrustations, film and iron sulfide deposits were significant representing aggressive anaerobic corrosion by SRB. In this anaerobic SRB surface corrosion, notable features such as deep pits, surface corrosion, and smooth barnacle attachment surfaces were observed. Due to general corrosion in the natural waters and aggressive anaerobic SRB surface corrosion, significant nominal corrosion rates were calculated.

9.2. Summary of Chapter 5 Results

9.2.1. Test Setup A

9.2.1.1. Microbiological Activity

With pulse increments of SRB and nutrients, SRB activity can proliferate in environments that can support SRB growth. Important environmental conditions include low oxygen levels. In supporting environments, sulfate additions apparently was not required to enhance to enhance the SRB activity. In naturally aerated environments, the pulse increments of SRB and nutrients did not show proclivity to sustain SRB in open (non-crevice environments) and crevice environments, but additions of sulfate appeared to be beneficial in those cases.

9.2.1.2. Electrochemical Behavior

SRB activity can cause electrochemical potential ennoblement consistent with the mechanisms commonly associated with cathodic depolarization. Renewed SRB activity maintained ennobled potentials. Relatively low corrosion currents develop in the neutral pH de-aerated solutions, but SRB activity can result in higher corrosion currents. In de-aerated solutions with SRB activity, high cathodic currents due to enhanced hydrogen reduction as part of the biotic reduction of sulfate to sulfide by SRB were measured.

9.2.1.3. Corrosion Development

Significant general corrosion can occur in the neutral pH test solution. Surface corrosion pits developed in solutions with the early presence of sulfates (2,000 ppm sulfate) regardless of

SRB inoculation. However, pits also developed in the inoculated control samples with low level sulfates indicating effect by SRB. Anaerobic SRB surface hole corrosion was observed for the crevice samples.

9.2.2. Test Setup B

9.2.2.1. Microbiological Activity

SRB activity after solution inoculation showed enhanced sulfide levels that corresponded well to high COD levels. As expected, and similar to results from test setup A, SRB activity was higher in de-aerated solutions. Higher nutrient levels (40 mL compared to 20 mL Postgate B) prior to SRB inoculation did not show strong differentiation in SRB proliferation. SRB activity was shown to be better supported under porous crevices presumably due to greater nutrient availability and development of local low-level oxygen, even in naturally aerated bulk solutions. In de-aerated solutions, crevices also appeared to have positive effects to support SRB. No strong differentiation in SRB activity was observed for surface conditions with rougher texture (269 micron compared to 10 micron).

9.2.2.2. Electrochemical Behavior

As in test setup A, potential ennobled was associated with SRB activity. Even though potential ennoblement occurred due to hydrogen consumption as part of SRB activity, corrosion currents did not correspondingly increase due to the early development of SRB surface biofilm development and sulfide precipitation. These currents are not associated with corrosion mitigation but rather proclivity for localized corrosion.

9.2.2.3. Corrosion Development

Pitting was observed in the inoculated de-aerated solution but was more adverse in presence of high sulfate concentrations (2,000 ppm sulfates). Anaerobic SRB surface hole corrosion was observed in the hard crevice but not in the soft crevices. The soft crevice showed non-uniformly distributed spotted surface oxidation.

9.3. Summary of Chapter 6 Results

The water-based copper-free anti-fouling coating showed relatively better antifouling performance and less barnacle growth compared to polyurea coated steel samples and had generally lower surface bacteria populations (SRB, IRB, APB and SFB) over the time of exposure. The polyurea coating did not prevent marine growth from developing in any of the test conditions and significant barnacle attachment was observed by the earliest days of exposure. The observations showed that barnacle larva can settle on the polyurea coating regardless of its mechanical surface properties. Relatively smooth surface roughness could still allow for secure barnacle attachment; however larger barnacle plate sizes were observed at surfaces with higher roughness. Electrochemical results indicated poor barrier properties of the

two coatings. Corrosion potential for all samples were in the range for the plain steel corrosion potential and high corrosion current and very low impedance values (<500 ohm at 1Hz) was measured for all samples showing coating degradation by exposure time. Severe corrosion condition was observed for samples with heavy fouling formation, which implicate the adverse effect of immersion and macrofoulers growth on coating durability.
In lab testing, MIC due to SRB only occurred with the presence of coating defects that exposed the steel substrate. SRB could develop on polyurea. SRB was also shown to develop on the surface of the antifouling coating. There, surface degradation of the coating occurred. It was posed that local concentrations of antifouling agents may be reduced near the steel interface.

9.4. Summary of Chapter 7 Results

9.4.1. Field Site Testing

System potentials ~-1,000 mV_{CSE} developed with the coupling of commercially available zinc anodes to coupled steel arrays placed at the Matanzas river and Alafia river test sites.Current densities afforded to the steel array by the zinc anodes exceeded 30 mA/m^2. No major differentiation in CP current was observed between the heavy marine fauna and mature barnacles in Matanzas R. and the interlayered encrustation of barnacles at Alafia R.

Separate anode sites on the steel array could not be well differentiated by isolating current measurements. However, differentiation in CP current between sites gave indication of varying conditions of reduction reactions. The steel array at the Matanzas river. site was posed to have conditions where oxygen was not readily accessible to the steel substrate as well as less available cathode surfaces (possibly due to dense and tight coverage by marine fouling).

Both sites are aggressive in terms of corrosion development of submerged steel, but the free corrosion rate for submerged steel was higher at Matanzas river. site than Alafia river. site. Application of CP reduced the general apparent corrosion rate at both test sites. However, comparison of measured current to the apparent corrosion rate gave indication that there may be portions of the steel array submerged at Matanzas river. site that did not receive sufficient cathodic polarization. It was proposed that localized corrosion continue when marine fouling create local corrosion cells where regions are unprotected by CP.Proliferation of bacteria was not inhibited in the presence of cathodic polarization at ~-1,000 mV_{CSE}.

9.4.2. Laboratory Polarization Testing

Crevice environments reduce effectiveness of cathodic protection by decreasing the level of cathodic current in the occluded regions.Cathodic reactions related to SRB activity (sulfate reduction) is significant in the presence of cathodic polarization.Small lab geometries gave indication of positive effect of cathodic polarization to reduce SRB growth. However, SRB presence was maintained during the length of lab testing.Non-uniform cathodic polarization of steel developed for steel samples with crevice geometries. With the presence of cathodic polarization, irregular surface oxidation of steel developed for samples with crevice geometries

and was enhanced with the presence of SRB. Surface heterogeneities due to sulfide precipitates and biofilm also contribute in a similar manner even with presence of CP.SRB can proliferate even on steel anodic surfaces.

9.5. Summary of Chapter 8 Results

9.5.1. Laboratory Samples Results for Plain Concrete

9.5.1.1. Microbiological Activity

The stereo-microscope images confirmed concrete deterioration, characterized by a rougher surface (some cement paste degradation) combined with the presence of white products on top of the surfaces. It may be possible that the leaching of alkaline compounds from the concrete promoted deterioration, also combined with the SRB bacteria activity. The hard crevice cases didn't show the presence of white products (efflorescence) on top of the surface presumably due to fast buildup of alkaline solution within the occluded space as detected by high surface pH ~12.

Sulfide analysis confirmed the SRB activity in all the tested cases, with the highest values for the hard crevice environments. In general, COD values didn't give clear indication of SRB activity.

SRB sessile test confirmed the presence of SRB bacteria in all the inoculated tested cases. The highest SRB count were found for all non-aerated tested cases and the aerated case with hard crevice, indicating that SRB may be active even in environments with oxygen and it is more active in anoxic conditions, such as the hard crevice. The leaching of alkaline compounds from concrete pore solution to the exterior could be the cause of concrete deterioration observed.

9.5.1.2. Electrochemical and Resistivity Behavior

The impedance modulus decreased with time, indicating the degradation of the concrete dielectric properties with time. The non-inoculated cases showed higher resistivity values than the inoculated cases. Also, the highest values were observed for those samples with hard crevices, independently of the presence or absence of bacteria in the media. This indicates that the presence of bacteria in the test solution will influence in concrete resistivity, which is also related to concrete deterioration related to SRB presence.

9.5.2. Field Samples Results for Plain Concrete

The results of field samples served as control testing in natural conditions to validate lab observations. Three different outdoor exposure conditions were used for field testing: SR-312 (seawater), US-41 (brackish water) and US-301 (fresh water), all of them with different nutrient levels.

Visual photo-documentation of the samples surface with time confirmed the presence of flora and fauna on the concrete samples, of different species according to the environment, whose size and density was closely related to water depth and nutrients availability. The SR-312 site had hard fouling from barnacle encrustations representing hard crevice environments and soft fouling from marine flora representing porous crevices. The US-41 and US-301 sites had hard fouling from barnacle encrustation that can create hard crevices. BART test demonstrated to be a fast and easy test to determine bacteria presence in the samples surface. Resistivity and EIS measurements appeared to provide electrical characteristics consistent to the environmental exposure including salinity and immersion level.

9.5.3. Laboratory and Field Coated-concrete Specimen Results

In laboratory testing, formation of iron sulfide in the test solution and chemical oxygen demand (COD) trends provided indication of SRB activity. SRB sessile tests confirmed the presence of SRB in all the tested cases. Visual inspection of the coated concrete surface after immersion tests showed less surface degradation relative to the comparative plain concrete specimens in the test solutions. EIS initially showed large impedance with barrier coating characteristics; however, impedance values decreased with time and showed smaller values of pore resistances indicating moisture penetration. Testing did not elucidate the role of SRB on coating parameters.

Polyurea coatings didn’t prevent the formation of marine flora and fauna on the coated concrete samples, whose size and density was closely related to water depth and nutrients availability. The SR-312 site had hard fouling from barnacle encrustations and soft fouling from marine flora representing porous crevices. The US-41 and US-301 sites had hard fouling from barnacle encrustation that can create hard crevices. BART test confirmed that SRB, IRB, APB, and SFB bacteria could develop on the samples surface.

REFERENCES

Abdollahi, Hamid, and Julian WT Wimpenny. "Effects of oxygen on the growth of Desulfovibrio desulfuricans." *Microbiology*136.6 (1990): 1025-1030.

ACI 515-66 “Guide for the Protection of Concrete against Chemical Attack by Means of Coatings and Other Corrosion Resistant Materials”, Part 5 ACI, C., (1992). "201.2 R-92--Guide to Durable Concrete." American Concrete Institute.

Alam, Bashir, *et al*., (2012). "Sulphate Attack in High-Performance Concrete-A Review." International journal of Advanced Structures and Geotechnical Engineering, 1, p. 15-18.

Alcantara, S., (2004). “Sulfur formation by steady-state continuous cultures of a sulfoxidazing consortium and *Thiobacillus thioparus* ATCC 23645.” Environmental Technology 25, p. 1151–1157.

Al-Darbi, M. M., et al. "Control of microbial corrosion using coatings and natural additives." *Energy Sources* 24.11 (2002): 1009-1018.

ASTM G1-03(2017)” Standard Practice for Preparing, Cleaning, and Evaluating Corrosion Test Specimens”

Aviam, O., Bar-Nes, G., Zeiri, Y., Sivan, A., (2004). “Accelerated bio- degradation of cement by sulfur-oxidizing bacteria as a bioassay for evaluating immobilization of low-level radio-active waste”. Applied Environmental Microbiology 70, p. 6031-6036.

Ayoub, G., Azar, N., Fadel, M., Hamad, B., (2004). “Assessment of hydrogen sulphide corrosion of cementitious sewer pipes: A case study”. Urban Water Journal 1, p. 39−53.

Barlo. T.J and.Berry. W.E, material performance, (1984), p14

Barton, L.L. ,Tomei.F.A. "Characteristics and activities of sulfate-reducing bacteria." Sulfate-reducing bacteria. Springer US, 1(995):p.1-32.

Baumgärtner, M., et al. "Release of nitric oxide from building stones into the atmosphere." *Atmospheric Environment. Part B. Urban Atmosphere* 24.1 (1990): 87-92.

Beech, A.B., A. Mollica, H.-C. Flemming, V. Scotto, W. Sand. Simple methods for the investigation of the role of biofilms in corrosion. in Brite Euram Thematic Network on MIC of Industrial Materials. Task Group 1, Biofilm Fundamentals. 2000.

Beech, Iwona B., and Christine C. Gaylarde. "Recent advances in the study of biocorrosion: an overview." *Revista de microbiologia* 30.3 (1999): 117-190.

Beeldens, A., Monteny, J., Vincke, E., De Belie, N., Van Gemert, D., Taerwe, L., and Verstraete, W., (2001). “Resistance to biogenic sulphuric acid corrosion of polymer- modified mortars.” Cement and Concrete Composites 23, p. 47-56.

Bielefeldt, A., Gutierrez-Padilla, M.G.D., Ovtchinnikov, S., Silverstein, J., Hernandez, M., (2009). “Bacterial kinetics of sulfur oxidizing bacteria and their biodeterioration rates of concrete sewer pipe samples.” Journal of Environmental Engineering 136, p. 731–8.

Blackburn, Freeman E. "Non-Bioassay Techniques for Monitoring MIC." *CORROSION 2004*. NACE International, 2004.

Blackwood, C.S. Lim, S.L.M. Leo, X, Hu, J. Pang. "Macrofouling induced localized corrosion of stainless steel in Singapore seawater." *Corrosion Science* 129 (2017): 152-160.

Blackwood, D. J., C. S. Lim, and S. L. M. Teo. "Influence of fouling on the efficiency of sacrificial anodes in providing cathodic protection in Southeast Asian tropical seawater." *Biofouling* 26.7 (2010): 779-785.

Booth, G. H., and A. K. Tiller. "Polarization studies of mild steel in cultures of sulphate-reducing bacteria." *Transactions of the Faraday Society* 56 (1960): 1689-1696.

Borenstein, S.W., (1994). “Microbiologically influenced corrosion handbook.” (Abington Hall, England: Woodhead Publishing Ltd.), p. 288.

Bouillon, Jean, et al. An introduction to Hydrozoa. 2006.

Brady, Robert F. "Fouling-release coatings for warships." *Defence Science Journal* 55.1 (2005): 75.

Brancato, M. S., and R. M. Woollacott. "Effect of microbial films on settlement of bryozoan larvae (Bugula simplex, B. stolonifera and B. turrita)." *Marine Biology* 71.1 (1982): 51-56.

Broekaert. M. "Polyurea spray coatings." *The technology and latest developments. http://www. huntsman. com/portal/page/portal/polyurethanes* (2002).

Bryant, Richard D., and Edward J. Laishley. "The role of hydrogenase in anaerobic biocorrosion." *Canadian Journal of Microbiology* 36.4 (1990): 259-264.

BS 6349: Part 1: (2000), “Maritime structures. Code of practice for general criteria”.

Castaneda, H., and Benetton, X.D., (2008). "SRB-biofilm influence in active corrosion sites formed at the steel-electrolyte interface when exposed to artificial seawater conditions," Corrosion Science 50, p. 1169–1183.

Cayford, B., Dennis, P., Keller, J., Tyson, G., Bond, P., (2012). “High- throughput amplicon sequencing reveals distinct communities within a corroding concrete sewer system.” Applied and Environmental Microbiology 78, p. 7160−7162.

Chambers, Lily D., et al. "Modern approaches to marine antifouling coatings." *Surface and Coatings Technology* 201.6 (2006): 3642-3652

Characklis, W. G. "Fouling biofilm development: a process analysis."*BIOTECHNOLOGY AND BIOENGINEERING* 102.2 (2009), p. 310-347.

Chess, Paul M., and John P. Broomfield, eds. *Cathodic protection of steel in concrete*. CRC Press, 2003.

Clapp, W. P. "Macro-organisms in sea water and their effect on corrosion." *The corrosion handbook. New York: John Wiley & Sons, Inc* (1948): 433À41.

Costello, J. A. "Corrosion Of Metals By Micro-Organisms A Literature Survey." *International Biodeterioration Bulletin* 5.3 (1969): 101.

Costerton, J. W., and G. G. Geesey. "The microbial ecology of surface colonization and of consequent corrosion." *Biologically Influenced Corrosion, Gaithersburg, MD, National Association of Corrosion Engineers, Paper* 223 (1986).

Costerton, J. William, and J. Boivin. "Biofilms and corrosion." *Biofouling and Biocorrosion in industrial water systems*. Springer Berlin Heidelberg, 1991. 195-204.

Crisp, "Factors influencing the settlement of marine invertebrate larvae." Chemoreception in Marine Organisms, (1974): 177-265.

Cwalina, B., (2008). "Biodeterioration of concrete." Architecture Civil Engineering Environment 1, p. 133-140.

De Brito, L.V. Coutinho, R. Cavalcanti, E.H. Benchimol. M. "The influence of macrofouling on the corrosion behaviour of API 5L X65 carbon steel." Biofouling 23.3 (2007):193-201.

de Romero, M., Ocando, L., de Rincón, O., Parra, J., Ruiz, R., Bracho, M., ... & Quintero, A. (2006, January). Cathodic Polarization effect on sessile SRB growth and iron protection. In *CORROSION 2006*. NACE International.

de Romero, Matilde F., et al. "Evaluation of Cathodic Protection in presence of Sulfate Reducing Bacteria mixed cultures." *CORROSION 2008* (2008).

de Romero, Matilde, Oladis De Rincon, and Lisseth Ocando. "Cathodic protection efficiency in the presence of SRB: State of the art." *CORROSION 2009*. NACE International, 2009.

Dexter, S.C., and La Fontaine, J.P., (1998). "Effect of natural marine biofilms on galvanic corrosion," Corrosion 54, p. 851-861.

Dickinson, W. H., and Z. Lewandowski. "Manganese biofouling and the corrosion behavior of stainless steel." *Biofouling* 10.1-3 (1996): 79-93.

Dickinson, W. H., Z. Lewandowski, and R. D. Geer. "Evidence for surface changes during ennoblement of type 316L stainless steel: Dissolved oxidant and capacitance measurements." *Corrosion* 52.12 (1996): 910-920.

Diercks, M., Sand, W., Krumbein, E., (1991) “Microbial corrosion of concrete.” Experientia 47, p. 514-516.

Dilling, Waltraud, and Heribet Cypionka. "Aerobic respiration in sulfate-reducing bacteria." *FEMS Microbiology Letters* 71.1-2 (1990): 123-127.

Donham, J. E., et al. "The Role of Bacteria in the Corrosion of Oil Field Equipment." *TPC Publication* 3 (1976).

Duana, J., Wua, S., Zhanga, X., Huangb, G., Duc, M., Houa, B., (2008). “Corrosion of carbon steel influenced by anaerobic biofilm in natural seawater.” Electrochimica Acta, 54, p. 22–28.

Eashwa, M. Subramanian G., Chandrasekaran P., Balakrishnan. K. "Mechanism for barnacle-induced crevice corrosion in stainless steel." Corrosion 48.7 (1992): 608-612.

Eashwar, M. Subramanian, G. and Chandrasekaran. P. "Marine fouling and corrosion studies in the coastal waters of Mandapam, India." Bulletin of Electrochemistry 6.08 (1990): 699-702.

Eashwar, M., Subramanian, G., Chandrasekaran, P., Manickam, S. T., Maruthamuthu, S., & Balakrishnan, K. (1995). The interrelation of cathodic protection and marine macrofouling. *Biofouling*, *8*(4), 303-312.

Edyvean, R. G. J., L. A. Terry, and G. B. Picken. "Marine fouling and its effects on offshore structures in the North Sea. A review." *International biodeterioration* 21.4 (1985): 277-284.

Egan, et al. "Correlation between pigmentation and antifouling compounds produced by Pseudoalteromonas tunicata." Environmental Microbiology 4.8 (2002), p. 433-442.

Enos, D.G., Taylor, S.R., (1996). "Influence of sulfate-reducing bacteria on alloy 625 and austenitic stainless steel weldments," Corrosion, 52, p. 831-842.

Eštokov, A., *et al*., (2012). "Study of the deterioration of concrete influenced by biogenic sulphate attack." Procedia Engineering 42, p.1731-1738.

F.L. LaQue, "Topics for research in marine corrosion." Canada. Materials Performance 21.4 (1982):p. 13-18.

Feio, M. J., et al. "The influence of the Desulfovibrio desulfuricans 14 ATCC 27774 on the corrosion of mild steel." *Materials and Corrosion* 51.10 (2000): 691-697.

Fischer, K. P. "Cathodic protection in saline mud containing sulfate reducing bacteria." *Mater. Perform.* 20 (1981): 41.

Flemming, Hans-Curt, et al., eds. *Marine and industrial biofouling*. Springer Berlin Heidelberg, 2009.
Fofonoff PW, Ruiz GM, Steves B, & Carlton JT. 2003. National Exotic Marine and Estuarine Species Information System." http://invasions.si.edu/nemesis/. "
Fonseca, Inês TE, et al. "The influence of the media on the corrosion of mild steel by Desulfovibrio desulfuricans bacteria: an electrochemical study." *Electrochimica Acta* 43.1 (1998): 213-222.
Fritsch, Felix Eugene. The structure and reproduction of the algae. At The University Press; Cambridge, 1948
Gandy, Anthony F., and Elizabeth T. Gandy. *Microbiology for environmental scientists and engineers*. McGraw-Hill, 1980.
Gaylarde, C., Ribas, M., and Warscheid, Th., (2003). "Microbial impact on building materials: an overview." Materials and Structures 36, p. 342-352.
Geesey, G.G., Biofilm formation, in A practical manual on microbiologically influenced corrosion, G. Kobrin, Editor. 1993, NACE: Houston, TX, USA.
Geesey, J.W., *et al*., (1986). "The microbial ecology of surface colonization and of consequent corrosion", in Biologically Influenced Corrosion (NACE reference book 8), S.C. Dexter, Editor. (Houston, TX: NACE).
Gehrke, T. and Sand, W., (2003). "Interactions between Microorganisms and Physicochemical factors Cause MIC of Steel Pilings In Harbors (ALWC)." Corrosion/2003, Paper No. 03557, NACE International, Houston, TX).
Gu, J.D., Ford, T.E., Berke, N.S., Mitchell, R., (1998). "Biodeterioration of concrete by the fungus *Fusarium*." International Biodeterioration &Biodegradation, 41, p. 101–109.
Gubner, Rolf J., and Iwona B. Beech. "Statistical assessment of the risk of the accelerated low-water corrosion in the marine environment." *CORROSION 99*. NACE International, 1999.
Gutierrez-Padilla, Ma. *et al*., (2007). "Monitoring of microbially induced concrete corrosion in pipelines." Corrosion 2007. NACE International, 2007.
H.C. Flemming, et al., eds. *Marine and industrial biofouling*. Springer Berlin Heidelberg, 2009.
Haile, T., Nakhla, G., Allouche, E., and Vaidya, S., (2009). "Evaluation of the bactericidal characteristics of nano-copper oxide or functionalized zeolite coating for bio-corrosion control in concrete sewer pipes*."* Corrosion Science, 50, p. 713-720.
Hamilton, W. A. "Microbially influenced corrosion as a model system for the study of metal microbe interactions: a unifying electron transfer hypothesis." *Biofouling* 19.1 (2003): 65-76.
Hao, Oliver J., et al. "Sulfate-reducing bacteria." *Critical reviews in environmental science and technology* 26.2 (1996): 155-187.
Hardy, J. A.; Hamilton, W. A. (1981). "The oxygen tolerance of sulfate-reducing bacteria isolated from the North Sea waters." C~rr.i.entMicrobiology, 6, pp259-262.
Hellio, et al. "Natural marine products with antifouling activities." Advances in marine antifouling coatings and technologies. (2009), p 572-622.
Herrera, L.K., and Videla, H.A., (2009). "Role of iron-reducing bacteria in corrosion and protection of carbon steel." International Biodeterioration & Biodegradation, 63, p. 891–895.

Hodgkiess, T., and A. Nevilie. *Localized effects of macrofouling species on electrochemical corrosion of high grade alloys*. No. CONF-980316-. NACE International, Houston, TX (United States), 1998

Horvath, J., and Mihaly Novak. "Potential/pH equilibrium diagrams of some Me-S-H2O ternary systems and their interpretation from the point of view of metallic corrosion." *Corrosion Science* 4.1-4 (1964): 159-178.

Houghton, D. R. "Marine fouling and offshore structures." *Ocean Management* 4.2-4 (1978): 347-352.

Hu, An. *Investigation of sulfate-reducing bacteria growth behavior for the mitigation of microbiologically influenced corrosion (MIC)*. Diss. Ohio University, 2004.

Islander, R.L, Devinny, J.S., Mansfeld, F., Postyn, A., Shih, H., (1991). “Microbial ecology of crown corrosion in sewers.” Journal of Environmental Engineering, 117, p, 751-770.

Iversen, Anna. "MIC on Stainless Steels in Wastewater Treatment Plants-Field Tests and a Risk Assessment." *CORROSION 2002*. NACE International, 2002.

Jack, T. R., et al. *Evaluation of coating performance after exposure to biologically active soils*. No. CONF-950304-. NACE International, Houston, TX (United States), 1995.

Jack, Thomas R., et al. "External corrosion of line pipe--A summary of research activities." *Materials performance* 35.3 (1996).

Javaherdashti, C.Nwaoha, and H. Tan, eds. Corrosion and materials in the oil and gas industries. CRC Press, (2013).

Javaherdashti, R., (1999). "A review of some characteristics of MIC caused by sulphate reducing bacteria: Past, present and future," Anticorrosion Methods and Materials, 46, p.173-180.

Javaherdashti, R., (2008). “Microbiologically Influenced Corrosion. An Engineering Insight.” (London, England: Springer-Verlag), p. 164.

Javaherdashti, Reza, Chikezie Nwaoha, and Henry Tan, eds. *Corrosion and materials in the oil and gas industries*. CRC Press, 2013.

Javaherdashti, Reza. *Microbiologically influenced corrosion: an engineering insight*. Springer, 2016.

Javaherdashti, Reza. *Microbiologically influenced corrosion: an engineering insight*. Springer Science & Business Media, 2008.

Jayaraman, A., Earthman, J.C., Wood, T.K., (1997). “Corrosion inhibition by aerobic biofilms on SAE 1018 steel.” Applied Microbiology and Biotechnology, 47, p. 62–68.

Jayaraman, A., *et al*., (1997b). "Axenic aerobic biofilms inhibit corrosion of SAE 1018 steel through oxygen depletion." Applied microbiology and biotechnology, 48, p. 11-17.

Jayaraman, A., Sun, A.K. and Wood. T. K., (1998). "Characterization of axenic Pseudomonas fragi and Escherichia coli biofilms that inhibit corrosion of SAE 1018 steel." Journal of Applied Microbiology, 84, p. 485-492.

Jones, J., B. Little, and F. Mansfeld. "ESEM/EDS, SEM/EDS and EIS studies of coated 4140 steel exposed to marine, mixed microbial communities including SRB." *International Power Generation Conference, Atlanta-Georgia*. 1992.

Jones-Meehan, Joanne, et al. *Advanced Nontoxic Fouling Release Coatings*. No. NRL/PU/6110--99-388. NAVAL RESEARCH LAB WASHINGTON DC, 1999.

Kazuyuki, T., and Kawamura, M., (1994). "Effects of fly ash and silica fume on the resistance of mortar to sulfuric acid and sulfate attack." Cement and Concrete Research, 24, p. 361-370.

Keough, Michael J., and Peter T. Raimondi. "Responses of settling invertebrate larvae to bioorganic films: effects of different types of films." *Journal of Experimental Marine Biology and Ecology* 185.2 (1995): 235-253

Keough. M.J. and Raimondi. P.T.. "Responses of settling invertebrate larvae to bioorganic films: effects of different types of films." Journal of Experimental Marine Biology and Ecology, 185.2 (1995): 235-253

Kobrin, G., Corrosion by microbiological organisms in natural water. Material Performance, 1976. 15.

Kuehr C. von Wolzogen, (1923). “Water and Gas”, Corrosion, 26, 277-282.

Lamond, J.F., (2006). “Significance of tests and properties of concrete and concrete-making materials STP 169D.” P (256-258), ASTM International.

Lau, Stanley CK, et al. "Bioactivity of bacterial strains isolated from marine biofilms in Hong Kong waters for the induction of larval settlement in the marine polychaete Hydroides elegans." *Marine Ecology Progress Series* 226 (2002): 301-310.

Lee, Anthea K., Martin G. Buehler, and Dianne K. Newman. "Influence of a dual-species biofilm on the corrosion of mild steel." *Corrosion Science* 48.1 (2006): 165-178.

Lee, W. *et al*., (1995). "Role of Sulfate-reducing Bacteria in Corrosion of Mild Steel: a Review," Biofouling 8, p.165-168.

Lehaitre, M. Delauney, L. and Compère. C. "Biofouling and underwater measurements." Real-time observation systems for ecosystem dynamics and harmful algal blooms: Theory, instrumentation and modelling. Oceanographic Methodology Series. UNESCO, Paris (2008), p. 463-493.

Lehaitre, M., L. Delauney, and C. Compère. "Biofouling and underwater measurements." *Real-time observation systems for ecosystem dynamics and harmful algal blooms: Theory, instrumentation and modelling. Oceanographic Methodology Series. UNESCO, Paris* (2008): 463-493.

Lin, Johnson, and Bafana B. Madida. "Biofilms affecting progression of mild steel corrosion by Gram positive Bacillus sp." *Journal of basic microbiology* 55.10 (2015): 1168-1178.

Linda Z. Holland, ”Tunicates”, current biology, Volume 26, Issue 4, 22 February 2016, Pages R146–R152

Ling, A.L., *et al*. (2014). "Carbon dioxide and hydrogen sulfide associations with regional bacterial diversity patterns in microbially induced concrete corrosion." Environmental Science & Technology, 48, p. 7357-7364.

Linhardt, P., (2006). "MIC of Stainless Steel in Freshwater and the Cathodic Behaviour of Biomineralized Mn-Oxides," Electrochimica Acta, 12, p. 6081-6084.

Littauer, E., and D. M. Jennings. "The prevention of marine fouling by electrical currents." *Proc. 2nd Int. Congress on Marine Corrosion and Fouling*. 1968.

Little, B. J. "A perspective on the use of anion ratios to predict corrosion in Yucca Mountain." *Corrosion* 59.8 (2003): 701-704.

Little, B. J. and Lee, J.S., (2014). "Microbiologically influenced corrosion: An Update," International Materials Reviews, 59, p.384-393.

Little, B., P. Wagner, and D. Duquette. "Technical note: microbiologically induced increase in corrosion current density of stainless steel under cathodic protection." *Corrosion* 44.5 (1988): 270-274.
Little, B., Wagner, P., Mansfeld, F., (1991). “Microbiologically influenced corrosion of metals and alloys”. International Materials Reviews, 36, p. 253-272.
Little, B.J. Lee, J.S., (2007). in: R.W. Revie (Ed.), “Microbially Influenced Corrosion”, Wiley Series in Corrosion, Wiley, Hoboken.
Little, B.J., Lee, J.S., Ray, R.I., (2015). “Diagnosing microbiologically influenced corrosion: A state of the art review”, B.J. Little, J.S. Lee and R.I. Ray, taken from the Book, Introduction to managing microbiologically influenced corrosion, Editor: Richard Bruce Eckert, NACE International, Houston, TX.
Little, Brenda J., and Jason S. Lee. "Microbiologically influenced corrosion." *Kirk-Othmer Encyclopedia of Chemical Technology* (2009).
Little, Brenda J., and Jason S. Lee. "Microbiologically influenced corrosion: an update." *International Materials Reviews* 59.7 (2014): 384-393.
Little, Brenda J., and Patricia A. Wagner. *The interrelationship between marine biofouling and cathodic protection*. No. NRL/PP/7333--92-0002. NAVAL RESEARCH LAB STENNIS SPACE CENTER MS, 1993.
Little, Brenda, et al. *The role of metal-reducing bacteria in microbiologically influenced corrosion*. No. CONF-970332--. NACE International, Houston, TX (United States), 1997.
Little, Brenda, Patricia Wagner, and Florian Mansfeld. "An overview of microbiologically influenced corrosion." *Electrochimica acta* 37.12 (1992): 2185-2194.
Little, et al. Microbiologically Induced Corrosion, New York: John Wiley & Sons Inc. (2007)
Little, J.L., Microbiologically influenced corrosion: An Update. International Materials Reviews, 2014. 59.
Little, J.S.L., Microbiologically Induced Corrosion. 2007, New York: John Wiley & Sons Inc.
Liu, H., Xu, L., Zeng, J., (2000). "Role of corrosion products in biofilms in microbiologically induced corrosion of carbon steel," British Corrosion Journal, 35, p. 131-135.
Maki, J. S., et al. "Inhibition of attachment of larval barnacles, Balanus amphitrite, by bacterial surface films." *Marine Biology* 97.2 (1988): 199-206.
Mansfeld, F., (2007). "The interaction of bacteria and metal surfaces," Electrochimica Acta 52, p.7485-7488.
Mansfeld, F., and Little, B., (1992). “Electrochemical techniques applied to studies of microbiologically influenced corrosion (MIC), Trends in Electrochemistry”. Book, (http://www.dtic.mil/dtic/tr/fulltext/u2/a268497.pdf).
Mansfeld, F., The interaction of bacteria and metal surfaces. Electrochimica Acta 2007. 52.
Mansfield, C.C. Lee, L.T. Han, G. Zhang, X. Xiao, J. Jones-Meehan, B.J. Little, P. Wagner, R. Ray, J. Jones-Meehan. *The Impact of Microbiologically Influenced Corrosion on Protective Polymer Coatings*. University of Southern California Los Angeles Dept of Materials Science and Engineering, 1998.
Marquez, J.F., Sanchez-Silva, M., and Husserl, J. (2013). "Review of reinforced concrete biodeterioration mechanisms." Proceedings, 8th international conference on fracture mechanics of concrete and concrete structures, Toledo, Spain. Vol. 9.

Maruthamuthu, S., Eashwar, M., Manickam, S. T., Ambalavanan, S., Venkatachari, G., & Balakrishnan, K. (1990). Marine fouling on test panels and in-service structural steel in Tuticorin harbour.

Melchers, R. E. "Effect of nutrient-based water pollution on the corrosion of mild steel in marine immersion conditions." *Corrosion* 61.3 (2005): 237-245.

Melchers, R. E. "Modelling immersion corrosion of structural steels in natural fresh and brackish waters." *Corrosion Science* 48.12 (2006): 4174-4201.

Melchers, R. E. "The effects of water pollution on the immersion corrosion of mild and low alloy steels." *Corrosion Science* 49.8 (2007): 3149-3167.

Melchers, R. E., and Jeffrey, R.J., (2013). "Accelerated low water corrosion of steel piling in harbors," Corrosion Engineering, Science and Technology, 48, p. 496-505.

Melchers, R. E., and R. J. Jeffrey. "Accelerated low water corrosion of steel piling in harbours." *Corrosion Engineering, Science and Technology* 48.7 (2013): 496-505.

Melchers, Robert E. "Long-term immersion corrosion of steels in seawaters with elevated nutrient concentration." *Corrosion Science* 81 (2014): 110-116.

Melchers, Robert E., and Robert Jeffrey. "Corrosion of long vertical steel strips in the marine tidal zone and implications for ALWC." *Corrosion Science* 65 (2012): 26-36.

Milde, K., Sand, W., Wolff, W., Bock, E., (1983). "Thiobacilli of the corroded concrete walls of the Hamburg sewer system." Journal of General Microbiology, 129, p.1327–1333.

Millero, Frank J. "The thermodynamics and kinetics of the hydrogen sulfide system in natural waters." *Marine Chemistry* 18.2-4 (1986): 121-147.

Minteny, E., Vincke, E., Beeldens, A., Belie, N.D., Taewe, L., Gemert, D.V., Verstraete, W., (2000). "Chemical, microbiological, and in situ test methods for biogenic sulfuric acid corrosion of concrete." Cement Concrete Research, 30, p. 623-634.

Mohanty, S. S., et al. "Kinetics of SO4− 2 reduction under different growth media by sulfate reducing bacteria." *BioMetals* 13.1 (2000): 73-76.

Mori, T., Nonaka, T., Tazaki, K., Koga, M., Hikosaka, Y., Noda, S., (1992). "Interactions of nutrients, moisture, and pH on microbial corrosion of concrete sewer pipes." Water Research, 26, p. 29−37.

Moser, R.D., *et al*., (2014). "An Investigation of Concrete Deterioration at South Florida Water Management District Structure S65E. No. ERDC/GSL-TR-14-4." Engineer Research and Development Center Vicksburg Ms Geotechnical and Structures Lab.

Moulin, J.M., Marsh, E., Chau, W.T., Karius, R., Beech, I.B., Gubner, R., Raharinaivo, A., (2001). "Prevention of accelerated low corrosion on steel piling structures due to microbially influenced corrosion mechanisms", Report EUR 20043 EN, 2001, ECSC Steel Publications, European Commission, B-1049 Brussels.

Muntasser, Zeiad, et al. "Prevention of microbiologically influenced corrosion using coatings." *CORROSION 2002*. NACE International, 2002.

Myers, Charles R., and Kenneth H. Nealson. "Bacterial manganese reduction and growth with manganese oxide as the sole electron acceptor." *Science* 240.4857 (1988): 1319.

NACE standard,TM0194-2014 "Field Monitoring of Bacterial Growth in Oil and Gas Systems" ISBN: 1-57590-192-7

Narayan, Roger, Susmita Bose, and Amit Bandyopadhyay, eds. *Biomaterials Science: Processing, Properties and Applications II: Ceramic Transactions*. Vol. 237. John Wiley & Sons, 2012.

Neville, T. Hodgkiess. "Comparative study of stainless steel and related alloy corrosion in natural sea water." British Corrosion Journal 33.2 (1998): 111-120.

Newman, et al. "Pitting of stainless steels by thiosulfate ions." *Corrosion* 45.4 (1989), p. 282-287.

Newman, R. C., B. J. Webster, and R. G. Kelly. "The electrochemistry of SRB corrosion and related inorganic phenomena." *ISIJ international* 31.2 (1991): 201-209.

Nica, D., *et al*., (2000). "Isolation and Characterization of Microorganisms Involved in the Biodeterioration of Concrete in Sewers." International Biodeterioration and Biodegradation, 46, p. 61-68.

Nielsen, A.H., *et al*., (2005). "Simulation of sulfide buildup in wastewater and atmosphere of sewer networks." Water science and technology, 52, p. 201-208.

O. de Rincon ,E. Morris. "Studies on selectivity and establishment of "Pelo de Oso"(Garveia franciscana) on metallic and non-metallic materials submerged in Lake Maracaibo, Venezuela." Anti-corrosion methods and materials 50.1 (2003): 17-24.

Obuekwe, Christian O., et al. "Surface changes in mild steel coupons from the action of corrosion-causing bacteria." *Applied and environmental microbiology* 41.3 (1981): 766-774.

O'Connor, Nancy J., and Donnia L. Richardson. "Attachment of barnacle (Balanus amphitrite Darwin) larvae: responses to bacterial films and extracellular materials." *Journal of Experimental Marine Biology and Ecology* 226.1 (1998): 115-129.

O'Connor, Nancy J., and Donnia L. Richardson. "Effects of bacterial films on attachment of barnacle (Balanus improvisus Darwin) larvae: laboratory and field studies." *Journal of Experimental Marine Biology and Ecology* 206.1-2 (1996): 69-81.

O'Dea, V., (2007). "Coatings & linings - understanding biogenic sulfide corrosion." Materials Performance, 46, p. 36-39.

O'Dell, J. W. "The determination of chemical oxygen demand by semi-automated colorimetry, method 410.4." *Cincinnati, Ohio: Environmental Monitoring Systems Laboratory, Office of Research and Development, US Environmental Protection Agency* (1993).

Odom, J. M. "Industrial and environmental activities of sulfate-reducing bacteria." *The sulfate-reducing bacteria: Contemporary perspectives*. Springer New York, 1993. 189-210.

Okabe, S., Odagiri, M., Ito, T., Satoh, H., (2007). "Succession of Sulfur-Oxidizing bacteria in the microbial community on corroding concrete in sewer systems" Applied and Environmental Microbiology, 73, p. 971-980.

Olivares, Geraldo Zavala, et al. "Sulfate Reducing Bacteria Influence on the Cathodic Protection of Pipelines That Transport Hydrocarbons." *CORROSION 2003*. NACE International, 2003.

Olivares, Geraldo Zavala, et al. "Sulfate Reducing Bacteria Influence on the Cathodic Protection of Pipelines That Transport Hydrocarbons." *CORROSION 2003*. NACE International, 2003.

Olmstead, W., Hamlin, H., (1900). "Converting portions of the Los Angeles outfall sewer into a septic tank", Engineering News, 44, p.317– 318.

Palanichamy, S. ,Subramanian. G. "Hard foulers induced crevice corrosion of HSLA steel in the coastal waters of the Gulf of Mannar (Bay of Bengal), India." Journal of Marine Science and Application 13.1 (2014): 117-126.

Palraj, S., and G. Venkatachari. "Corrosion and bio fouling characteristics of mild steel in Mandapam waters." *Materials performance* 45.6 (2006): 46-50.

Palraj,S, Venkatachari, G.and Subramanian. G. "Bio-fouling and corrosion characteristics of 60/40 brass in Mandapam waters." Anti-Corrosion Methods and Materials 49.3 (2002):194-198.

Parker, C.D., (1945). "The Corrosion of Concrete 2. The Function of *Thiobacillus concretivorus* (Nov. Spec.) in The Corrosion of Concrete Exposed To Atmospheres Containing Hydrogen Sulphide." Australian Journal of Experimental Biology & Medical Science, 23, p. 91-97.

PCA, (2002). “Types and causes of concrete deterioration.” Portland Cement Association, IS536, p. 1-16.

Pedersen, A., Hermansson, M., (1991). “Inhibition of metal corrosion by bacteria.” Biofouling, 3, p. 1–11.

Pipe, "North Sea fouling organisms and their potential effects on the corrosion of North Sea structures." Marine Corrosion of Offshore Structures*, 1981,* (1981), p. 13-22.

Postage, J.R, the sulphate reducing bacteria, 2nd ed, (Cambridge, England, Cambridge university Press, (1984)

Potekhina, J.S., Sherisheva, N.G., Povetkina, L.P., Pospelov, A.P., Rakitina, T.A., Warnecke, F., Gottschal Sahar k, G., (1999). “Role of microorganisms in corrosion inhibition of metals in aquatic habitats.” Applied Microbiology and Biotechnology, 52, p. 639–646.

Rajakaruna, P. S. (2010). Microbial Deterioration of Concrete Infrastructure. (Thesis). Oklahoma State University. Retrieved from http://hdl.handle.net/11244/10161

Rajasekar, Y.T., Role of Inorganic and Organic Medium in the Corrosion Behavior of Bacillus megaterium and Pseudomonas sp. in stainless steel SS 304. Industrial and Engineering Chemistry Research, 2011. 50.

Ray, R. Lee, J., Little, B., (2009). "Factors contributing to corrosion of steel pilings in Duluth-Superior Harbor," Corrosion, 65, p. 707-717.

Ribas, M., (1993). “Study of concrete deterioration through its microstructure”, Materiales de Construccion, 43, p. 15-24.

Rim-Rukeh, A., and G. Irerhievwie. "Estimation of microbiologically influenced corrosion of X60 steel exposed to a natural freshwater environment." *Journal of Emerging Trends in Engineering and Applied Sciences* 3.6 (2012): 953-958.

Rincon, O. and Morris, E. (2003), “Studies on selectivity and establishment of ‘Pelo de Oso’ (*Garveia franciscana*) on metallic and non-metallic materials submerged in Lake Maracaibo, Venezuela”, *Anti-Corrosion Methods and Materials*, Vol. 50 No. 1, pp. 17-24.

Roberts, D. Rittschof, E. Holm, A.R, Schmidt. "Factors influencing initial larval settlement: temporal, spatial and surface molecular components." Journal of Experimental Marine Biology and Ecology 150.2 (1991): 203-221.

Rogers, R.D., (1995). "Assessment of the Effects of Microbially Influenced Degradation on a Massive Concrete Structure Final Report." (1995).

Salvago, et al. "A statistical evaluation of AISI 316 stainless steel resistance to crevice corrosion in 3.5% NaCl solution and in natural sea water after pre-treatment in HNO3." *Corrosion science* 27.9 (1987):p.927-936.

Sanchez-Silva, M., and Rosowsky, D.V., (2008). "Biodeterioration of construction materials: state of the art and future challenges." Journal of Materials in Civil Engineering, 20, p. 352-365.

Sand, W., (1987). “Importance of hydrogen sulfide, thiosulfate, and methylmercaptan for growth of *Thiobacilli* during simulation of concrete corrosion.” Australian Journal of Experimental Biology 23, p. 93-98

Sand, W., (2008). "Microbial corrosion and its inhibition." Biotechnology Set, Second Edition, p. 265-316.

Sand, W., and Bock, E., (1991). "Biodeterioration of mineral materials by microorganisms—biogenic sulfuric and nitric acid corrosion of concrete and natural stone." Geomicrobiology Journal, 9, p. 129-138.

Sanders, P. F. "M0nit0ring And C0ntr0l 0f Sessile Microbes: Cost Effective Ways T0 Reduce Microbial Corrosion." *Microbial Corrosion-1* 1 (1988): 191.

Sanders, P. F., and S. Maxwell. "Microfouling, macrofouling and corrosion of metal test specimens in seawater." *Microbial Corrosion* (1983): 74-83.

Sangeetha., et al. "Understanding the structure of the adhesive plaque of Amphibalanus reticulatus." Materials Science and Engineering: C 30.1 (2010): p.112-119.

Santo Domingo, J.W., *et al*., (2011). "Molecular survey of concrete sewer biofilm microbial communities." Biofouling, 27, 993-1001.

Schippers, Axel, T. Rohwerder, and Wolfgang Sand. "Intermediary sulfur compounds in pyrite oxidation: implications for bioleaching and biodepyritization of coal." *Applied microbiology and biotechnology* 52.1 (1999): 104-110.

Scott, P. J. B. "Expert consensus on MIC: failure analysis and control." *Materials performance* 43.4 (2004): 46-50.

Shreir, L.L., 1963, "The Microbiology of Corrosion," Corrosion,1,Wiley,J.,New York,pp 252-264

Soleimani, S., (2012). “Prevention and control of microbiologically influenced concrete deterioration in wastewater concrete structures using *E. coli* biofilm.”

Soracco, R. J., et al. *Microbiologically influenced corrosion investigations in electric power generating stations*. No. CONF-880314--. Houston, TX; National Assoc. of Corrosion Engineers, 1988.

Starkey, R.L. (1935). "Products of the oxidation of thiosulfate by bacteria in mineral media." The Journal of general physiology, 18, p. 325-349.

Stoodley, Paul, et al. "Influence of hydrodynamics and nutrients on biofilm structure." *Journal of applied microbiology* 85.S1 (1998).

Subramanian, and S. Palanichamy. "Influence of fouling assemblage on the corrosion behaviour of mild steel in the coastal waters of the Gulf of Mannar, India." *Journal of Marine Science and Application* 12.4 (2013), p. 500-509

Swain, G. W., and J. Patrick-Maxwell. "The effect of biofouling on the performance of Al-Zn-Hg sacrificial anodes." *Corrosion* 46.3 (1990): 256-260.

Taylor, K.B., (2003). “Hydrogen Sulfide and Microbiologically Induced Corrosion of Concrete, Steel and Ductile Iron in Waste Water Facilities” NACE-03060, Corrosion, 16-20 March, San Diego, California.

Thiyagarajan, V. "A review on the role of chemical cues in habitat selection by barnacles: new insights from larval proteomics." Journal of Experimental Marine Biology and Ecology 392.1 (2010): 22-36.

Tomlinson, Michael, and John Woodward. *Pile design and construction practice*. CRC Press, 2014

Trejo, David, et al. "Analysis and assessment of microbial biofilm-mediated concrete deterioration." *Texas Transportation Institute, Texas, USA* 26 (2008).

Unabia, C. R. C., and M. G. Hadfield. "Role of bacteria in larval settlement and metamorphosis of the polychaete Hydroides elegans." *Marine Biology* 133.1 (1999): 55-64.

Videla, H.A., (1996). “Manual of biocorrosion,” ed. K. McCombs. (USA: CRC Press, Inc.)

Videla, H.A., (2002). "Prevention and control of biocorrosion." International Biodeterioration & Biodegradation, 49, p. 259-270.

Videla, H.A., (2002). "Prevention and control of biocorrosion." International Biodeterioration & Biodegradation, 49, p. 259-270.

Videla, H.A., and Herrera, L.K., (2009). "Understanding microbial inhibition of corrosion. A comprehensive overview," International Biodeterioration & Biodegradation, 63, p. 891–895.

Videla, H.A., Herrera, L.K., and Edyvean, R.G.J., (2005). "An Updated Overview of SRB Induced Corrosion and Protection of Carbon Steel, CORROSION/2005, Paper No. 488." NACE International, Houston, TX.

Videla, H.A., Manual of biocorrosion, ed. K. McCombs. 1996, USA: CRC Press, Inc.

Videla, Hector A., Liz Karen Herrera, and G. Edyvean. "An updated overview of SRB induced corrosion and protection of carbon steel." *CORROSION 2005*. NACE International, 2005.

Vincke, E., Boon, N. and Verstraete, W., (2001). "Analysis of the microbial communities on corroded concrete sewer pipes–a case study." Applied Microbiology and Biotechnology, 57, p. 776-785.

VR de Messano, et al. "Evaluation of biocorrosion on stainless steels using laboratory-reared barnacle Amphibalanus amphitrite." Anti-Corrosion Methods and Materials 61.6 (2014): 402-408.

VR. de Messano, L. Sathler, L. Reznik, LYl. Coutinho, R.. "The effect of biofouling on localized corrosion of the stainless steels N08904 and UNS S32760." International Biodeterioration & Biodegradation 63.5 (2009): 607-614.

Vupputuri, S., *et al*., (2013). "Characterization and mediation of microbial deterioration of concrete bridge structures." Final report.

Walters, L.J. . Hadfield M. G, and Smith C. M.. "Waterborne chemical compounds in tropical macroalgae: positive and negative cues for larval settlement." Marine Biology 126.3 (1996): 383-393.

Wei, S., *et al*., (2010). "Microbial mediated deterioration of reinforced concrete structures." International biodeterioration & biodegradation, 64, p. 748-754.

Wei, S., *et al*., (2013). "Microbiologically induced deterioration of concrete: a review." Brazilian Journal of Microbiology, 44, p. 1001-1007.

Wei,S. Sanchez M., D. Trejo, C. Gillis. "Microbial mediated deterioration of reinforced concrete structures." *International Biodeterioration & Biodegradation* 64.8 (2010): 748-754.

Wells, Steven, and Mark Sytsma. "A review of the use of coatings to mitigate biofouling in freshwater." *Portland State University Center for Lakes and Reservoirs* (2009).

Wen, Jie, Tingyue Gu, and Srdjan Nesic. "Investigation of the effects of fluid flow on SRB biofilm." *NACE International Corrosion Conference Series, Corrosion/2007 Paper*. No. 07516. 2007.

Wen, K. Zhao, T. Gu and S. Nesic, Effects of mass transfer and flow conditions on SRB corrosion of mild steel, Paper No. 06666, *Corrosion/2006*, NACE International, Houston, TX, 2006.

Yebra, Diego Meseguer, Søren Kiil, and Kim Dam-Johansen. "Antifouling technology—past, present and future steps towards efficient and environmentally friendly antifouling coatings." *Progress in organic coatings* 50.2 (2004): 75-104.

Yilmaz, K., (2010). “A study on the effect of fly ash and silica fume substituted cement past and mortars.” Scientific Research and Essays, 5, p. 990-998

Yuzwa, G. F., and P. Eng. "Corrosion by sulphate reducing bacteria." *Alberta Public Works, Supply and Services. Edmonton, Alberta. APPENDICES A. Dependency* (1991).

Zardus, John D., et al. "Microbial biofilms facilitate adhesion in biofouling invertebrates." *The Biological Bulletin* 214.1 (2008): 91-98.

Zavala-Olivares, G., Esquivel, R. G., Gayosso, M. J., Trejo, A. G., Gurrión, C. C., & Villalobos, E. B. (2006, January). Influence of Sulfate Reducing Bacteria on the Cathodic Protection Potential of XL52 Steel. In *CORROSION 2006*. NACE International.

Zhang, H-J., and Stephen C. Dexter. "Effect of biofilms on crevice corrosion of stainless steels in coastal seawater." *Corrosion* 51.1 (1995), p.56-66.

APPENDIX. WATER CHARACTERISTIC OF SELECTED FLORIDA TEST SITES

Table A. Initial Survey of Selected River Water Characteristics.

	Parameters	Matanzas R.	Alafia R. (Downstream)	Alafia R. (Upstream)
General	Water Type	Estuarial/Brackish	Estuarial/Brackish	~Fresh
	Max. Water Depth/ft	~30	~5	~5
	Dissolved Oxygen /mg.L^{-1}	4.20	7.90	6.53
	Avg. Salinity /ppth	30-35	15-20	10-15
	Conductivity/ mS.cm^{-1}	38.2	36.55	10.73
	Macrofouler[1]	Tunicates, Hydroids, Barnacles, Sponge	Barnacles	Barnacles
Water Chemistry	Sulfate/mg.L^{-1}	2,700 (2,800)	620 (1,900)	2,200 (58)
	Chloride/mg.L^{-1}	19,000 (21,000)	3,800 (14,000)	71
	Phosphorous/mg.L^{-1}	0.12 (0.081)	0.28 (0.096)	0.71 (0.95)
	Ammonia/mg.L^{-1}	0.03 (0.1)	0.08 (0.029)	0.04 (0.12)
	Iron/mg.L^{-1}	0.08 (0.049)	3.5 (1)	0.15 (0.64)
	Nitrate/mg.L^{-1}	0.50	0.65 (8.8)	0.5 (0.76)
	Total Organic Nitrogen /mg.L^{-1}	0.41 (0.25)	0.48 (0.80)	0.52 (0.80)
	Total Nitrogen/mg.L^{-1}	0.93	1.1 (9.72)	0.56 (0.76)
Microorganismst	Sulfate Reducing Bacteria (SRB)/CFU.mL^{-1}	27,000 (A)	325.00 (M)	500,000 (A)
	Iron-Reducing Bacteria (IRB)/CFU.mL^{-1}	500 (M)	9,000 (A)	9,000 (A)
	Acid Producing Bacteria (APB)/CFU.mL^{-1}	450 (M)	82,000 (A)	82,000 (A)
	Slime-Forming Bacteria (SFB)/CFU.mL^{-1}	13,000 (M)	1,750,000 (A)	1,750,000 (A)

Data in parenthesis was at time of sample installation. Aggressivity. (NA) Not Aggressive, (M) Moderately Aggressive, (A) Aggressive 1. General guidelines for BART test for corrosion